

THE ORBITAL INTERACTION COMPONENT OF CONFORMATIONAL EFFECTS

by

Ronald Y.N. Leung

B.Sc., University of Ulster, 1982.

THESIS SUBMITTED IN PARTIAL FULFILLMENT OF  
THE REQUIREMENTS FOR THE DEGREE OF  
DOCTOR OF PHILOSOPHY  
in the Department  
of  
Chemistry

© Ronald Y.N. Leung 1991

SIMON FRASER UNIVERSITY

February 1991

All rights reserved. This work may not be reproduced in whole or in part, by photocopy or other means, without permission of the author.

**APPROVAL**

Name: Ronald Y. N. Leung

Degree: Doctor of Philosophy

Title of thesis: The Orbital Interaction Component of  
Conformational Effects

Examining Committee:

Chairman: Dr. P. W. Percival

---

Dr. B. M. Pinto  
Senior Supervisor

---

Dr. Y. L. ~~Chow~~  
Committee Member

---

Dr. A. S. Tracey  
Committee Member

---

Dr. S. Wolfe  
Internal Examiner

---

Dr. A. Rauk  
External Examiner  
Department of Chemistry  
University of Calgary

Date of Approval: Mar 15, 91

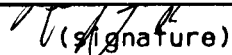
PARTIAL COPYRIGHT LICENSE

I hereby grant to Simon Fraser University the right to lend my thesis, project or extended essay (the title of which is shown below) to users of the Simon Fraser University Library, and to make partial or single copies only for such users or in response to a request from the library of any other university, or other educational institution, on its own behalf or for one of its users. I further agree that permission for multiple copying of this work for scholarly purposes may be granted by me or the Dean of Graduate Studies. It is understood that copying or publication of this work for financial gain shall not be allowed without my written permission.

Title of Thesis/Project/Extended Essay

THE ORBITAL INTERACTION COMPONENT OF  
CONFORMATIONAL EFFECTS

Author:

  
(signature)

RONALD Y. N. LEUNG

(name)

Mar. 20, 91

(date)

## ABSTRACT

A combination of experimental and computational approaches has provided details for the analysis of the steric, electrostatic and orbital interaction components of conformational effects operating in substituted heterocycles containing the O-C-N, S-C-N, O-C-O, S-C-O, O-C-C-N, S-C-C-N, O-C-C-O and S-C-C-O fragments. The orbital interactions in these heterocycles have been interpreted in terms of the interplay of the endo- and exo-anomeric gauche interactions and the attractive and repulsive ethane-type gauche interactions.

*Ab initio* molecular orbital calculations of acyclic molecules containing N-C-O fragments have been used for the parameterization of the MM2(85) force field. The geometric and energetic behaviour of a number of acyclic and heterocyclic molecules containing N-C-O anomeric fragments are reasonably well reproduced with the parameterized force field.

An *ab initio* MO study, with the MINI-1\* and 3-21G\* basis sets, of HXCH<sub>2</sub>YH (X,Y=S,Se,Te) molecules has been used to probe the existence of anomeric interactions involving second, third and fourth row heteroatoms. Bond length and bond angle trends in different conformations, the relative energies of conformers, and the methyl stabilization energies obtained in

isodesmic reactions suggest that anomeric effects exist in these systems.

Analysis of the results of semi-empirical MO (MNDO) and molecular mechanics calculations of a series of  $\text{CH}_2=\text{CH}-\text{CH}_2\text{X}$  molecules ( $\text{X}=\text{H}, \text{CH}_3, \text{OCH}_3, \text{OCOCH}_3, \text{OH}, \text{F}, \text{Cl}$ ) and the *ab initio* MO (3-21G) calculations of the molecules ( $\text{X}=\text{H}, \text{OH}, \text{F}, \text{Cl}$ ) indicate that the orbital interaction component is significant. Quantitative PMO analysis of the *ab initio* results for the molecules in which  $\text{X}=\text{F}, \text{Cl}$  has shown that the conformational preferences are dominated by the destabilizing orbital interactions and the unfavourable electrostatic interactions in gauche conformations.

The geometrical preferences and the rotational barriers in sterically hindered diselenides and ditellurides have been probed by dynamic NMR measurements. Semiempirical MO (MNDO) calculations of model compounds are also described. The results are discussed in terms of steric factors and orbital interaction components.

## ACKNOWLEDGEMENTS

The years I spent at Simon Fraser University have certainly been worthwhile. My senior supervisor, Professor B. M. Pinto has demonstrated his patience and dedication to help me throughout my study. His demand for excellence has set a good example for me to follow, not only in scientific research, but in life as a whole. I would also like to show my appreciation to all the other teachers who have taught me in the various aspects of Chemistry.

I am grateful to Dr. B. D. Johnston for his assistance in the synthesis of one of the thiacyclohexanes required for the NMR studies and to Dr. J. Korppi-Tommola for his assistance in the MINI-1\* basis set implementation.

I am grateful to Professor S. Wolfe for his valuable instruction in the use of *ab initio* MO methods and for the hospitality shown to me while in his laboratory at Queen's University. I also thank him for the quantitative PMO analysis of allyl chloride and fluoride.

Finally, I thank my wife and my parents for their wholehearted support and patience.

## TABLE OF CONTENTS

Approval .....	ii
Abstract .....	iii
Acknowledgements .....	v
Table of Contents .....	vi
List of Tables .....	ix
List of Figures .....	xiv
1. Introduction .....	1
1.1 Anomeric effect .....	2
1.2 Exo-anomeric effect .....	18
1.3 Reverse anomeric effect .....	24
1.4 Second and lower row anomeric effect .....	31
1.5 Solvent effect .....	38
1.6 Enthalpic anomeric effect .....	40
1.7 Attractive and repulsive gauche effect .....	43
1.8 Overview of thesis .....	61
2. Experimental .....	64
2.1 General information .....	64
I. Synthesis and NMR analysis .....	64
II. Determination of thermodynamic and kinetic data.	66
i. Direct determination of equilibrium constants .....	66
ii. Kinetic parameters from line shape analysis .....	67
III. Molecular mechanics calculations .....	68

IV.	<i>Ab initio</i> calculations .....	69
V.	Semi-empirical MO calculations .....	70
2.2	Synthesis .....	70
I.	Synthetic schemes .....	70
II.	General description of syntheses .....	82
III.	Procedures .....	86
3.	The study of attractive and repulsive gauche effects ..	133
3.1	Introduction .....	133
3.2	Results .....	136
I.	5-Substituted-1,3-diheterocyclohexanes .....	136
i.	NMR analysis .....	136
ii.	Conformational analysis .....	141
II.	2-Substituted-1,4-diheterocyclohexanes .....	147
i.	NMR analysis .....	147
ii.	Conformational analysis .....	151
3.3	Discussion .....	155
I.	Solvent effects on the conformational equilibria of 5-substituted-1,3-dioxacyclohexanes .....	155
II.	Anomeric effect .....	163
i.	2-Methoxyoxacyclohexane .....	163
ii.	2-Methylaminoxacyclohexane .....	164
iii.	2-Methoxythiacyclohexane .....	167
iv.	2-Methylaminothiacyclohexane.....	168
III.	Ethane-type gauche interactions .....	171
IV.	2- or 3-Substituted-1,4-diheterocyclohexanes ..	185
V.	Additivity of effects ? .....	193



4.	Parameterization of the MM2 force field for the O-C-N system .....	196
4.1	Introduction .....	196
4.2	Development of the force field .....	198
	I. <i>Ab initio</i> calculations .....	203
	II. Development of anomeric bond length parameters .....	207
	III. Development of bond angle parameters .....	208
	IV. Development of torsional parameters .....	209
5.	Theoretical investigation of anomeric systems containing second and lower row heteroatoms .....	218
6.	Theoretical investigation of the allylic anomeric effect .....	252
6.1	Introduction .....	252
6.2	Results and Discussion .....	259
7.	Rotational barriers in sterically hindered dichalcogenides .....	275
7.1	Introduction .....	275
7.2	Compounds .....	280
7.3	Results .....	281
7.4	Discussion .....	285
	I. Interactions in the ground state .....	286
	II. Interactions in the transition state .....	289
	III. Effects on the rotational barriers .....	290
7.5	Theoretical investigation of the rotational barriers in model dichalcogenides .....	292
	References .....	302

## LIST OF TABLES

Table	Page
3.1	Low-temperature $^{13}\text{C}$ NMR chemical shift data for 5-substituted-1,3-dioxacyclohexanes .....138
3.2	$^{13}\text{C}$ NMR chemical shift data ( $\delta_a$ and $\delta_e$ ) of C-5 for compounds 6-11 at 298 K .....138
3.3	$^{13}\text{C}$ NMR chemical shift data ( $\delta_a$ and $\delta_e$ ) of C-4 and C-6 for compounds 6-11 at 298 K .....139
3.4	Low-temperature $^{13}\text{C}$ NMR chemical shift data of cis-2-methyl-5-methoxy-1,3-dithiacyclohexane and 5-methylamino-1,3-dithiacyclohexanes .....140
3.5	$^{13}\text{C}$ NMR chemical shift data of axial- and equatorial-3-X-substituted-thiacyclohexanes ..... 141
3.6	Equilibrium data for 5-substituted-1,3-diheterocyclohexanes .....142
3.7	2-Isopropyl-induced $^{13}\text{C}$ NMR chemical shift corrections of 1,3-dioxacyclohexane .....144
3.8	$^1\text{H}$ coupling constants of H-5 ( $W_{1/2}$ ) in Hz for 5-X-substituted-2-isopropyl-1,3-dioxacyclohexanes (6-11) at 298 K .....145
3.9	$^1\text{H}$ Coupling constants of H-5 ( $W_{1/2}$ ) for 5-X-substituted-1,3-dioxacyclohexanes (3-5) at 298 K .....145
3.10	Calculated mole fraction of the axial conformers (I) at 298 K .....146
3.11	$^{13}\text{C}$ NMR chemical shift data ( $\delta_{\text{obs}}$ ) of C-4 and C-6 for compounds 3-5 at 298 K .....146
3.12	Calculated mole fraction of the axial conformer at 298 K using C-4 and C-6 as the probe .....147

3.13	Low-temperature $^{13}\text{C}$ NMR chemical shifts of 2-methoxy and 2-methylamino-1,4-diheterocyclohexanes ...	149
3.14	Equilibrium data for 2-substituted-1,4-diheterocyclohexanes .....	150
3.15	Conformational free energy data for 2-methoxy and 2-methylaminoheterocyclohexanes and 1,4-diheterocyclohexanes .....	154
3.16	Total interaction energy ( $\text{kcalmol}^{-1}$ ) between X and Y groups in $\text{XCH}_2\text{Y}$ calculated at the 6-31G*//6-31G* level .....	170
3.17	Experimental and calculated energy differences ( $e = a$ ) for 5-methoxy and 5-methylamino-1,3-dioxane and dithiacyclohexanes .....	173
3.18	Comparison of the orbital interactions in the 2-substituted-1,4-diheterocyclohexanes and the two corresponding types of gauche interaction in 2-substituted-heterocyclohexanes and 5-substituted-1,3-diheterocyclohexanes .....	187
3.19	Optimized bond lengths ( $\text{\AA}$ ) and bond angles ( $^\circ$ ) in the gauche,gauche conformation of $\text{XCH}_2\text{Y}$ and the corresponding staggered monosubstituted methanes, evaluated at the 6-31G* level .....	192
4.1	Relative energies and selected structural parameters of fully optimized conformers (true minima) of aminomethanol (AMOL) at the 3-21G level: bond lengths in $\text{\AA}$ ; angles in degrees .....	206
4.2	Bond lengths (in $\text{\AA}$ ) obtained by the full geometry optimization of AMOL .....	208
4.3	Relative energies $E$ ( $\text{kcalmol}^{-1}$ ) of AMOL with different N-C-O bond angles $\theta$ (degrees) .....	209

4.4	Relative energies $E$ (kcalmol <sup>-1</sup> ) of aminomethanol (AMOL) with different dihedral angles $\omega$ (degrees) ....	211
4.5	Relative energies $E$ (kcalmol <sup>-1</sup> ) of methylamino-methanol (MAMOL) with different C-N-C-O dihedral angles $\omega$ (degrees) .....	212
4.6	Relative energies $E$ (kcalmol <sup>-1</sup> ) of aminomethoxy-methane (AMM) with different C-O-C-N dihedral angles $\omega$ (degrees) .....	212
4.7	Torsional constants obtained for the parameterization of the MM2 force field for the N-C-O fragment .....	212
4.8	Predicted relative energies (kcalmol <sup>-1</sup> ) of the conformers of aminomethanol (AMOL), methylamino-methanol (MAMOL), 1-aminomethoxymethane (AMM) and 1-methoxy-N,N-dimethylmethylamine (MDMMA) with the newly parameterized MM2 force field, MM2*, and <i>ab initio</i> MO calculations .....	214
4.9	Relative energies (kcalmol <sup>-1</sup> ) of the axial and equatorial conformers of heterocycles having N-C-O units as calculated by MM2* vs literature values.....	215
4.10	Predicted bond length (Å) and bond angle (degrees) parameters of aminomethanol, as calculated by MM2*.....	216
5.1	Optimized parameters (bond lengths in Å; bond angles in degrees) of diselenomethane .....	226
5.2	Optimized parameters (bond lengths in Å; bond angles in degrees) of selenothiomethane .....	227
5.3	Optimized parameters (bond lengths in Å; bond angles in degree) of dithiomethane .....	228
5.4	Optimized geometric parameters (bond lengths in Å; bond angles in degrees) of dithiomethane (g,a conformer) at various levels of computation .....	229

5.5	Optimized geometric parameters (bond lengths in Å; bond angles in degrees) of dithiomethane (g,g conformer) at various levels of computation .....	230
5.6	Selected geometrical parameters and relative energies of HX-CH <sub>2</sub> -YH .....	232
5.7	Optimized parameters (bond lengths in Å, bond angles in degrees) of dihydroxymethane .....	233
5.8	Calculated bond separation energies (kcalmol <sup>-1</sup> ) for XCH <sub>2</sub> Y .....	234
5.9	Calculated relative energies(ΔE) and methyl stabilization energies (ΔMS) of dithiomethane and dihydroxymethane .....	235
5.10	Optimized parameters (bond lengths in Å; bond angles in degrees) of diselenomethane .....	238
5.11	Optimized parameters (bond lengths in Å; bond angles in degrees) of selenothiomethane .....	239
5.12	Optimized parameters (bond lengths in Å; bond angles in degrees) of dithiomethane .....	240
5.13	Optimized parameters (bond lengths in Å; bond angles in degrees) of ditelluromethane .....	241
5.14	Optimized parameters (bond lengths in Å; bond angles in degrees) of tellurothiomethane .....	242
5.15	Optimized parameters (bond lengths in Å; bond angles in degrees) of selenotelluromethane .....	243
5.16	Calculated conformational energies of different conformers of dithiomethane .....	244
5.17	Calculated relative energies (ΔE) and methyl stabilization energies (ΔMS) of diheterosubstituted methanes .....	245

5.18	The methyl stabilization energies of diselenomethane calculated by the isodesmic reaction .....	247
5.19	Relative energies of diselenomethane at different levels of computation .....	248
5.20	Optimized parameters of diselenomethane at different levels of computation .....	249
5.21	Effect of Electron Correlation on Relative Energies of Dimethoxymethane .....	250
6.1	Relative energies of cis and gauche rotamers of 1-X-substituted-2-propenes .....	260
6.2	Torsional terms obtained from the Fourier expansion analysis of the total potential functions of 1-X-substituted-2-propenes .....	262
6.3	<i>Ab initio</i> MO calculation for allyl alcohol at the 6-31G basis level (bond lengths in Å, angles in degrees) relative energy ( $\Delta E$ ) in kcalmol <sup>-1</sup> ) .....	267
6.4	<i>Ab initio</i> MO calculation for allyl alcohol at the 3-21G basis level (bond lengths in Å, angles in degrees, relative energy ( $\Delta E$ ) in kcalmol <sup>-1</sup> ) .....	268
6.5	Orbital interactions in allyl fluoride .....	272
6.6	Orbital interactions in allyl chloride .....	273
7.1	Rate constants ( <i>k</i> ) derived from line-shape analysis ..	284
7.2	Activation parameters for restricted rotation in 7.2 and 7.3 .....	285
7.3	Critical structural data for diaryl dichalcogenides in the solid state .....	287
7.4	(CSSC) Dihedral angles ( $\omega$ (°)) of disulfides with bulky substituents .....	294

7.5	Optimized parameters (bond lengths in Å; bond angles in degrees) of dialkyl disulfides .....	295
7.6	<i>Ab initio</i> MO calculated rotational barriers (kcalmol <sup>-1</sup> ) of hydrogen disulfide and methyl disulfide .....	296
7.7	Potential energy profile for internal rotation of hydrogen peroxide at the 6-31G* level of computation..	297
7.8	Potential energy profile for internal rotation of hydrogen disulfide at the 6-31G* level of computation	299

## LIST OF FIGURES

Figure	Page
1.1 Configurational equilibrium of $\alpha$ - and $\beta$ -D-glucose in aqueous medium .....	3
1.2 A definition of the anomeric effect (E) in heterocyclohexanes .....	4
1.3 Dipole-dipole interactions in 2-axial- and equatorial-hydroxyoxacyclohexanes .....	5
1.4 Lone pair orientations in 2-hydroxyoxacyclohexane. "Rabbit ear" effect in the equatorial conformation .....	6
1.5 Double bond-no bond resonance in polyhalogenated methanes .....	7
1.6 2,3-Dihalogenosubstituted-1,4-diheterocyclohexanes .....	7
1.7 Lone pair delocalization in 2-halogenated-1,4-diheterocyclohexanes .....	8
1.8 Molecular orbital counterpart of double bond-no bond resonance .....	8
1.9 Two orbital-two electron ( $\pi \rightarrow \sigma^*$ ) orbital interaction diagram .....	9
1.10 Bond length variations in the cis- and trans-2,3-dichloro-1,4-dioxacyclohexanes .....	10
1.11 Non-equivalent $\pi$ and $\sigma$ lone pair orbitals in H <sub>2</sub> O .....	12
1.12 The two highest lying molecular orbitals of dimethoxymethane in the gauche, gauche conformation .....	13
1.13 Through space and through bond orbital interactions in the anti, anti conformation of dimethoxymethane .....	14



1.14	FCH <sub>2</sub> OH as a model for 2-fluorooxacyclohexane in the qualitative PMO analysis .....	17
1.15	PMO analysis of the orbital interactions in the antiperiplanar and gauche conformations of FCH <sub>2</sub> OH .....	17
1.16	Conformational equilibrium of tri-O-benzoyl- $\beta$ -D-xylopyranosylfluoride .....	18
1.17	The three possible rotamers in the axial and equatorial conformations of 2-alkoxyoxacyclohexane .....	19
1.18	The preferred conformers in axial and equatorial alkylglycosides .....	20
1.19	$\pi$ -Type lone pair donations in the exo- and endo-anomeric interactions .....	21
1.20	Model $\alpha$ -glycoside A and $\beta$ -glycoside B .....	22
1.21	Conformational preferences of $\alpha$ -glycosides and the corresponding C-glycosides .....	23
1.22	Conformational equilibrium of N-imidazolidinium glycoside .....	24
1.23	Conformational equilibrium of 2-aminooxacyclohexane ...	26
1.24	The relationship between the equatorial and axial conformations of 2-aminooxacyclohexane and the anti, gauche and gauche, gauche conformations of aminomethanol .....	28
1.25	Trimethylsilyloxy- (TMSO) and tert-butoxy- (TBO) substituted-1,4-dioxacyclohexanes .....	30
1.26	The relationship between the axial and equatorial-X-substituted oxacyclohexanes and CH <sub>3</sub> CH(XH)(YH) .....	32
1.27	Conformational equilibria of cyclic esters of phosphorus and thiophosphorus acids .....	33

1.28	Conformational equilibrium of a cyclic phenyl phosphate ester .....	34
1.29	Conformational equilibrium of a 5-tert-butyl-cyclic sulfite .....	34
1.30	Schematic representations of the stabilizing orbital interactions operating in the axial- and equatorial-2-(4-substituted-phenylseleno)-1,3-dithiacyclohexanes..	35
1.31	Charge transfer in the axial-2-(4-substituted-phenyl-seleno)-1,3-dithiacyclohexane .....	36
1.32	Conformational equilibria in 5-methyl-2-phenylthio- and 2-phenylseleno-1,3-diselenanes .....	36
1.33	Conformational equilibrium of 2-(4-methoxyphenyl)-seleno-1,3-dithiacyclohexane in $\text{CFCl}_3/\text{CDCl}_3$ .....	42
1.34	Dipole-dipole interactions present in the axial and equatorial conformers of 2-C(O)R-5-methyl-5-aza-1,3-dithiacyclohexane .....	43
1.35	Potential energy diagram for rotation of the C-C bond of ethane .....	45
1.36	Potential energy diagram for rotation about the C2-C3 bond of n-butane .....	45
1.37	Some examples of 1,2-disubstituted ethanes with a more favoured gauche conformation .....	46
1.38	Configurational equilibria of 2-isopropyl-5-fluoro-, 5-methoxy-, and 5-cyano-1,3-dioxacyclohexanes .....	46
1.39	Coordinate diagram of $\Delta G^\circ_{X/Y} - E_V$ versus $\Delta E_D$ for 1,2-disubstituted-cyclohexanes .....	48
1.40	Configurational equilibria of 5-methoxy- and 5-methylthio-1,3-dithiacyclohexanes .....	49
1.41	Energy level diagram of two orbital-four electron destabilizing orbital interaction .....	50

1.42	Conformational equilibria of 2-X-substituted-1,4-dioxa-cyclohexanes and 2-X-substituted-1,4-oxathia-cyclohexanes .....	51
1.43	Conformational equilibria of 3,7,9-trihetero derivatives of bicyclo [3.3.1]nonanes .....	52
1.44	The combination of through space orbital interactions ( $\phi_1+\phi_2$ , $\phi_1-\phi_2$ ) with $\sigma$ and $\sigma^*$ through bond orbital interactions .....	53
1.45	The three possible conformations ( $C_e$ , $C_a$ and TB) of 3-X-substituted -1,5-benzodioxepins (X=I, Br, Cl, F and OMe) .....	56
1.46	The axial conformation of 1,3-dioxan-5-yl methyl sulfone and the analogously substituted oxacyclohexane.	58
1.47	The three possible staggered conformations of 2-alkylthio-1,1-dimethoxyethanes .....	60
1.48	The more stable rotamers of conformations I and III of 2-alkylthio-1,1-dimethoxyethanes .....	61
3.1	5-Substituted-1,3-diheterocyclohexanes and 2- or 3-substituted-1,4-diheterocyclohexanes synthesized for the study of attractive and repulsive gauche effects .....	133
3.2	Possible rotamer of 5-methylamino-1,3-dioxacyclohexane .....	137
3.3	Conformational equilibria of 3-X-substituted-thiacyclohexanes .....	140
3.4	Dipolar interactions in axial and equatorial 5-substituted-1,3-dioxacyclohexanes .....	144
3.5	Comparison of steric requirements of substituted cyclohexane and 2-substituted-oxacyclohexane .....	152

3.6	Calculated energy differences of the methyl substituent in cyclohexane and 1,4-dioxacyclohexane ..	152
3.7	Dipole-dipole interpretation of the anomeric interactions in 2-substituted-oxacyclohexanes .....	155
3.8	Trans-2,3-dimethoxy- and trans-2,5-dimethoxy-1,4-dioxacyclohexanes .....	156
3.9	Model of $n_p \rightarrow \sigma^*_{C-X}$ orbital interaction in truncated fragment .....	157
3.10	Charge transfer model of $n_p \rightarrow \sigma^*_{C-X}$ orbital interaction	157
3.11	Dipole-dipole interactions in 5-axial, and 5-equatorial-substituted-1,3-dioxacyclohexanes .....	158
3.12	Intramolecular electrostatic attraction in 5-axial-acetyl-1,3-dioxacyclohexane .....	159
3.13	Conformational equilibrium of 5-amino-5-methyl-1,3-dioxacyclohexane .....	160
3.14	Bifurcated intramolecular hydrogen bonding in cis-2-phenyl-5-hydroxy-1,3-dioxacyclohexane .....	160
3.15	Intramolecular hydrogen bonding in protonated cis-2-tert-butyl-5-methoxy-1,3-dithiacyclohexane .....	161
3.16	Intramolecular hydrogen bonding in 5-axial-hydroxy-1,3-dithiacyclohexane .....	161
3.17	Intermolecular hydrogen bonding of axial-amino substituted-1,3-dioxacyclohexane with solvent, dimethylsulfoxide .....	162
3.18	Hyperconjugative interactions in O-C-O fragments .....	164
3.19	Predicted orientation of the NH proton of 2-axial-methylaminooxacyclohexane .....	166
3.20	The four possible stable conformations of aminomethoxymethane .....	167

3.21	Predicted orientation of the NHCH <sub>3</sub> group in 5-axial-methylamino-1,3-diheterocyclohexanes .....	173
3.22	Possible orientation of the 5-methylamino substituent in 1,3-diheterocyclohexanes .....	174
3.23	Resultant dipoles of the diheterocyclohexane ring and the methoxy substituent .....	175
3.24	Resultant charge distribution in 5-methylamino-1,3-diheterocyclohexanes .....	176
3.25	Combinations of through space and through bond orbital interactions for 5-methylamino-1,3-dioxacyclohexane (4) .....	179
3.26	Possible through bond interactions in 5-substituted-1,3-diheterocyclohexanes .....	182
3.27	The two orbital interaction components in 2- or 3-substituted-1,4-diheterocyclohexanes .....	186
3.28	Gauche interactions in hetero-substituted fragments ..	186
3.29	Orientation of the equatorial methylamino substituent in 5-substituted-1,3-diheterocyclohexanes .....	188
3.30	Orientation of the equatorial methylamino substituent in 2-substituted-heterocyclohexanes .....	188
3.31	Orientation of the equatorial methylamino substituent in 2-substituted-1,4-diheterocyclohexanes .....	189
3.32	Through space lone pair repulsion in axial-2-methoxy-1,4-diheterocyclohexane (Y=S) .....	190
3.33	Hydrogen bond between NH proton and the ring heteroatom in axial-2-methylamino-1,4-diheterocyclohexanes .....	191
3.34	Atomic charges on XCH <sub>2</sub> Y (X=O, S; Y=NH <sub>2</sub> ) ,given by Mulliken population analysis .....	192

3.35	The $n_x \rightarrow \sigma^*_{C-Z}$ orbital interaction in the anomeric type gauche fragment and the $\sigma_{C-H} \rightarrow \sigma^*_{C-Z}$ orbital interaction in the ethane type gauche fragment .....	193
3.36	Orientations of the anomeric type and ethane type gauche orbital interactions .....	194
4.1	Schematic representation of a dipole/dipole interaction .....	201
4.2	Schematic representation of a torsional angle $\omega$ described by the connected atoms A-B-C-D .....	202
4.3	The periodicity and behaviour of the MM2 torsional terms .....	203
4.4	The four possible conformers of aminomethanol .....	204
4.5	Aminomethanol (AMOL, 4-1), methylaminomethanol (MAMOL, 4-2) and aminomethoxymethane (AMM, 4-3) .....	205
5.1	The five relevant conformations of disubstituted methanes ( $X=Y$ , $G, A \equiv A, G$ ) .....	219
5.2	The relationship between the axial and equatorial conformations of 2-substituted-heterocyclohexanes and their truncated models .....	219
5.3	The orbitals involved in the $\pi$ and $\sigma$ type interactions in disubstituted methanes .....	223
6.1	Conformational equilibrium of 3-substituted-cyclohexenes in the half-chair conformation .....	252
6.2	Double bond-no bond resonance interaction in 3-substituted-cyclohexenes .....	253
6.3	Dipole-dipole interactions in the axial and equatorial 2-substituted-cyclohexanones .....	254

6.4	The two electron-two orbital $\sigma_{C-X} \rightarrow \pi^*_{C=O}$ interaction in the axial conformation of 2-substituted-cyclohexanones .....	254
6.5	Allylic $A^{1,3}$ strain in the equatorial conformation of 2-substituted-methylenecyclohexanes .....	255
6.6	The $n_O \rightarrow \pi^*_{C=C}$ orbital interaction in axial-2-methoxy- and 2-acetoxymethylenecyclohexanes .....	256
6.7	Orbital interactions in 7-X-substituted-2-methoxy-methylenecyclohexanes .....	256
6.8	The planar conformation of benzyl fluoride .....	258
6.9	Cis and gauche rotamers of 1-X-substituted-2-propene .	260
6.10	The Cg and Gg forms of allyl alcohol .....	263
6.11	The gauche and cis conformations of 3-buten-2-ol .....	264
6.12	The two different sets of rotamers of allyl alcohol in the gauche and cis conformations .....	264
6.13	The bond lengths (Å) of allyl alcohol calculated at the 6-31G level .....	266
6.14	The orbital interactions of allyl halides in the cis rotameric form .....	270
6.15	The orbital interaction of allyl halides in the gauche rotameric form .....	271
7.1	Chalcogen-chalcogen bond rotation in acyclic dichalcogenides .....	276
7.2	Structure of bis(2,4,6-tri-substituted-phenyl)-dichalcogenides .....	276
7.3	Rotation about the chalcogen-chalcogen (X-X) bond and about the carbon-chalcogen (C-X) bond in sterically hindered dichalcogenides .....	278

7.4	Dominant orbital interactions that contribute to the HOMO of R-X-X-R molecules in the (a) perpendicular, (b) syn and (c) anti conformations .....	288
7.5	Fourier decomposition analysis of the potential function of hydrogen peroxide .....	298
7.6	Dipolar interactions in the syn and anti rotameric forms of hydrogen peroxide .....	299
7.7	Fourier decomposition analysis of the potential function of hydrogen disulfide .....	300



## CHAPTER 1

### INTRODUCTION

Conformational analysis is one of the fields in chemistry that only received attention at the end of the nineteenth century. The tetrahedral geometry of saturated carbon was first proposed by van't Hoff<sup>1</sup> and Le Bel<sup>2</sup> in 1874/1875. In 1890, Sachse<sup>3</sup> suggested that cyclohexane could exist in two arrangements, free from energy strain, which were later termed chair and boat conformations. However, the term "conformation" was introduced by Haworth<sup>4</sup> only at the end of the 1920's. About a decade later, Kohlrausch<sup>5</sup> demonstrated experimentally that there were two types of bonds in the chair form of cyclohexane (now termed axial and equatorial). The experimental work on cyclohexane was then extended by Hassel,<sup>6</sup> and in 1943, he recognized that in all cases known, the equatorial position was favoured in substituted cyclohexanes. The major breakthrough was made by Barton<sup>7</sup> who built on Hassel's ideas to explain the greater stability of equatorial over axial substituents on the basis of steric hindrance and non-bonded repulsion. As a result of their distinctive work, Hassel and Barton were jointly awarded the Nobel Prize for

chemistry in 1969 for developing and applying the principles of conformation in chemistry.

The principles of conformational analysis developed for the case of cyclohexane were then extended to a wide variety of other cyclic and acyclic systems and subsequently to heterocyclic systems.<sup>8-10</sup> In most cases, the concept of steric bulk or size enables a prediction of the relative stabilities of conformers, their reactivities, and the stereochemistry of the products formed. The rationale that has developed over the years is based on the minimization of repulsive forces. For example, in six-membered rings, in the majority of cases, conformers bearing axial substituents are less stable than those with equatorial ones. There are only one or two exceptions in the case of monosubstituted cyclohexanes: the axial conformation in cyclohexylmercuric acetate and chloride is preferred.<sup>11</sup> However, there are also exceptions where electronegative groups prefer the axial orientation in systems containing heteroatoms, electron pairs, or polar bonds. This "anomalous" behaviour has been classified in terms of special conformational effects.<sup>12</sup>

### 1.1 Anomeric Effect

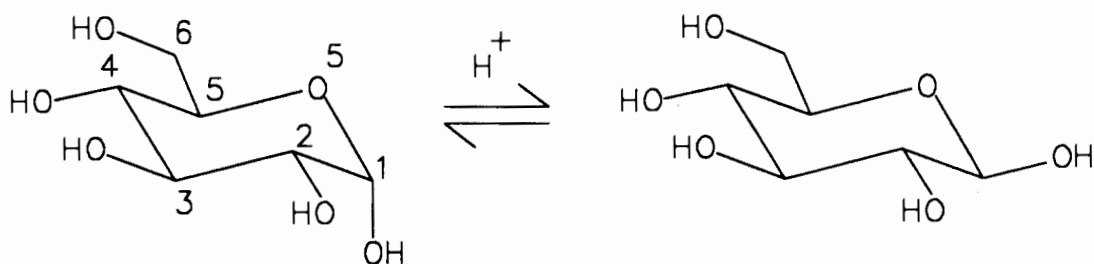
One of the most studied conformational effects is the anomeric effect. The behaviour was first noted by Edward<sup>13</sup> in

his investigation of the relative stability of methyl- $\alpha$ - and  $\beta$ -glycopyranosides to acid hydrolysis. The term "anomeric effect" was introduced in 1959 by Lemieux<sup>14</sup> as a result of the investigation of the equilibria of peracetylated pento- and hexo-pyranoses.<sup>15</sup> Since then, extensive literature has appeared on studies of this "special" conformational effect.<sup>16-30</sup>

The configurational equilibrium between  $\alpha$ - and  $\beta$ -D-glucose provides a classic illustration of the anomeric effect (Fig.1.1). Calculation of the free energy difference

Figure 1.1

Configurational equilibrium of  $\alpha$ - and  $\beta$ -D-glucose in aqueous medium.

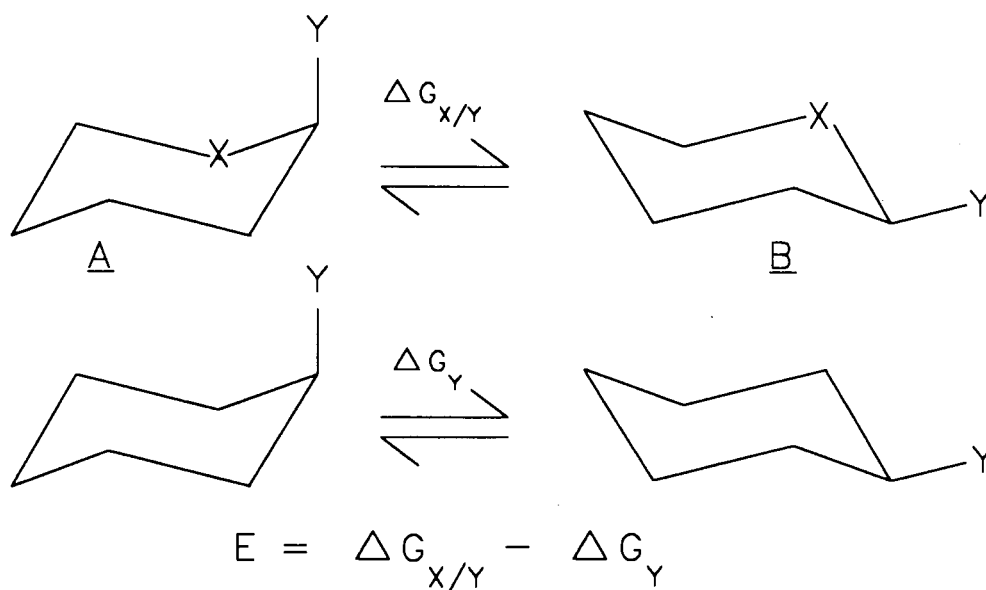


between these two isomers using the "A-value" of the hydroxyl group predicted a value of  $1.25 \text{ kcal mol}^{-1}$ ,<sup>31</sup> which gives an equilibrium  $\beta$ : $\alpha$  mixture of 89:11. However, experimentally<sup>31</sup> one finds a  $\beta$ : $\alpha$  mixture of 64:36 in water solution. The difference is attributed to the presence of the anomeric

effect. For cyclic systems of type A, with or without additional ring substituents, the magnitude of the anomeric effect (E), has been defined as the difference between the conformational free energy for the equilibrium  $A \rightleftharpoons B$  ( $\Delta G_{X/Y}$ ) and the corresponding process in the analogously substituted cyclohexane ( $\Delta G_Y$ ) (Fig.1.2).

Figure 1.2

A definition of anomeric effect (E) in heterocyclohexanes.

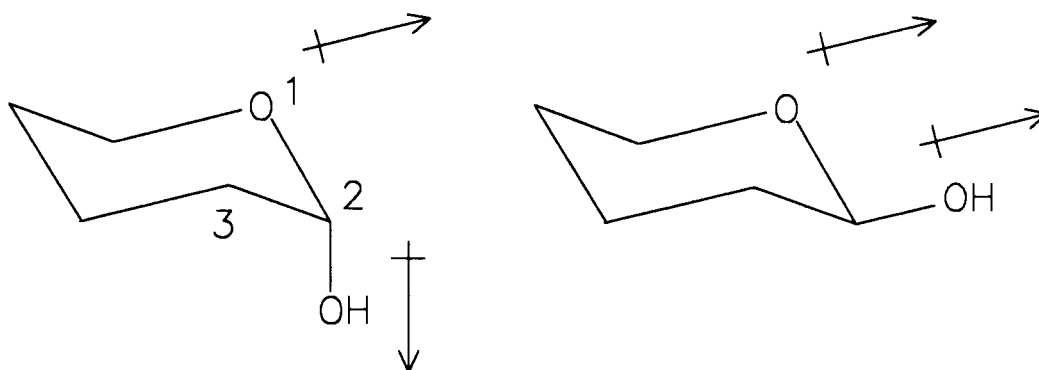


The origin of the anomeric effect was initially attributed to the electrostatic interactions between the carbon-substituent dipole and the resultant dipole of the lone pairs on the ring oxygen in 2-substituted-heterocyclohexanes.<sup>16</sup> A greater stabilization is obtained with the substituent in the axial orientation since this put the C2-O2

bond dipole perpendicular to the ring oxygen dipole. In the equatorial orientation, the two dipoles are parallel and in much closer proximity, as illustrated in Fig.1.3.

Figure 1.3

Dipole-dipole interactions in 2-axial- and equatorial-hydroxyoxacyclohexanes.

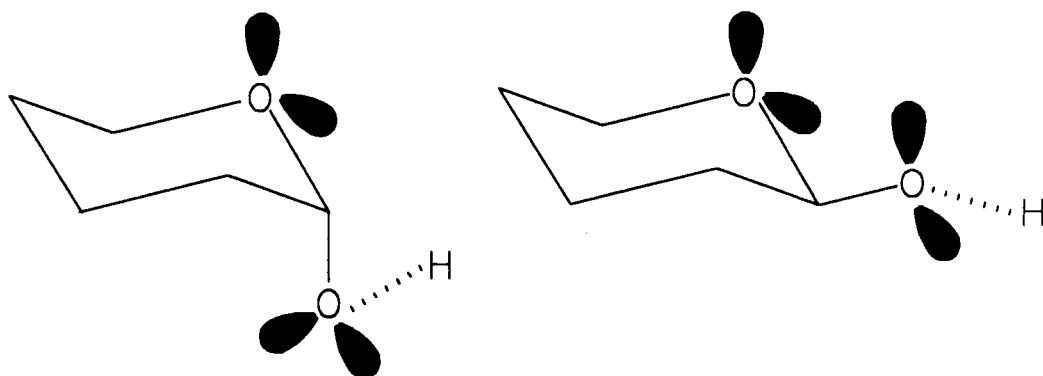


This interpretation of the anomeric effect is supported by the observed solvent dependence of the conformational equilibria of acetals.<sup>16,32</sup> However, this rationalization is unable to account for the observed<sup>33</sup> and calculated<sup>21,34-39</sup> systematic changes in geometry as a function of conformation. Obviously, this suggests that dipole-dipole interactions may not be the only driving force for the anomeric effect. A different view of this electrostatic interaction, picturesquely known as the "rabbit-ear" effect,<sup>40,41</sup> is based on the premise that lone pair-lone pair interactions are significantly greater than either lone pair-bonding pair or bonding pair-bonding pair interactions. In the axial

orientation of the acetal, there is no lone pair-lone pair interaction whereas all possible rotamers of the substituent in the equatorial orientation have at least one such interaction (Fig.1.4). However, theoretical calculations on 2-methoxyoxacyclohexane and on fluoromethanol have shown no support for an electrostatic interaction of heteroatom unshared electron pairs, and this model has for the most part been abandoned in the current view of the anomeric effect.<sup>42,43</sup>

Figure 1.4

Lone pair orientations in 2-hydroxyoxacyclohexane. "Rabbit ear" effect in the equatorial conformation.

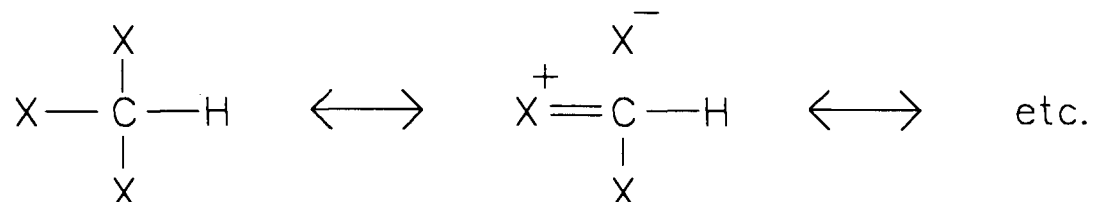


An alternative explanation is based on the concept of double bond-no bond resonance,<sup>44-46</sup> and was forwarded by Altona.<sup>47,48</sup> It was found that the carbon-halogen bonds in polyhalogenated methanes are shorter than those in the parent methyl halides,<sup>44</sup> and the effects are additive with the number

of halogen atoms (Fig.1.5). This was readily explained by the double bond-no bond resonance theory.<sup>44-46</sup>

Figure 1.5

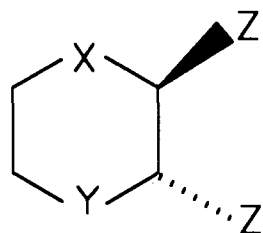
Double bond-no bond resonance in polyhalogenated methanes.



In halogenated 1,4-dioxacyclohexanes, dithiacyclohexanes and p-oxathiacyclohexanes (Fig.1.6), which exhibit anomeric

Figure 1.6

2,3-Dihalogenosubstituted-1,4-diheterocyclohexanes.



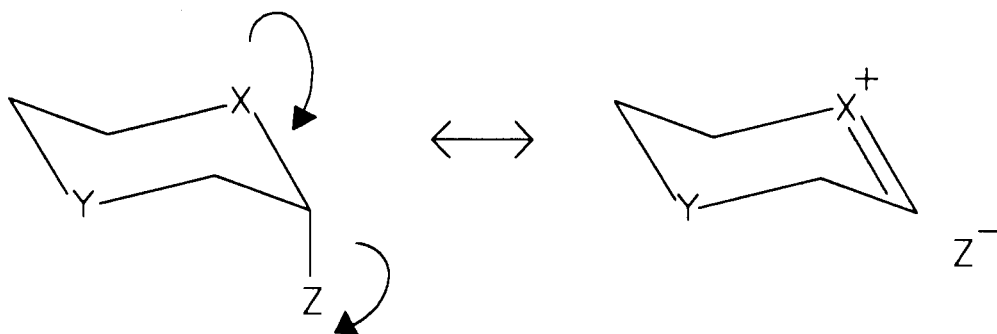
1,4-dioxacyclohexane	X=Y=O	Z=Cl, Br
1,4-dithiacyclohexane	X=Y=S	Z=Cl
1,4-oxathiacyclohexane	X=O, Y=S	Z=Br

effects, the shortening of the endocyclic carbon-heteroatom bonds and the lengthening of the exocyclic carbon-Z bonds was also rationalized in terms of a double bond-no bond resonance interaction resulting from the delocalization of the hybrid lone pair on the ring heteroatoms<sup>49-56</sup> that was antiperiplanar

to the carbon-substituent bond (Fig.1.6, 1.7). Although this explanation was accepted for some time, it could not account for the relative shortening of both the endocyclic  $C_1-O_5$  bond and the exocyclic  $C_1-O_1$  bond in glycopyranoses and in methyl- $\alpha$ -D-glycopyranosides.<sup>20</sup>

Figure 1.7

Lone pair delocalization in 2-halogenated-1,4-diheterocyclohexanes.



A molecular orbital counterpart of double bond-no bond resonance was first suggested by Lucken.<sup>54</sup> According to this interpretation<sup>54,56</sup> the anomeric stabilization in heterocyclic systems is brought about by the charge transfer between a lone pair orbital on the ring heteroatom X, and the  $\sigma^*$  antibonding orbital of the adjacent polar C-Y bond. (Fig.1.8 & 1.9).

Maximum overlap between the interacting orbitals results when the lone pair on Y is oriented antiperiplanar to the C-X bond. This theory was applied to the interpretation of the anomeric effect by Altona<sup>47</sup>, based mainly on the x-ray crystallographic data of heterocycles. An important aspect of the finding<sup>47</sup> is



Figure 1.8

Molecular orbital counterpart of double bond-no bond resonance.

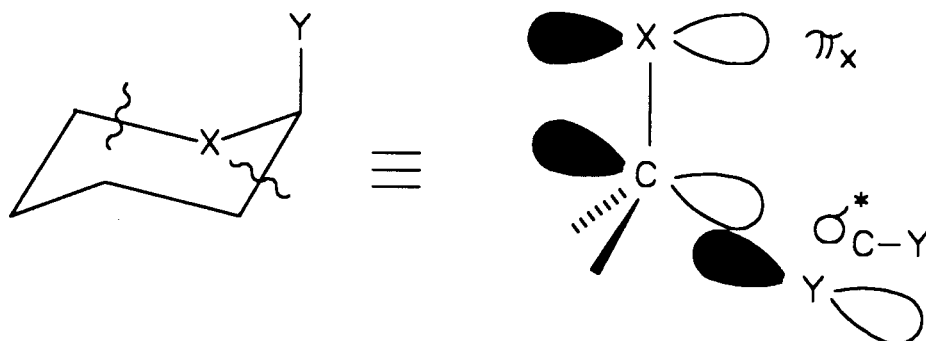
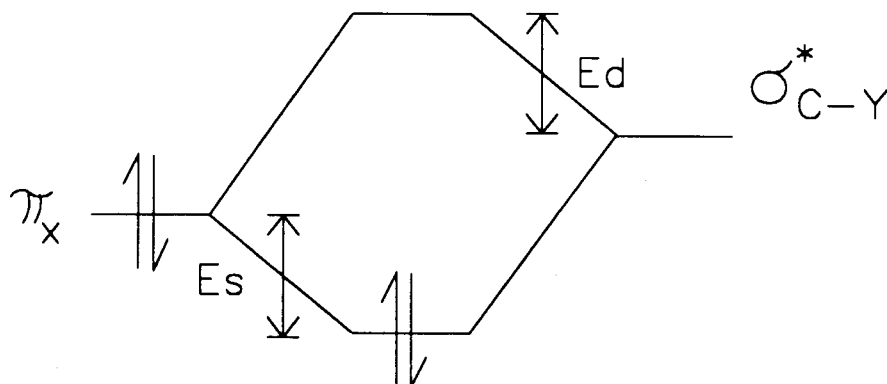


Figure 1.9

Two orbital-two electron ( $\pi \rightarrow \sigma^*$ ) orbital interaction diagram.

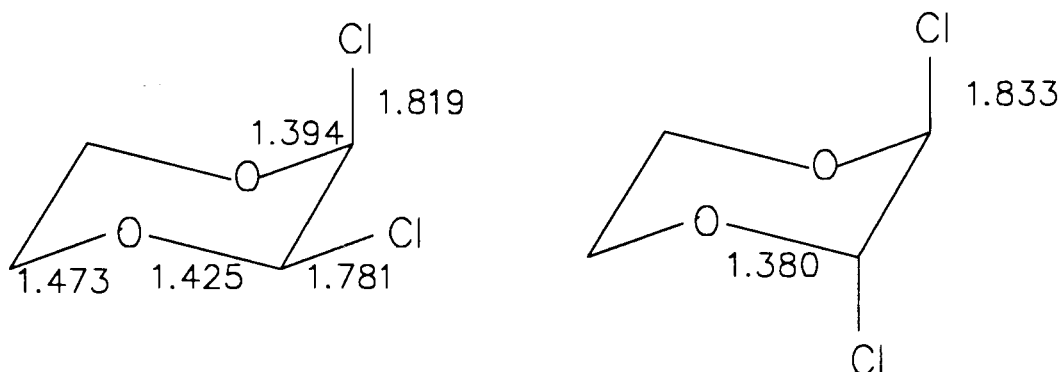


that the C-Y bond (Fig.1.8) is longer than normal and the C-X bond is shorter than normal as a result of the mixing between the lone pair and the antibonding orbitals. Experimental evidence was obtained by examination of bond length variations in  $\alpha$ -halogenoethers as shown above.<sup>20,49-54</sup> The bond length variations in the cis- and trans-2,3-dichloro-1,4-dioxanes<sup>33</sup>

provide a clear demonstration of this interpretation (Fig.1.10).

Figure 1.10

Bond length variations in the cis- and trans-2,3-dichloro-1,4-dioxacyclohexanes.



In order to better understand the orbital interactions, 2-chlorooxacyclohexane was studied by experimental and theoretical means.<sup>57-59</sup> The orbital populations of the axial and equatorial conformers were calculated by *ab initio* MO methods at the STO-3G level and the  $\pi$  orbital populations on the halogen atoms were related to the  $^{35}\text{Cl}$  NQR frequencies. These studies, together with those of the  $^{35}\text{Cl}$  NQR frequencies of axial and equatorial pyranosyl chlorides<sup>59</sup> were interpreted in terms of a higher  $3p_z$  orbital population on the axial chlorine atom or a greater ionicity of the C-Cl bond in the compounds having the chlorine atom in the axial orientation. In the same way, the lone pair orbital on X is also capable of

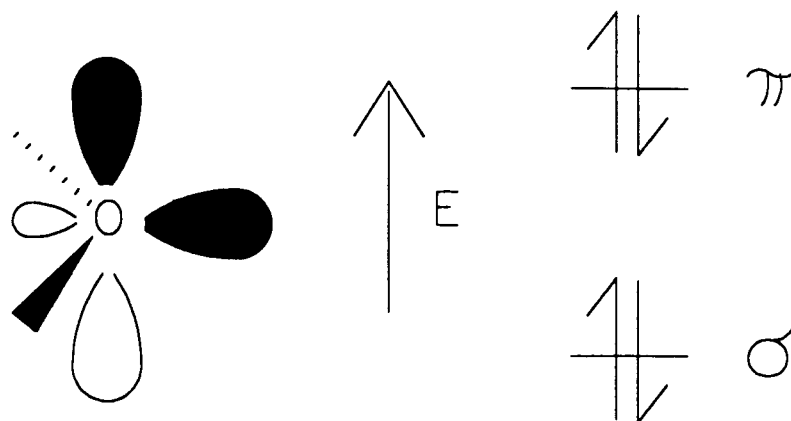
interacting with a  $\sigma^*_{\text{C-H}}$  orbital, although the interaction should be much weaker in the latter case.

The observed stereoselectivity of the reactions of electrophiles with aldopyranoses and pyranosides may be interpreted in terms of an increase in electron density on the axial hydrogen atom, resulting from the  $\pi_{\text{O}} \rightarrow \sigma^*_{\text{C-H}}$  orbital interaction.<sup>60</sup> For instance, the preferential oxidation by bromine of aldopyranose anomers having axial C<sub>1</sub>-H bonds,<sup>61</sup> the complete inertness of glycosides with equatorial C<sub>1</sub>-H bonds to ozone oxidation under conditions that convert glycosides with axial C<sub>1</sub>-H bonds to the corresponding glyconates,<sup>62</sup> and the selectivity of the chromium trioxide oxidation of methyl glycosides<sup>63</sup> have all been considered<sup>60</sup> as experimental evidence for a  $\pi_{\text{O}} \rightarrow \sigma^*_{\text{C-H}}$  interaction. In fact, the *ab initio* MO calculation on dihydroxymethane<sup>64</sup> indicated a higher electron density in a C-H bond antiperiplanar to an oxygen lone pair.

At this point it is instructive to introduce briefly the concept of canonical or delocalized molecular orbitals. Consideration of the molecular orbitals of H<sub>2</sub>O indicates that there are two non-equivalent lone pair orbitals on oxygen,<sup>65</sup> one with  $\pi$ - and the other with  $\sigma$ -character (Fig.1.11). (This contrasts with the valence bond interpretation which considers these lone pair orbitals as being energetically equivalent).

Figure 1.11

Non-equivalent  $\pi$  and  $\sigma$  lone pair orbitals in  $H_2O$ .



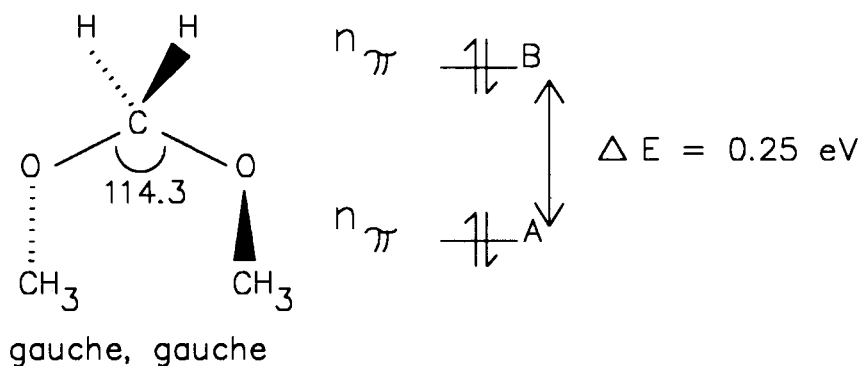
The potential energy of the  $\sigma$ -type oxygen lone-pair is lower than that of the  $\pi$ -type lone-pair. In  $H_2O$ , the experimentally determined energy difference between these lone-pairs is 0.5 eV ( $11.5 \text{ kcal mol}^{-1}$ ).<sup>66,67</sup> Therefore, in the context of Lucken's model, the interaction of the oxygen  $\pi$ -type lone pair with an adjacent antibonding orbital should be energetically more favourable than with an oxygen  $\sigma$ -type lone pair since the interaction is inversely proportional to the energy difference between interacting orbitals.<sup>68-70</sup>

Generally, the interaction of two filled non-bonding orbitals,  $\phi_a$  and  $\phi_b$ , can be observed experimentally by the splitting into two bands in the photoelectron spectrum.<sup>71</sup> In a study of the electronic structure of dimethoxymethane, Jorgensen et al.<sup>72,73</sup> found that the theoretically calculated oxygen lone pair orbital energies agreed well with

experimentally determined vertical ionization potentials of the two orbitals resulting from interaction of the highest lying molecular orbitals ( $n_\pi$ ). Their energies (Fig.1.12) in the gauche, gauche (g,g) conformer were calculated as a function of the O-C-O bond angle. The calculation also predicted that the energy difference between the  $n_\pi$  orbital having B symmetry and the other lone pair orbital with A symmetry would be 0.25 eV for an O-C-O angle of 114.3, the bond angle obtained from electron diffraction studies (Fig.1.12). The first band of the photoelectron spectrum of

Figure 1.12

The two highest lying molecular orbitals of dimethoxymethane in the gauche, gauche conformation.

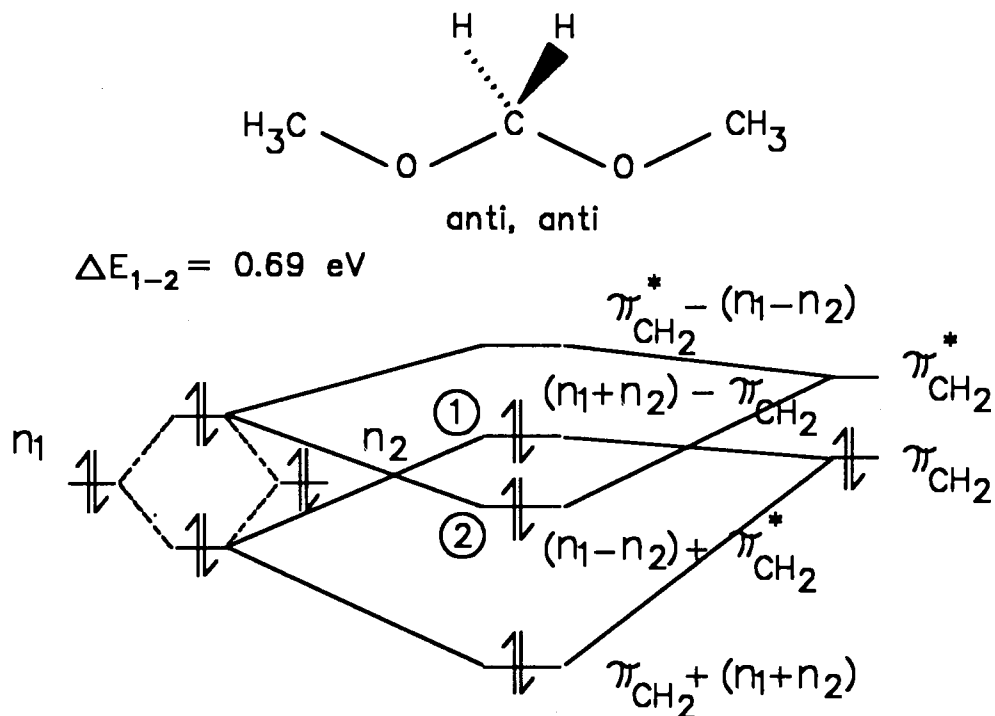


dimethoxymethane indeed showed two peaks with  $\Delta E = 0.24 \text{ eV}$ . When the conformation about the C-O bonds was altered from the g,g to the anti,anti (a,a), molecular orbital calculations showed that the energy gap between the two  $n_\pi$  orbitals

increased, suggesting a stronger  $n_{\pi}-n_{\pi}$  orbital interaction coupled through the  $\pi(\text{CH}_2)$  orbitals (Fig.1.13).

Figure 1.13

Through space and through bond orbital interactions in the anti,anti conformation of dimethoxymethane.



The molecular orbital interpretation described above is an example of the currently used Perturbation Molecular Orbital (PMO) approach to conformational problems.<sup>74,68-70,75</sup> The hypothesis of the PMO approach is that the MO's of a molecule can be regarded as the result of orbital interactions between different "functional group" orbitals which are dissected from the molecule.<sup>21</sup> For a molecular system A-B, in which A and B are fragments or "functional" groups, A and B

are allowed to approach each other in different orientations, and the possible orbital interactions are considered. The most stable conformation is achieved by maximizing the stabilizing and by minimizing the destabilizing interactions between the group or fragment orbitals of A and B. The magnitude of the stabilizing interaction of two orbitals  $i$  and  $j$  is proportional to  $S_{ij}/\Delta e_{ij}$ , where  $S_{ij}$  is the overlap matrix element and  $\Delta e_{ij}$  is the energy difference between the interacting orbitals. The magnitude of the destabilizing interaction is proportional to  $S_{ij}^2(e_i+e_j)/2$ .<sup>69,70</sup> Provided that there is constant overlap, the largest stabilizing and destabilizing orbital interactions are those associated with the frontier orbitals of A and B,<sup>76,77</sup> and there is extensive precedent that the behaviour of the HOMO parallels that of the total energy behaviour of various molecular systems.

In order to obtain the magnitude of the energy changes resulting from orbital interactions between fragment molecular orbitals in different conformations of a particular molecular system, a quantitative PMO approach was developed by Wolfe *et al.*<sup>21,78</sup> The fragment orbitals of A and B are obtained from the *ab initio* wave functions of the molecule A-B. A molecular fragment is a near transferrable mechanical entity, and this is justified by the observation that the Fock matrix elements are transferrable from one molecule to another.<sup>79-84</sup> The total energy behaviour of various molecular systems is

reproduced semi-quantitatively by the behaviour of the  $\pi$ -type orbital interactions between the fragments. The  $\sigma$ -type orbital which represents dissected bonds, is conformationally invariant and therefore does not make a significant contribution to the total energy behaviour. Using this approach, the authors have shown that the experimentally observed trends in the magnitudes of the anomeric effect can be correlated with the trends in stabilizing orbital interactions between the  $\pi$ -type lone pair orbitals on Y and the  $\sigma^*$  antibonding orbital of  $\text{CH}_2\text{X}$  of the  $\text{XCH}_2\text{YH}$  molecular systems. Consider, for example, the case of  $\text{FCH}_2\text{OH}$  which serves as a model for 2-fluorooxacyclohexane (Fig.1.14). The PMO treatment focuses on the two orbital-two electron stabilizing orbital interactions that contribute to the HOMO of the molecules. Figure 1.15 illustrates the application of the PMO procedure to the model axial and equatorial conformers of 2-fluorooxacyclohexane, with the interaction taken as  $\text{HO}\cdots\text{CH}_2\text{F}$ . In each conformation shown, the doubly occupied orbital is  $n_\pi$ , the  $\pi$ -type nonbonding orbital on O, and the acceptor orbital is the unoccupied orbital of  $\text{CH}_2\text{F}$  that has the proper symmetry for non-zero primary overlap with  $n_\pi$ . In the antiperiplanar conformation, this is  $\pi^*(\text{CH}_2\text{X})^\#$ , and in the

---

<sup>#</sup> Since this orbital is antibonding in the region between the CH bonds, it is also referred to as a  $\sigma^*_{\text{CH}}$  orbital. Similarly, a  $\pi(\text{CH}_2\text{X})$  orbital is regarded as a  $\sigma_{\text{CH}}$  orbital. These two descriptions are used interchangeably in this thesis.



perpendicular or gauche conformation, the acceptor orbital is  $\sigma^*(\text{CH}_2\text{X})$ . Since the  $\sigma^*$  orbital lies lower than the  $\pi^*$  orbital

Figure 1.14

FCH<sub>2</sub>OH as a model for 2-fluorooxacyclohexane in the qualitative PMO analysis.

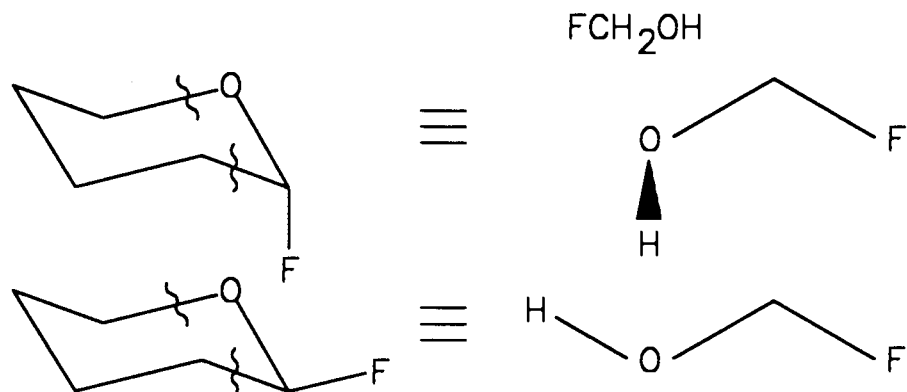
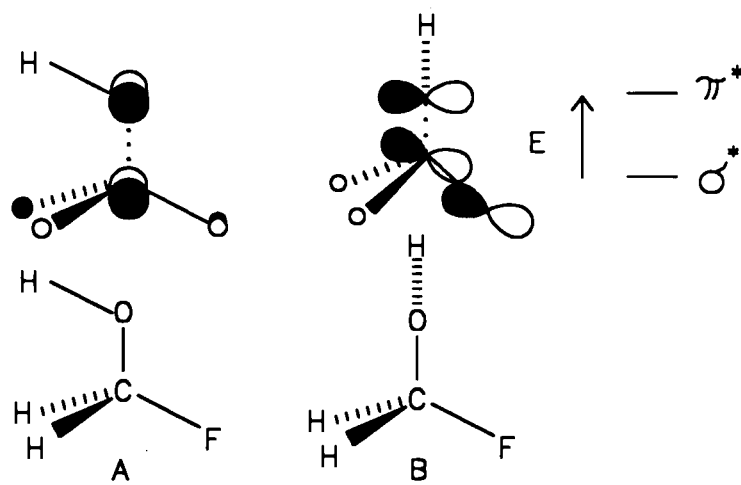


Figure 1.15

PMO analysis of the antiperiplanar and gauche conformations of FCH<sub>2</sub>OH.

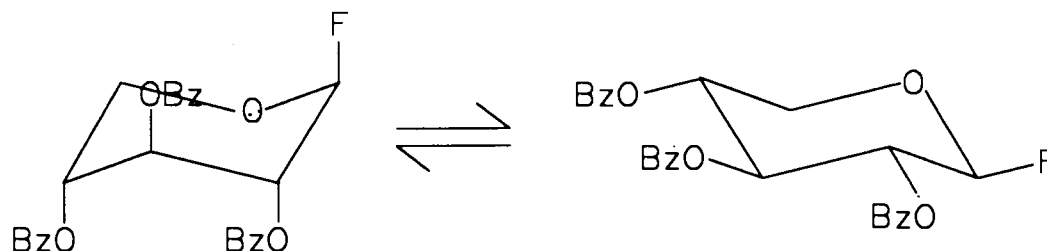


,78,84 there is greater stabilization in the  $n \rightarrow \sigma^*$  interaction than in the  $n \rightarrow \pi^*$  interaction. This analysis accounts for the

greater stability of the gauche conformations of FCH<sub>2</sub>OH molecules in comparison to the antiperiplanar conformations. Furthermore, this analysis can account for the dominance in solution (>90%) of the all axial conformer of tri-O-benzoyl-β-D-xylopyranosyl fluoride (Fig.1.16).<sup>85,86</sup>

Figure 1.16

Conformational equilibrium of Tri-O-benzoyl-β-D-xylopyranosyl fluoride.



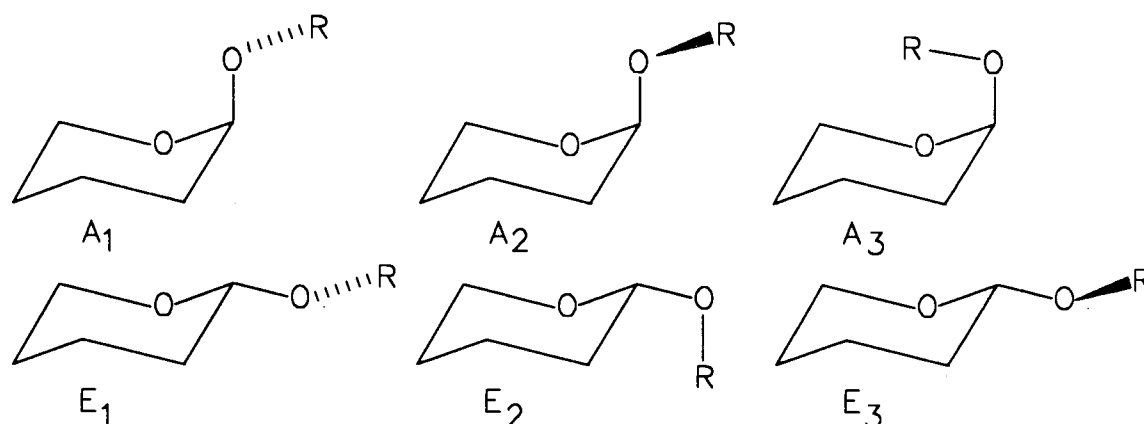
## 1.2 Exo-anomeric effect

While the conformations of XCH<sub>2</sub>YH molecules and the axial preference of electronegative substituents at the 2-position of oxacyclohexane are governed by the anomeric effect, in glycopyranosides, the preferred orientation of the 2-substituent groups are influenced by the exo-anomeric effect. This refers to the preference for the gauche conformation about the aglyconic carbon of glycopyranosides relative to the rest of the sugar ring.<sup>87</sup> Thus, in a 2-alkoxyoxacyclohexane, three staggered rotamers are possible for the axial and

equatorial conformations. These are referred to as A1-A3 and E1-E3, respectively (Fig.1.17). The gauche conformations

Figure 1.17

The three possible rotamers in the axial and equatorial conformations of 2-alkoxyoxacyclohexane.



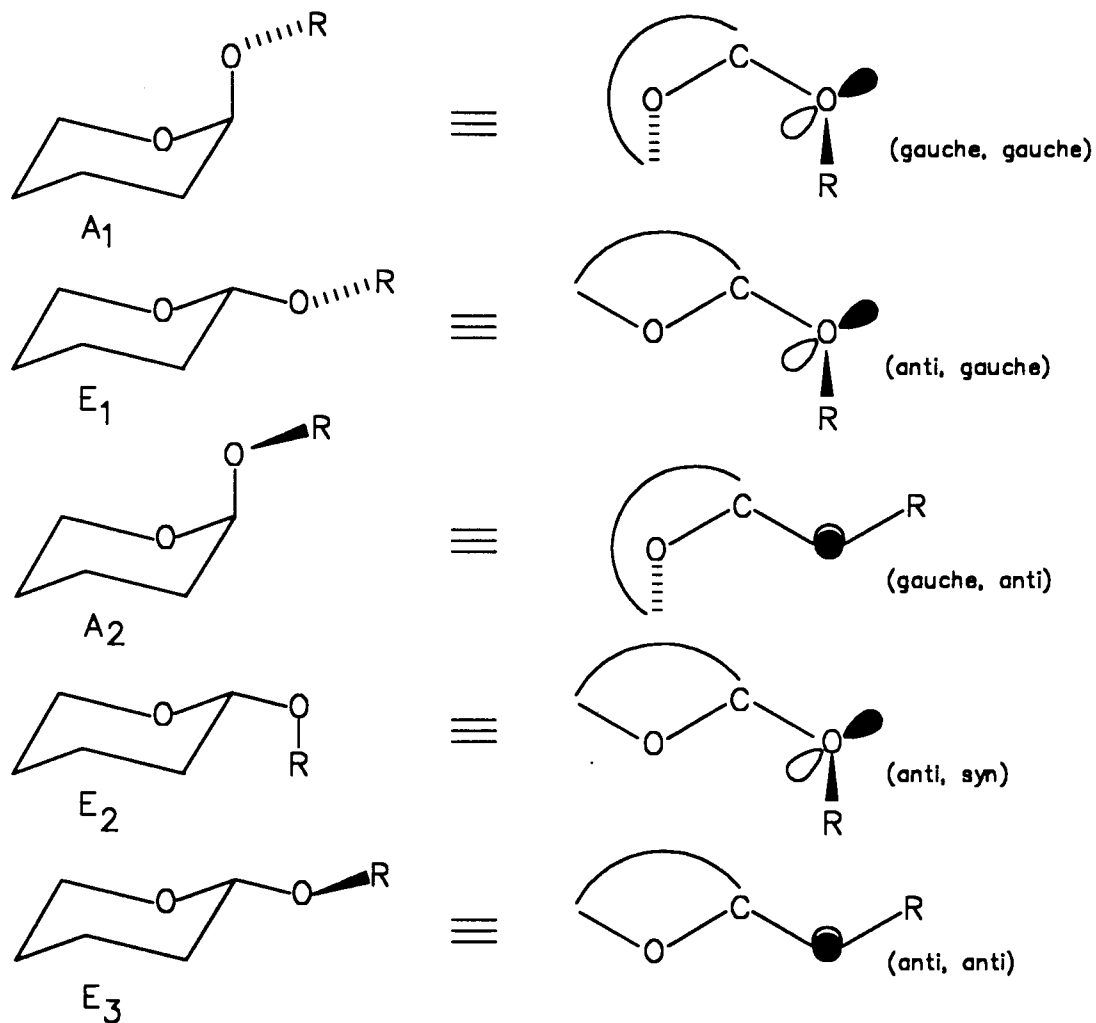
(A1,E1) were thought to be the only preferred conformations of the axial and equatorial alkyl glycosides<sup>88</sup> although Fuchs *et al.*<sup>89</sup> have recently shown, based on an examination of x-ray crystal structure data, that conformation E2 is also appreciably (25%) populated.

The origin of the exo-anomeric effect can be considered to be analogous to that of the anomeric effect in that conformations in which the  $\pi$ -type lone pair orbital on the glycosidic oxygen is in near antiperiplanar orientation to the  $\sigma^*$  antibonding orbital associated with the adjacent endocyclic

C-O bond, are stabilized through orbital interactions (Fig.1.18). This type of orbital interaction is "turned off"

Figure 1.18

The preferred conformers in the axial and equatorial alkyl glycosides.

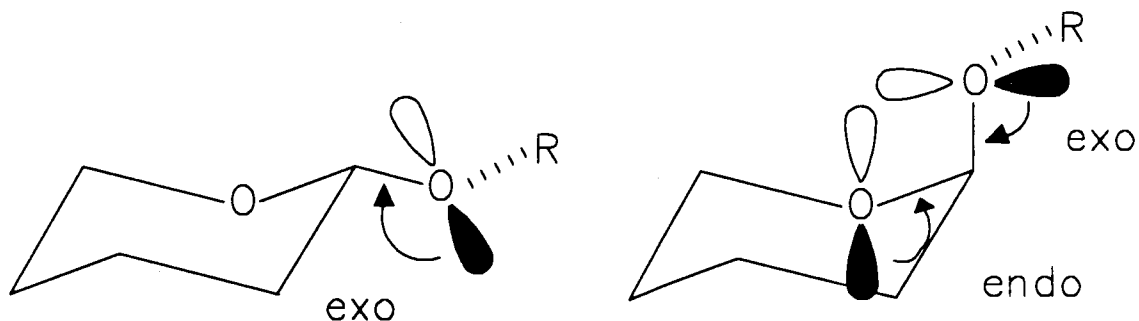


in rotamers A<sub>2</sub> and E<sub>3</sub>, and the rotamer A<sub>3</sub> is disfavoured energetically because of the steric repulsion of the OR group with the ring carbons and hydrogens. The exo-anomeric effect

is calculated to be stronger in the equatorial conformer (E1).<sup>89,90</sup> In this conformer (E1), the  $\pi$ -type lone pair on the ring oxygen is syn-clinal to the exocyclic C-O bond and therefore has minimal anomeric type interaction. The exo-anomeric effect thus has no competition with the charge transfer (back bonding) from the endocyclic oxygen orbitals<sup>88,91</sup> (the endo-anomeric effect). In the axial conformer (A1), which is stabilized by the endo-anomeric effect, the exo-anomeric effect is attenuated by the back bonding (Fig.1.19).

Figure 1.19

$\pi$ -Type lone pair donations in the exo- and endo-anomeric interactions.

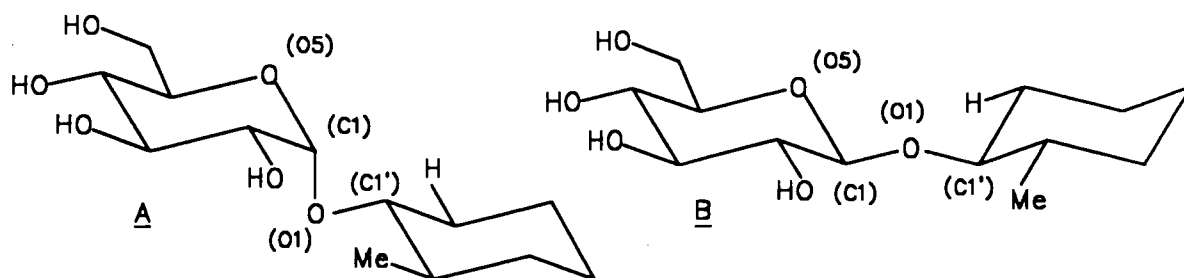


Evidence for the exo-anomeric effect has been obtained from the examination of the coupling constants between the  $^{13}\text{C}$ -labelled aglyconic carbons and the anomeric hydrogens in a number of  $\alpha$ - and  $\beta$ -D-glycopyranosides.<sup>88,92</sup> The results indicated a near constant ( $3.7 \pm 0.5$  Hz) value for the coupling of  $^{13}\text{C}$  atoms at the aglyconic carbon with the

anomeric hydrogen ( $^1J_{13C-H}$ ). It was concluded on the basis of an approximate Karplus relationship<sup>93,94</sup> that the torsion angle defined by the aglyconic carbon and the anomeric hydrogen was strongly maintained in the range  $|55| \pm 5^\circ$ . The X-ray crystallographic data for many carbohydrate structures showed that the orientations of the aglycon, are compatible with stabilization by way of an exo-anomeric effect.<sup>84,88,95</sup> For example, the bond lengths obtained in model glycosides such as A and B (Fig.1.20) were in accord with expectations, based on the PMO theory described previously.<sup>96</sup> The bond

Figure 1.20

Model  $\alpha$ -glycoside A and  $\beta$ -glycoside B.



angles obtained are also in support of the operation of the exo-anomeric effect. The valence bond angle C5-O5-C1, O5-C1-O1, and C1-O1-C1', in the  $\alpha$ -anomer were all substantially greater than the tetrahedral angle; however, in the  $\beta$ -anomer both C5-O5-C1 and O5-C1-O1 were close to the tetrahedral angle but C1-O1-C1' was much greater ( $115.1^\circ$ ) than  $109.5^\circ$ . Both effects are expected to render the atoms involved more

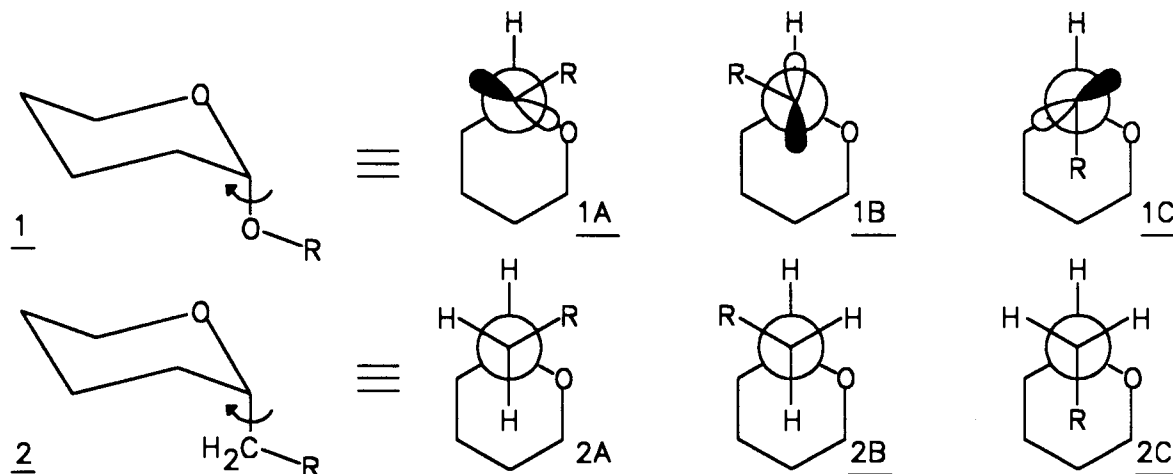
trigonal in character; however, in the latter case only the exo-anomeric effect is operative.

Furthermore, hard sphere calculations, containing the contribution of the exo-anomeric effect, on the human blood group B trisaccharide provided a structure that was comparable with that inferred from the  $^1\text{H}$  NMR data determined in aqueous solution.<sup>97</sup> In the conformational analysis of oligosaccharides, the inclusion of the exo-anomeric effect is thought to be crucial since it adds rigidity about the glycosidic bonds of the oligosaccharides.<sup>98</sup> The effect is of special importance in aqueous media and Lemieux has suggested that it may even be sufficient to overcome non-bonded interactions in some conformations. Although this interpretation agrees with the existence of the exo-anomeric effect, the conformational preference of  $\alpha$ - and  $\beta$ -C-glycosides (Fig.1.21) corresponds well to the one predicted solely on the basis of steric interactions.<sup>99</sup> Kishi et al.<sup>99</sup> define the exo-anomeric effect as the additional stabilization of  $\alpha$ - and  $\beta$ -glycosides over the corresponding C-glycosides in a given conformation due to the stereoelectronic effect. The  $^1\text{H}$  NMR spectra of a series of  $\alpha$ - and  $\beta$ -C-glycosides were used to determine the conformation around the C1-C1' bonds. The spin-spin coupling constants led to the conclusion that  $\alpha$ - and  $\beta$ -C-glycosides exist predominantly in the conformations 1A and 2A

respectively. The conformations 1C and 2C are destabilized over the other conformations owing to steric effects.

Figure 1.21

Conformational preferences of  $\alpha$ -glycosides and the corresponding C-glycosides.



However, 1B and 2B are sterically destabilized over 1A and 2A due to an additional gauche-butane type interaction.<sup>100</sup> The conformational preferences of C-glycosides are similar therefore to those of the corresponding O-glycosides and the authors suggest that the exo-anomeric effect is not one of the major factors determining the conformational preferences of glycosides.<sup>99</sup>

### 1.3 Reverse Anomeric Effect

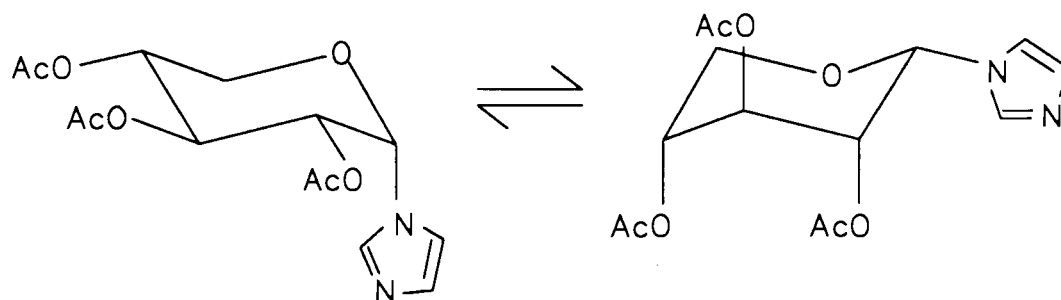
In its original formulation, the reverse anomeric effect was defined by Lemieux and Morgan<sup>101</sup> as the tendency of an



aglycon bearing a positive charge to adopt the equatorial orientation. For example, groups such as N-pyridinium show a stronger preference for the equatorial position than the usual steric preference found in the correspondingly substituted cyclohexanes. This is the reverse anomeric effect. The hypothesis was originally based on  $^1\text{H}$  NMR data which showed that  $\alpha$ -D-glycopyranosyl pyridinium salts exist in the  $^1\text{C}_4$  conformation. In the conformational investigation of N-imidazolidinium glycosides, the equilibrium mixture (Fig.1.22)

Figure 1.22

Conformational equilibrium of N-imidazolidinium glycoside.



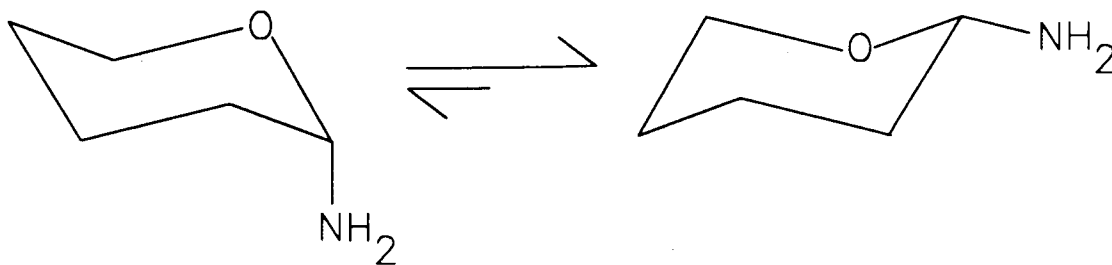
in  $\text{CCl}_4$  was found to contain 35% of the equatorial form.<sup>101</sup> The equatorial preference was greater in more polar solvents (65% in  $\text{CDCl}_3$ , 85% in acetone- $d_6$ ). When the imidazole group was completely protonated, only the equatorial conformer was present. The steric environment of the heterocyclic ring has not changed on going from the unprotonated to the protonated forms. The greater preference of the equatorial conformer

upon protonation of the imidazole group must therefore be due to an electronic effect.

Finch and Nagpurkar<sup>102</sup> have suggested a stereoelectronic interpretation of the reverse anomeric effect in compounds containing pyridinium or imidazolidinium as substituents. The stabilization of the equatorial orientation is attributed to the interaction between the p-type lone pair orbital of the ring oxygen and the  $e_{2u}\pi^*$  antibonding orbital of the aromatic system in this conformation, in which the aromatic ring and C<sub>1</sub>-O<sub>5</sub> bond are coplanar. However, this hypothesis still remains to be proven. When oxacyclohexane is substituted with neutral nitrogen substituents such as methylamino, the equatorial conformer is more stable than the axial one.<sup>103,104</sup>

Figure 1.23

Conformational equilibrium of 2-aminooxacyclohexane.



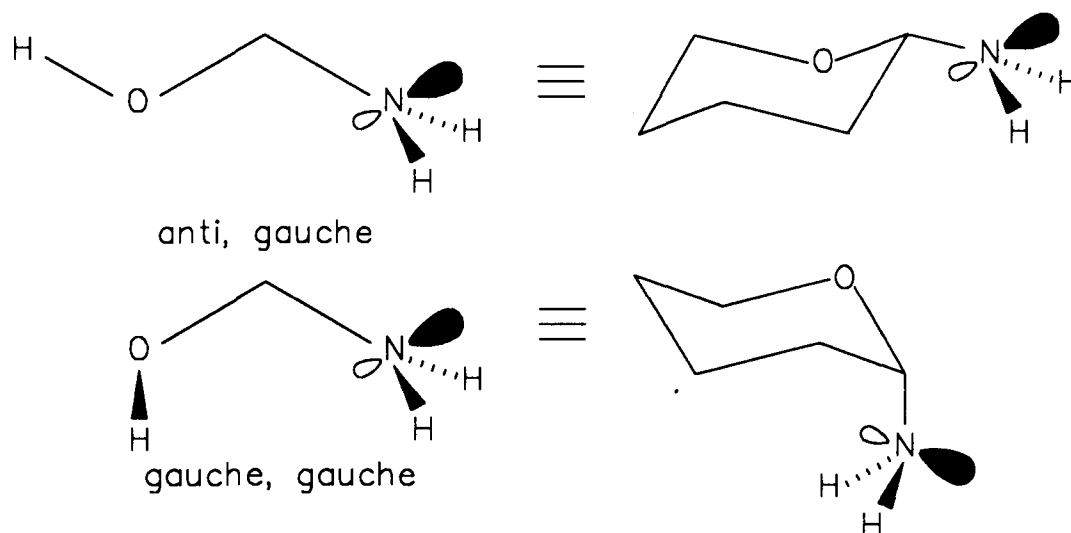
These observations were suggested to be the result of a reverse anomeric effect.<sup>104</sup> Glacet *et al.*<sup>104</sup> reported an equilibrium containing 85% cis- and 15% trans-isomers for 2-methylamino-4-methyloxacyclohexane. Furthermore, in a study

of the reactivities of 2-(1-aziridinyl)-oxacyclohexane, Glacet and coworkers<sup>105</sup> found that the reactivity of the aziridinyl derivative is weaker than for the corresponding 2-dialkylamino derivatives. This observation was rationalized in terms of the decrease in the positive "electromeric" effect of nitrogen. Booth et al.<sup>106</sup> also recently concluded that the methylamino group has a small reverse anomeric effect. This was based on the fact that 2-methylaminooxacyclohexane has a stronger preference than methylaminocyclohexane for the equatorial conformation. The *ab initio* MO calculation results obtained by Schafer et al.<sup>107</sup> and Pinto et al.<sup>26</sup> however, did not agree with the above conclusion. In their calculations of aminomethanol ( $\text{H}_2\text{NCH}_2\text{OH}$ ), the perpendicular conformation was found to be more stable than the antiperiplanar conformation by  $\approx 1 \text{ kcal mol}^{-1}$  (Fig.1.24). The former conformation corresponds to the axial orientation of the amino group in the oxacyclohexane ring and the latter to the equatorial orientation. Although the perpendicular conformer is calculated to be more stable than the antiperiplanar one, the energy difference is much smaller than in the 2-hydroxy analogs which have an energy difference of  $4.51 \text{ kcal mol}^{-1}$ .<sup>26</sup> In another explanation offered by Wolfe et al.,<sup>78</sup> the behaviour of the amino-substituted compounds is discussed in terms of orbital interactions, based on PMO calculations of  $\text{H}_2\text{NCH}_2\text{OH}$ . The important finding of this treatment is the fact

that in aminomethanol, the nitrogen lone pair is higher-lying in energy than the lone pair on oxygen and, therefore, makes the dominant contribution to the HOMO of the molecule. It was suggested that the stabilizing interaction between the nitrogen lone pair orbital and the  $\sigma^*_{C-O}$  orbital dictates the conformational behaviour of aminomethanol, and that this interaction was most favourable in the conformations in which the nitrogen lone pair orbital was antiperiplanar to the C-O bond. This requirement is fulfilled by two low energy conformations of aminomethanol (Fig.1.24). The authors

Figure 1.24

The relationship between the equatorial and axial conformations of 2-aminoxyclohexane and the anti, gauche and gauche, gauche conformations of aminomethanol.



concluded that the preference for the anti orientation is governed by orbital interactions which can be taken as the "origin" of the generalized reverse anomeric effect in systems of this type.\* However, the equatorial preference of amino-substituents in heterocyclic rings of this type may be accounted for simply in terms of endo- and exo-anomeric interactions.<sup>108</sup> The equatorial conformer is dominant in the equilibrium mixture of 2-methylaminoxacyclohexane;<sup>109</sup> this preference ( $\Delta A$ ) was interpreted as the difference between the sum of the endo- and exo-anomeric effects in the equatorial conformer ( $A_e$ ) and the sum ( $A_a$ ) of the same effects in the axial conformer.<sup>24,110</sup> The endo- $A_e$  contributions are considered to be negligible, as mentioned previously; therefore,  $A_e$  is assumed to be equal to exo- $A_e$ . The anomeric effect ( $\Delta A$ ) is defined as shown in the following expression:

$$\begin{aligned}\Delta A &= (\text{exo-}A_e + \text{endo-}A_e) - (\text{exo-}A_a + \text{endo-}A_a) \\ &= A_e - A_a\end{aligned}$$

Within this formulation, anomeric effects will have a wide range of values, including positive and negative values, depending on the relative magnitudes of the various exo- and endo-anomeric effects. According to the PMO analysis of aminomethanol,<sup>78</sup> the nitrogen lone pair is higher-lying in

---

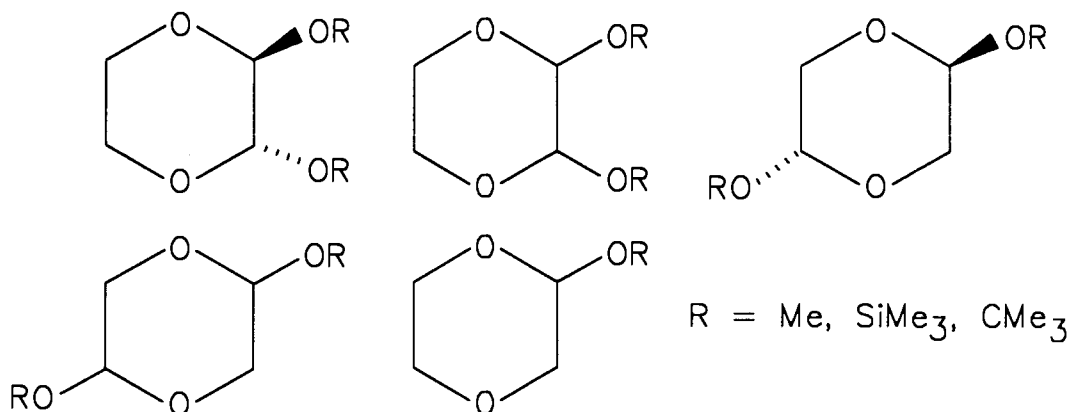
\*It should be noted, however, that these results were based on ab initio MO calculations,<sup>78</sup> at the STO-3G level, with partial geometry optimization; the calculations showed incorrectly that the most favourable conformation of  $\text{H}_2\text{NCH}_2\text{OH}$  corresponds to that conformation of 2-aminotetrahydropyran in which the amino group is equatorially oriented.

energy than the lone pair on oxygen, and the nitrogen is expected to possess strong exo-anomeric effects which may be even greater than the oxygen endo-anomeric effect.

Although this interpretation is satisfying, it is questionable whether one can account for the equatorial preference of substituents in the 2-position of heterocyclic rings solely in terms of the dominance of the exo-anomeric effect. With bulky substituents, in particular, one must make allowance for steric interactions. Other factors may also contribute to the overall equatorial predominance. For instance, the population of the equatorial form of a series<sup>111</sup> of trimethylsilyloxy- (TMSO) and tert-butoxy-(TBO) substituted 1,4-dioxacyclohexanes are lower than in the corresponding alkoxy derivatives<sup>112,113</sup> due to (1). the strong attractive nonbonded  $\text{OSi}\cdots\text{O}$  interaction which also reduces the O-C-O-Si dihedral angle; and (2). the inductive electron donating ability of the  $\text{SiMe}_3$  or  $\text{CMe}_3$  groups which lowers the effective electronegativity of the TMSO or TBO group (Fig.1.25).

Figure 1.25

Trimethylsilyloxy- (TMSO) and tert-butoxy- (TBO) substituted-1,4-dioxacyclohexanes.



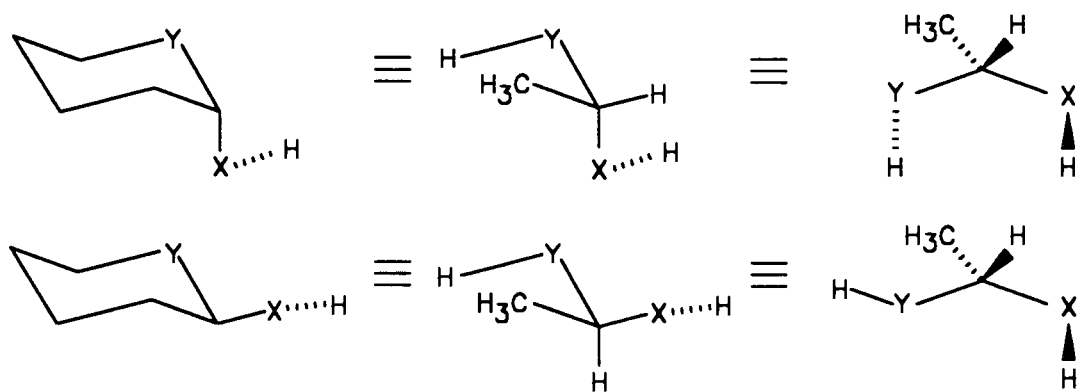
#### 1.4 Second and Lower Row Anomeric Effects

Studies of the anomeric effect focused initially on the conformational analysis of 2-substituted heterocyclohexanes containing first-row heteroatoms.<sup>13-25,106-121</sup> However, anomeric effects are also observed in heterocycles containing second-row elements.<sup>33,54,122-129</sup> The effect was found to be significant in 1,3-dithianes<sup>30,130</sup> and 1,3,5-trithianes.<sup>131</sup> The sulfur anomeric effect has even been implicated in the control of stereochemistry in the asymmetric synthesis of Erythromycin.<sup>132</sup> As with the 1,3-dioxacyclohexanes, the 1,3-dithiacyclohexane systems<sup>30,130-135</sup> have provided a very

convenient backbone for the study of the anomeric effect. The greater axial conformational preference of 2-alkoxythiacyclohexanes than the corresponding oxacyclohexanes indicates either that the anomeric effect is greater for sulfur,<sup>136-139</sup> or alternatively, that the steric effect is less in the sulfur system. In contrast, the anomeric effect in 2-alkylthiooxacyclohexanes was found to be stronger than that in the corresponding 2-alkylthiothiacyclohexanes.<sup>136</sup> It would appear that the magnitude of the anomeric effect cannot be predicted simply as a function of the ring heteroatom.<sup>21</sup> Fully optimized *ab initio* MO calculations at the 6-31G\* level on molecules of the type CH<sub>3</sub>CHXHYH (X, Y = O, S), have shown that the magnitude of the anomeric effect was similar for model systems containing endocyclic oxygen and exocyclic X at the anomeric centre (Fig 1.26).<sup>140</sup> On the other hand, there

Figure 1.26

The relationship between the axial and equatorial substituted oxacyclohexanes and CH<sub>3</sub>CH(XH)(YH).





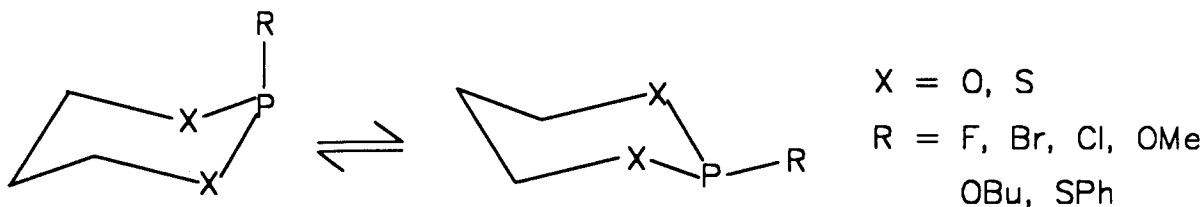
is an approximately 1 kcal mol<sup>-1</sup> energy difference for model systems containing a common X, with different endocyclic heteroatoms (Fig.1.26).

*Ab initio* MO calculations of a series of HY-CH<sub>2</sub>-X molecules indicated that the gauche conformation was energetically favoured relative to the anti conformation for X=Cl, F; Y=S, and that the gauche, gauche conformation was preferred relative to the gauche, anti conformation for X=OH, SH; Y=S.<sup>54-56</sup> These results are in accord with expectations based on the anomeric effect since the conformations are predicted to increase in energy in the sequence gauche, gauche < anti, gauche < anti, anti.<sup>26,85</sup> Furthermore, the bond angle and bond length variations as a function of torsion about the C-X and C-Y bonds<sup>26,39</sup> are also consistent with the interplay of hyperconjugative interactions associated with the endo and exo-anomeric effect.<sup>106</sup>

The transmission of anomeric interactions through second row atoms has also been documented. Thus, a preference for the gauche conformation was observed in cyclic esters of phosphorus and thiophosphorus acid (Fig.1.27).<sup>142</sup>

Figure 1.27

Conformational equilibria of cyclic esters of phosphorus and thiophosphorus acids.



In six membered cyclic phenyl phosphate esters in  $\text{CDCl}_3$ , the conformer in which the phenoxy (PhO) group is axial is preferred almost exclusively (>95%)<sup>143</sup>, a preference that is also manifested in the solid state (Fig.1.28).<sup>144</sup> While the oxygen atom of the thiacyclohexane sulphoxide only showed a small preference for the axial conformation,<sup>145</sup> there was a strong axial preference of the oxygen atom in the corresponding cyclic sulfites.<sup>146-149</sup> The axial preference of the S=O group in the t-butyl substituted cyclic sulfite (Fig.1.29) was estimated to be  $3.5 \text{ kcal mol}^{-1}$ .<sup>146</sup>

Figure 1.28

Conformational equilibrium of a cyclic phenyl phosphate ester.

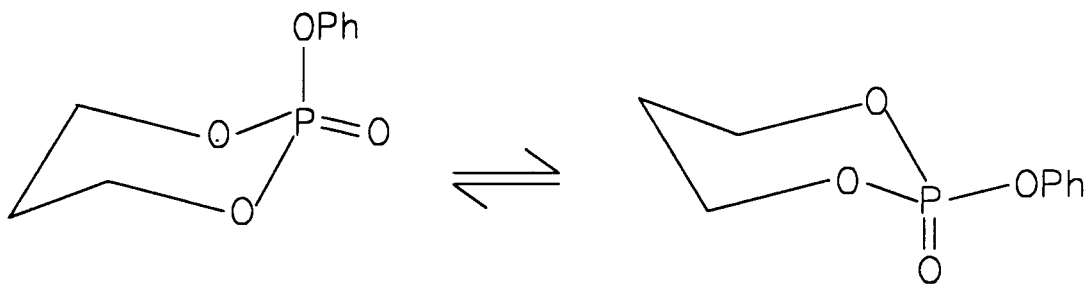
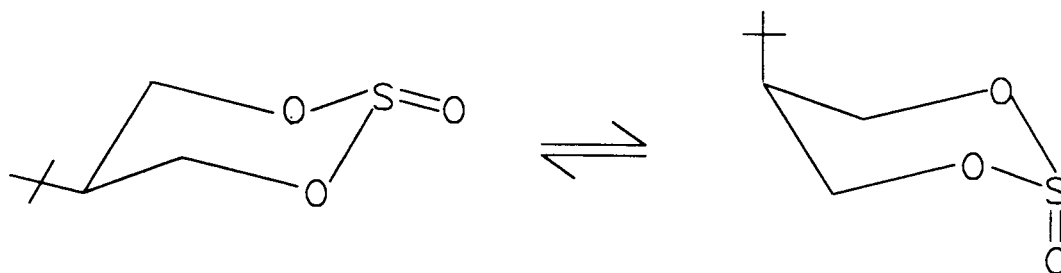


Figure 1.29

Conformational equilibrium of a 5-tert-butyl-cyclic sulfite.



The transmission of anomeric interactions through central atoms such as phosphorus and sulfur has also been substantiated recently by theoretical calculations on model systems.<sup>27,39,150-152</sup>

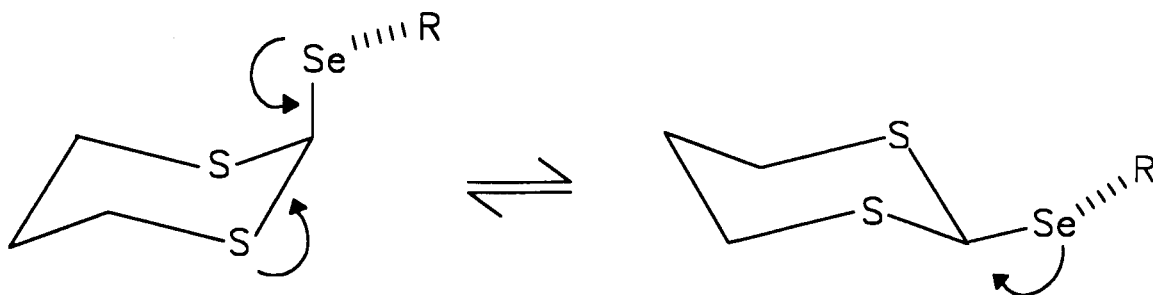
Other contributions to the study of the second-row anomeric effect include the study of S-C-P anomeric interactions in 2-diphenylphosphinoyl-1,3-dithiacyclohexanes by Juaristi *et al.*<sup>125,127,153,154</sup> and in 2-phosphoryl, 2-thiophosphoryl, and 2-selenophosphoryl-1,3-dithiacyclohexanes and 1,3,5-trithianes by Mikolajczyk *et al.*<sup>128,155</sup>

Recently, the study of the anomeric effect was extended to third-row heteroatoms by Pinto *et al.*<sup>28,29,38,156</sup> The conformational analysis of heterocyclic systems containing S-C-Se and Se-C-Se units were studied extensively. Conformational analysis of 2-(4-substituted-phenylseleno)-1,3-dithiacyclohexanes in solution by means of <sup>1</sup>H and <sup>77</sup>Se NMR spectroscopy<sup>157</sup> provided systematic evidence for the role of

stabilizing orbital interactions operating in S-C-Se fragments (Fig.1.30). The experimental data suggested the presence of a

Figure 1.30

Schematic representations of the stabilizing orbital interactions operating in the axial- and equatorial-2-(4-substituted-phenyl-seleno)-1,3-dithiacyclohexanes.



sulfur endo-anomeric effect and a selenium exo-anomeric effect. The postulate was reinforced by analysis of the data by means of a dual substituent parameter approach<sup>158,159</sup> which suggested that increased electron density was present on selenium in the axial conformers. This result is consistent with charge transfer interactions associated with the endo anomeric effect (Fig.1.31). The presence of increased negative charge on the Se atom in the axial conformer was substantiated by the trends in  $^{13}\text{C}$  and  $^{77}\text{Se}$  NMR data. The study was extended to the 1,3-diselenane analogues (Fig.1.32). The conformational behaviour of 5-methyl-2-phenylthio- and 2-phenylseleno-1,3-diselenane was studied by dynamic  $^{13}\text{C}$  and  $^{77}\text{Se}$  NMR spectroscopy. From the conformational free energies

Figure 1.31

Charge transfer in the axial-2-(4-substituted-phenylseleno)-1,3-dithiacyclohexane.

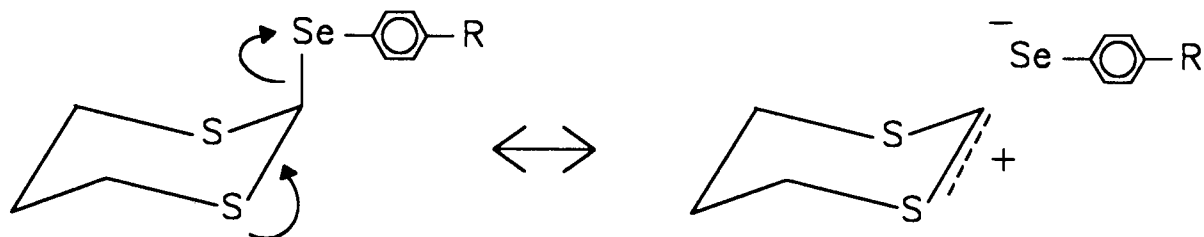
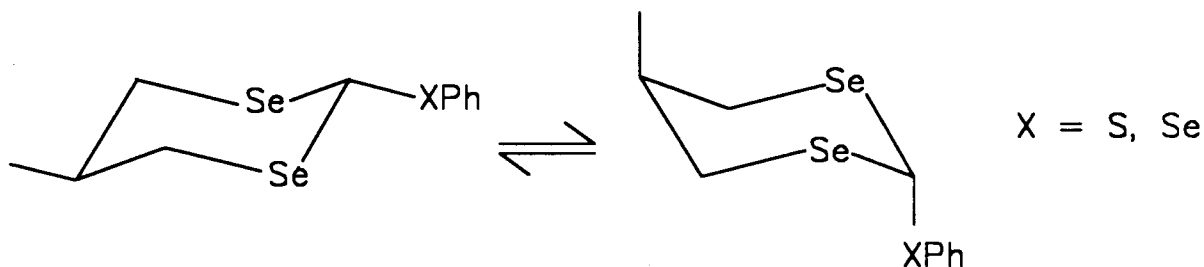


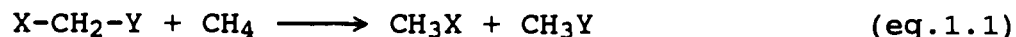
Figure 1.32

Conformational equilibria in 5-methyl-2-phenylthio- and 2-phenylseleno-1,3-diselenanes.



obtained ( $\Delta G^\circ_{147K} = -0.33 \text{ kcal mol}^{-1}$  (SPh),  $\Delta G^\circ_{147K} = -0.08 \text{ kcal mol}^{-1}$  (SePh)) and the conformational free energy of 5-methyl-1,3-diselenane ( $\Delta G^\circ_{147K} = 0.87 \text{ kcal/mol}$ ), Pinto et al.<sup>28</sup> argued that there exists a significant Se-C-S ( $\Delta G^\circ_{147K} = -1.20 \text{ kcal/mol}$ ) and Se-C-Se ( $\Delta G^\circ_{147K} = -0.96 \text{ kcal/mol}$ ) anomeric effect. The unusual solid-state conformational preference of a selenium coronand<sup>28</sup> provided additional evidence for a selenium anomeric effect.

In an earlier study of anomeric effects involving second-row substituents (Cl, SH and PH<sub>2</sub>), Schleyer and coworkers<sup>39</sup> found that anomeric effects were less significant when second row substituents were involved and proposed that anomeric effects would tend to vanish when elements of the lower rows in the periodic table were involved. They suggested that the stabilization energies obtained from the isodesmic equation (eq.1.1) were directly associated with the magnitude of the anomeric effect. They found that, whereas stabilization of



over 10 kcalmol<sup>-1</sup> were present for all combinations of the first-row elements, (X,Y = F, OH and NH<sub>2</sub>), all combinations of the second-row substituents, (X,Y = Cl, SH and PH<sub>2</sub>) did not show significant effects.

The significance and origin of second-row anomeric interactions has also been questioned by Anet and Kopelevich<sup>160</sup> on the basis of the absence of a conformational deuterium isotope effect in 2-deuterio-5,5-dimethyl-1,3-dithiacyclohexane. The absence of  $n_s \rightarrow \sigma^*_{C-H(D)}$  hyperconjugative interactions led these authors to propose that  $\pi$  donation by sulfur may not be responsible for the preferred axial orientation of electronegative substituents at C-2 of thianes and dithiacyclohexanes.

## 1.5 Solvent Effects

The conformational analysis of compounds that contain polar bonds and atoms with unshared pairs of electrons requires a consideration of solvent effects. One of the early explanations of the anomeric effect was based on the minimization of dipolar repulsion,<sup>13</sup> as illustrated previously in this section. Increasing the polarity of the solvent is predicted to minimize dipolar interactions and to maximize the proportion of the more polar conformer. Indeed, in the conformational study of 2-methoxytetrahydropyran, the solvent CD<sub>3</sub>CN was found to favour the more polar equatorial conformer to a greater extent than the nonpolar CCl<sub>4</sub>.<sup>87</sup> However, the weakly polar CDCl<sub>3</sub> was as effective as CD<sub>3</sub>CN in favouring the more polar equatorial conformer (mole fraction 0.29 (CDCl<sub>3</sub>) versus 0.32 (CD<sub>3</sub>CN)). However, solvent polarity may not be the only solvent effect in determining the magnitude of the anomeric effect. The conformational equilibrium for methyl 3-deoxy- $\beta$ -L-erythropentopyranoside was more sensitive to the chemical nature of the solvent than to its polarity.<sup>161</sup> The influence of solvent on the magnitude of the anomeric effect can be interpreted in terms of how the solvent affects the competition between the endo- and exo-anomeric effects.<sup>162</sup> The effects of solvent on the relative magnitude of the endo- and exo-anomeric effects may be considered to arise from the formation of specific complexes with the solvent, the exo-

anomeric effect being more strongly influenced. Solvents which can provide a proton to hydrogen bond to the ring heteroatom are particularly effective in strengthening the exo-anomeric effect. Other factors may also contribute, for example, in the conformational study of 2-carbomethoxy-1,3-dithiacyclohexane, Juaristi et al.<sup>154</sup> have observed an increase in the proportion of the less polar axial conformer with increasing solvent polarity at low temperature and have suggested an explanation based on a solvent compression effect<sup>163</sup> to explain this anomaly. An alternative explanation advanced by Fuchs et al.,<sup>164</sup> suggests that when the molecular dipoles of the axial and equatorial conformers are of similar magnitudes, the more polar double-bond no-bond structure<sup>45</sup> resulting from hyperconjugative interactions in the axial conformer, will be stabilized in the more polar solvent. In the systematic evaluation of the anomeric effect in 2-arylseleno-1,3-dithiacyclohexanes, Pinto et al.<sup>157</sup> found that an increase in the proportion of the less polar axial conformer was observed in the more polar solvent, acetone, relative to that in methylene chloride, although similar substituent effects were observed in non-polar and polar solvents. The results suggested that dipole/dipole interactions do not have a dominating influence and that other electronic factors were important in these systems.



## 1.6 Enthalpic anomeric effect

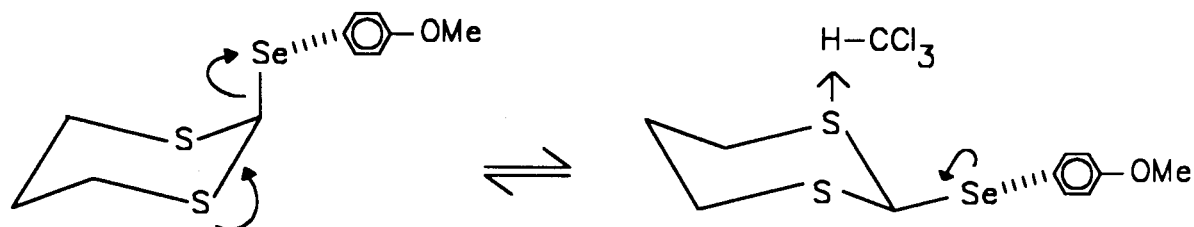
The magnitude of anomeric effect is defined<sup>165,166</sup> as the difference between the conformational free energy  $(\Delta G^\circ_X)_{A-E}$  for the equilibrium under consideration and the conformational free energy  $(\Delta G^\circ_X)_{A-E}$  for the corresponding equilibrium in the substituted cyclohexane. The equilibria in cyclohexane systems are determined largely by steric effects, especially in non polar solvents. However, the position of the equilibrium in heterocyclic systems involves steric, polar and electronic effects, and solvent effects play an important role as well (see previous discussion). In a conformational study of substituted oxacyclohexanes, Booth et al.,<sup>106</sup> have stressed that in studies of the anomeric effect, it is the  $\Delta H^\circ$  values that correlate with the various "effects" of interest. The conformational free energy obtained in an equilibrium is a compromise between the enthalpy and entropy terms ( $\Delta G^\circ = \Delta H^\circ - T\Delta S^\circ$ ).

In a series of 2-substituted-oxacyclohexanes,<sup>106</sup> the anomeric effect was found to be dominated by the  $\Delta H^\circ$  term with little influence from the variation in the  $\Delta S^\circ$  term. Although steric repulsion also plays a role in controlling the axial/equatorial equilibrium, the trend in the  $\Delta H_{a \rightarrow e}$  values supports the orbital interaction model.<sup>106</sup> The competition between the endo and exo anomeric effects is a function of the

donor power of the heteroatom and the acceptor power of the C-heteroatom bond. For instance, the change from 2-chlorooxacyclohexane to 2-methoxyoxacyclohexane causes a weakening of the endo-anomeric effect and a strengthening of the exo-anomeric effect. Thus, an increase in the proportion of the equatorial conformer and a decrease in the  $\Delta H^\circ$  term is observed ( $\Delta H^\circ \approx 0$ ). The same argument can be applied to rationalize the dominance of the equatorial conformer of 2-methylaminooxacyclohexane in which the exo-anomeric effect is stronger than the endo-anomeric effect.<sup>106</sup> On the other hand, Lemieux *et al.*,<sup>161</sup> have suggested that the near temperature independence of the change in  $\Delta G^\circ$  of 2-methoxyoxacyclohexane is due to a stronger H-bonding of the solvent used (CFCl<sub>3</sub>/CDCl<sub>3</sub>) with the equatorial conformer to form solvated species of nearly equal enthalpy contents. A similar rationale accounts for the results obtained in the equilibrium of 2-(4-methoxyphenyl)seleno-1,3-dithiacyclohexane.<sup>157</sup> In the latter case, the preferential hydrogen-bonding between the solvent, chloroform and the ring sulfur atom in the equatorial isomer, owing to greater  $n_{se} \rightarrow \sigma^*_{C-S}$  exo-anomeric interactions, would favour this isomer enthalpically and would offset the stabilization due to the  $n_S \rightarrow \sigma^*_{C-Se}$  endo-anomeric effect in the axial isomer. Conversely, the axial isomer would be favoured entropically (Fig.1.33).

Figure 1.33

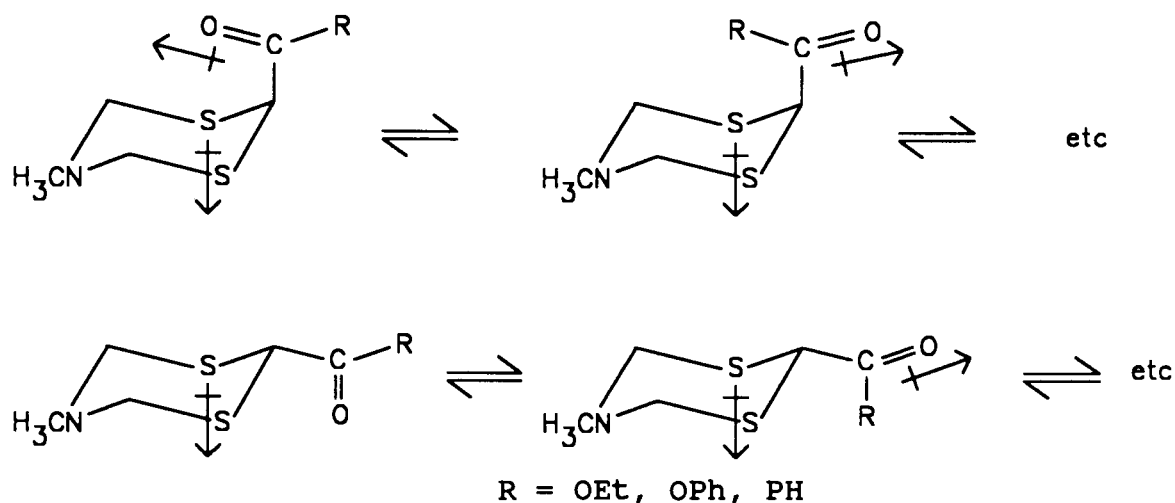
Conformational equilibrium of 2-(4-methoxyphenyl)seleno-1,3-dithiacyclohexane in  $\text{CFCl}_3/\text{CDCl}_3$ .



Juaristi et al.,<sup>30</sup> in the study of 2-substituted-5-methyl-5-aza-1,3-dithiacyclohexanes, have evaluated the S-C-Y anomeric effect in terms of the enthalpic and entropic contributions. For the S-C-S anomeric effect, the thermodynamic data obtained showed that the axial preference of the thiophenyl group was of enthalpic origin. The entropic term which favours the equatorial conformer is overcome by the enthalpic term. In contrast to the S-C-S segment, the thermodynamic data for the S-C-C(O)R groups showed that the  $\Delta H^\circ$  term in most solvents was close to zero. The axial preference of these derivatives is controlled by the entropic term which was attributed to the local dipole-dipole interactions present in the axial and equatorial conformers.<sup>30</sup>

Figure 1.34

Dipole-dipole interactions present in the axial and equatorial conformers of 2-C(O)R-5-methyl-5-aza-1,3-dithiacyclohexane.



### 1.7 Attractive and Repulsive Gauche Effects

The gauche effect was originally defined by Wolfe<sup>19</sup> as the tendency for a molecule to adopt that structure which has the maximum number of gauche-interactions between adjacent electron pairs and/or polar bonds. It has been suggested that the anomeric effect in its generalized form causes a preference for the gauche over the anti arrangement in compounds of the type C-X-C-Y.<sup>167,168</sup> As the concepts of conformational analysis have developed over the years, however, this definition has been extended<sup>169</sup> in that the gauche effect is not understood only as the predominance of the gauche over the anti form in a 1,2-disubstituted framework

but rather as the preference for the gauche form in excess of that predicted on the basis of steric and polar factors. The gauche effect in its original form is associated, therefore, with additional gauche attraction and is now termed the attractive gauche effect. The greater preference for the anti form than predicted on the basis of steric and polar interactions can be attributed then to additional gauche repulsion.

The minimum energy conformation of a molecule is one that minimizes its repulsive interactions and maximizes its attractive interactions. In an ethane molecule, the staggered conformations are favoured over the eclipsed conformations (Fig.1.35) by  $\approx 3 \text{ kcalmol}^{-1}$ .<sup>170</sup> This energy difference is commonly known as the ethane barrier and may be taken as the standard rotational barrier for an acyclic hydrocarbon when analyzing the contribution of torsional strain to the total energy strain.

However, in n-butane, the potential energy diagram is more complicated with 3 energy minima and 3 energy maxima (Fig.1.36). The minima correspond to the staggered conformations of which the energy of the anti conformation is lower than the gauche conformations by  $0.8 \text{ kcalmol}^{-1}$ .<sup>171,172</sup> This methyl-methyl gauche repulsion ( $0.8 \text{ kcalmol}^{-1}$ ) is known as the n-butane gauche interaction.

Figure 1.35

Potential energy diagram for rotation of the C-C bond of ethane.

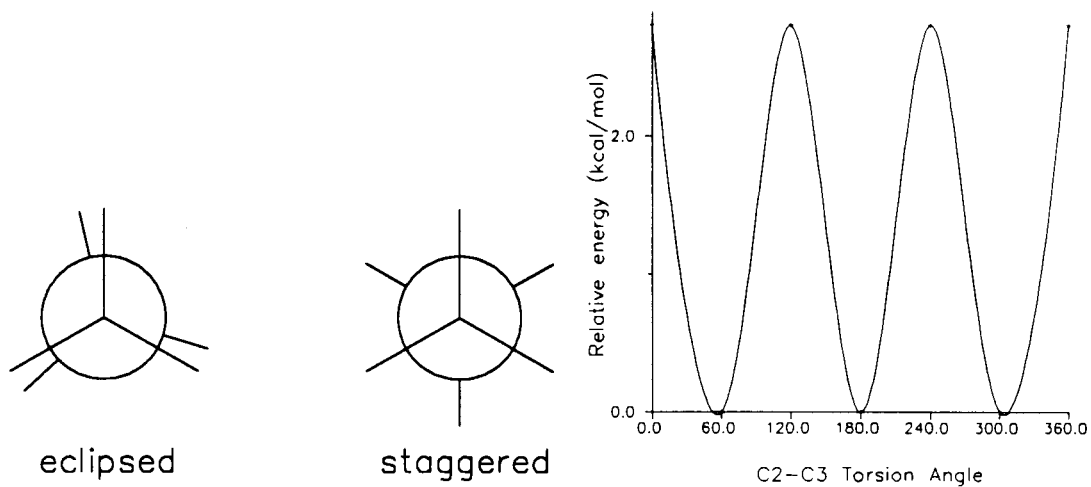
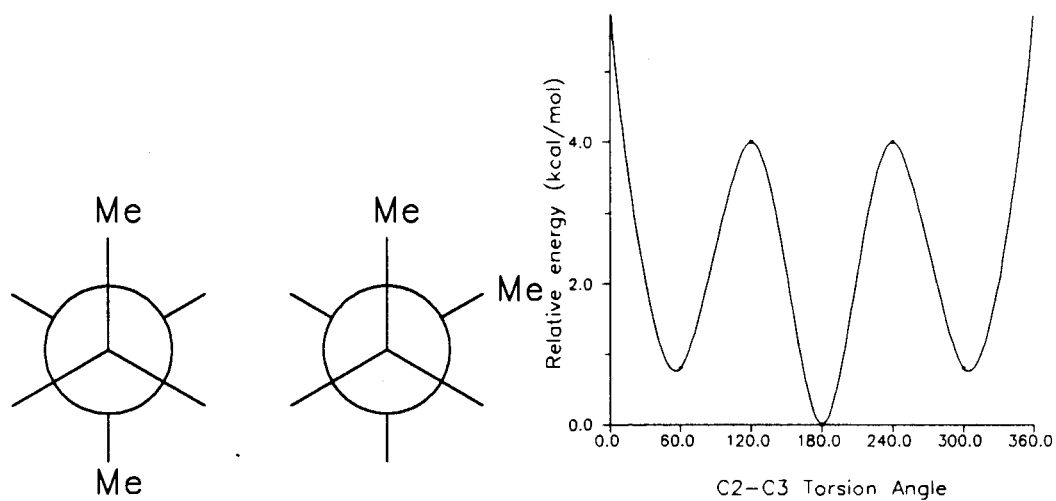


Figure 1.36

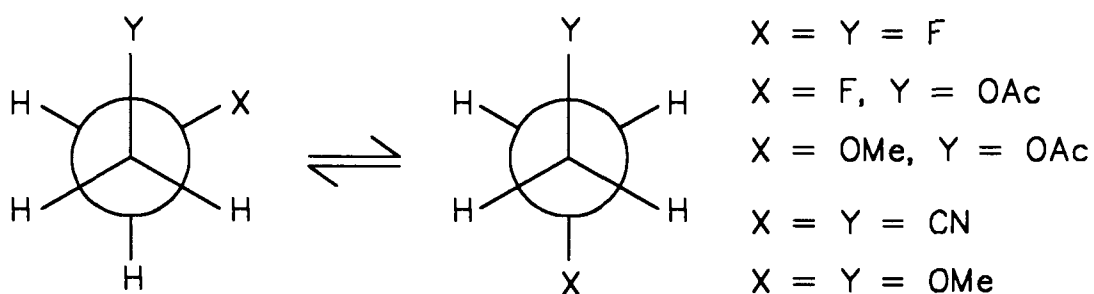
Potential energy diagram for rotation about the C2-C3 bond of n-butane.



In some 1,2-diheterosubstituted ethanes with electronegative elements,<sup>178-184</sup> in spite of the non-bonded repulsion and dipolar repulsion between the substituents in the gauche arrangement, the gauche conformations are favoured over the anti conformations (Fig.1.37).

Figure 1.37

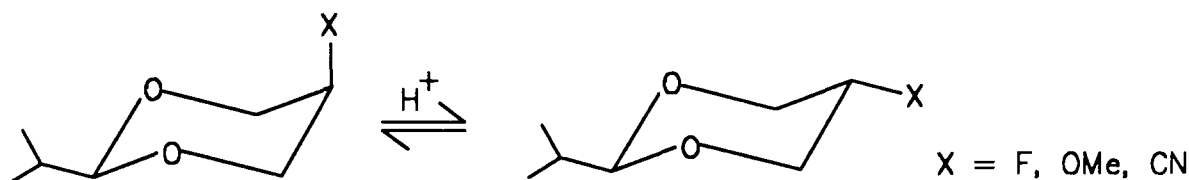
Some examples of 1,2-disubstituted ethanes with a more favoured gauche conformation.



The same butane type gauche attraction is also observed in 2-isopropyl-5-fluoro-, 5-methoxy-, and 5-cyano-1,3-dioxacyclohexanes (Fig.1.38).<sup>185</sup> The diastereomers in which

Figure 1.38

Configurational equilibria of 2-isopropyl-5-fluoro-, 5-methoxy-, and 5-cyano-1,3-dioxacyclohexanes.



the substituents are axially oriented are found to be more stable in contrast to the results with the analogously substituted cyclohexanes.

In some trans-1,2-disubstituted cyclohexanes,<sup>186-187</sup> the experimentally determined equilibria were compared with those calculated on the basis of known conformational energies ( $\Delta G^\circ_X$ ,  $\Delta G^\circ_Y$ ) of the monosubstituted cyclohexanes and the repulsive interaction ( $\Delta G^\circ_{X/Y}$ ) between substituents X and Y in the gauche conformation, according to the equation:

$$\Delta G^\circ_{\text{exp}} = \Delta G^\circ_{X/Y} + \Delta G^\circ_X + \Delta G^\circ_Y \quad (\text{eq.1.2})$$

In principle, if there are no additional conformational effects, the value of  $\Delta G^\circ_{X/Y}$  should be approximated by the sum of the steric ( $E_V$ ) and polar ( $\Delta E_D$ ) interactions of X and Y.

$$\Delta G^\circ_{X/Y} = E_V + \Delta E_D \quad (\text{eq.1.3})$$

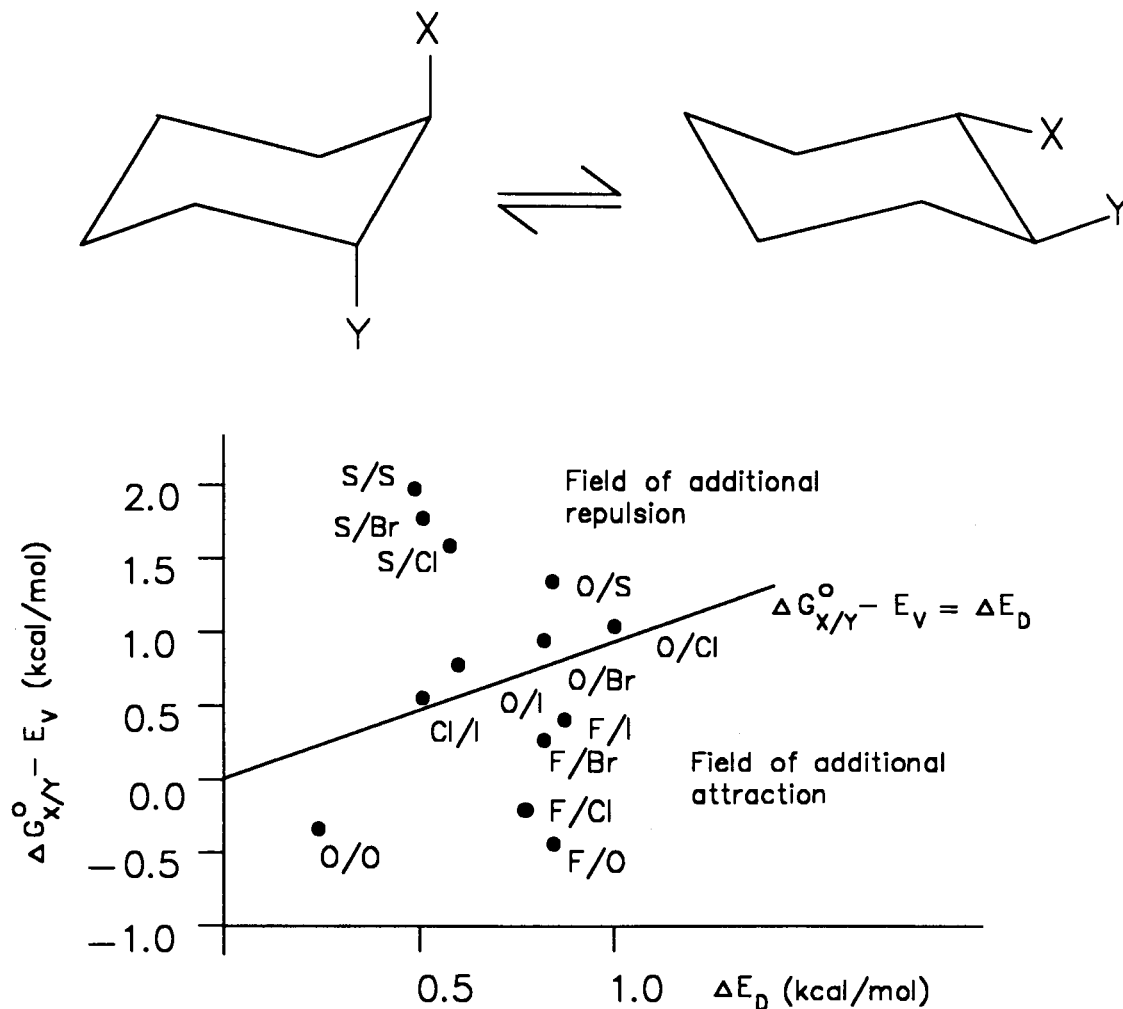
$$\text{or } \Delta G^\circ_{X/Y} - E_V = \Delta E_D \quad (\text{eq.1.4})$$

A coordinate diagram of  $\Delta G^\circ_{X/Y} - E_V$  versus  $\Delta E_D$  was constructed (Fig.1.39). The field above the straight line of unit slope indicated additional gauche repulsion and the field below indicated additional gauche attraction. The ordinate distance from the experimental point to the line of unit slope corresponded to the energy of additional gauche attraction or repulsion.



Figure 1.39

Coordinate diagram of  $\Delta G^\circ_{X/Y} - E_V$  versus  $\Delta E_D$  for 1,2-disubstituted cyclohexanes.



Using this approach, Zefirov et al.<sup>186,187</sup> have found that the O/Cl, O/Br, O/I, and Cl/I interactions could be interpreted adequately in terms of steric and polar interactions whereas the O/O, F/I, F/Br, F/Cl and F/O systems exhibited additional gauche attraction, and the S/S, S/Cl,

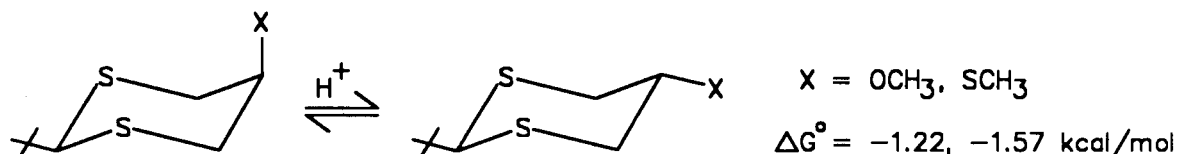
S/Br and S/O systems exhibited additional gauche repulsion (Fig.1.39). The same approach has been used by Eliel and Juaristi<sup>188</sup> to obtain evidence for additional gauche repulsion in 5-methoxy- and 5-methylthio-1,3-dithiacyclohexanes (Fig.1.40). The experimental  $\Delta G^\circ$  values were compared with those obtained by the calculation of steric ( $E_v$ ) and polar interactions ( $\Delta E_D$ ).

$$\Delta G_{\text{diff}} = \Delta G^\circ - E_v - \Delta E_D \quad (\text{eq.1.5})$$

The magnitude of the additional gauche interactions between S/S and S/O were reflected by  $\Delta G_{\text{diff}}$ . Results of these studies showed that additional repulsion was present in both systems and that the magnitude of the repulsive gauche effect was greater for the S/S than for the S/O interaction.

Figure 1.40

Configurational equilibria of 5-methoxy- and 5-methylthio-1,3-dithiacyclohexanes.



The additional attractive and repulsive gauche interactions can be rationalized in terms of Allen's dissection of the total energy of a system into attractive and repulsive components.<sup>19,189</sup> The stability of a system depends

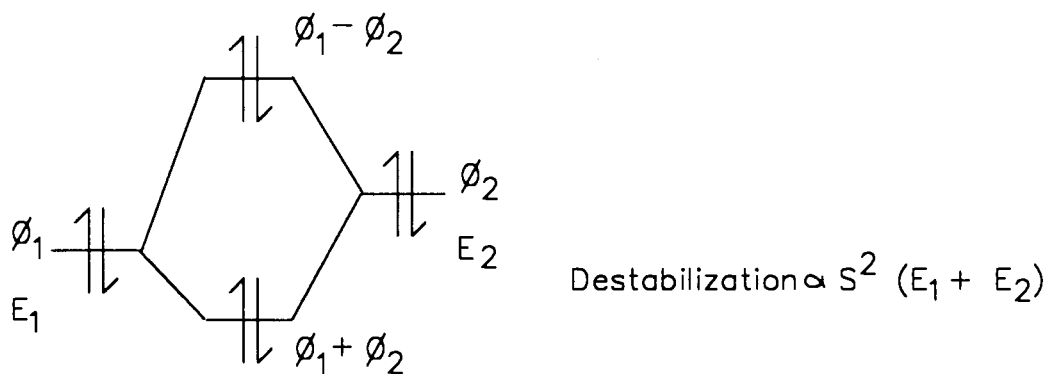
on the nuclear-electron attraction ( $V_{ne}$ ) between groups or atoms relative to the nuclear-nuclear repulsion ( $V_{nn}$ ), electron-electron repulsion ( $V_{ee}$ ) and the kinetic energy ( $T$ ).

$$E = V_{ne} + (V_{nn} + V_{ee} + T) \quad (\text{eq.1.6})$$

A different explanation has been offered in terms of "through-space" and "through-bond" orbital interactions.<sup>68</sup> The "through-space" orbital interaction resulting from overlap of lone pair orbitals on the heteroatoms, X and Y in the X-C-C-Y fragments, leads to the formation of bonding,  $\phi_1 + \phi_2$ , and antibonding,  $\phi_1 - \phi_2$ , combinations. Since the antibonding combination orbital (Fig.1.41) is destabilized more than the

Figure 1.41

Energy level diagram of two orbital-four electron destabilizing orbital interaction.

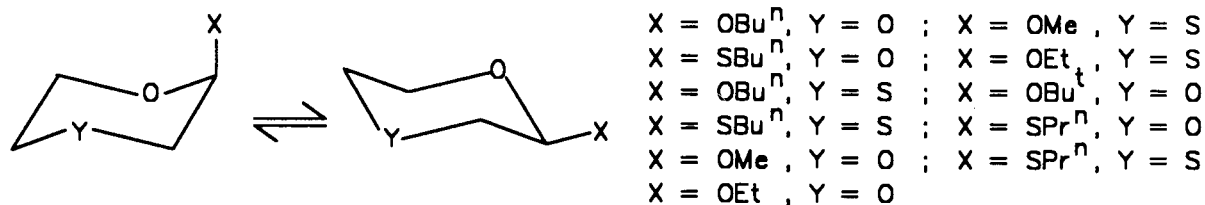


bonding combination orbital is stabilized,<sup>67,68,190</sup> and the orbitals are occupied by four electrons, the overall interaction is destabilizing. This type of lone pair orbital

overlap was recognized as being a manifestation of gauche repulsion, and was described by Zefirov and coworkers<sup>191</sup> as the "hockey stick effect". Evidence for the "hockey stick effect" was provided by the conformational behaviour of 2-substituted-1,4-oxathiacyclohexanes and 1,4-dioxacyclohexanes (Fig.1.42). For 2-alkoxy- or 2-alkylthio-substituted

Figure 1.42

Conformational equilibria of 2-X-substituted-1,4-dioxacyclohexanes and 2-X-substituted-1,4-oxathiacyclohexanes.

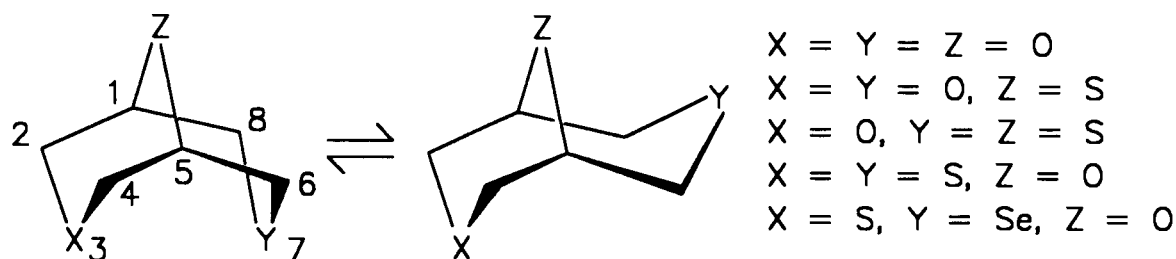


compounds, the proportion of the axial conformer decreased significantly in the 1,4-oxathiacyclohexanes relative to that in the 1,4-dioxacyclohexanes. This result was taken as evidence for stronger repulsive S/S interactions than O/S interactions, which were, in turn, stronger than O/O interactions. The greater diffuseness of the 3p and 3s orbitals of the second row heteroatoms was in agreement with greater electron-electron repulsion. However, Zefirov and coworkers<sup>192</sup> have shown by means of photoelectron spectroscopy that the interaction between the electron pairs of the heteroatoms in the 3,7,9-trihetero derivatives of

bicyclo[3.3.1]nonane (Fig.1.43) is governed mainly by "through-bond" interactions, as in the case of the monocyclic compounds 1,4-dioxacyclohexane, 1,4-oxathiacyclohexane, and 1,4-dithiacyclohexane.<sup>65,193</sup>

Figure 1.43

Conformational equilibria of 3,7,9-trihetero derivatives of bicyclo [3.3.1]nonanes.

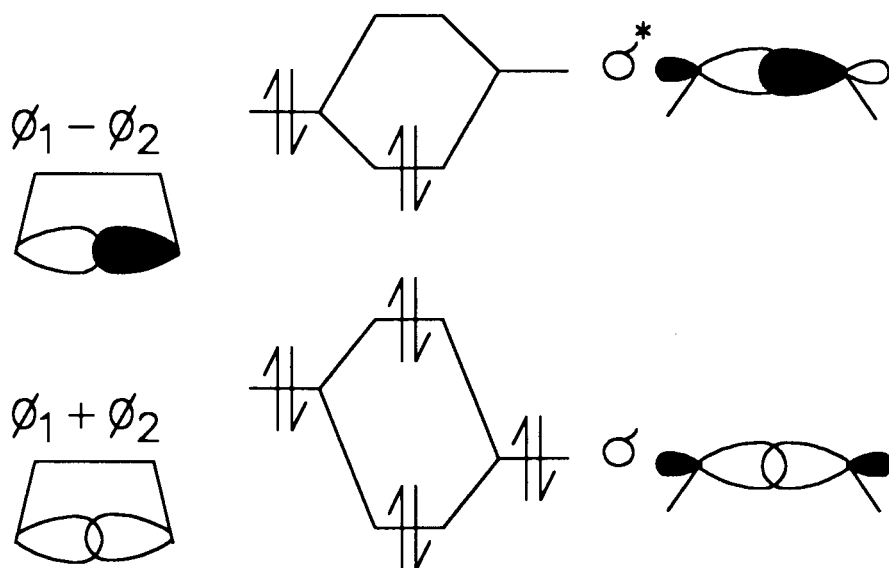


The concept of "through-bond" interaction was developed by Hoffmann.<sup>68</sup> According to this theory, the four electron "through-space" interaction results in destabilization as described above. However, now the resulting bonding and antibonding combinations interact with the  $\sigma$  and  $\sigma^*$  orbitals of the  $\sigma$ -bond, to give appropriate in-phase and out-of-phase combinations (Fig.1.44). One of these "through-bond" interactions is a two-electron, two-orbital interaction and is, therefore, stabilizing while the other is a four-electron, two-orbital net destabilizing interaction. Since the two interactions oppose one another, the relative contribution of each interaction can result in a lone pair interaction that is

net attractive or net repulsive. "Through-bond" and "through-space" interactions have been suggested as the origin of additional gauche attraction.<sup>194</sup>

Figure 1.44

The combination of through space orbital interactions ( $\phi_1 + \phi_2$ ,  $\phi_1 - \phi_2$ ) with  $\sigma$  and  $\sigma^*$  through bond orbital interactions.



Although these proposals can be used to explain the experimental observations, the possible influence and significance of dipolar and/or non-bonded repulsions were not included in the discussion. A theoretical approach was therefore used to analyze the additional gauche interactions especially in 1,2-disubstituted ethanes.<sup>195</sup> In this treatment, the potential function,  $V(\phi)$ , describing internal rotation about the carbon-carbon bond, is resolved into its

Fourier components by means of the truncated Fourier expansion:

$$V(\phi) = 1/2V_1(1 - \cos\phi) + 1/2V_2(1 - \cos 2\phi) + 1/2V_3(1 - \cos 3\phi) \quad (\text{eq.1.7})$$

where  $\phi$  is the XCCY dihedral angle of the X,Y-disubstituted fragment.<sup>195</sup> Each of the Fourier components is then given some physical meaning in terms of various conformational interactions. The one-fold potential,  $V_1$ , is related to through-space interactions and is usually taken as an indication of steric and dipolar interactions. The three-fold potential,  $V_3$ , is associated with the intrinsic preference for staggered as opposed to eclipsed conformations. The two-fold potential,  $V_2$ , is overlap dependent and is associated with conjugative and hyperconjugative interactions and is related to the orbital interaction component. Using this approach, the conformational behaviour of the  $\text{XCH}_2\text{CH}_2\text{Y}$  molecule can be analyzed in terms of the relative importance of stabilizing and destabilizing orbital interactions, electrostatic interactions, and intrinsic, "ethane-type" interactions. However, it is known from experience that estimation of the contributions of the one-fold and two-fold potential to the total potential function is dependent on the choice of the basis set employed in the calculation. This type of calculation has been widely adopted in the field of conformational analysis especially in molecular mechanics

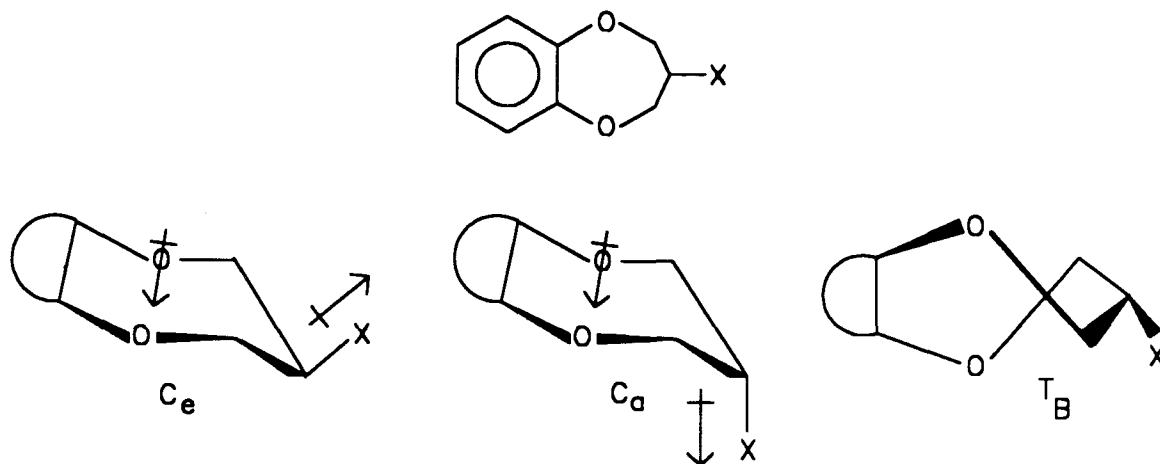
calculations, although its success depends on the appropriate choice of the one-fold, two-fold and three-fold potential terms. In this connection, molecular mechanics calculations were recently applied<sup>111</sup> to a series of cis- and trans-2,3-di(R)oxy-1,4-dioxacyclohexanes (R=Me, Ph, Ac). These empirical calculations using Allinger's MM2 program<sup>197</sup>, modified for oxygen containing compounds<sup>198</sup>, confirmed the experimental findings that the equilibrium in these compounds could be interpreted in terms of combined anomeric and gauche effects. However, the experimental observations in a series of glycol ethers such as 1,2-dimethoxyethane and 1,2-dimethoxypropane could not be reproduced by MM2 calculations.<sup>199</sup> The difference was suggested to arise mostly from the through-bond interaction which was not accounted for in the MM2 force field.

In an investigation of the main contributing factors to the gauche effect, St.-Jacques et al.<sup>200</sup> have concluded that intramolecular orbital interactions between vicinal polar bonds were the most important factors amongst an array of prominent factors such as electrostatic, solvation and steric interactions. Thus, in the conformational studies of a series of 3-X-substituted-1,5-benzodioxepins (X=I, Br, Cl, F and OMe), the results showed that the number of conformations varied from one to three ( $C_e$ ,  $C_a$  and TB), depending on the substituent electronegativity and solvent polarity (Fig.1.45).



Figure 1.45

The three possible conformations ( $C_e$ ,  $C_a$  and  $T_B$ ) of 3-X-substituted -1,5-benzodioxepins where X=I, Br, Cl, F and OMe.



The greater flexibility of the 7-membered ring provided a convenient probe for the investigation of the stereoelectronic effect. Intramolecular orbital interactions of the  $\sigma \rightarrow \sigma^*$  type were assumed to be more important for the heavier halogens (I, Br and Cl). The increase in the  $T_B$  form from I to Cl was attributed to an increase in the  $\sigma_{C-H} \rightarrow \sigma^*_{C-X}$  interaction, and the decrease in the  $C_e$  form to an increase in the  $\sigma_{C-X} \rightarrow \sigma^*_{C-O}$  interaction. From MO theory, the interactions of two orbitals with two electrons are stabilizing.<sup>21,201</sup> In a fragment such as X-C-C-Y, the orbital interactions between C-X and C-Y bonds are at a maximum when X and Y are antiperiplanar. For a  $\sigma^*_{C-X}$  orbital, an increase in the electronegativity of X leads to an increase in the charge transfer towards the carbon atom; as a consequence, there is better overlap in a  $\sigma_{C-Y} \rightarrow \sigma^*_{C-X}$

interaction as the electronegativity of X increases, for a given Y.<sup>202</sup> This prediction is valid for a series of X in the same row of the periodic table<sup>201</sup> and for the series of halides.<sup>203-205</sup> The relative energy levels of the  $\sigma^*_{C-X}$  orbitals given by CNDO/2 calculations<sup>47</sup> follow the order  $\sigma^*_{C-H} > \sigma^*_{C-O} > \sigma^*_{C-F} > \sigma^*_{C-Cl} > \sigma^*_{C-Br} > \sigma^*_{C-I}$ , while the order of the  $\sigma$  orbitals is  $\sigma_{C-I} > \sigma_{C-Br} > \sigma_{C-Cl} > \sigma_{C-H} > \sigma_{C-O} > \sigma_{C-F}$ , as revealed by CNDO/2 and *ab initio* calculations<sup>206</sup>, and an analysis of ionization potentials of CH<sub>3</sub>X molecules.<sup>205,207#</sup> Deviation from this general trend was observed by St.-Jacques *et al.*<sup>200</sup> for the substituents F and OMe; the latter results were interpreted in terms of the increased competition between the  $\sigma \rightarrow \sigma^*$  type interactions and dipolar interactions.

In 3-X-substituted-1-benzoxepins (X=I, Br, Cl, F and OMe), where one of the oxygen atoms in the analogous benzodioxepins is replaced by a carbon atom, only a single O-C-C-X vicinal interaction remains between the polar bonds.<sup>208</sup> Conformational analysis also revealed that intramolecular orbital interactions of the  $\sigma \rightarrow \sigma^*$  type constituted an important force, complementing electrostatic interactions and solvation. However, the two analogous systems, having two and one O-C-C-X vicinal interactions between the polar bonds, showed that the

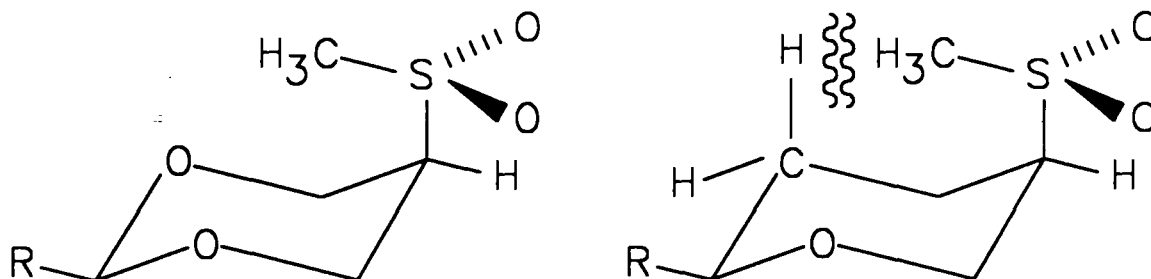
---

# It is noteworthy that the studies on 3-halotetrahydropyrans over a decade ago,<sup>49</sup> before the PMO approach became popular, suggested that some effects other than dipolar forces are responsible for the conformational behaviour.

effect of orbital interactions on conformations was not predictable using straightforward additivity schemes.<sup>208</sup> The same conclusion was made by Eliel et al.<sup>209</sup> in their conformational studies of 3-substituted oxacyclohexanes. Unlike nonpolar substituents in oxacyclohexanes,<sup>210</sup> the  $\Delta G^\circ$  values for polar substituents were not necessarily midway between those in cyclohexanes and those in 1,3-dioxacyclohexanes. The reason for this discrepancy between polar and nonpolar substituents may be visualized by looking at an example.<sup>209</sup> In the axial conformer of 1,3-dioxan-5-yl methyl sulfone, the methyl group was turned inside the ring with the sulfonyl oxygens pointing to the outside.<sup>211</sup> This created a small Me/O/O steric repulsion, as opposed to a rather strong destabilizing dipolar O/O/O interaction if the sulfonyl oxygens were pointing inside the ring (Fig.1.46). However, in

Figure 1.46

The axial conformation of 1,3-dioxan-5-yl methyl sulfone and the analogously substituted oxacyclohexane.



the analogously substituted oxacyclohexane (Fig.1.46), if the methyl group turns itself inside the ring, there is a severe Me/H steric repulsion whereas turning the oxygens into the ring causes a strong dipolar repulsion. As a result, the conformational energy of the methyl sulfone substituted oxacyclohexane is much greater than the average of the values in the analogously substituted cyclohexane and 1,3-dioxacyclohexane.<sup>209</sup>

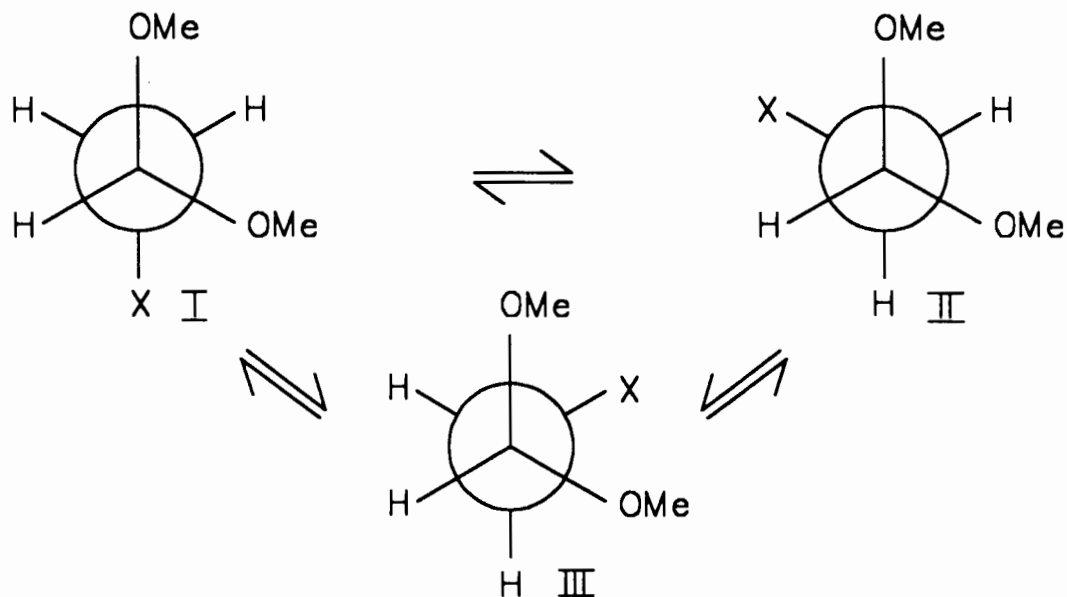
In the conformational studies of the 2-alkylthio derivatives of 1,1-dimethoxyethane,<sup>212</sup> an unexpected result was obtained in which the sterically most hindered conformation (conformer III) was preferred in the conformational equilibrium (Fig.1.47). This preference was for the gauche conformation.

In Figure 1.48, the more stable rotamers for conformations I and III are illustrated (conformer II is the enantiomer of I and is therefore excluded). On steric grounds, the rotamer IIIa could be considered to be less stable than Ia and Ib owing to the stronger Me/S steric repulsion than the Me/H repulsion. Although IIIb is not especially destabilized by steric factors, it has two strong through space lone pair repulsive interactions. The steric interaction in this conformer should be diminished because of

the flattening of the acetal function by the anomeric effect.<sup>22,23,213</sup>

Figure 1.47

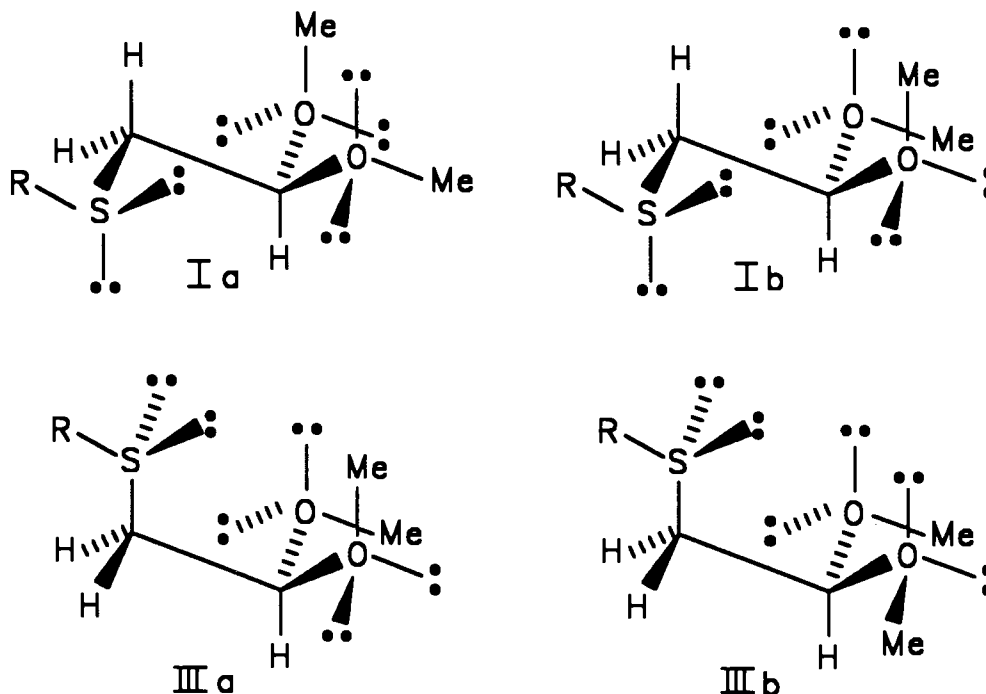
The three possible staggered conformations of 2-alkylthio-1,1-dimethoxyethanes.



Furthermore, the stabilizing  $\sigma \rightarrow \sigma^*$  type orbital interaction, as discussed above, was also given an important role. Thus, the rotamers Ia and Ib, with  $\sigma_{\text{C-H}} \rightarrow \sigma^*_{\text{C-O}}$  and  $\sigma_{\text{C-S}} \rightarrow \sigma^*_{\text{C-O}}$  interactions were judged to be less stable than rotamers IIIa and IIIb in which there are two  $\sigma_{\text{C-H}} \rightarrow \sigma^*_{\text{C-O}}$  interactions and one  $\sigma_{\text{C-S}} \rightarrow \sigma^*_{\text{C-H}}$  interaction.<sup>214</sup> The steric destabilizations in IIIa and stereoelectronic stabilization in IIIb, are attenuated by the structural modifications brought about by the anomeric effect and other orbital interactions.

Figure 1.48

The more stable rotamers of conformations I and III of 2-alkylthio-1,1-dimethoxyethanes.



### 1.8 Overview of thesis

This thesis describes several studies aimed at an understanding of orbital interactions operating through bonds and through space. The studies deal specifically with various aspects of the endo and exo-anomeric effect and the attractive and repulsive gauche effect.

In Chapter 2, the general experimental and theoretical procedures, the syntheses of all the compounds required for

the conformational analysis and the corresponding spectroscopic data are documented.

Chapter 3 describes the study of the conformational effects operating in O-C-N, S-C-N, O-C-O, S-C-O, O-C-C-N, S-C-C-N, O-C-C-O, and S-C-C-O fragments. Thus, different heterocyclic systems incorporating these fragments have been subjected to conformational analysis by NMR studies and molecular mechanics calculations. During the course of the latter studies, it became obvious that there was a serious need for parameterization of molecular mechanics force fields for these specific fragments. Chapter 4 illustrates such a procedure for the O-C-N fragment.

Experimental studies have shown that the magnitude of the anomeric effect is significant in substituted heterocycles containing second and lower row heteroatoms.<sup>122-129</sup> However, theoretical MO calculations using the isodesmic approach have suggested that the existence of the effect is questionable in these systems. The discrepancy may be due to the difference in the definition of the anomeric effect. In order to probe this aspect further, Chapter 5 reports the *ab initio* MO calculations and the isodesmic analysis of a series of disubstituted methanes containing second, third and fourth row heteroatoms.

Chapter 6 describes the study of the anomeric effect operating in allylic systems by computational methods. Calculations by MNDO and *ab initio* MO methods, together with a quantitative perturbational molecular orbital analysis of the results were used to provide an estimate of the significance of the "allylic anomeric effect".

Chapter 7 describes the dynamic NMR studies of the rotational barriers in sterically hindered dichalcogenides. The theoretical investigation of model compounds is also described. Orbital interactions are also of importance in these systems.



**CHAPTER 2**  
**EXPERIMENTAL**

**2.1 General Information.**

**I. Synthesis and NMR Analysis**

Melting points were determined on a Fisher-Johns melting-point apparatus and are uncorrected.  $^1\text{H}$  NMR (400.13 MHz) and  $^{13}\text{C}$  (100.6 MHz) NMR spectra were recorded on a Bruker WM-400 NMR spectrometer at 297 K for solutions in  $\text{CDCl}_3$  and at 273 K for solutions in  $\text{CFCl}_3/\text{CD}_2\text{Cl}_2$  (85/15). Chemical shifts and coupling constants were obtained from a first-order analysis of the spectra. Chemical shifts are given in ppm downfield from  $\text{SiMe}_4$ . All  $^{13}\text{C}$  NMR spectra were proton decoupled. The following abbreviations are employed in descriptions of NMR spectra: *s* (singlet); *d* (doublet); *t* (triplet); *q* (quartet); *bs* (broad singlet); *dd* (doublet of doublets), etc.; *m* (multiplet), *a* (axial), *e* (equatorial). In the dynamic  $^{13}\text{C}$  NMR and  $^1\text{H}$  NMR experiments, the spectra were measured on 0.1 M and 0.01 M solutions, respectively in 85:15 mixtures of  $\text{CFCl}_3/\text{CD}_2\text{Cl}_2$ . The conformational equilibria data obtained in the  $^{13}\text{C}$  NMR experiments were measured at temperatures at which exchange was slow on the NMR time scale in the temperature range 273 to 163 K. Spectra required for line shape analysis were recorded. The thermocouple readings of the spectrometer are believed to be accurate to  $\pm 2$  K; the thermocouple was

calibrated in the following manner. Peak separations of the signals from a standard methanol sample within the broadband probe were measured by use of the  $^1\text{H}$  decoupler coils for observation of the  $^1\text{H}$  NMR signals. The peak separations were converted into temperature values using the quadratic equation of Van Geet,<sup>215</sup> scaled to 400 MHz,<sup>216</sup> and a calibration curve for the probe thermocouple was constructed. In the case of some  $^1\text{H}$  and  $^{13}\text{C}$  NMR experiments, lower temperatures were required, and the temperatures were obtained from the above curve by extrapolation.

Analytical TLC was performed on pre-coated aluminum plates with Merck silica gel 60F-254 as the adsorbent. The developed plates were air dried, exposed to uv light and/or sprayed with 10%  $\text{H}_2\text{SO}_4$  in ethanol, and heated to 100°C. Medium pressure column chromatography was performed on Kieselgel 60(230-400 mesh) according to a published procedure<sup>217</sup>.

Solvents were distilled before use and were dried, as necessary, by literature procedures. Moisture and/or oxygen sensitive reactions were performed under nitrogen by use of standard Schlenk-tube techniques.

Microanalyses were performed by Mr. M.K. Yang of the Microanalytical Laboratory of Simon Fraser University.

High resolution mass spectra were recorded at the University of British Columbia Regional Mass Spectrometry Centre.

## II. Determination of Thermodynamic and Kinetic Data

### i. Direct determination of equilibrium constants:

The equilibrium constants at  $\approx 160$  K were determined from direct measurements of the relative areas of pair/pairs of signals in the  $^{13}\text{C}$  NMR spectra due to structurally identical carbon pairs in the two conformations. Sections of the spectra were expanded to 10Hz/cm prior to computer integration or hand planimetry. The values reported represent means obtained from several spectra as well as from 5 integrations of each spectrum. The errors in K are the standard deviations of the measurements. The errors in  $\Delta G^\circ$  derive from the errors in K and the error in the temperature, T. The relative intensities obtained from the routine  $^1\text{H}$  decoupled spectra with a pulse angle of  $18^\circ$  were found to be in good agreement with those obtained with the "inverse gated decoupling" technique. The Nuclear Overhauser enhancement is relatively insignificant in the determination of the conformational equilibria.

ii. Kinetic parameters from line shape analysis:

Spectra required for line-shape analysis were recorded using a 500 Hz sweep width and chemical shifts were obtained by analysis of several spectra. Chemical shift differences between exchanging signals in the exchange-broadened region were derived by linear extrapolation of the values from the slow-exchange region to higher temperatures. Changes in chemical shift differences with temperature were small. Similarly, linear extrapolation of the line widths in the spectra at the slow exchange limit to higher temperatures were used to derive effective transverse relaxation times for use in the calculations of exchange-broadened spectra.

Calculations of simulated line shapes were performed by the use of a version of the CLATUX program<sup>218</sup> for two-site exchange on an IBM 3081 computer equipped with a CALCOMP plotter.

Rate constants ( $k$ ) were obtained by visual comparison of the experimental spectra with those calculated for various  $k$  values. The errors in  $k$  were considered to be the ranges in rate constants over which it was impossible to distinguish between the experimental and calculated spectra. Activation parameters and errors were calculated by the use of a weighted, non-linear least-squares program (RATES)<sup>219</sup>. The program calculates Eyring parameters from the equation of the

form  $\ln k = a/T + b + \ln T$ . The equations for the algorithm underlying the program were obtained from Wolberg.<sup>220</sup> The program weights the data in accordance with their estimated errors, and specifically treats errors in both temperatures and rate constants.

Uncertainties in extrapolated values of  $\Delta G^\ddagger$  calculated at specific values of T were obtained from the unbiased estimates of the standard deviations of least-squares parameters a and b, and are reported at the 95% confidence level.

### III. Molecular Mechanics Calculations

Calculation of molecular geometries and energies using the molecular mechanics method with Allinger's MM2 program<sup>199,221</sup> were performed with the VAX 11/750 computer with a math-coprocessor. The MM2(85) version<sup>222</sup> was used in all the calculations. The force field in this version was parameterized for the C-O-C-O-C anomeric fragments.<sup>198</sup> It accounts not only for the relative stabilities but also for the characteristic bond lengths and bond angles associated with these groupings. Potential curves were derived by calculation about the appropriate torsional angles at 30° intervals.

#### IV. Ab Initio Calculations

The geometries of all the conformations studied were optimized without geometrical constraints by using closed-shell Hartree-Fock theory<sup>223</sup> and Pulay's method<sup>224</sup> using the Gaussian 86 program.<sup>225</sup> The calculations were carried out on a VAX 750, VAX 8600 or an IBM 3081 computer. The large number of calculations and the speed of the computer dictated a certain restraint in the choice of the basis set, and the 3-21G or 3-21G\* basis sets<sup>226</sup> appeared suitable for most compounds, given these constraints.<sup>227</sup> In certain cases other basis sets were used; for example, 4-31G or 4-31G\* and 6-31G or 6-31G\* basis sets<sup>71</sup> were used in some allylic and HXCH<sub>2</sub>XH systems. Huzinaga's MINI-1\* basis set was used for systems containing hetroatoms whose basis functions are not available in the Gaussian program. For the systems containing Se and Te, the 3-21G\* basis set and the Gaussian 85 program<sup>228</sup> were used. The latter calculations were carried out by S.D.Kahn on a Silicon Graphics 4D-70 computer. The relevant bond lengths, bond angles, and dihedral angles were optimized individually, and eventually complete optimization was carried out to provide the final geometry.

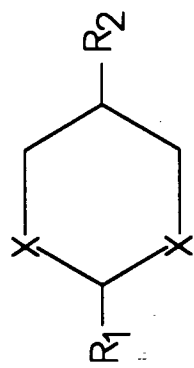
## V. Semi-Empirical Molecular Orbital Calculations

The MNDO method<sup>229</sup> was used for the calculation of heats of formation and molecular geometries. Two computer programs were used. The original program developed by Dewar and Thiel<sup>230</sup> and the modified version by Gilbert and Gajewski<sup>231</sup>. All the results were derived from RHF calculations with complete geometry optimization by the Davidon-Fletcher-Powell method<sup>232,233</sup>. The gradient norms were minimized by a non-linear least squares gradient minimization routine (NLLSQ) until they were less than 5; the gradient norms were then minimized further using McIver-Komornicki minimization routines<sup>234</sup>.

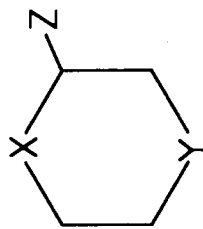
### 2.2 Synthesis

#### I. Synthetic Schemes

The compounds required for the conformational analysis in this study are listed in CHART 1 and their synthetic schemes in SCHEMES 1-10.



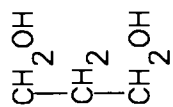
- |       |     |                      |                                  |
|-------|-----|----------------------|----------------------------------|
| 1.    | X=O | R <sub>1</sub> =H    | R <sub>2</sub> =H                |
| 2.    | X=O | R <sub>1</sub> =i-Pr | R <sub>2</sub> =H                |
| 3.    | X=O | R <sub>1</sub> =H    | R <sub>2</sub> =NH <sub>2</sub>  |
| 4.    | X=O | R <sub>1</sub> =H    | R <sub>2</sub> =NHMe             |
| 5.    | X=O | R <sub>1</sub> =H    | R <sub>2</sub> =NMe <sub>2</sub> |
| 6,9.  | X=O | R <sub>1</sub> =i-Pr | R <sub>2</sub> =NH <sub>2</sub>  |
| 7,10. | X=O | R <sub>1</sub> =i-Pr | R <sub>2</sub> =NHMe             |
| 8,11. | X=O | R <sub>1</sub> =i-Pr | R <sub>2</sub> =NMe <sub>2</sub> |
| 12.   | X=O | R <sub>1</sub> =H    | R <sub>2</sub> =OMe              |
| 13.   | X=S | R <sub>1</sub> =H    | R <sub>2</sub> =NHMe             |
| 14.   | X=S | R <sub>1</sub> =H    | R <sub>2</sub> =OMe              |
| 15.   | X=S | R <sub>1</sub> =Me   | R <sub>2</sub> =OMe              |



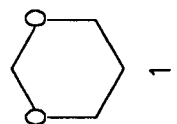
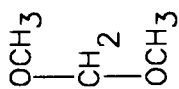
- |     |     |        |        |
|-----|-----|--------|--------|
| 16. | X=S | Y=S    | Z=NHMe |
| 22. | X=S | Y=S    | Z=OMe  |
| 17. | X=S | Y=CH   | Z=NHMe |
| 23. | X=S | Y=CH   | Z=OMe  |
| 24. | X=S | Y=CHMe | Z=OMe  |
| 19. | X=S | Y=O    | Z=NHMe |
| 26. | X=S | Y=O    | Z=OMe  |
| 20. | X=O | Y=S    | Z=NHMe |
| 25. | X=O | Y=S    | Z=OMe  |
| 18. | X=O | Y=O    | Z=NHMe |
| 27. | X=O | Y=O    | Z=OMe  |
| 21. | X=O | Y=CHMe | Z=NHMe |
| 28. | X=O | Y=CHMe | Z=OMe  |

CHART 1

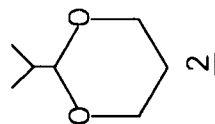
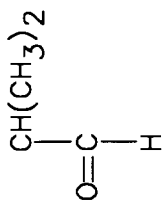




+

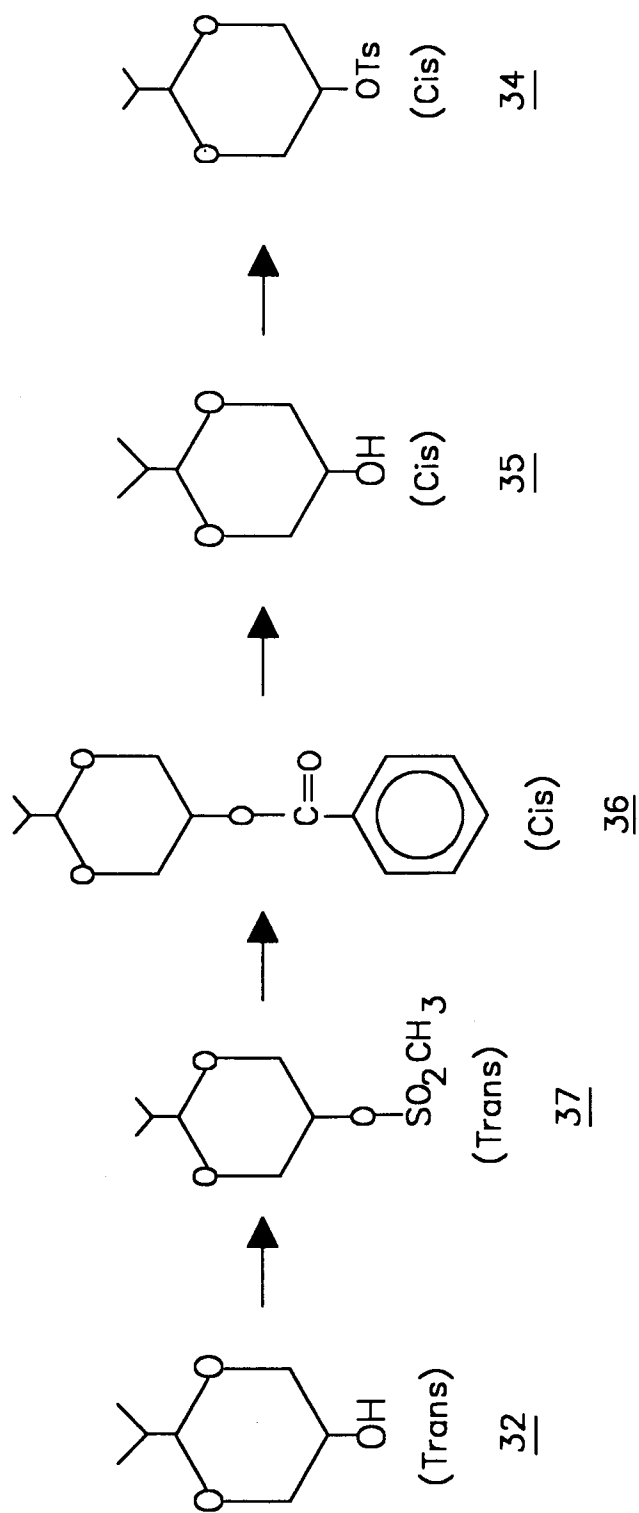


+

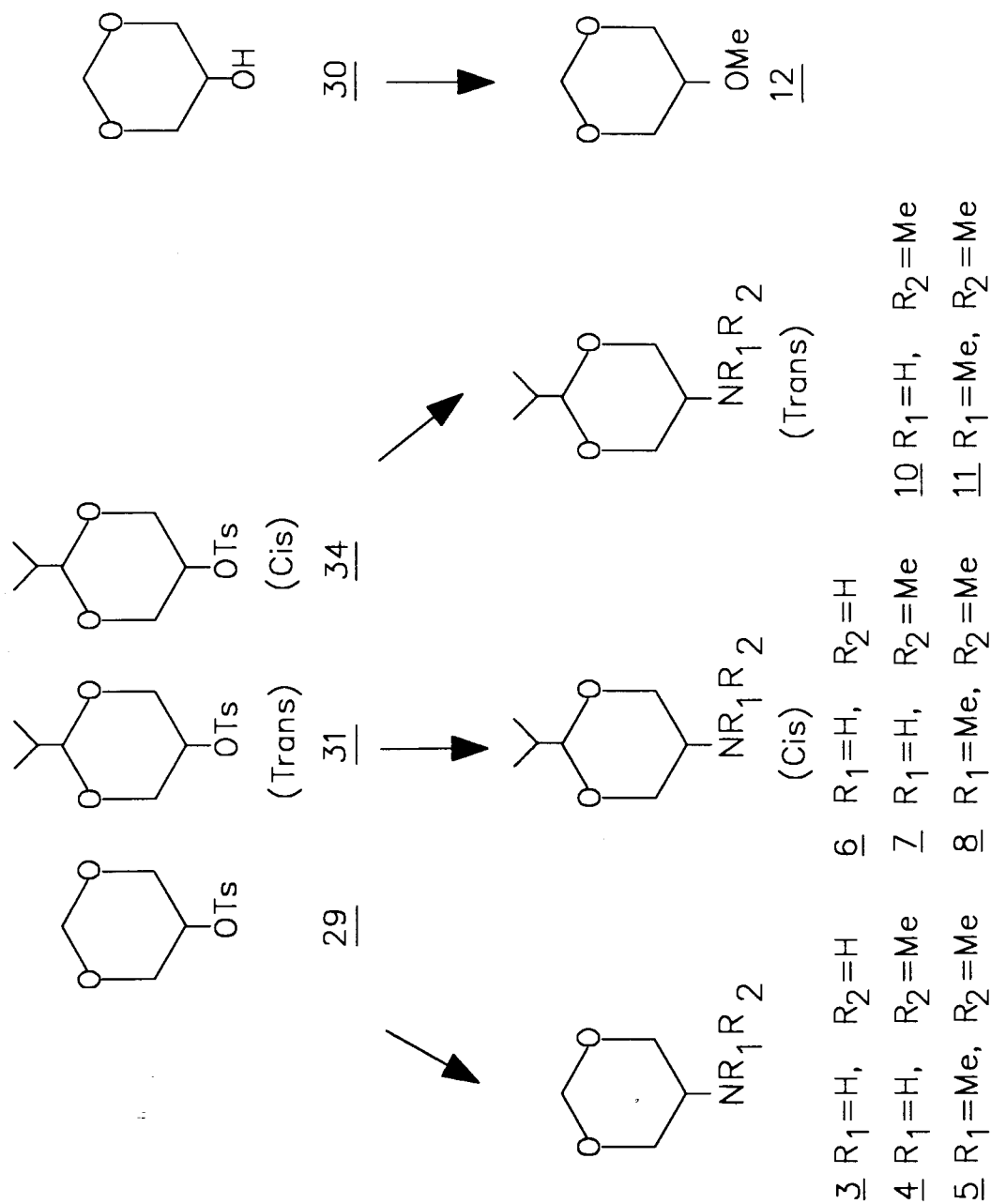


SCHEME 1

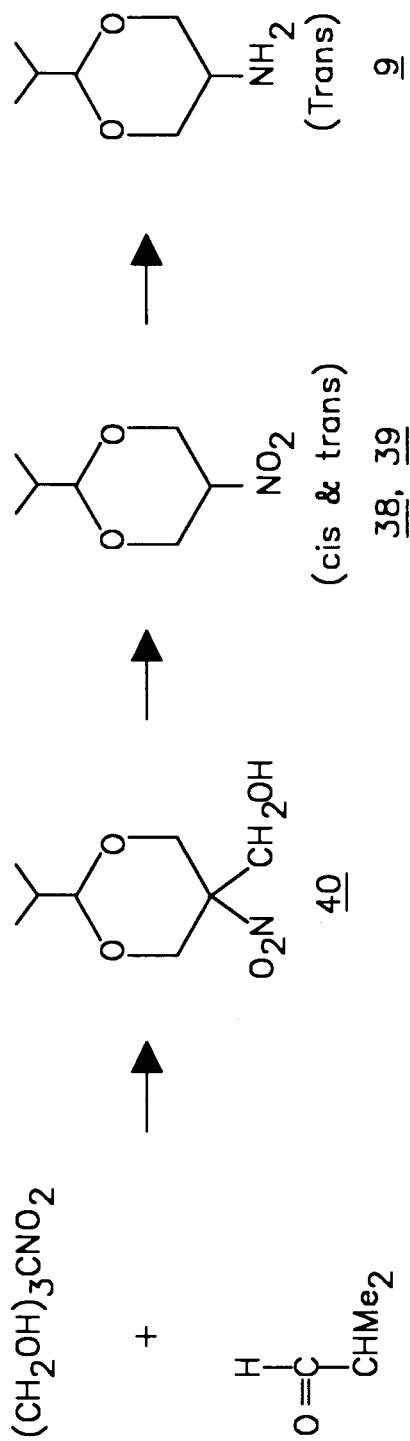




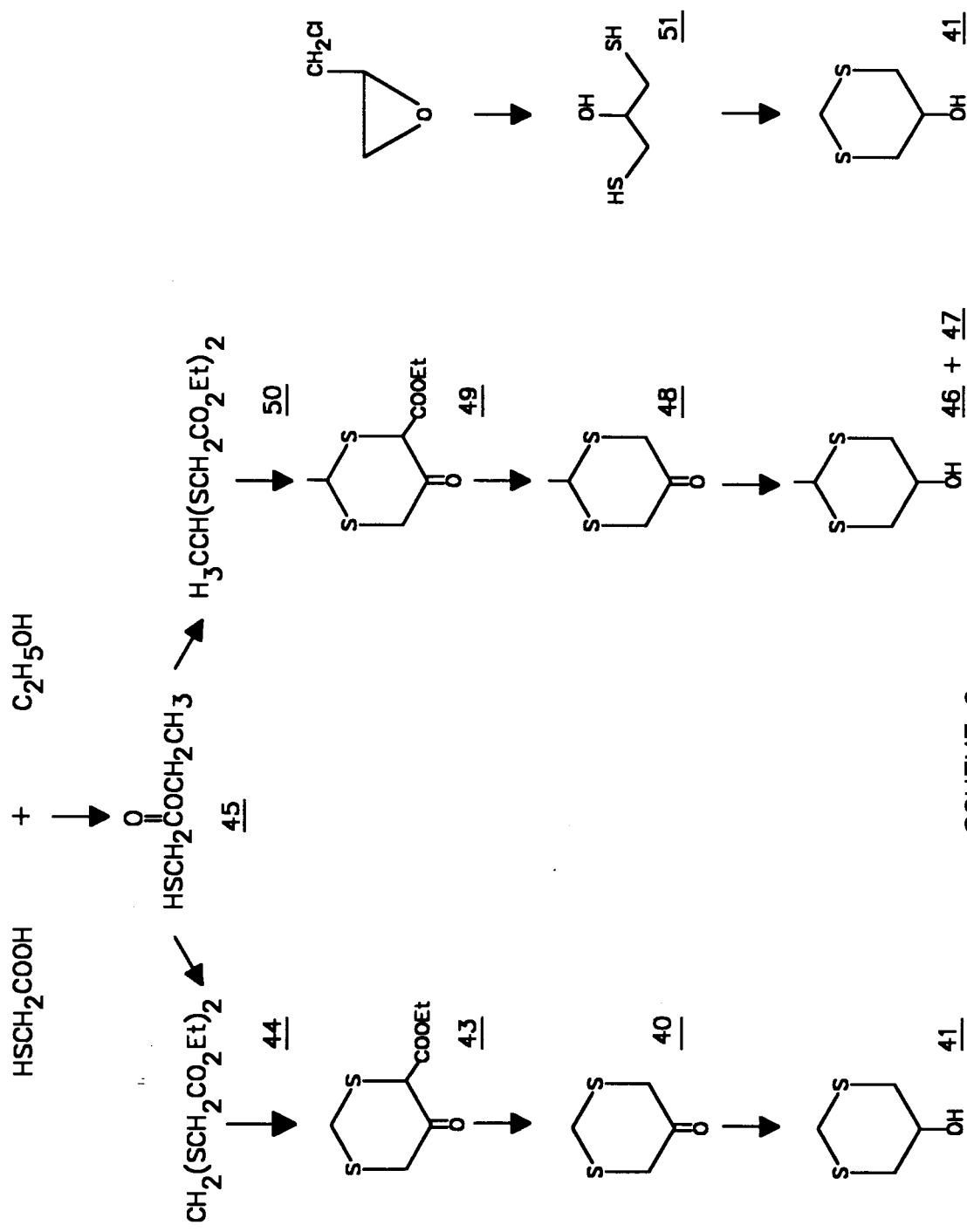
SCHEME 3



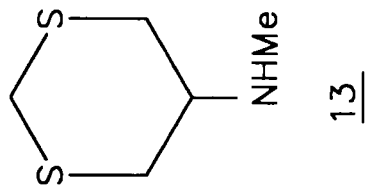
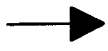
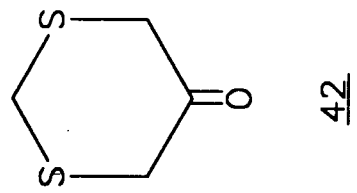
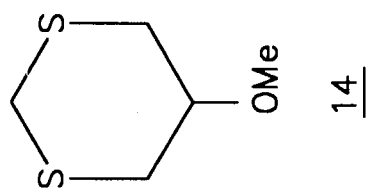
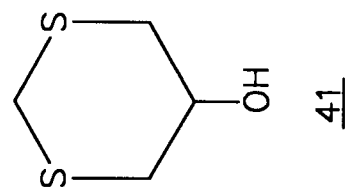
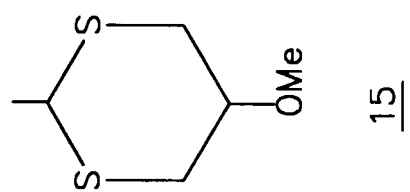
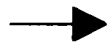
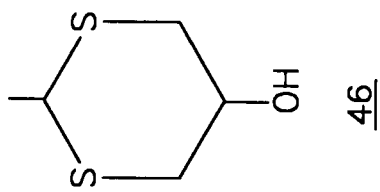
SCHEME 4



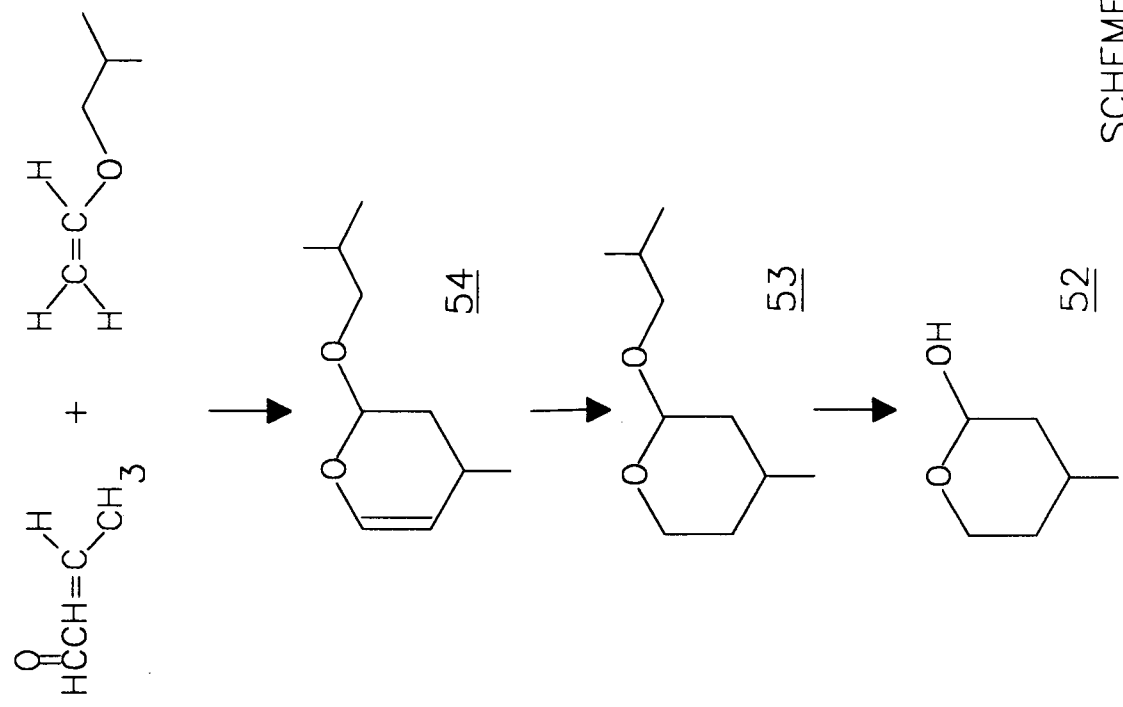
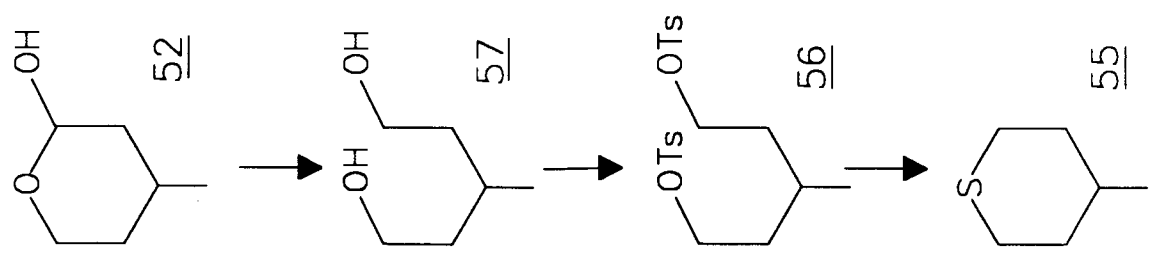
SCHEME 5



SCHEME 6



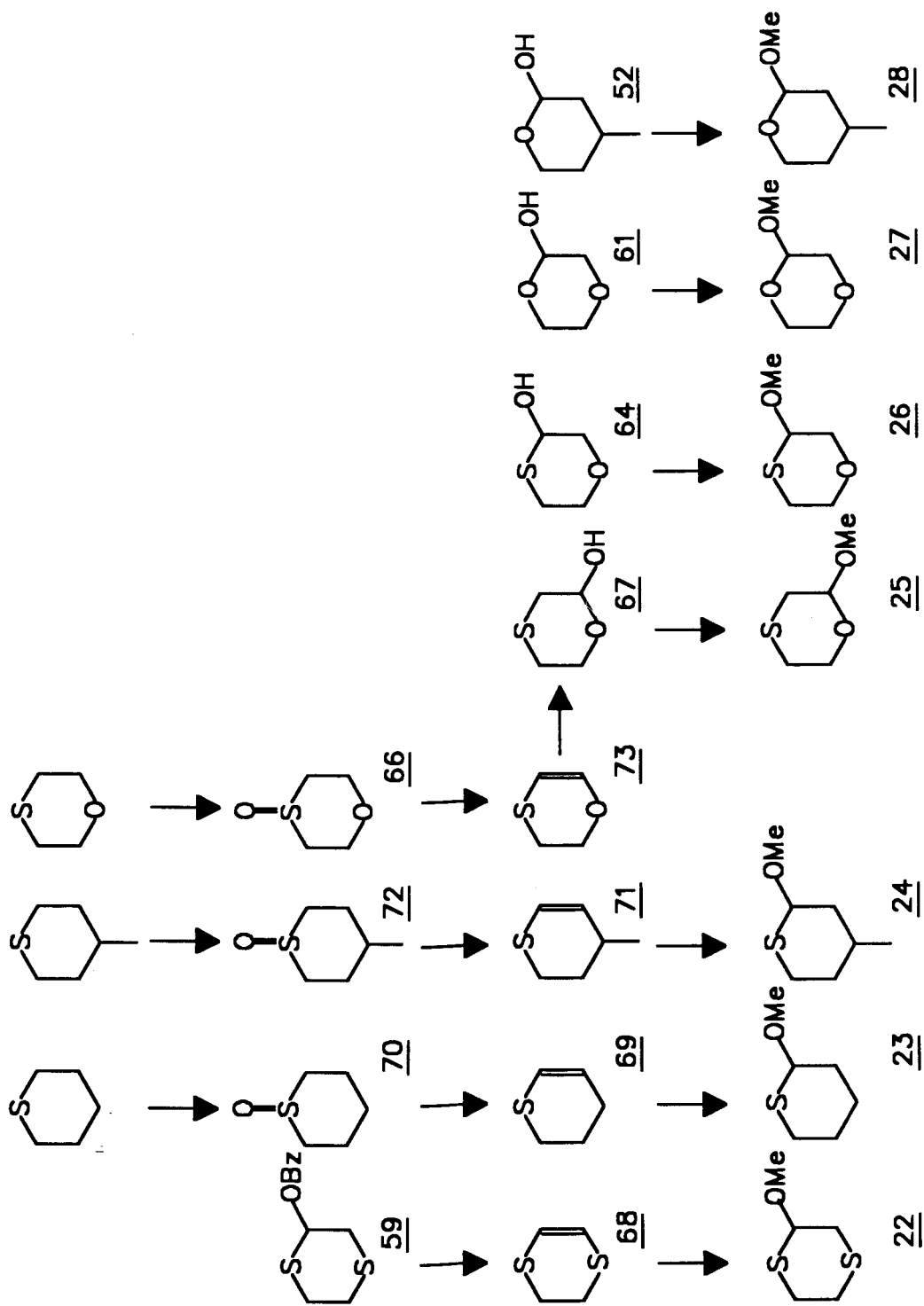
SCHEME 7



SCHEME 8







SCHEME 10

## II. General Description of Syntheses

### i. 5-Substituted-1,3-dioxacyclohexanes and their 2-isopropyl analogues.

The parent 5-hydroxy-1,3-dioxacyclohexane (30) was prepared by the acid catalysed condensation of glycerol and dimethoxymethane (SCHEME 1).<sup>185</sup> The corresponding 2-isopropyl analogue (32) was prepared by condensing glycerol and isobutyraldehyde (SCHEME 2). The 5-methoxy derivative (12) was made by methylation of the hydroxy precursors (30) using dimethylsulfate. The amine derivatives (3-8,10,11) were prepared by the amine substitution reactions on the corresponding 5-O-p-toluenesulfonyl-1,3-dioxacyclohexanes (29,31,34) (SCHEME 4). However, the trans-5-amino-2-isopropyl-1,3-dioxacyclohexane (9) was synthesized by the hydrogenation of the trans-2-isopropyl-5-nitro-1,3-dioxacyclohexane (39). This nitro compound was prepared, in turn, by condensing commercially available 2-hydroxymethyl-2-nitro-1,3-propanediol  $(\text{HOCH}_2)_3\text{CNO}_2$  with isobutyraldehyde, and elimination of formaldehyde from the resulting 5-hydroxymethyl-2-isopropyl-5-nitro-1,3-dioxacyclohexane (40) using lithium amide (SCHEME 5).<sup>211</sup>

1,3-Dioxacyclohexane and 2-isopropyl-1,3-dioxacyclohexane were prepared according to published procedures.<sup>235,236</sup>

ii. 5-Substituted-1,3-dithiacyclohexanes and their 2-methyl analogues.

The synthesis of the parent 5-hydroxy-2-methyl-1,3-dithiacyclohexane (46,47) was achieved by the reduction of the corresponding ketone (48) with sodium borohydride (SCHEME 6).<sup>188</sup> The ketone was prepared by the acid catalyzed addition of ethyl-2-mercaptoacetate (45) and acetaldehyde, followed by the acid hydrolysis and the subsequent decarboxylation of the resulting 4-carboethoxy derivative (49). The 5-hydroxy-1,3-dithiacyclohexane (41) was made by the reduction of 1,3-dithia-5-one (40) which was prepared from the acid hydrolysis and decarboxylation of the 4-carboethoxy derivative (43). The 4-carboethoxy-1,3-dithia-5-one (43) was synthesized, in turn, by the cyclization of diethyl-3,5-dithiapimelate (44); the latter was made by the acid catalyzed condensation of ethyl-2-mercaptoacetate (45) and dimethoxymethane.

An alternative route for the synthesis of 5-hydroxy-1,3-dithiacyclohexane (41) was provided by the acid catalyzed addition of 1,3-dimercapto-2-propanol (51) and dimethoxymethane. The 1,3-dimercapto-2-propanol was prepared, in turn, by the addition of epichlorohydrin and sodium hydrogen sulfide (SCHEME 6).<sup>238</sup>

The 5-methoxy derivatives (14,15) were prepared by the methylation of the corresponding hydroxides (41,46) with

iodomethane. 5-Methylamino-1,3-dithiacyclohexane (13) was prepared from the corresponding ketone (42) by using Leuckart's reaction (SCHEME 7).<sup>239</sup>

iii. 2-Substituted-oxa and thiacyclohexanes and 2- or 3-substituted 1,4-diheterocyclohexanes

The hemiacetal, 2-hydroxy-4-methyloxacyclohexane (52) was prepared by the acid hydrolysis of the 2-isobutoxy derivative (53) which was prepared, in turn, from the [2+4] cycloaddition of crotonaldehyde and isobutyl vinyl ether, followed by Pd/C catalyzed hydrogenation (SCHEME 8).<sup>165,250</sup>

The 2-hydroxythiacyclohexane (60) was prepared by the base catalyzed solvolysis<sup>248</sup> of 2-benzoyloxythiacyclohexane (61) which was prepared from thiacyclohexane by treatment with tert-butyl- peroxybenzoate in benzene according to the procedure of Sosnovsky and Yang (SCHEME 9).<sup>243</sup> The same procedure was used to prepare 2-hydroxy-1,4-dioxacyclohexane (62) from 1,4-dioxacyclohexane and 2-hydroxy-1,4-dithiacyclohexane (58) from 1,4-dithiacyclohexane. 2-Hydroxy-1-oxa-4-thiacyclohexane (67) was prepared by acid hydrolysis of the corresponding 1-oxa-4-thiacyclohex-2-ene (73) ; compound (73) was obtained as the side product from the Pummerer rearrangement of 1-oxa-4-thiacyclohexane 4-oxide (66) (SCHEME 10).<sup>244,251</sup>

3-Hydroxy-1-oxa-4-thiacyclohexane (64) was prepared from the methanolysis of the 3-acetoxy derivative (65) (SCHEME 9). Compound (65) was obtained from the Pummerer rearrangement of 1-oxa-4-thia-cyclohexane 4-oxide (66).<sup>244,251</sup>

Thiacyclohex-2-ene (69) was obtained as the elimination product from the Pummerer rearrangement<sup>244,251</sup> of thiacyclohexane oxide (70) (SCHEME 10).

1,4-Dithiacyclohex-2-ene (68) was prepared from the acid catalyzed elimination reaction of the corresponding 2-benzoyloxy derivative (59) (SCHEME 10).

The methoxy substituted derivatives of the heterocyclohexanes (22-28) were prepared by treatment of the corresponding olefins or the 2-hydroxy derivatives with acid and methanol (SCHEME 10).

The methylamine derivatives (16-21) were prepared from the corresponding hydroxy derivatives by treatment with aqueous methylamine according to the procedure of Glacet and Veron (SCHEME 9).<sup>252</sup>

### III. Procedures

#### 1,3-Dioxane<sup>235</sup> (1) (Scheme 1)

Dimethoxymethane (3.8 g, 0.05 mol) was added into a solution of 1,3-propanediol (3.8 g, 0.05 mol) containing catalytic amounts of lithium bromide and *p*-toluenesulfonic acid monohydrate. The solution was stirred overnight at RT. It was buffered with anhydrous sodium acetate, stirred for 20 min., filtered, diluted with ether (20 ml) and washed with water (2x20 ml). The solution was dried with anhydrous magnesium sulfate, filtered and concentrated to give a colourless liquid. It was then distilled to give (1) (1.0 g, 0.012 mol, 25%), b.p.103-105°, lit.<sup>235</sup> 105°. <sup>1</sup>H NMR (100 MHz, CDCl<sub>3</sub>): $\delta$  1.80 (2H,*d*, *J*=5.8 Hz, 2H-5's), 3.91 (4H,*t*, *J*=5.8 Hz, 2H-4's, 2H-6's), 4.87 (2H,*s*, 2H-2's).

#### 2-Isopropyl-1,3-dioxane<sup>236</sup> (2) (Scheme 1)

A solution of isobutyraldehyde (5.38 g, 0.075 mol), 1,3-propanediol (5.68 g, 0.075 mol) and a catalytic amount of *p*-toluene sulfonic acid monohydrate in petroleum ether (35 ml) was heated under reflux with a Dean-Stark trap. After ca. 1.35 ml (0.075 mol) of water had been collected in the trap, the solution was cooled, buffered by addition of anhydrous sodium acetate (0.5 g), stirred for an additional 20 min.,

filtered, diluted with ether (50 ml) and washed with water (2x20 ml). The solution was dried over anhydrous magnesium sulfate, filtered and concentrated to give a colourless liquid. It was distilled to give (2) (6.4 g, 0.05 mol, 67%), b.p.140-142°, lit.<sup>236</sup> 142-143°. <sup>1</sup>H NMR (100 MHz, CDCl<sub>3</sub>): $\delta$  0.91 (6H,*d*, *J*=6.9 Hz, 2CH<sub>3</sub>'s), 1.25 (1H,*dm*, *J*=13.1 Hz, H-5e), 1.73 (1H,*m*, CHMe<sub>2</sub>), 1.99 (1H,*ddd*, *J*=13.1,12.5,1.6 Hz, H-5a), 3.72 (2H,*ddd*, *J*=12.5, 11.8, 2.5 Hz, H-4a,6a), 4.05 (2H,*ddt*, *J*=11.8, 1.6, 1.6 Hz, H-4e,6e), 4.21 (1H,*d*, *J*=5.0 Hz, H-2a).

5-O-*p*-Toluenesulfonyl-1,3-dioxacyclohexane (29) (Scheme 2)

Freshly distilled glycerol (10.0 g, 0.11 mol) was reacted with dimethoxymethane (15.0 g, 0.20 mol) in the presence of hydrochloric acid (5 drops, pH<2), following a modified procedure of Hibbert and Trister.<sup>243</sup> Methanol and unreacted dimethoxymethane were evaporated before the mixed acetals were equilibrated at 90° for 24 h using catalytic amounts of *p*-toluenesulfonic acid. The crude mixed acetals were tosylated with *p*-toluenesulfonyl chloride (15.0 g, 0.08 mol) and pyridine in the usual manner. The tosylated acetals were extracted with methylene chloride and concentrated to give a syrup. Column chromatography of the resulting syrup, with ethylacetate/ hexane (1/2) as eluant, gave a component having an *R<sub>f</sub>* value of 0.39. It was identified as being (29) and was recrystallized from ethanol (2.8 g, 0.041 mol, 37%), m.p.88-



90°, lit.<sup>108</sup> 89-90.5°. <sup>1</sup>H NMR (400 MHz, CDCl<sub>3</sub>):δ 2.45 (3H,*s*, Me), 3.45-4.20 (4H,*m's*, 2H-4's,2H-6's), 4.42 (1H,*m*, H-5), 4.74 (2H,*s*, 2H-2's), 7.35-7.90 (4H,2*d*,*J*=8.5 Hz, Ar). <sup>13</sup>C NMR (100.6 MHz, CDCl<sub>3</sub>):δ 21.47 (C-11), 68.42 (C-4,C-6), 70.92 (C-5), 93.32 (C-2), 127.67 (C-9), 129.96 (C-8), 133.49 (C-10), 145.19 (C-7)

trans-5-Benzoyloxy-2-isopropyl-1,3-dioxacyclohexane (33)  
(Scheme 2)

A mixture of freshly distilled glycerol (433 g,4.60 mol), isobutyraldehyde (167 g, 2.30 mol) and 40% sulfuric acid (2.5 ml) in a 2l flask fitted with a reflux condenser and a Dean-Stark trap was refluxed until no more water was collected (6 h). The solution was cooled and the acetals were allowed to equilibrate at 5° for 2 days. The resulting solution was neutralized with 10% aqueous sodium hydroxide solution, and extracted with ether. The ethereal extract was dried over anhydrous potassium carbonate, filtered and concentrated to give a colourless liquid. Distillation yielded the mixed acetals (303 g, 90%); b.p.84-88/1.5mm Hg (lit.<sup>185</sup> 79-93/5-6mm Hg).

The mixed acetals (303 g,2.08 mol) in pyridine (327 ml) were benzoylated with benzoyl chloride (322 g,266 ml,2.30 mol) in pyridine (266 ml) overnight. The pyridine solution was

poured slowly with vigorous stirring into ice-cold distilled water (2l). A yellow oil was separated and the aqueous layer was extracted with ether. The ethereal extracts were combined with the oil, washed with 3% sulfuric acid, 5% sodium carbonate solution and finally with water. It was then dried over anhydrous sodium sulfate and concentrated to give an oil that was heated to 100°/28mm Hg for 2 h in order to remove all traces of pyridine. The desired product, (33), was fractionally crystallized from hexane (60 g, 0.24 mol, 11.5%), m.p. 58-59, lit.<sup>185</sup> mixed benzoates 70.5-72.0°. <sup>1</sup>H NMR (400 MHz, CDCl<sub>3</sub>): δ 0.97 (6H, d, J=6.8 Hz, CHMe<sub>2</sub>), 1.86 (1H, m, CHMe<sub>2</sub>), 3.60 (2H, dd, J<sub>gem</sub>=11.5 Hz, J<sub>aa</sub>=11.0 Hz, H-4a, 6a), 4.25 (1H, d, J=4.8 Hz, H-2a), 4.38 (2H, dd, J<sub>gem</sub>=11.5 Hz, J<sub>ae</sub>=5.0 Hz, H-4e, 6e), 5.13 (1H, m, H-5), 7.45-7.58 (3H, m, H-8's, H-9), 8.00 (2H, d, J=6.8 Hz, H-7's)

trans-5-O-p-Toluenesulfonyl-2-isopropyl-1,3-dioxacyclohexane (31) (Scheme 2)

The trans-benzoate (33) (32.0 g, 0.13 mol) was saponified with potassium hydroxide (15 g) dissolved in water (15 ml) and diethylene glycol (90 ml), by heating at 80° with swirling for 3 min, followed by vigorous shaking in a stoppered flask and heating for an additional 2 min. After cooling, the mixture was extracted continuously for 48 h with hexane. The extracts were dried over anhydrous magnesium sulfate, filtered, and

concentrated to give, after crystallization from hexane, (32) (18.0 g, 0.12 mol, 92%), m.p.41°, lit.<sup>185</sup> 40.5-41°.

To a solution of (32) (18.0 g, 0.12 mol) in pyridine (150 ml) in an ice bath was added *p*-toluenesulfonyl chloride (27.0 g, 0.14 mol) in small portions over a period of 30 min. The mixture was stirred overnight at room temperature. It was then diluted with 2N HCl until the pH was below 4. The ester, (31) was collected on a buchner funnel and was recrystallized from methanol (26.5 g, 0.89 mol, 74%), m.p.70-71°, lit.<sup>108</sup> 67-68.5°. <sup>1</sup>H NMR (400 MHz, CDCl<sub>3</sub>):δ 0.91 (6H,*d*,*J*=6.4 Hz, CHMe<sub>2</sub>), 1.82 (1H,*m*, CHMe<sub>2</sub>), 2.44 (3H,*s*, Me), 3.82 (2H,*d*,*J*=12.5 Hz, H-4a,6a), 4.05 (2H,*d*, *J*=12.5 Hz, H-4e,6e), 4.19 (1H,*d*,*J*=5.0 Hz, H-2), 4.32 (1H,*s*, H-5), 7.31-7.78 (4H,2*d*'s, *J*=8.0 Hz, Ar). <sup>13</sup>C NMR (100.6 MHz, CDCl<sub>3</sub>):δ 16.61 (C-1), 21.35 (C-10), 32.38 (C-2), 68.45 (C-4), 72.98 (C-5), 105.43 (C-3), 127.47 (C-8), 134.05 (C-9), 144.73 (C-6)

cis-5-Benzoyloxy-2-isopropyl-1,3-dioxacyclohexane (36)

(Scheme 3)

Ice cold solutions of (32) (2.0 g, 14 mmol) in pyridine and methanesulfonyl chloride (4 ml) in pyridine (16 ml) were mixed and stirred at room temperature for 6 h. The mixture was then poured into ice-water (ca.200 ml) and the precipitate was collected, washed with water, and recrystallized from

ethanol to give the methanesulfonate (3.0 g, 13 mmol;96% yield).

The solution of (37) (3.0g;13 mmol) in dimethylformamide (100 ml) was boiled under reflux for 6 h in the presence of sodium benzoate (8.6 g,0.06 mol). Water was then added to the cooled solution and the product was extracted with methylene chloride (3x100 ml). The methylene chloride extracts were combined and dried with anhydrous potassium carbonate and concentrated to give a brown solid; the solid was then redissolved in ethyl acetate and purified by filtering through a thin layer of TLC grade silica gel. After evaporating off the solvent, the slightly yellowish solid was recrystallized from ethanol to give colourless crystals which were identified as being (36) (0.84 g, 3 mmol ;26%), m.p.54-55°, lit.<sup>185</sup> mixture of benzoates 70.5-72°. <sup>1</sup>H NMR (400 MHz, CDCl<sub>3</sub>):δ 0.98 (6H, d, J=6.7 Hz, CHMe<sub>2</sub>), 1.89 (1H, m, CHMe<sub>2</sub>), 4.02 (2H, dd J<sub>gem</sub>=13.0 Hz, J<sub>ae</sub>=1.8Hz, H-4a,6a), 4.27 (2H, dd, J<sub>gem</sub>=13.0 Hz, J<sub>ee</sub>=1.3Hz, H-4e,6e), 4.36 (1H, d, J=5.0 Hz, H-2a), 4.85 (1H, t, J=1.8 Hz, H-5e), 7.45-7.58 (3H, m, H-8's, H-9), 8.15 (2H, d, J=7.8 Hz, H-7's).

cis-5-O-p-Toluenesulfonyl-2-isopropyl-1,3-dioxacyclohexane  
(34) (Scheme 3)

The cis tosylate (34) was prepared from the benzoate (36), as described for the trans isomer (31) in 53% yield.  $^1\text{H}$  NMR (400 MHz,  $\text{CDCl}_3$ ):  $\delta$  0.92 (6H, *d*,  $J=6.5$  Hz,  $\text{CHMe}_2$ ), 1.68 (1H, *m*,  $\text{CHMe}_2$ ), 2.48 (3H, *s*, Me), 3.49 (2H, *dd*,  $J_{\text{gem}}=10.5$  Hz,  $J_{\text{aa}}=10.0$  Hz, H-4a,6a), 4.07 (2H, *dd*,  $J_{\text{gem}}=10.5$  Hz,  $J_{\text{ae}}=5.4$  Hz, H-4e,6e), 4.12 (1H, *d*,  $J=4.5$  Hz H-2a), 4.41 (1H, *m*, H-5), 7.37-7.80 (4H, *2d's*,  $J=8.0$  Hz, Ar).  $^{13}\text{C}$  NMR (100.6 MHz,  $\text{CDCl}_3$ ):  $\delta$  16.81 (C-1), 21.47 (C-10), 32.02 (C-2), 68.25 (C-4), 68.42 (C-5), 105.62 (C-3), 127.76 (C-8), 129.99 (C-7), 133.20 (C-9), 145.27 (C-6)

5-Amino-1,3-dioxacyclohexane (3) (Scheme 4)

A solution of (29) (1.0 g, 4 mmol) in saturated methanolic ammonia (8 ml) was heated in a sealed tube at  $100^\circ$  for 4 days. The reaction mixture was poured into sodium hydrogen carbonate solution (15 ml) and extracted with methylene chloride (3x15 ml). The extracts were dried over anhydrous potassium carbonate and concentrated. The light yellow liquid obtained was distilled to give (3) as a colourless liquid (0.2 g, 2 mmol, 50%), b.p.  $90^\circ/34\text{mm Hg}$ .  $^1\text{H}$  NMR (400 MHz,  $\text{CDCl}_3$ ):  $\delta$  2.88 (1H, *dt*,  $J_{\text{ax}}=6.3$  Hz,  $J_{\text{ex}}=3.5$  Hz, H-5), 3.46 (2H, *dd*,  $J_{\text{gem}}=11.2$ ,  $J_{\text{ax}}=6.3$  Hz, H-4a, H-6a), 3.97 (2H, *dd*,  $J_{\text{gem}}=11.2$ ,  $J_{\text{ex}}=3.5$  Hz, H-4e, H-6e), 4.70 (1H, *d*,  $J=6.1$  Hz,

H-2a), 4.80 (1H,*d*,  $J=6.1$  Hz, H-2e).  $^{13}\text{C}$  NMR (100.6 MHz,  $\text{CDCl}_3$ ): $\delta$  45.5 (C-5), 73.2 (C4, C6), 93.8 (C-2)

Anal. Calcd. for  $\text{C}_4\text{H}_9\text{NO}_2$ : C,46.59; H,8.80; N;13.58.  
Found: C,46.55; H,8.93; N;13.68.

#### 5-Methylamino-1,3-dioxacyclohexane (4) (Scheme 4)

A mixture of (29) (0.5 g, 1.9 mmol) in methanol (2 ml) and methylamine (4.0 ml, 40% aqueous solution) was heated in a sealed tube at  $100^\circ$  for 72 h. The mixture was poured into sodium hydrogen carbonate solution (10 ml) and then extracted with methylene chloride (3x100 ml). The extracts were dried over anhydrous potassium carbonate and concentrated. The pale yellow liquid obtained was distilled to give (4) (0.12 g, 1 mmol, 54%), b.p. $140^\circ$  /34mm Hg.  $^1\text{H}$  NMR (400 MHz,  $\text{CDCl}_3$ ): $\delta$  2.44 (3H,*s*, Me), 2.56 (1H,*m*, H-5), 3.70 (2H,*dd*,  $J_{\text{gem}}=11.4$ ,  $J_{\text{ax}}=5.3$  Hz, H-4a, H-6a), 3.96 (2H,*dd*,  $J_{\text{gem}}=11.4$ ,  $J_{\text{ex}}=3.2$  Hz, H-4e, H-6e), 4.76 (1H,*d*,  $J=6.1$  Hz, H-2a), 4.81 (1H,*d*,  $J=6.1$  Hz, H-2e).  $^{13}\text{C}$  NMR (100.6 MHz,  $\text{CDCl}_3$ ): $\delta$  33.5 (C-7), 53.1 (C-5), 69.7 (C-4, C-6), 94.1 (C-2).

Anal. Calcd. for  $\text{C}_5\text{H}_{11}\text{NO}_2$ : C,51.26, H,9.46, N;11.95.  
Found: C,50.98, H,9.69, N;11.85.

5-Dimethylamino-1,3-dioxacyclohexane (5) (Scheme 4)

A mixture of (29) (1.0 g, 3.8 mmol) in methanol (8 ml) and dimethylamine (8 ml, 25% aqueous solution) was heated in a sealed tube at 100° for 4 days. The mixture was worked up as described above to give (5) (0.28 g, 2.1 mmol, 56%) as a colourless liquid, b.p.98-100°/34mm Hg. <sup>1</sup>H NMR (400 MHz, CDCl<sub>3</sub>):δ 2.26 (6H,*s*, two Me's), 2.40 (1H,*m*, H-5), 3.60 (2H,*dd*, *J*<sub>gem</sub>=11.3, *J*<sub>ax</sub>=10.2 Hz, H-4a, H-6a), 4.14 (2H,*dd*, *J*<sub>gem</sub>=11.3, *J*<sub>ex</sub>=4.2 Hz, H-4e, H-6e), 4.57 (1H,*d*, *J*= 6.1 Hz, H-2a), 4.90 (1H,*d*, *J*=6.1 Hz, H-2e). <sup>13</sup>C NMR (100.6 MHz, CDCl<sub>3</sub>):δ 42.6 (C-7), 57.5 (C-5), 69.3 (C-4, C-6), 93.6 (C-2).

Anal. Calcd. for C<sub>6</sub>H<sub>13</sub>NO<sub>2</sub>: C,54.94; H,9.99; N,10.68.

Found: C,54.76; H,9.77; N,10.85.

cis-5-Amino-2-isopropyl-1,3-dioxacyclohexane (6) (Scheme 4)

A solution of (31) (0.30 g, 1 mmol) in saturated methanolic ammonia (10 ml) was heated in a sealed tube at 100° for 4 days. The mixture was worked up as described above to give (6) (0.10 g, 0.69 mmol, 69%) as a colourless liquid, b.p.110°/ 34mm Hg. <sup>1</sup>H NMR (400 MHz, CDCl<sub>3</sub>):δ 0.92 (6H,*d*, *J*=6.9 Hz, CHMe<sub>2</sub>), 1.78 (1H,*m*, CHMe<sub>2</sub>), 2.65 (1H,*t*, *J*=1.8 Hz, H-5), 3.84 (4H,*m*, H-4's, H-6's), 4.24 (1H,*d*, *J*=4.8 Hz, H-2a). <sup>13</sup>C NMR (100.6 MHz, CDCl<sub>3</sub>):δ 16.7 (C-9), 32.8 (C-8), 45.98 (C-5), 72.9 (C-4, C-6), 106.6 (C-2).

Anal. Calcd. for  $C_7H_{15}NO_2$ : C, 57.90; H, 10.41; N, 9.65.

Found: C, 57.67; H, 10.45; N, 9.59.

cis-2-Isopropyl-5-methylamino-1,3-dioxacyclohexane (7)  
(Scheme 4)

A mixture of (31) (0.2 g, 0.67 mmol) in methanol (2 ml) and methylamine (4.0 ml, 40% aqueous solution) was heated in a sealed tube at 100° for 4 days. The mixture was worked up as described above to give (7) (0.084 g, 0.53 mmol, 79%), b.p. 110°/34mm Hg.  $^1H$  NMR (400 MHz,  $CDCl_3$ ):  $\delta$  0.90 (6H, *d*,  $J=6.9$  Hz,  $CHMe_2$ ), 1.76 (1H, *m*,  $CHMe_2$ ), 2.27 (1H, *m*, H-5), 2.44 (3H, *s*,  $NHMe$ ), 3.79 (2H, *d*,  $J=11.9$  Hz, H-4a, H-6a), 4.10 (2H, *d*,  $J=11.9$  Hz, H-4e, H-6e), 4.24 (1H, *d*,  $J=4.9$  Hz, H-2).  $^{13}C$  NMR (100.6 MHz,  $CDCl_3$ ):  $\delta$  16.8 (C-9), 32.7 (C-8), 33.3 (C-7), 53.1 (C-5), 68.9 (C-4, C-6), 106.2 (C-2)

Anal. Calcd. for  $C_8H_{17}NO_2$ : C, 60.35; H, 10.76; N, 8.80.

Found: C, 60.09; H, 10.88; N, 9.00

cis-5-Dimethylamino-2-isopropyl-1,3-dioxacyclohexane (8)  
(Scheme 4)

A mixture of (31) (0.56 g, 1.88 mmol) in methanol (2 ml) and dimethylamine (4.0 ml, 25% aqueous solution) was heated in a sealed tube at 100° for 3 days. The mixture was worked up as described above to give (8) (0.21 g, 1.2 mmol, 65%),



b.p.110°/34mm Hg.  $^1\text{H}$  NMR (400 MHz,  $\text{CDCl}_3$ ): $\delta$  0.89 (6H,*d*, $J=6.9$  Hz,  $\text{CHMe}_2$ ), 1.79 (1H,*m*,  $\text{CHMe}_2$ ), 2.09 (1H,*m*, H-5), 2.44 (6H,*s*,  $\text{NMe}_2$ ), 3.83 (2H,*d*, $J=12.8$  Hz, H-4a,H-6a), 4.26 (1H,*d*,  $J=4.8$  Hz, H-2), 4.28 (2H,*d*, $J=12.8$  Hz, H-4e,H-6e).  $^{13}\text{C}$  NMR (100.6 MHz,  $\text{CDCl}_3$ ): $\delta$  16.9 (C-9), 32.6 (C-8), 43.5 (C-7), 57.1 (C-5), 67.8 (C-4, C-6), 105.9 (C-2).

Anal. Calcd. for  $\text{C}_9\text{H}_{19}\text{NO}_2$ : C,62.39; H,11.05; N,8.08.

Found: C,62.05; H,11.35; N,8.30

trans-2-Isopropyl-5-methylamino-1,3-dioxacyclohexane (10)  
(Scheme 4)

Compound (34) (0.055 g, 0.2 mmol) was treated with methylamine, as described for the preparation of the *cis*-isomer (7). (10) (0.021 g, 0.13 mmol, 72%) was obtained as a colourless liquid, b.p.100°/34mm Hg.  $^1\text{H}$  NMR (400 MHz,  $\text{CDCl}_3$ ): $\delta$  0.88 (6H,*d*,  $J=6.9$  Hz,  $\text{CHMe}_2$ ), 1.75 (1H,*m*,  $\text{CHMe}_2$ ), 2.39 (3H,*s*,  $\text{NHMe}$ ), 2.77 (1H,*m*, H-5), 3.20 (2H,*dd*, $J_{\text{gem}}=10.8$  Hz,  $J_{\text{aa}}=10.6$  Hz, H-4a,H-6a), 4.08 (1H,*d*, $J=5.0$  Hz, H-2), 4.19 (2H,*dd*, $J_{\text{gem}}=10.8$  Hz,  $J_{\text{ea}}=4.8$  Hz, H-4e, H-6e).  $^{13}\text{C}$  NMR (100.6 MHz,  $\text{CDCl}_3$ ): $\delta$  17.0 (C-9), 32.4 (C-8), 33.8 (C-7), 52.0 (C-5), 71.4 (C-4, C-6), 105.8 (C-2).

Anal. Calcd. for  $\text{C}_8\text{H}_{17}\text{NO}_2$ : C,60.35; H,10.76; N,8.80.

Found: C,60.59; H,10.89; N,9.01

trans-5-Dimethylamino-2-isopropyl-1,3-dioxacyclohexane (11)  
(Scheme 4)

Compound (34) (0.055 g, 0.2 mmol) was treated with dimethylamine, as described for the preparation of the cis-isomer (8). (11) (0.014 g, 0.081 mmol, 41%) was obtained as a colourless liquid, b.p. 110°/34mm Hg.  $^1\text{H}$  NMR (400 MHz,  $\text{CDCl}_3$ ):  $\delta$  0.90 (6H, *d*,  $J=6.9$  Hz,  $\text{CHMe}_2$ ), 1.75 (1H, *m*,  $\text{CHMe}_2$ ), 2.22 (6H, *s*,  $\text{NMe}_2$ ), 2.41 (1H, *dd*,  $J_{aa}=10.7$ ,  $J_{ae}=4.8$  Hz, H-5), 3.45 (2H, *dd*,  $J_{gem}=11.2$ ,  $J_{aa}=10.7$  Hz, H-4a, H-6a), 4.08 (1H, *d*,  $J=5.0$  Hz, H-2), 4.24 (2H, *dd*,  $J_{gem}=11.2$ ,  $J_{ae}=4.8$  Hz, H-4e, H-6e).  $^{13}\text{C}$  NMR (100.6 MHz,  $\text{CDCl}_3$ ):  $\delta$  17.0 (C-9), 32.4 (C-4), 42.6 (C-7), 57.1 (C-5), 69.6 (C-4, C-6), 105.5 (C-2).

Anal. Calcd. for  $\text{C}_9\text{H}_{19}\text{NO}_2$ : C, 62.39; H, 11.05; N, 8.08.

Found: C, 61.98; H, 11.09; N, 8.07.

5-Methoxy-1,3-dioxacyclohexane (12) (Scheme 4)

The mixed acetals from the reaction of glycerol and dimethoxymethane (4.2 g, 0.04 mol) was added into a stirred suspension of sodium hydride 50% oil dispersion (2.4 g, 0.05 mol) in dry THF (15 ml) at 0° over a period of 30 min. Dimethylsulfate (5.7 g, 4.25 ml, 0.045 mol) was then added slowly and the mixture was stirred at RT for 16 h. TLC (hexane/ethyl acetate (3:1)) showed the presence of a new component having an  $R_f$  value of 0.61. The mixture was

quenched with 1N sodium hydroxide solution (10 ml) and was extracted with methylene chloride (3x20 ml). The methylene chloride extracts were dried with anhydrous potassium carbonate and the solvent was evaporated to give a colourless liquid. Chromatography on silica gel using the TLC solvent as eluant gave 4-methoxy-methyl-1,3-dioxolane (0.74 g, 6 mmol, 15%) which had an  $R_f$  value of 0.61.  $^1\text{H}$  NMR (400 MHz,  $\text{CDCl}_3$ ):  $\delta$  3.40 (3H, s,  $\text{OCH}_3$ ), 3.44 (1H, dd,  $J=10.2, 5.1$  Hz, H from  $\text{CH}_3\text{OCH}_2$ ), 3.50 (1H, dd,  $J=10.2, 5.9$  Hz, H from  $\text{CH}_3\text{OCH}_2$ ), 3.68 (1H, dd,  $J=8.1, 6.0$  Hz, H-5e), 3.96 (1H, dd,  $J=8.1, 7.0$  Hz, H-5a), 4.89, 5.03 (2H, 2s's, H-2a, H-2e).  $^{13}\text{C}$  NMR (100.6 MHz,  $\text{CDCl}_3$ ):  $\delta$  59.2 ( $\text{OCH}_3$ ), 66.9 ( $\text{CH}_2$ ), 72.9 (C-5), 74.3 (C-4), 95.3 (C-2).

A more polar component was obtained as a colourless liquid and was identified as being (12) (0.62 g, 5 mmol, 12.5%). This compound was not visible on the TLC plate.  $^1\text{H}$  NMR (400 MHz,  $\text{CDCl}_3$ ):  $\delta$  3.31 (1H, dtt,  $J_{ax}=6.6$  Hz,  $J_{ex}=3.3$  Hz, H-5), 3.43 (3H, s,  $\text{OCH}_3$ ), 3.73 (2H, dd,  $J_{gem}=11.3$  Hz,  $J_{ax}=6.6$  Hz, H-4a, H-6a), 4.05 (2H, dd,  $J_{gem}=11.3$  Hz,  $J_{ex}=3.3$  Hz, H-4e, H-6e), 4.75 (1H, d,  $J=6.0$  Hz, H-2a or H-2e), 4.87 (1H, d,  $J=6.0$  Hz, H-2a or H-2e).  $^{13}\text{C}$  NMR (100.6 MHz,  $\text{CFCl}_3/\text{CD}_2\text{Cl}_2$  (85/15)):  $\delta$  57.6 ( $\text{OCH}_3$ ), 70.3 (C-4, C-6), 72.1 (C-5), 94.6 (C-2)

Anal. Calcd. for  $\text{C}_5\text{H}_{10}\text{O}_3$ : C, 50.84; H, 8.53. Found: C, 50.59; H, 8.58

5-Hydroxymethyl-2-isopropyl-5-nitro-1,3-dioxacyclohexane (40)  
(Scheme 5)

A solution of 50% aqueous 2-hydroxymethyl-2-nitro-1,3-propanediol (194.0 g, 0.73 mol) and isobutyraldehyde (53.9 g ;68 ml, 0.75 mol) in benzene (300 ml) containing *p*-toluene-sulfonic acid monohydrate (2 g) in a 1-litre round bottom flask equipped with a reflux condenser and Dean-Stark trap was heated under reflux for 16 h as described by Eliel *et al.*<sup>211</sup> The cooled mixture was diluted with ether (500 ml) and washed with 2% aqueous sodium bicarbonate (4x200 ml), and water (400 ml). The organic layer was dried with anhydrous sodium sulfate and concentrated to give a brown paste which was then recrystallized from diethyl ether to yield (40) (82.0 g, 0.4 mol, 55%).

cis- and trans-5-Nitro-2-isopropyl-1,3-dioxacyclohexanes (38 & 39)  
(Scheme 5)

Ammonia (11) was condensed into a 2litre 3 necked flask fitted with a mechanical stirrer and dry-ice ethanol condenser. A few crystals of  $\text{Fe}(\text{NO}_3)_3 \cdot 9\text{H}_2\text{O}$  were added and stirring was commenced. Lithium (1.5 g) was added in small pieces until the colour of the solution turned grey. When all the lithium had reacted, (40) (27.0 g, 0.13 mol) was added in small portions over 20 min. The suspension was stirred for 6 h, and ammonium chloride (15 g) was then added. The ammonia

was allowed to evaporate overnight with stirring. Water was added to the suspension and stirring was continued for another 1 h. The suspension was extracted with ether (3x200 ml). The extracts were washed with water (3x100 ml) and then dried over anhydrous magnesium sulfate and concentrated to a black tar. The tar was then distilled to give a colourless liquid which was identified as being a mixture of (38 & 39) (8.5 g, 0.06 mol, 40%), b.p.50-58°/0.3mm Hg, lit.<sup>211</sup> 50-53/0.2 Torr. Column chromatography with hexane/ethyl acetate (10/1) as eluant gave two components having  $R_f$  values 0.47 and 0.08 which were identified as being the trans and cis isomers, respectively. (38)  $^1\text{H}$  NMR (100.13 MHz,  $\text{CDCl}_3$ ): $\delta$  0.89 (6H,*d*, $J=6.5$  Hz,  $\text{CHMe}_2$ ), 1.87 (1H,*m*,  $\text{CHMe}_2$ ), 4.30 (1H,*d*,  $J=4.9$  Hz, H-2), 3.95 (1H,*m*, H-5e), 4.10 (2H,*dd*, $J_{gem}=11.6$  Hz, H-4a,H-6a), 4.87 (2H,*dd*, $J_{gem}=11.6$  Hz, H-4e,H-6e). (39)  $^1\text{H}$  NMR (at 100 MHz in  $\text{CDCl}_3$ ): $\delta$  0.91 (6H,*d*, $J=6.5$  Hz,  $\text{CHMe}_2$ ), 1.90 (1H,*m*,  $\text{CHMe}_2$ ), 4.19 (1H,*d*,  $J=4.8$  Hz, H-2), 3.93 (2H,*m*, H-4a,H-6a), 4.48 (1H,*dd*, $J=5.6$  Hz, H-5a), 4.68 (2H,*m*, H-4e, H-6e)

trans-5-Amino-2-isopropyl-1,3-dioxacyclohexane (9) (Scheme 5)

Compound (39) (1 g, 5.7 mmol) was hydrogenated at room temperature in 95% ethanol over 0.1g 5% Pd/C catalyst at a pressure of 32 p.s.i. for 2 h. The catalyst was filtered through a thin layer of silica gel and the solvent was

evaporated to give a colourless liquid which was identified as being (9) (0.78 g, 5.4 mmol, 94%).  $^1\text{H}$  NMR (400 MHz,  $\text{CDCl}_3$ ):  $\delta$  0.93 (6H, *d*,  $J=6.8$ ,  $\text{CHMe}_2$ ), 1.80 (1H, *m*,  $\text{CHMe}_2$ ), 3.03 (1H, *dd*,  $J_{aa}=10.5$ ,  $J_{ae}=5.0$  Hz, H-5a), 3.21 (2H, *dd*,  $J_{gem}=11.0$ ,  $J_{aa}=10.5$  Hz, H-4a, H-6a), 4.12 (1H, *d*,  $J=5.0$  Hz, H-2a), 4.14 (2H, *dd*,  $J_{gem}=11.0$ ,  $J_{ae}=5.0$  Hz, H-4e, H-6e).  $^{13}\text{C}$  NMR (100.6 MHz,  $\text{CDCl}_3$ ):  $\delta$  17.0 (C-9), 32.5 (C-8), 44.2 (C-5), 73.5 (C-4, C-6), 105.6 (C-2).

Anal. Calcd. for  $\text{C}_7\text{H}_{15}\text{NO}_2$ : C, 57.90; H, 10.41; N, 9.65.

Found: C, 58.30; H, 10.16; N, 8.90

#### Ethyl-2-mercaptoacetate (45) (Scheme 6)

Ethanol (10 ml, 7.85 g, 0.17 mol) was added to a mixture of mercaptoacetic acid (12.2 g, 0.13 mol) and concentrated sulfuric acid (1 ml). A slightly exothermic reaction ensued and the solution was stirred for 0.5 h. The solution was diluted with methylene chloride (100 ml), washed with water (2x20 ml) and saturated sodium bicarbonate solution (2x20 ml). It was then dried over anhydrous magnesium sulfate and concentrated to give a colourless liquid which was distilled to give (45) (11.8 g, 98 mmol, 78%), b.p. 74-75°/28mm Hg.  $^1\text{H}$  NMR (at 100 MHz in  $\text{CDCl}_3$ ):  $\delta$  1.28 (3H, *t*,  $J=6.7$  Hz,  $\text{CH}_3$ ), 2.00 (1H, *t*,  $J=8.3$  Hz, SH), 3.25 (2H, *d*,  $J=8.3$  Hz,  $\text{COCH}_2$ ), 4.20 (2H, *q*,  $J=6.7$  Hz,  $\text{CH}_2\text{CH}_3$ ).

Diethyl-3,5-dithiapimelate<sup>188</sup> (44) (Scheme 6)

To a mixture of (45) (5.45 g, 0.045 mol) and boron trifluoride etherate (5.5 ml, 6.35 g, 0.04 mol) in refluxing chloroform (50 ml) was added a solution of dimethoxymethane (1.7 g, 0.024 mol) in chloroform (100 ml). After the addition was completed, the solution was cooled and washed with 2N aqueous sodium hydroxide solution (50 ml). It was dried with anhydrous magnesium sulfate and concentrated to give a colourless liquid. Column chromatography of the liquid with ethyl acetate/hexane (1/3) as eluant gave a component having an  $R_f$  value of 0.6. It was identified as being (44) (5.78 g, 0.023 mol, 51%).  $^1\text{H NMR}$  (400 MHz,  $\text{CDCl}_3$ ):  $\delta$  1.29 (6H, t,  $J=7.1$  Hz, two  $\text{OCH}_2\text{CH}_3$ ), 3.37 (4H, s, two  $\text{SCH}_2\text{CO}$ ), 3.95 (2H, s,  $\text{SCH}_2\text{S}$ ), 4.20 (4H, q,  $J=7.1$  Hz, two  $\text{OCH}_2\text{CH}_3$ ).

4-Carboethoxy-1,3-dithiacyclohexane-5-one<sup>188</sup> (43) (Scheme 6)

Sodium hydride (1.6 g, 0.067 mol) in THF (100 ml) was warmed to 60° in an oil bath. (42) (5.78g, 0.023 mol) in THF (60 ml) was added dropwise under  $\text{N}_2$  over a period of 1 h. The solution was refluxed for 2 h and set aside overnight. The unreacted sodium hydride was destroyed by addition of ethanol. The solution was then poured into ice-water/acetic acid mixture. The two layers were separated and the aqueous layer was extracted with ether (2x100 ml). The organic extracts

were combined, dried over anhydrous magnesium sulfate and concentrated to give a yellowish liquid. It was distilled to give (43), b.p.108-110°/0.7mm Hg. and solidified upon standing (2.1 g, 0.011 mol, 48%). <sup>1</sup>H NMR (400MHz, CDCl<sub>3</sub>):δ 1.36 (3H,t, J=7.2 Hz, CH<sub>3</sub>), 3.42 (2H,s, SCH<sub>2</sub>CO), 3.80 (2H,s, SCH<sub>2</sub>S), 4.29 (2H,q, J=7.2 Hz, OCH<sub>2</sub>CH<sub>3</sub>), 12.61 (1H,s, SCHCO).

Alternative route for the synthesis of (41).

1,3-Dimercaptopropan-2-ol<sup>238</sup> (51) (Scheme 6)

A solution of sodium hydroxide (75 g, 1.9 mol) in methanol (1.5 l) was saturated with hydrogen sulfide at 0°. Epichlorohydrin (18.5 g, 0.2 mol) was added to the sodium hydrogen sulfide solution and the reaction was set aside for 18 h. The cooled and stirred mixture was then brought to pH 4-5 by addition of concentrated hydrochloric acid. The white precipitate was filtered and the solvent was evaporated in vacuum to give a paste. Water was added and the product was extracted with chloroform (3x30 ml). The chloroform extracts were combined and washed with water (15 ml). After drying over anhydrous magnesium sulfate, a little ammonium acetate was added as a stabilizer and the solvent was evaporated. The oil obtained was distilled to give a colourless liquid, b.p.68-72°/2.8mm Hg. TLC (hexane/ethyl acetate (1/1))



indicated the presence of a component having an  $R_f$  value of 0.42. The sample was chromatographed on silica gel using the TLC solvent as eluant to give (51) (1.5 g, 0.01 mol, 5%).  $^1\text{H}$  NMR (400 MHz,  $\text{CDCl}_3$ ):  $\delta$  1.47 (2H, t,  $J=8.5$  Hz, 2SH's), 2.72 (4H, m, 2 $\text{CH}_2$ 's), 3.69 (1H, m,  $\text{CHOH}$ ).  $^{13}\text{C}$  NMR (100.6M Hz,  $\text{CDCl}_3$ ):  $\delta$  29.5 ( $\text{CH}_2$ ), 72.8 ( $\text{CHOH}$ ).

#### 5-Hydroxy-1,3-dithiacyclohexane (41) (Scheme 6)

A mixture of (51) (1.2 g, 9.7 mmol) and dimethoxymethane (0.8 g, 11 mmol) in chloroform (10 ml) was added slowly into a refluxing solution of boron trifluoride etherate (1.2 ml), acetic acid (2.3 ml) and chloroform (5 ml) over a period of 15 min. The solution was cooled to room temperature and washed successively with water (2x10 ml), aqueous potassium carbonate (10 ml) and water (10 ml). It was then dried over anhydrous potassium carbonate and concentrated to give a light yellow syrup. TLC (solvent hexane/ethyl acetate (7/3)) indicated the presence of a component having an  $R_f$  value of 0.47. The sample was chromatographed on silica gel using the TLC solvent as eluant to give a yellow semi-solid. It was distilled to give (41) (0.95 g, 7 mmol, 72%), b.p. 110°/3mm Hg. Recrystallization from hexane/ethyl acetate gave white crystals; m.p. 61-62°.  $^1\text{H}$  NMR (400 MHz,  $\text{CDCl}_3$ ):  $\delta$  2.77 (2H, ddd,  $J=1.7, 6.2, 13.8$  Hz, H-4a, H-6a), 3.07 (2H, dd,  $J=1.6, 13.8$  Hz, H-

4e,H-6e), 3.32 (2H,d,  $J=14.0$  Hz, H-2a with OH overlapped), 3.84 (1H,d,  $J=14.0$  Hz, H-2e), 3.97 (1H,bs,  $w_x=10.8$  Hz, H-5).  $^{13}\text{C}$  NMR (100.6MHz,  $\text{CDCl}_3$ ): $\delta$  30.6 (C-2), 36.4 (C-4,C-6), 59.9 (C-5).

Anal. Calcd. for  $\text{C}_4\text{H}_8\text{OS}_2$ : C,35.27, H,5.91. Found: C,35.51, H,5.80

2-Methyl-1,3-dithiacyclohexane-5-one<sup>188</sup> (48) (Scheme 6)

To a mixture of (45) (4.68 g, 0.039 mol) and acetaldehyde (0.65 g, 0.015 mol) at  $0^\circ$  was added boron trifluoride etherate (2.0 ml, 2.3 g, 0.015 mol). The solution was stirred overnight at  $4^\circ$ , and was then washed with 2N aqueous sodium hydroxide solution (40 ml) and water (40 ml). It was dried with anhydrous magnesium sulfate and concentrated to give the crude diester (4.91 g). The crude diester was cyclized as described for the case of (44) to give (49).

Compound (49) was hydrolyzed in 2N sulfuric acid as described above to give (48). It was distilled to give a colourless liquid, b.p.86-90°/2mm Hg, which crystallized upon standing. It was recrystallized in ethyl acetate/light petroleum ether (1.5 g, 0.01 mol, 26% ), m.p.38-39°.  $^1\text{H}$  NMR (400 MHz,  $\text{CDCl}_3$ ): $\delta$  1.62 (3H,d,  $J=6.8$  Hz,  $\text{CH}_3$ ), 3.32 (2H,d,  $J=14.5$  Hz, H-4a,H-6a), 3.59 (2H,d,  $J=14.5$  Hz, H-4e,H-6e), 4.54

(1H,q,  $J=6.8$  Hz, H-2).  $^{13}\text{C}$  NMR (100.6 MHz,  $\text{CDCl}_3$ ): $\delta$  36.91 (C-4, C-6), 39.94 (C-2), 201.75 (C-5)

cis- and trans-5-Hydroxy-2-methyl-1,3-dithiacyclohexane (46, 47) (Scheme 6)

To a solution of (48) (2.81 g, 19 mmol) in dry methanol (60 ml) was added sodium borohydride (0.98 g, 25 mmol). The solution was refluxed for 3 h. After cooling, the solution was washed with 1N HCl (10 ml) and water. It was dried with anhydrous magnesium sulfate and concentrated to give a colourless liquid. Column chromatography of the mixed hydroxides with hexane/ethyl acetate (2:1) as eluant gave (46) (2.18 g, 15 mmol) with an  $R_f$  value of 0.53 and the more polar, (47) (0.28 g, 1.8 mmol) with an  $R_f$  value of 0.40 (combined yield 2.46 g, 16 mmol, 86%).  $^1\text{H}$  NMR (400 MHz,  $\text{CDCl}_3$ ): $\delta$  (46) 1.42 (3H,d,  $J=7.0$  Hz,  $\text{CH}_3$ ), 2.81 (2H,dd,  $J_{gem}=13.8$  Hz,  $J_{ae}=4.7$  Hz, H-4a,H-6a), 3.12 (2H,dd,  $J_{gem}=13.8$  Hz,  $J_{ee}=1.4$  Hz, H-4e,H-6e), 3.55 (1H,d,  $J=11.9$  Hz, OH), 3.88 (1H,dt,  $J_{HOH}=11.9$  Hz,  $J_{ea}=4.7$  Hz,  $J_{ee}=1.4$  Hz, H-5e), 4.01 (1H,q,  $J=7.0$  Hz, H-2a). (47) 1.55 (3H,d,  $J=6.9$  Hz,  $\text{CH}_3$ ), 2.33 (1H,bs, OH), 2.75 (2H,dd,  $J_{gem}=13.9$  Hz,  $J_{aa}=9.0$  Hz, H-4a,H-6a), 2.93 (2H,dd,  $J_{gem}=13.9$  Hz,  $J_{ae}=3.0$  Hz, H-4e,H-6e), 3.94 (1H,q,  $J=6.9$  Hz, H-2a), 3.96 (1H,m, H-5a).

1,3-Dithiane-5-one (42) (Scheme 6)

Compound (43) (2.03 g, 0.01 mol) was hydrolyzed by refluxing for 4 h with 2N sulfuric acid (15 ml). After cooling, it was extracted with methylene chloride (3x40 ml). The organic extracts were combined, washed with water (3x20 ml) and aqueous sodium bicarbonate (20 ml). They were then dried with magnesium sulfate and concentrated to give a yellowish powder. Recrystallization from ethyl acetate/hexane gave (42) (1.30 g, 0.097 mol, 98%), m.p.103-104°. <sup>1</sup>H NMR (at 100 MHz in CDCl<sub>3</sub>):δ 3.44 (4H,s, 2H-4's,2H-6's), 3.91 (2H,s, 2H-2's). <sup>13</sup>C NMR (100.6 MHz, CDCl<sub>3</sub>):δ 29.72 (SCH<sub>2</sub>S), 37.90 (2x SCH<sub>2</sub>CO), 201.01 (C=O).

Anal. Calcd. for C<sub>4</sub>H<sub>6</sub>OS<sub>2</sub>: C,35.80, H,4.51. Found: C,35.87, H,4.42.

5-Hydroxy-1,3-dithiacyclohexane (41) (Scheme 6)

To (42) (0.35 g, 2.6 mmol) in dry methanol (40 ml) was added sodium borohydride (0.1 g, 2.6 mmol). The solution was refluxed for 3 h. After cooling, the solution was washed with 1N HCl (10 ml), and washed with water. It was then dried with anhydrous magnesium sulfate and concentrated to give a colourless liquid which was identified as being (41) (0.33 g, 2.4 mmol, 92%).

5-Methylamino-1,3-dithiacyclohexane (13) (Scheme 7)

Methylamine (1.73 g, 60 mmol) was bubbled into formic acid (85%, 4 ml) in an ice bath. Compound (42) (1.34 g, 10 mmol) was then added, the solution was warmed slowly to reflux during 1 h and kept refluxing for 1 h. 6M HCl (15 ml) was added and the solution was refluxed for another 1 h.<sup>239</sup> The solution was cooled and was basified with sodium hydroxide solution (8 g, 50 ml). The aqueous layer was separated and the insoluble residue formed was rinsed with water. The washings were added to the basic solution. The combined aqueous solution was extracted with ether (3x50 ml), the ethereal extracts were washed with water (10 ml) and dried over anhydrous potassium carbonate. The extracts were concentrated and the residue was distilled to give a yellowish oil which was identified as being (13) (0.26 g, 1.7 mmol, 17%), b.p.85-90°/0.3mm Hg. <sup>1</sup>H NMR (400 MHz, CDCl<sub>3</sub>): δ 2.42 (3H, s, NCH<sub>3</sub>), 2.69 (2H, dd, J<sub>gem</sub>=13.2 Hz, J<sub>ax</sub>=6.8 Hz, H-4a, H-6a), 2.78 (1H, dt, J<sub>ax</sub>=6.8, J<sub>ex</sub>=2.0 Hz, H-5), 2.95 (2H, dd, J<sub>gem</sub>=13.2, J<sub>ex</sub>=2.0 Hz, H-4e, H-6e), 3.44 (1H, d, J= 13.8 Hz, H-2e), 3.76 (1H, d, J=13.8 Hz, H-2a). <sup>13</sup>C NMR (100.6 MHz, CDCl<sub>3</sub>): δ 31.28 (C-2), 32.76 (NCH<sub>3</sub>), 34.11 (C-4, C-6), 50.61 (C-5). Mass spect. exact mass M, 149.0333. C<sub>5</sub>H<sub>11</sub>NS<sub>2</sub> requires M, 149.0334.

5-Methoxy-1,3-dithiacyclohexane (14) (Scheme 7)

To a suspension of sodium hydride (0.05 g, 0.02 mol) in THF (20 ml) was added a solution of (41) (0.15g, 1.1 mmol) in THF (10 ml). Iodomethane (0.18 g, 1.2 mmol) was added slowly and the mixture was stirred overnight at room temperature. The reaction was quenched by the addition of 1N sodium hydroxide solution (2 ml). The organic layer was separated, washed with water (5 ml) and dried with anhydrous potassium carbonate. It was concentrated to give (14) (0.15g, 1 mmol, 91%).  $^1\text{H}$  NMR (400 MHz,  $\text{CDCl}_3$ ): $\delta$  2.65 (2H, *dd*,  $J=14.0, 10.0$  Hz, H-4a,6a), 2.93 (2H, *dm*,  $J=14.0$  Hz, H-4e,6e), 3.34 (1H, *dt*,  $J=13.8, 1.5$  Hz, H-2e), 3.40 (3H, *s*,  $\text{OCH}_3$ ), 3.55 (1H, *m*, H-5a), 3.86 (1H, *d*,  $J=13.8$  Hz, H-2a).  $^{13}\text{C}$  NMR (100.6 MHz,  $\text{CFCl}_3/\text{CD}_2\text{Cl}_2$ ): $\delta$  31.9 (C-2), 34.6 (C-4,C-6), 56.8 ( $\text{OCH}_3$ ), 77.5 (C-5).

Anal. Calcd. for  $\text{C}_5\text{H}_{10}\text{OS}_2$ : C,40.00, H,6.67. Found: C,40.14, H,6.78.

cis-5-Methoxy-2-methyl-1,3-dithiacyclohexane (15) (Scheme 7)

Compound (15) (0.31 g, 1.9 mmol, 60%) was prepared from (46) (0.48 g, 3.2 mmol), as described for the synthesis of (14).  $^1\text{H}$  NMR (400 MHz,  $\text{CDCl}_3$ ): $\delta$  1.59 (3H, *d*,  $J=7.0$  Hz,  $\text{CH}_3$ ), 2.93 (2H, *dd*,  $J_{\text{gem}}=14.0$  Hz,  $J_{\text{ex}}=3.2$  Hz, H-4e, H-6e), 2.98 (2H, *dd*,  $J_{\text{gem}}=14.0$ ,  $J_{\text{ax}}=5.5$  Hz, H-4a,H-6a), 3.46 (1H, *tt*,

$J_{ax}=5.5, J_{ex}=3.2$  Hz, H-5), 3.97 (1H, q,  $J=7.0$  Hz, H-2a).  $^{13}\text{C}$  NMR (at 100.6 MHz in  $\text{CFCl}_3/\text{CD}_2\text{Cl}_2$  (85/15)):  $\delta$  23.17 ( $\text{CH}_3$ ), 31.37 (C-4, C-6), 39.63 (C-2), 56.58 ( $\text{OCH}_3$ ), 72.88 (C-5).

Anal. Calcd. for  $\text{C}_6\text{H}_{12}\text{OS}_2$ : C, 43.87; H, 7.36. Found: C, 43.54; H, 7.05

cis- and trans-2-Hydroxy-4-methyloxacyclohexanes<sup>240,241</sup> (52)  
(Scheme 8)

A mixture of freshly distilled crotonaldehyde (30.0 g, 0.43 mol) and isobutyl vinyl ether (47.3 g, 0.47 mol) was heated in a bomb at 210-220° for 3 h. The resulting yellow liquid was distilled to give 2-isobutoxy-4-methyl-5,6-dihydropyran (54) as a colourless liquid (48.7 g, 0.29 mol, 67%), b.p. 75-77°/20mm Hg, lit.<sup>240</sup> 86-90°/13mm Hg.

Compound (54) (5 g, 0.029 mol) in 95% ethanol was hydrogenated at 40 psi, at room temperature over 10% Pd/C catalyst (5.0 g) for 24 h. After filtration through celite, the solution was distilled to yield 2-isobutoxy-4-methyloxacyclohexane (53) (4.6 g, 0.027 mol, 92%), b.p. 40-41°/0.3mm Hg, lit.<sup>241</sup> 79-86°/4-5mm Hg.

A mixture of (53) (35.0 g, 0.2 mol) and 10% sulfuric acid (70 ml) was heated on a steam bath for 1 h and then steam distilled. The aqueous layer of the distillate was

continuously extracted with ether for 48 h. The ether extract was combined with the organic layer of the steam distillate and dried over anhydrous potassium carbonate. Evaporation of the solvent followed by distillation gave crude (52); b.p. 95-100°/20mm Hg (lit.<sup>240</sup> 75-80°/5mm Hg). TLC with hexane/ethyl acetate (4/1) indicated the presence of a non-polar and polar component with  $R_f$  values of 0.79 and 0.16, respectively. The sample was chromatographed on silica gel using the TLC solvent as eluant to eliminate the non-polar impurity and the desired product (2.5 g, 0.02 mol, 10%) was eluted with ethyl acetate.

The  $^{13}\text{C}$  and  $^1\text{H}$  NMR signals of the cis and trans isomers could not be distinguished owing to their similarities in chemical shifts and population.  $^1\text{H}$  NMR (400 MHz,  $\text{CDCl}_3$ ):  $\delta$  0.91, 0.96 (3H, 3H, *d*,  $J=6.6$  Hz,  $\text{CH}_3$ 's), 1.02, 1.23 (2H, 2H, *m*, H-5a's, H-3a's), 1.48, 1.56 (1H, 1H, *dm*,  $J_{\text{gem}}=13.5$  Hz, H-5e's), 1.66, 1.99 (1H, 1H, *m*, H-4a's), 1.73 (1H, *dddd*,  $J=13.5$ , 3.8, 1.9, 1.9 Hz, H-3e), 1.88 (1H, *dddd*,  $J=12.8$ , 3.8, 1.9, 1.9 Hz, H-3e), 3.47 (1H, *ddd*,  $J=10.8$ , 10.8, 2.4 Hz, H-6a), 3.62 (1H, *ddd*,  $J=11.1$ , 4.5, 2.1 Hz, H-6e), 3.99 (2H, *m*, H-6a, H-6e), 4.65 (1H, *dd*,  $J_{\text{aa}}=9.5$  Hz,  $J_{\text{ae}}=2.1$  Hz, H-2a), 5.27 (1H, *bd s*, H-2e).  $^{13}\text{C}$  NMR (100.6 MHz,  $\text{CDCl}_3$ ):  $\delta$  21.6, 21.9 ( $\text{CH}_3$ 's), 23.4, 29.2 (C-4's), 33.4, 33.9 (C-5's), 38.6, 41.3 (C-3's), 59.4, 65.4 (C-6), 91.3, 96.0 (C-2's).



#### 4-Methylthiacyclohexane (55) (Scheme 8)

Compound (52) (0.57 g, 4.9 mmol) in water (5 ml) was added dropwise, with stirring to a solution of sodium borohydride (0.16 g, 4.2 mmol) in water (8 ml). The temperature of the reaction was kept at  $\approx 30^\circ$ . After stirring for an additional 20 min., Rexyn 101(H) was added until the evolution of gas stopped. The solution was diluted with water (30 ml) and additional Rexyn 101(H) ( $\approx 1$  g) was added. After filtration, the solution was concentrated to give the diol (57) as a syrup (0.41 g, 3.4 mmol, 70%).

Compound (57) (0.41 g, 3.4 mmol) was tosylated in the usual manner with *p*-toluenesulfonyl chloride (2.19 g, 11.5 mmol) to give the crude 1,5-di-*p*-toluenesulfonyl-3-methylpropane (56) (0.35 g, 0.8 mmol, 23%). The desired product (0.20 g, 0.47 mmol, 14%) was purified by column chromatography with hexane/methylene chloride (1/1) as the eluant.

Compound (54) (0.20 g, 0.47 mmol) in THF (5ml) and sodium sulfide (3 ml, 2M) in ethanol (70%) were added to a refluxing solution of sodium sulfide (5 ml, 2M) in ethanol (70%). The solution was refluxed overnight. The resulting solution was steam distilled. The distillate was diluted with water and extracted with pet. ether (40-60°) (4x100 ml). The extracts were combined, washed with water (3x50 ml) and dried over anhydrous sodium sulfate. The solvent was evaporated to give

a yellowish liquid which was distilled to give (55) (0.04 g, 0.34 mmol, 75%), b.p. 155-160°, lit.<sup>242</sup> 156-159° as a colourless liquid. <sup>1</sup>H NMR (400 MHz, CDCl<sub>3</sub>): δ 0.88 (3H, d, J=6.1 Hz, CH<sub>3</sub>), 1.29 (2H, ddd, J=12.2, 12.0, 3.1 Hz, H-3a, 5a), 1.37 (1H, m, H-4a), 1.91 (2H, dm, J=12.0 Hz, H-3e, 5e), 2.54 (2H, dm, J=13.5 Hz, H-2e, 6e), 2.62 (2H, ddd, J=13.5, 12.2, 3.5 Hz, H-2a, 6a). <sup>13</sup>C NMR (100.6 MHz, CDCl<sub>3</sub>): δ 23.1 (CH<sub>3</sub>), 30.0 (C-2, C-6), 32.3 (C-4), 36.3 (C-3, C-5).

2-Benzoyloxy-1,4-dithiacyclohexane<sup>243</sup> (59) (Scheme 9)

A solution of 1,4-dithiacyclohexane (3.0 g, 0.025 mol) in benzene (30 ml) and benzoyl peroxide (6.0 g, 0.025 mol) in benzene (60 ml) were dropped into refluxing benzene (60 ml) dropwise during 2 h and the mixture was then refluxed under nitrogen for 6 h. The mixture was cooled, and was washed successively with sodium hydrogen carbonate solution (40 ml) and water (20 ml). The mixture was dried over anhydrous magnesium sulfate and the solvent was evaporated to give a syrup. TLC hexane/ethyl acetate (5/1) indicated the presence of a new component having an *R<sub>f</sub>* value of 0.56. The syrup was chromatographed on silica gel using the TLC solvent as eluant to give (59) as a white solid which was recrystallized from methanol to give white crystals (0.92 g, 0.004 mol, 15%), m.p. 84-85°, lit.<sup>108</sup> 83-85°. <sup>1</sup>H NMR (400 MHz, CDCl<sub>3</sub>): δ 2.79

(2H, *m*, H-5a, H-5e), 3.03 (1H, *dd*,  $J=5.2, 14.4$  Hz, H-3a), 3.13 (1H, *ddd*,  $J=2.0, 11.5, 13.5$  Hz, H-6a), 3.42 (1H, *dd*,  $J=2.1, 13.5$  Hz, H-6e), 3.45 (1H, *dd*,  $J=2.4, 14.4$  Hz, H-3e), 6.08 (1H, *dd*,  $J=2.4, 5.2$  Hz,  $w_{\frac{1}{2}}=9.4$  Hz, H-2), 7.44-7.66 (3H, *m*, Ph), 8.17 (2H, *m*, Ph).  $^{13}\text{C}$  NMR (100.6 MHz,  $\text{CDCl}_3$ ):  $\delta$  26.1 (C-6), 27.7 (C-5), 33.2 (C-3), 67.9 (C-2), 128.2, 129.6, 133.0 (Ph), 164.7 (CO).

### 2-Hydroxy-1,4-dithiacyclohexane (58) (Scheme 9)

To a solution of (59) (0.2 g, 0.8 mmol) in absolute methanol (10 ml) at 0° was added sodium metal (50 mg). The mixture was stirred at 4° for 16 h and then neutralized with moist Rexyn 101(H) at 0° to pH 8. The resin was removed by filtration and the solvent was evaporated to give a syrup which was shown by TLC hexane/ethyl acetate (3/1) to consist of a component having an  $R_f$  value of 0.38 and methyl benzoate. Chromatography on silica gel using the TLC solvent as eluant gave (58) as a white solid (0.06 g, 0.44 mmol, 53%).  $^1\text{H}$  NMR (400 MHz,  $\text{CDCl}_3$ ):  $\delta$  2.68 (2H, *m*, H-5a, H-5e), 2.88 (1H, *dd*,  $J=4.8, 13.6$  Hz, H-3a), 3.05, 3.34 (2H, *2ddd*,  $J=2.1, 11.5, 13.6$  Hz, H-6a, H-6e), 3.47 (1H, *dd*,  $J=1.7, 13.6$  Hz, H-3e), 3.65 (1H, *d*,  $J=9.6$  Hz, OH), 4.93 (1H, *dd*,  $J=4.8, 9.6$  Hz, H-2).  $^{13}\text{C}$  NMR (100.6 MHz,  $\text{CDCl}_3$ ):  $\delta$  25.5 (C-5), 28.7 (C-6), 37.4 (C-3), 67.6 (C-2).

Anal. Calcd. for  $C_4H_8OS_2$ : C, 35.30; H, 5.92. Found:  
C, 35.30; H, 5.86.

2-Methylamino-1,4-dithiacyclohexane (16) (Scheme 9)

A solution of (58) (0.19 g, 1.4 mmol) in methanol (20 ml) at 0° was added aqueous methylamine (2 ml, 40%). After 1 h, potassium carbonate (0.2 g) was added. The mixture was stirred at 0° for 2 h. The mixture was diluted with water (10 ml) and was extracted with methylene chloride (4x20 ml). The extracts were dried over potassium carbonate and concentrated to give a clear syrup which was identified as being (16) (0.14 g, 0.94 mmol, 67%).  $^1H$  NMR (400 MHz,  $CDCl_3$ ):  $\delta$  2.52 (3H, s, NCH<sub>3</sub>), 2.63 (2H, m, H-5e, H-6e), 2.82 (1H, dd,  $J_{vic}=4.8$ ,  $J_{gem}=13.5$  Hz, H-3a), 2.97 (2H, m, H-5a, H-6a), 3.45 (1H, dd,  $J_{vic}=2.5$ ,  $J_{gem}=13.5$  Hz, H-3e), 3.83 (1H, dd,  $J=2.5, 4.8$ ,  $w_x=10.0$  Hz, H-2).  $^{13}C$  NMR (100.6 MHz  $CFCl_3/CD_2Cl_2$  (85/15)):  $\delta$  26.0 (C-6), 30.1 (C-5), 34.1 (CH<sub>3</sub>), 37.8 (C-3), 60.5 (C-2).

Anal. Calcd. for  $C_5H_{11}NS_2$ : C, 40.23; H, 7.43. Found:  
C, 39.98; H, 7.29.

2-Benzoyloxythiacyclohexane<sup>243</sup> (61) (Scheme 9)

Solutions of thiacyclohexane (6.3 g, 0.06 mol) in benzene (25 ml) and tert-butylperoxybenzoate (11.1 g, 0.06 mol) in

benzene (100 ml) were dropped into a mixture of refluxing benzene containing cuprous chloride (0.02 g) over a period of 2 h and the mixture was refluxed under nitrogen for 36 h. The solution was cooled to RT, and was washed successively with 2N sodium carbonate solution (2x30 ml) and water (40 ml). The solution was dried over anhydrous magnesium sulfate and the solvent was evaporated to give a syrup. TLC hexane/ethyl acetate (9/1) indicated the presence of a new component having an  $R_f$  value of 0.70. The sample was chromatographed on silica gel using the TLC solvent as eluant to give (61) as a colourless liquid (8.5 g, 0.04 mol, 62%).  $^1\text{H}$  NMR (400 MHz,  $\text{CDCl}_3$ ):  $\delta$  1.73-2.14 (5H, *m*, H-3a, 2H-4's, 2H-5's), 2.22 (1H, *dd*,  $J=3.5, 14.0$  Hz, H-3e), 2.50 (1H, *ddd*,  $J=3.7, 3.7, 13.5$  Hz, H-6e), 3.09 (1H, *ddd*,  $J=2.9, 12.7, 13.5$  Hz, H-6a), 6.11 (1H, *m*,  $w_{1/2}=8.5$  Hz, H-2), 7.39-7.62 (3H, *m*, Ph), 8.08 (2H, *m*, Ph).  $^{13}\text{C}$  NMR (100.6 MHz,  $\text{CDCl}_3$ ):  $\delta$  20.6 (C-4), 25.3 (C-5), 26.2 (C-6), 32.2 (C-3), 72.3 (C-2), 128.3, 129.5, 130.4, 132.9 (Ph), 165.0 (CO).

#### 2-Hydroxythiacyclohexane<sup>245</sup> (60) (Scheme 9)

To a solution of (61) (1.5 g, 6.8 mmol) in absolute methanol (25 ml) at 0° was added sodium metal (20 mg). The mixture was stirred at 0° for 1 h, and then at RT for another 3 h. It was then neutralized with moist Rexyn 101(H) to pH 8.

The resin was removed by filtration and the solvent was evaporated to give a syrup which was shown by TLC (hexane/ethyl acetate (85/15)) to consist of one component having an  $R_f$  value of 0.35, and methyl benzoate. The sample was chromatographed on silica gel using the TLC solvent as eluant to give (60) as a colourless liquid (0.42 g, 3.6 mmol, 52%), 85-90°/0.5mm Hg, lit.<sup>243</sup> 71°/0.3mm Hg.  $^1\text{H}$  NMR (400 MHz,  $\text{CDCl}_3$ ):  $\delta$  1.53-2.03 (6H, *m*, 2H-3's, 2H-4's, 2H-5's), 2.44 (1H, *ddd*,  $J=4.2, 4.2, 13.5$  Hz, H-6e), 3.02 (1H, *ddd*,  $J=3.0, 11.5, 13.5$  Hz, H-6a), 4.97 (1H, *m*,  $w_{1/2}=8.0$  Hz, H-2).  $^{13}\text{C}$  NMR (100.6 MHz,  $\text{CDCl}_3$ ):  $\delta$  20.5 (C-4), 25.1 (C-5), 26.7 (C-6) 34.1 (C-3), 71.3 (C-2).

#### 2-Methylaminothiacyclohexane (17) (Scheme 9)

(17) (0.26 g, 2.0 mmol, 87%) was prepared from (60) (0.27 g, 2.3 mmol) as described for the synthesis of (16).  $^1\text{H}$  NMR (400 MHz,  $\text{CDCl}_3$ ):  $\delta$  1.41-1.92 (5H, *m*, H-4a, 4e, H-5a, 5e, H-3e), 2.13 (1H, *m*, H-3e), 2.52 (3H, *s*,  $\text{NCH}_3$ ), 2.53 (1H, *m*, H-6e), 2.68 (1H, *m*, H-6e), 3.78 (1H, *dd*,  $J=8.9, 3.2$  Hz, H-2).  $^{13}\text{C}$  NMR (100.6 MHz,  $\text{CFCl}_3/\text{CD}_2\text{Cl}_2$  (85/15)):  $\delta$  25.8 (C-4), 28.0 (C-5), 28.7 (C-6), 34.6 ( $\text{NCH}_3$ ), 36.9 (C-3), 64.6 (C-2).

Anal. Calcd. for  $\text{C}_6\text{H}_{13}\text{NS}$ : C, 54.91; H, 9.98; N, 10.67.

Found: C, 55.16; H, 9.72; N, 10.46.

2-Benzoyloxy-1,4-dioxacyclohexane<sup>243</sup> (63) (Scheme 9)

t-Butylperoxybenzoate (7.8 g, 0.04 mol) was added over a period of 0.5 h to a stirred mixture of p-dioxacyclohexane (8.8 g, 0.1 mol) and cuprous chloride (0.02 g, 0.2 mmol) maintained at 105-110°. The solution was refluxed for 2 h. After cooling, the solution was diluted with ether (20 ml), and was extracted with sodium carbonate solution (2N). The ethereal solution was washed with water, dried over anhydrous sodium sulfate and concentrated to a colourless liquid which was distilled to give (63) (4.5 g, 0.022 mol, 54%), bp 122-125°/1.5mm Hg, lit.<sup>243</sup> 105-107/0.1mm Hg. <sup>1</sup>H NMR (400 MHz, CDCl<sub>3</sub>): δ 3.62-4.27 (6H, *m*'s, 2H-3's, 2H-5's, 2H-6's), 6.08 (1H, *t*, *J*=2.6 Hz, H-2), 7.39-7.62 (3H, *m*, Ph), 8.08-8.16 (2H, *m*, Ph). <sup>13</sup>C NMR (100.6 MHz, CDCl<sub>3</sub>): δ 61.8 (C-5), 66.0 (C-6), 67.8 (C-3), 89.9 (C-2), 128.5, 130.0, 133.4 (Ph), 165.3 (CO).

Anal. Calcd. for C<sub>11</sub>H<sub>12</sub>O<sub>4</sub>: C, 63.45; H, 5.81. Found: C, 63.54; H, 5.83.

2-Hydroxy-1,4-dioxacyclohexane (62) (Scheme 9)

The compound was prepared from (63) (4.5 g, 0.022 mol), as described for the case of (58). The crude product was obtained as a syrup. TLC hexane/ethyl acetate (2:1) indicated one component having an *R<sub>f</sub>* value of 0.2, and methyl benzoate.

Column chromatography on silica gel using the same TLC solvent as eluant afforded a solid which was identified as being (62) (1.56 g, 0.015 mol, 68%). Recrystallization from hexane/ethyl acetate gave colourless crystals, m.p.37-38°. <sup>1</sup>H NMR (400 MHz, CDCl<sub>3</sub>):δ 3.38 (1H, *dd*, *J*=4.8, 11.8 Hz, H-3a), 3.58-3.76 (3H, *m*, 2H-5's, H-6e), 3.78 (1H, *dd*, *J*=2.2, 11.8 Hz, H-3e), 4.07 (1H, *m*, H-6a), 4.91 (1H, *dd*, *J*=2.2, 4.8 Hz, *w*<sub>1/2</sub>=9.1 Hz, H-2). <sup>13</sup>C NMR (100.6 MHz, CDCl<sub>3</sub>):δ 62.4 (C-5), 66.0 (C-6), 70.0 (C-3), 90.8 (C-2).

Anal. Calcd. for C<sub>4</sub>H<sub>8</sub>O<sub>3</sub>: C,46.15; H,7.75. Found: C,46.20; H,7.93.

### 2-Methylamino-1,4-dioxacyclohexane (18) (Scheme 9)

A mixture of (62) (0.12 g, 1.1 mmol) in methanol (2 ml) was treated with aqueous methylamine (2 ml, 40%) and potassium carbonate (0.2 g), as described for the synthesis of (16). Compound (18) was obtained as a clear liquid (0.11 g, 0.94 mmol, 85%). <sup>1</sup>H NMR (400 MHz, CDCl<sub>3</sub>):δ 2.52 (3H, *s*, NCH<sub>3</sub>), 3.20 (1H, *dd*, *J*<sub>vic</sub>=8.0, *J*<sub>gem</sub>=11.5 Hz, H-3a), 3.53 (1H, *ddd*, *J*<sub>ae</sub>=2.8, *J*<sub>aa</sub>=9.6, *J*<sub>gem</sub>=11.5 Hz, H-5a), 3.67 (1H, *dt*, *J*<sub>ea</sub>=2.6, *J*<sub>ee</sub>=2.6, *J*<sub>gem</sub>=11.5 Hz, H-5e), 3.73 (1H, *ddd*, *J*<sub>ae</sub>=2.8, *J*<sub>aa</sub>=9.6, *J*<sub>gem</sub>=12.1 Hz, H-6a), 3.82 (2H, *m*, H-6e, H-3e), 4.11 (1H, *dd*, *J*=2.5, 8.0 Hz, H-2). <sup>13</sup>C NMR (100.6 MHz, CDCl<sub>3</sub>):δ 31.7 (CH<sub>3</sub>), 64.3 (C-6), 66.3 (C-5), 70.4 (C-3), 85.9 (C-2). <sup>13</sup>C NMR



(100.6 MHz,  $\text{CFCl}_3/\text{CD}_2\text{Cl}_2$  (85/15)):  $\delta$  33.2 ( $\text{CH}_3$ ), 65.7 (C-6), 66.2 (C-5), 70.5 (C-3), 87.1 (C-2).

Anal. Calcd. for  $\text{C}_5\text{H}_{11}\text{NO}_2$ : C, 51.26; H, 9.46; N, 11.96.  
Found: C, 51.16; H, 9.42; N, 11.59.

### 3-Hydroxy-1-oxa-4-thiacyclohexane (64) (Scheme 9)

The compound was prepared from (65) (3.1 g, 0.019 mol), as described for the synthesis of (58). It was obtained as a syrup (1.5 g, 0.013 mol, 66%).  $^1\text{H}$  NMR data (400 MHz,  $\text{CDCl}_3$ ):  $\delta$  2.31 (1H, *dm*,  $J=14$  Hz, H-5e), 3.29 (1H, *ddd*,  $J=3.5, 11.5, 14.0$  Hz, H-5a), 3.81 (1H, *ddd*,  $J=2.3, 11.5, 11.5$  Hz, H-6a), 3.93 (1H, *dd*,  $J=1.8, 11.5$  Hz, H-6e), 4.06 (1H, *dd*,  $J=2.7, 12.0$  Hz, H-2e), 4.18 (1H, *ddd*,  $J=3.0, 3.0, 12.0$  Hz, H-2a), 4.68 (1H, *bd s*,  $w_{1/2}=8.5$  Hz, H-3)  $^{13}\text{C}$  NMR (100.6 MHz,  $\text{CDCl}_3$ ):  $\delta$  23.1 (C-5), 68.3 (C-6), 68.5 (C-2), 73.5 (C-3).

Anal. Calcd. for  $\text{C}_4\text{H}_8\text{O}_2\text{S}$ : C, 39.98; H, 6.71. Found: C, 39.93; H, 6.74

### 3-Methylamino-1-oxa-4-thiacyclohexane (19) (Scheme 9)

A solution of (64) (0.42 g, 3 mmol) in methanol (4 ml) at  $0^\circ$  was treated with aqueous methylamine (4 ml, 40%) with stirring. After 1 h, potassium carbonate (0.2 g) was added.

The solution was worked up as described for the case of (16). Compound (19) was obtained as a clear liquid (0.25 g, 2.1 mmol, 70%).  $^1\text{H}$  NMR (400 MHz,  $\text{CDCl}_3$ ):  $\delta$  2.36 (1H, *dt*,  $J_{ee}=J_{ea}=2.5$  Hz,  $J_{gem}=14.0$  Hz, H-5e), 2.53 (3H, *s*,  $\text{NCH}_3$ ), 2.88 (1H, *ddd*,  $J_{ae}=3.2$ ,  $J_{aa}=10.1$ ,  $J_{gem}=14.0$  Hz, H-5a), 3.65 (1H, *t*,  $J=3.3$  Hz,  $w_{1/2}=7.5$  Hz, H-3), 3.84 (1H, *ddd*,  $J_{ae}=2.5$ ,  $J_{aa}=10.0$ ,  $J_{gem}=11.8$  Hz, H-6a), 3.94 (1H, *dd*,  $J_{vic}=3.5$ ,  $J_{gem}=11.6$  Hz, H-2a), 4.01 (1H, *dt*,  $J_{ee}=2.5$ ,  $J_{ea}=3.2$ ,  $J_{gem}=11.8$  Hz, H-6e), 4.09 (1H, *dd*,  $J_{vic}=2.5$ ,  $J_{gem}=11.6$  Hz, H-2e).  $^{13}\text{C}$  NMR (100.6 MHz,  $\text{CDCl}_3$ ):  $\delta$  23.5 (C-5), 33.3 ( $\text{CH}_3$ ), 59.9 (C-3), 68.9 (C-6), 74.1 (C-2).  $^{13}\text{C}$  NMR (100.6 MHz,  $\text{CFCl}_3/\text{CD}_2\text{Cl}_2$  (85/15)):  $\delta$  24.6 (C-5), 34.6 ( $\text{CH}_3$ ), 61.6 (C-3), 70.2 (C-6), 75.6 (C-2).

Anal. Calcd. for  $\text{C}_5\text{H}_{11}\text{NOS}$ : C, 45.08; H, 8.32; N, 10.51.  
Found: C, 44.96; H, 8.51; N, 10.15.

#### 2-Methylamino-1-oxa-4-thiacyclohexane (20) (Scheme 9)

A solution of (67) (0.14 g, 1.2 mmol) in methanol (3 ml) at  $0^\circ$  was treated with aqueous methylamine (3 ml, 40%) and potassium carbonate (0.2 g), as described for (16). Compound (20) was obtained as a clear liquid (0.31 g, 0.98 mmol, 81%).  $^1\text{H}$  NMR (400 MHz,  $\text{CDCl}_3$ ):  $\delta$  2.38 (1H, *dm*,  $J_{gem}=14.0$  Hz, H-5e), 2.49 (3H, *s*,  $\text{NCH}_3$ ), 2.53 (1H, *dd*,  $J_{vic}=8.0$ ,  $J_{gem}=13.2$  Hz, H-3a), 2.65 (2H, *m*,  $J_{ae}=3.0$ ,  $J_{aa}=9.2$ ,  $J_{gem}=14.0$  Hz, H-5a, H-3e), 3.81 (1H, *ddd*,  $J_{ae}=2.5$ ,  $J_{aa}=9.2$ ,  $J_{gem}=12.0$  Hz, H-6a), 4.18 (2H, *m*, H-6e,

H-2).  $^{13}\text{C}$  NMR (100.6 MHz,  $\text{CDCl}_3$ ):  $\delta$  26.4 (C-5), 31.3 (C-3), 31.4 ( $\text{CH}_3$ ), 66.3 (C-6), 87.4 (C-2).  $^{13}\text{C}$  NMR (100.6 MHz,  $\text{CFCl}_3/\text{CD}_2\text{Cl}_2$  (85/15)):  $\delta$  27.6 (C-5), 32.6 (C-3,  $\text{CH}_3$ ), 67.4 (C-6), 88.6 (C-2).

Anal. Calcd. for  $\text{C}_5\text{H}_{11}\text{NOS}$ : C, 45.08; H, 8.32; N, 10.51.  
Found: C, 44.94; H, 8.42; N, 10.54.

#### 4-Methyl-2-methylaminooxacyclohexane (21) (Scheme 9)

A solution of (52) (0.28 g, 2.4 mmol) in methanol (20 ml) at  $0^\circ$  was treated with aqueous methylamine (6 ml, 40%), as described for the case of (16). Compound (21) was obtained as a colourless liquid (0.17 g, 1.4 mmol, 58%), b.p.  $73-75^\circ/24\text{mm Hg}$ , lit.<sup>250</sup>  $53^\circ/18\text{mm Hg}$ .  $^1\text{H}$  NMR (400 MHz,  $\text{CDCl}_3$ ):  $\delta$  cis isomer 0.89 (1H, *m*, H-3a), 0.95 (3H, *d*,  $J=6.5$  Hz,  $\text{CH}_3$ ), 1.13 (1H, *ddd*,  $J=12.5, 12.5, 12.5, 4.5$  Hz, H-5a), 1.50 (1H, *dm*,  $J=13.0$  Hz, H-3e), 1.64 (1H, *m*, H-4), 1.77 (1H, *dm*,  $J=12.5$  Hz, H-5e), 2.51 (3H, *s*,  $\text{NCH}_3$ ), 3.42 (1H, *dt*,  $J=12.0, 12.0, 2.1$  Hz, H-6a), 3.83 (1H, *dd*,  $J=10.1, 2.0$  Hz, H-2), 3.97 (1H, *ddd*,  $J=12.0, 4.5, 1.3$  Hz, H-6e).  $\delta$  trans isomer (minor): 0.98 (3H, *d*,  $J=6.6$  Hz,  $\text{CH}_3$ ), 1.23 (1H, *m*, H-5a), 2.44 (3H, *s*,  $\text{NCH}_3$ ), 3.63 (2H, *m*, H-6a, 6e), 4.32 (1H, *t*,  $J=4.3$  Hz, H-2).  $^{13}\text{C}$  NMR (100.6 MHz,  $\text{CDCl}_3$ ): cis isomer 22.0 ( $\text{CH}_3$ ), 30.5 (C-4), 31.8 (C-5), 34.4 (C-3), 41.1 ( $\text{NCH}_3$ ), 66.2 (C-6), 89.5 (C-2).

1,4-Dithiacyclohex-2-ene<sup>244</sup> (68) (Scheme 10)

Compound (59) (0.25 g, 1.04 mmol) was dissolved in benzene (30 ml) containing a catalytic amount of *p*-toluenesulfonic acid, and the mixture was refluxed for 2 h. The benzene solution was washed with sodium hydrogen carbonate solution (2x20 ml) and water (20 ml). The solution was dried over anhydrous magnesium sulfate and the solvent was evaporated to give (68) as a colourless liquid (0.11 g, 0.93 mmol, 89%), b.p.102-104/24mm Hg, lit.<sup>244</sup> 128-132/44mm Hg. <sup>1</sup>H NMR (100.13 MHz, CDCl<sub>3</sub>):δ 3.18 (4H,*s*, 2H-5's,2H-6's), 6.07 (2H,*s*, H-2,H-3). <sup>13</sup>C NMR (100.6 MHz, CDCl<sub>3</sub>):δ 26.3 (C-5,C-6), 114.4 (C-2,C-3).

Thiacyclohex-2-ene<sup>246</sup> (69) (Scheme 10)

To a solution of thiacyclohexane (10.4 g, 0.10 mol) in methanol (30 ml) at 0° was added a solution of sodium periodate (24.0 g, 0.11 mol) in water (250 ml). The solution was stirred at 4° for 16 h. The solvent was evaporated in vacuo and the residue was extracted with methylene chloride. The extract was filtered and concentrated to give a white solid (70) (10.8 g, 0.09 mol, 90%). The sulfoxide (70) was dissolved in dry benzene (100 ml) containing a catalytic amount of *p*-toluenesulfonic acid. Acetic anhydride (12.5 ml, 0.14 mol) was added and the mixture was refluxed for 24 h

under nitrogen. After cooling, sodium hydrogen carbonate solution was added and the mixture was stirred vigorously for 2 h. The two layers were separated and the benzene layer was washed with water (30 ml). The solution was dried over anhydrous sodium sulfate, and the solvent was evaporated to give a liquid which was distilled to give (69) as a colourless liquid (6.3 g, 0.06mol, 68%), b.p.48-51°/28mm Hg, lit.<sup>246</sup> 66°/57mm Hg. <sup>1</sup>H NMR (400 MHz, CDCl<sub>3</sub>):δ 2.00 (2H,*m*, 2H-5's), 2.14 (2H,*m*, 2H-4's), 2.87 (2H,*m*, 2H-6's), 5.73 (1H,*ddd*, *J*=4.4,4.4, 10.4 Hz, H-3), 6.00 (1H,*bd*, *J*=10.4 Hz, H-2). <sup>13</sup>C NMR (100.6 MHz, CDCl<sub>3</sub>):δ 22.2 (C-5), 23.4 (C-4), 26.0(C-6), 119.0 (C-3), 120.7 (C-2).

1,4-Oxathiane-4-oxide<sup>248,249</sup> (66) (Scheme 10)

Sodium periodate (23.4 g, 0.11 mol) in water (220 ml) was added to a solution of 1,4-*p*-oxathiacyclohexane (10.8 g, 0.1 mol) in methanol (25 ml) at 0°. The mixture was stirred at 4° for 16 h. The solvent was evaporated and the residue was extracted with methylene chloride. The suspension was dried with anhydrous potassium carbonate, filtered and concentrated to give the sulfoxide (66) as a syrup which solidified after storing in a dessicator overnight (10.4 g, 0.087 mol, 87%).

3-Acetoxy-1-oxa-4-thiacyclohexane (65) (Scheme 9) and 1-oxa-4-thiacyclohex-2-ene (73) (Scheme 10)

Acetic anhydride (3.6 ml, 0.038 mol) was added slowly to a refluxing solution of (66) (3.0 g, 0.025 mol) in benzene (30 ml) containing *p*-toluenesulfonic acid ( $\approx$ 50 mg), and the solution was refluxed for 6 h. TLC (hexane/ethyl acetate (1/3)) indicated the presence of two new components having  $R_f$  values of 0.85 and 0.42. Sodium hydrogen carbonate solution (50 ml) was added and the mixture was stirred for 2 h. The benzene layer was separated and washed with water (10ml). The solution was dried over anhydrous potassium carbonate and the solvent was evaporated to give a colourless syrup. The syrup was chromatographed on silica gel using the TLC solvent as eluant. The components having  $R_f$  values of 0.85 and 0.42 were identified as being (73) (0.8 g, 8 mmol) and (65) (1.3 g, 8 mmol) respectively, 64%. (65)  $^1\text{H}$  NMR (400 MHz,  $\text{CDCl}_3$ ):  $\delta$  2.15 (3H, *s*,  $\text{CH}_3$ ), 2.26 (1H, *dm*,  $J=14.0$ ,  $w_{1/2}=5.0$  Hz, H-5e), 3.29 (1H, *dq*,  $J=3.5, 11.5, 14.0$  Hz, H-5a), 3.78 (1H, *dt*,  $J=2.0, 11.5, 11.5$  Hz, H-6a), 3.94 (1H, *dd*,  $J=1.5, 12.5$  Hz, H-2e), 4.12 (1H, *dd*,  $J=2.0, 12.5$  Hz, H-2a), 4.22 (1H, *dt*,  $J=2.8, 3.5, 11.5$  Hz, H-6e), 5.54 (1H, *bs*,  $w_{1/2}=4.5$  Hz, H-3).  $^{13}\text{C}$  NMR (100.6 MHz,  $\text{CDCl}_3$ ):  $\delta$  21.0 ( $\text{CH}_3$ ), 23.2 (C-5), 67.8 (C-6), 68.0 (C-3), 71.1 (C-2), 169.8 (CO).

Anal. Calcd. for  $C_6H_{10}O_3S$ : C, 44.44; H, 6.17. Found:  
C, 44.27; H, 6.38

(73)  $^1H$  NMR (400 MHz,  $CDCl_3$ ):  $\delta$  2.98 (2H, *m*, H-5a, H-5e), 4.30 (2H, *m*, H-6a, H-6e), 5.03 (1H, *dt*,  $J=1.2, 1.2, 6.6$  Hz, H-3), 6.57 (1H, *d*,  $J=6.6$  Hz, H-2).  $^{13}C$  NMR (100.6 MHz,  $CDCl_3$ ):  $\delta$  24.5 (C-5), 64.8 (C-6), 92.9 (C-3), 139.8 (C-2).

Anal. Calcd. for  $C_4H_6OS$ : C, 47.03; H, 5.92. Found:  
C, 47.10; H, 5.99

#### 2-Hydroxy-1-oxa-4-thiacyclohexane (67) (Scheme 10)

Compound (73) (0.54 g, 5.3 mmol) was treated with 2N aqueous hydrochloric acid (5 ml) for 16 h. The mixture was extracted with methylene chloride (3x15 ml) and the extracts were dried over anhydrous potassium carbonate. The solvent was evaporated to give a colourless liquid which solidified on standing. The product was recrystallized from a methylene chloride/hexane mixture to give colourless crystals which were identified as being (67) (0.52 g, 4.3 mmol, 82%), m.p. 58-59°.  $^1H$  NMR (400 MHz,  $CDCl_3$ ):  $\delta$  2.51 (2H, *m*, H-5a, H-5e), 2.54 (1H, *dd*,  $J=6.0, 13.2$  Hz, H-3a), 2.82 (1H, *dd*,  $J=2.0, 13.2$  Hz, H-3e), 3.85 (1H, *ddd*,  $J=4.2, 6.4, 12.0$  Hz, H-6a), 4.27 (1H, *ddd*,  $J=3.7, 5.6, 12.0$  Hz, H-6e), 5.00 (1H, *bs*,  $w_{1/2}=12.0$  Hz, H-2).  $^{13}C$  NMR (100.6 MHz,  $CDCl_3$ ):  $\delta$  26.0 (C-3), 32.2 (C-5), 65.1 (C-6), 92.0 (C-2).

Anal. Calcd. for  $C_4H_8O_2S$ : C, 39.98; H, 6.71. Found:  
C, 39.98; H, 7.16

2-Methoxy-1,4-dithiacyclohexane (22) (Scheme 10)

Methanolic hydrogen chloride (2%, 2 ml) was added to a solution of (68) (0.1 g, 0.85 mmol) in methanol (1 ml). The solution was stirred at RT for 4 h. It was neutralized with a saturated solution of sodium hydrogen carbonate (5 ml) and extracted with methylene chloride (3x10 ml). The organic layer was dried with anhydrous potassium carbonate and the solvent was evaporated to give a yellowish liquid which was identified as being (22) (0.09g, 0.61mmol, 72%).  $^1H$  NMR (400 MHz,  $CDCl_3$ ):  $\delta$  2.60 (1H, ddd,  $J_{gem}=13.5$ ,  $J_{ee}=5.5$ ,  $J_{ea}=2.1$  Hz, H-5e), 2.72 (1H, ddd,  $J_{gem}=13.5$ ,  $J_{ee}=5.5$ ,  $J_{eq}=2.0$  Hz, H-6e), 2.90 (1H, dd,  $J_{gem}=13.7$ ,  $^3J=5.0$  Hz, H-3a), 3.03 (1H, ddd,  $J_{gem}=13.5$ ,  $J_{aa}=10.8$ ,  $J_{ea}=2.0$  Hz, H-6a), 3.35 (1H, dd,  $J_{gem}=13.7$ ,  $^3J=2.0$  Hz, H-3e), 3.52 (3H, s,  $OCH_3$ ), 4.41 (1H, m,  $w_{1/2}=9.3$  Hz, H-2).  $^{13}C$  NMR (100.6 MHz,  $CFCl_3/CD_2Cl_2$  (85/15)):  $\delta$  26.4 (C-5), 29.0 (C-6), 35.4 (C-3), 56.7 ( $OCH_3$ ), 78.3 (C-2).

Anal. Calcd. for  $C_5H_{10}OS_2$ : C, 39.97; H, 6.71. Found:  
C, 40.40; H, 6.63.



### 2-Methoxythiacyclohexane (23) (Scheme 10)

Compound (23) (0.12 g, 0.9 mmol, 28%) was prepared from (69) (0.32 g, 3.2 mmol), as described for the case of (22). The crude product was purified by column chromatography using hexane/ethyl acetate (85/15) as eluant to give the product as a clear liquid.  $^1\text{H}$  NMR (400 MHz,  $\text{CDCl}_3$ ):  $\delta$  1.54-2.11 (6H, *m*'s, 2H-3's, 2H-4's, 2H-5's), 2.30 (1H, *dt*,  $J=13.0$ , 3.7 Hz, H-6e), 2.86 (1H, *dq*,  $J=13.0$ , 11.6, 2.7 Hz, H-6a), 3.42 (3H, *s*,  $\text{OCH}_3$ ), 4.37 (1H, *t*,  $J=3.3$ ,  $w_{1/2}=8.0$  Hz, H-2).  $^{13}\text{C}$  NMR (100.6 MHz,  $\text{CFCl}_3/\text{CD}_2\text{Cl}_2$  (85/15)):  $\delta$  21.8 (C-4), 25.1 (C-5), 28.3 (C-3), 35.2 (C-6), 56.9 ( $\text{OCH}_3$ ), 81.9 (C-2).

Anal. Calcd. for  $\text{C}_6\text{H}_{12}\text{OS}$ : C, 54.51; H, 9.15. Found: C, 54.40; H, 9.00.

### 4-Methylthiacyclohex-2-ene (71) (Scheme 10)

Compound (71) (0.11 g, 0.97 mmol, 40%), b.p. 85°/22mm Hg, was prepared from (72) (0.29 g, 2.5 mmol), as described for the synthesis of (69).  $^1\text{H}$  NMR (100 MHz,  $\text{CDCl}_3$ ):  $\delta$  0.98 (3H, *d*,  $J=6.9$  Hz,  $\text{CH}_3$ ), 1.65 (2H, *m*, 2H-4's), 2.28 (1H, *m*, H-4), 2.87 (2H, *q*,  $J=3.6$  Hz, 2H-5's), 5.58 (1H, *dd*,  $J=10.1, 3.0$  Hz, H-3), 5.95 (1H, *d*,  $J=10.1$  Hz, H-2).  $^{13}\text{C}$  NMR (100.6 MHz,  $\text{CDCl}_3$ ):  $\delta$  21.4 ( $\text{CH}_3$ ), 24.5 (C-5), 28.2 (C-4), 30.5 (C-6), 118.5 (C-3), 127.1 (C-2).

cis and trans-2-Methoxy-4-methylthiacyclohexane (24)  
(Scheme 10)

Compound (24) (0.14 g, 0.96 mmol, 64%) was prepared from (71) (0.18 g, 1.5 mmol), as described for the synthesis of (22).  $^1\text{H}$  NMR (400 MHz,  $\text{CDCl}_3$ ):  $\delta$  0.85 (3H, *d*,  $J=6.5$  Hz,  $\text{CH}_3$ ), 1.31 (1H, *ddd*,  $J=13.0, 12.0, 3.5$  Hz, H-5a), 1.53-1.60 (1H, *m*, H-3a), 1.82 (1H, *m*, H-4), 1.91 (1H, *dm*,  $J=13.0$  Hz, H-3e), 2.05 (1H, *dt*,  $J=13.5, 3.0$  Hz, H-5e), 2.31 (1H, *dt*,  $J=13.2, 2.9$  Hz, H-6e), 2.84 (1H, *ddd*,  $J=13.2, 13.2, 2.5$  Hz, H-6a), 3.37 (3H, *s*,  $\text{OCH}_3$ ), 3.45 (1H, *ddd*,  $J=13.2, 3.5, 3.5$  Hz, H-6e), 4.43 (1H, *bs*,  $w_{\frac{1}{2}}=8.2$  Hz, H-2).  $^{13}\text{C}$  NMR (100.6 MHz,  $\text{CFCl}_3/\text{CD}_2\text{Cl}_2$  (85/15)):  $\delta$  24.2 ( $\text{CH}_3$ ), 24.9 (C-5), 27.1 (C-4), 36.7 (C-3), 43.3 (C-6), 56.8 ( $\text{OCH}_3$ ), 82.4 (C-2).

Anal. Calcd. for  $\text{C}_7\text{H}_{14}\text{OS}$ : C, 57.49; H, 9.65. Found: C, 56.76; H, 9.78.

2-Methoxy-1-oxa-4-thiacyclohexane (25) (Scheme 10)

Compound (25) (0.17 g, 1.3 mmol, 76%) was prepared from (67) (0.2 g, 1.7 mmol), as described for the synthesis of (22).  $^1\text{H}$  NMR (400 MHz,  $\text{CDCl}_3$ ):  $\delta$  2.43-2.64 (3H, *m's*, H-3e, 2H-5's), 2.70 (1H, *dm*,  $J=12.8$  Hz, H-3a), 3.45 (3H, *s*,  $\text{OCH}_3$ ), 3.80 (1H, *dq*,  $J=12.0, 8.0, 3.0$  Hz, H-6a), 4.25 (1H, *dq*,  $J=12.0, 5.7, 3.0$  Hz, H-6e), 4.55 (1H, *dd*,  $J=6.0, 2.1$  Hz,  $w_{\frac{1}{2}}=10.0$  Hz, H-2).

$^{13}\text{C}$  NMR (100.6 MHz,  $\text{CFCl}_3/\text{CD}_2\text{Cl}_2$ ):  $\delta$  27.1 (C-5), 31.4 (C-3), 56.2 (OCH<sub>3</sub>), 67.0 (C-6), 101.1 (C-2).

Anal. Calcd. for  $\text{C}_5\text{H}_{10}\text{O}_2\text{S}$ : C, 44.75, H, 7.51. Found: C, 44.57, H, 7.62.

3-Methoxy-1-oxa-4-thiacyclohexane (26) (Scheme 10)

Compound (**26**) (0.28 g, 2.09 mmol, 50%) was prepared from (**64**) (0.5 g, 4.2 mmol), as described for the synthesis of (**22**). The crude product was purified by column chromatography on silica gel using hexane/ethyl acetate (6/1) as eluant to give the product as a colourless syrup.  $^1\text{H}$  NMR (400 MHz,  $\text{CDCl}_3$ ):  $\delta$  2.12 (1H, *d*,  $J=14.0$  Hz, H-6e), 3.15 (1H, *ddd*,  $J_{\text{gem}}=14.0$ ,  $J_{\text{aa}}=11.6$ ,  $J_{\text{ae}}=3.0$  Hz, H-6a), 3.45 (3H, *s*, OCH<sub>3</sub>), 3.78 (1H, *ddd*,  $J_{\text{gem}}=11.6$ ,  $J_{\text{aa}}=11.6$ ,  $J_{\text{ae}}=2.2$  Hz, H-5a), 3.92 (1H, *dd*,  $J_{\text{gem}}=12.5$ ,  $^3J=2.0$  Hz, H-3e), 4.11 (1H, *dm*,  $J=12.5$  Hz, H-3a), 4.15 (1H, *m*,  $w_{1/2}=7.5$  Hz, H-2).  $^{13}\text{C}$  NMR (100.6 MHz,  $\text{CFCl}_3/\text{CD}_2\text{Cl}_2$ ):  $\delta$  23.8 (C-6), 57.0 (OCH<sub>3</sub>), 69.2 (C-5), 73.3 (C-3), 78.5 (C-2).

Anal. Calcd. for  $\text{C}_5\text{H}_{10}\text{O}_2\text{S}$ : C, 44.75, H, 7.51. Found: C, 44.44; H, 7.28.

2-Methoxy-1,4-dioxacyclohexane (27) (Scheme 10)

Compound (27) was prepared from (60) (0.14 g, 1.3 mmol), as described for the synthesis of (22). It was obtained as a clear syrup (0.09 g, 0.76 mmol, 58%).  $^1\text{H}$  NMR (400 MHz,  $\text{CDCl}_3$ ):  $\delta$  3.47 (3H, *s*,  $\text{OCH}_3$ ), 3.54-3.60 (2H, *m*, H-5a, 5e), 3.68-3.77 (3H, *m*, H-6e, 3a, 3e), 4.03 (1H, *ddd*,  $J_{\text{gem}} = 11.50$ ,  $J_{\text{aa}} = 7.4$ ,  $J_{\text{ae}} = 3.1$  Hz, H-6a), 4.47 (1H, *dd*,  $J = 2.8$ , 2.1 Hz,  $w_{\frac{1}{2}} = 6.5$  Hz, H-2).  $^{13}\text{C}$  NMR (100.6 MHz,  $\text{CFCl}_3/\text{CD}_2\text{Cl}_2$  (85/15)):  $\delta$  62.1 (C-6), 66.9 (C-5), 69.6 (C-3), 97.9 (C-2). Mass spect., M.Found: 118.0630.  $\text{C}_5\text{H}_{10}\text{O}_3$  requires M.118.0630.

Anal. Calcd. for  $\text{C}_5\text{H}_{10}\text{O}_3$ : C, 50.84; H, 8.53. Found: C, 51.10; H, 8.64.

cis and trans-2-Methoxy-4-methyloxacyclohexane (28)  
(Scheme 10)

Methanolic hydrogen chloride (3%, 10 ml) was added to a solution of cis and trans (52) (0.64 g, 5.6 mmol) in methanol (25 ml). The solution was stirred at RT for 5 h. Methylene chloride (20 ml) was added and the solution was washed successively with saturated sodium hydrogen carbonate (2x10 ml) and water (10 ml). After drying with anhydrous sodium sulfate, the solvent was evaporated to give a clear syrup which was identified as being (28) (0.51 g, 3.9 mmol, 69%),

b.p. 50°/24mm Hg, lit.<sup>165</sup> 35-45°/10mm Hg. <sup>1</sup>H NMR (400 MHz, CDCl<sub>3</sub>): δ trans isomer 0.88 (3H, d, J=6.4 Hz, CH<sub>3</sub>), 1.24 (2H, m, H-3a, H-5a), 1.53 (1H, dm, J=13.0 Hz, H-5e), 1.72 (1H, dm, J=13.1 Hz, H-3e), 1.93 (1H, m, H-4a), 3.55 (3H, s, OCH<sub>3</sub>), 3.52 (1H, ddd, J=11.2, 4.8, 1.6 Hz, H-6e), 3.70 (1H, td, J=12.5, 11.2, 2.5 Hz, H-6a), 4.70 (1H, d, J=3.0 Hz, w<sub>1/2</sub>=6.5 Hz, H-2). cis isomer (minor) 0.98 (3H, d, J=6.6 Hz, CH<sub>3</sub>), 1.08 (1H, ddd, J=12.5, 12.0, 9.0 Hz, H-3a), 1.20 (1H, dq, J=13.0, 12.0, 12.0, 4.5 Hz, H-5a), 1.50 (1H, ddd, J=13.0, 2.5, 2.0 Hz, H-5e), 1.81 (1H, dm, J=12.5 Hz, H-3e), 3.43 (1H, td, J=12.0, 11.5, 2.5 Hz, H-6a), 3.48 (3H, s, OCH<sub>3</sub>), 4.03 (1H, ddd, J=11.5, 4.5, 2.0 Hz, H-6e), 4.23 (1H, dd, J=9.1, 2.0 Hz, H-2). <sup>13</sup>C NMR (100.6 MHz, CDCl<sub>3</sub>): δ trans isomer 23.4 (C-4), 25.4 (CH<sub>3</sub>), 35.1 (C-5), 39.8 (C-3), 55.2 (OCH<sub>3</sub>), 60.3 (C-6), 99.3 (C-2). δ cis isomer (minor) 22.9 (C-4), 30.7 (CH<sub>3</sub>), 35.0 (C-5), 41.0 (C-3), 56.7 (OCH<sub>3</sub>), 66.0 (C-6), 104.1 (C-2).

Anal. Calcd. for C<sub>7</sub>H<sub>14</sub>O<sub>2</sub>: C, 64.58, H, 10.84. Found: C, 64.29, H, 10.59.

## CHAPTER 3

### THE STUDY OF ATTRACTIVE AND REPULSIVE GAUCHE EFFECTS

#### 3.1 Introduction

This chapter describes the study of attractive and repulsive gauche effects in controlling the conformational preferences of 2- or 3-substituted-1,4-diheterocyclohexanes. The compounds shown in Fig.3.1 were synthesized for this study (see Chapter 2):-

Figure 3.1

5-Substituted-1,3-diheterocyclohexanes and 2- or 3-substituted-1,4-diheterocyclohexanes synthesized for the study of attractive and repulsive gauche effects.



1.	X=O	R <sub>1</sub> =H	R <sub>2</sub> =H	16.	X=S	Y=S	Z=NHMe
2.	X=O	R <sub>1</sub> =i-Pr	R <sub>2</sub> =H	17.	X=S	Y=CH <sub>2</sub>	Z=NHMe
3.	X=O	R <sub>1</sub> =H	R <sub>2</sub> =NH <sub>2</sub>	18.	X=O	Y=O	Z=NHMe
4.	X=O	R <sub>1</sub> =H	R <sub>2</sub> =NHMe	19.	X=S	Y=O	Z=NHMe
5.	X=O	R <sub>1</sub> =H	R <sub>2</sub> =NMe <sub>2</sub>	20.	X=O	Y=S	Z=NHMe
6,9.	X=O	R <sub>1</sub> =i-Pr	R <sub>2</sub> =NH <sub>2</sub>	21.	X=O	Y=CHMe	Z=NHMe
7,10.	X=O	R <sub>1</sub> =i-Pr	R <sub>2</sub> =NHMe	22.	X=S	Y=S	Z=OMe
8,11.	X=O	R <sub>1</sub> =i-Pr	R <sub>2</sub> =NMe <sub>2</sub>	23.	X=S	Y=CH <sub>2</sub>	Z=OMe
12.	X=O	R <sub>1</sub> =H	R <sub>2</sub> =OMe	24.	X=S	Y=CHMe	Z=OMe
13.	X=S	R <sub>1</sub> =H	R <sub>2</sub> =NHMe	25.	X=O	Y=S	Z=OMe
14.	X=S	R <sub>1</sub> =H	R <sub>2</sub> =OMe	26.	X=S	Y=O	Z=OMe
15.	X=S	R <sub>1</sub> =Me	R <sub>2</sub> =OMe	27.	X=O	Y=O	Z=OMe
				28.	X=O	Y=CHMe	Z=OMe

The 2-substituted-1,4-diheterocyclohexanes can exhibit two types of conformational effects, namely, the X-C-Z anomeric type gauche effect and the Y-C-C-Z ethane type gauche effect. Initially, the individual two-centered conformational effects, the anomeric effects in 2-substituted-oxacyclohexanes and thiacyclohexanes, and the gauche effects in 5-substituted-1,3-dioxa- and dithiacyclohexanes, were examined. The additivity of these two effects was then compared with the composite effect observed in the 1,4-diheterocyclohexanes. Additional three-centered interactions may be involved since the interactions of two heteroatoms will be "sensed" by the third one. The exocyclic nitrogen substituents are of particular interest since anomeric systems with this substituent appear not to show an anomeric effect.<sup>25,105-107</sup>

We chose to examine the O/O, O/N, S/O and S/N ethane-type gauche interactions in 5-substituted-1,3-diheterocyclohexanes (3-15) and the O/O, O/N, S/O and S/N anomeric type gauche effects in 2-substituted-oxacyclohexanes (21,28) and 2-substituted-thiacyclohexanes (17,23).

The conformational equilibria of compounds 3-28 were evaluated by means of low temperature <sup>13</sup>C NMR spectroscopy. In order to estimate the magnitudes of the gauche effects, the procedure outlined in the following sections was adopted.

The magnitudes of the anomeric and gauche interactions are usually defined as the difference of the conformational free energy for the equilibrium studied and the conformational energy for the same substituent in cyclohexane.<sup>253</sup> However, this is not an accurate representation. The steric requirements and the dipole/dipole interactions of a substituent in the cyclohexane and in the heterocyclohexanes are different, and are not accounted for in the above definition. In this thesis, we define the anomeric and gauche interactions as the additional interactions which cannot be accounted for in terms of steric and electrostatic interactions.<sup>25,30,31,45</sup> According to this definition, the anomeric and gauche interactions are the manifestations of the electronic interactions, which are brought about by the through bond or through space interaction of the lone pairs.

The differences in steric interactions of an axial or equatorial polar substituent in heterocyclohexanes can be estimated by adding a coefficient to the conformational free energy difference of that axial or equatorial polar substituent in cyclohexane. The coefficient was calculated by comparing the free energy difference of a non-polar substituted cyclohexane with that of the similarly substituted heterocyclohexanes. The electrostatic interaction was calculated by the application of Abraham's formula for charge/charge interaction:  $E_{\text{electrostat}} = 332q_i \cdot q_j / r_{ij} \cdot \epsilon$  where  $q_i$ ,



$q_j$  are the charges of atom X and atom Y,  $\epsilon$  is the dielectric constant and  $r_{ij}$  is the distance between the charges.<sup>254</sup>

The remaining electronic component (gauche effect) in each system was then evaluated by subtracting the steric and electrostatic components from the total conformational free energy.

### 3.2 Results

#### I. **5-substituted-1,3-diheterosubstituted-cyclohexanes (3-15)**

##### i. NMR Analysis

The 1,3-dioxacyclohexane systems were chosen to be the model compounds for the study of the Y-C-C-Z gauche interaction because of their symmetry and because the chemical shifts of the non-equivalent protons were well separated, thus permitting first-order analysis of the spectra. Initially, however, conformational equilibria of the compounds 3-5 and 12 were measured directly by integration of the two sets of decoalesced signals of each compound in the low temperature  $^{13}\text{C}$  NMR spectra. The  $^{13}\text{C}$  NMR spectra of 3-5 and 12 at 153 K (Table 3.1) showed a major and a minor resonance. The signals of C-5 or C-4/C-6 were used as the probes since they were well resolved in all of the spectra. Assignment of the major and minor  $^{13}\text{C}$  NMR resonances of the low temperature spectra of the

5-substituted-1,3-dioxacyclohexanes (3-5) was based on the  $^{13}\text{C}$  chemical shift data of C-4, C-5 and C-6 of the cis- and trans-2-isopropyl-1,3-dioxacyclohexanes (6-11) (see Tables 3.2 and 3.3). In  $\text{CD}_2\text{Cl}_2$ , the induced  $\alpha$  shifts of C-5 are always smaller for the equatorial substituted conformers. However, the induced  $\beta$  shifts of C-4 and C-6 are greater for the equatorial amino and methylamino-substituted conformers. For the dimethylamino-substituted conformers, the induced  $\beta$  shifts of C-4 and C-6 of the equatorial conformer are smaller than the axial one; this may be due to the  $\gamma$  gauche effect of the N-methyl group (Fig.3.2). The assignments of the two conformers of 12 were based on the interpretations of the spectra of the cis- and trans-5-methoxy-2-isopropyl-1,3-dioxacyclohexanes,<sup>185</sup> the correlations of the  $^{13}\text{C}$  chemical shift parameters, and the normal sequence of  $\alpha$ -substituent-induced chemical shifts due to the methoxy substituent.

Figure 3.2

Possible rotamer of 5-methylamino-1,3-dioxacyclohexane.

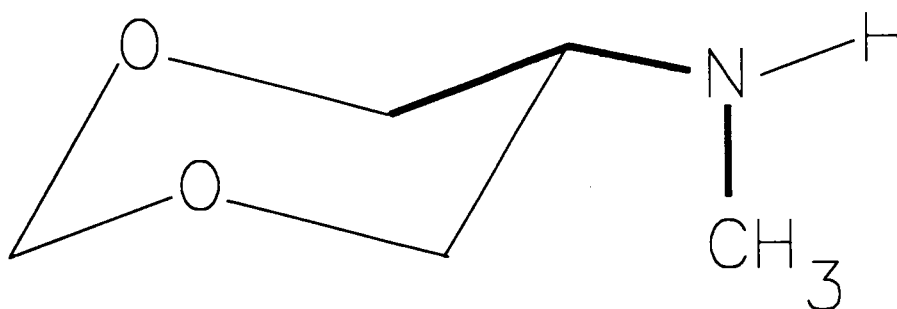


**Table 3.1**

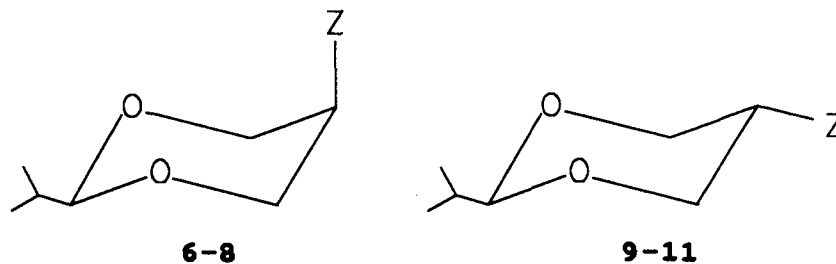
Low-temperature  $^{13}\text{C}$  NMR chemical shift data of 5-substituted-1,3-dioxacyclohexanes<sup>a</sup>.

Compd (Subst)	Isomer <sup>b</sup>	C2	C4,C6	C5	CH <sub>3</sub>
<b>12</b> (OCH <sub>3</sub> )	major	95.1	68.8	74.0	57.7
	minor	94.6	70.8	70.8	58.3
<b>3</b> (NH <sub>2</sub> )	major	94.5	73.6	44.8	
	minor	93.2	73.0	46.6	
<b>4</b> (NHCH <sub>3</sub> )	major	94.5	68.7	54.3	33.4
	minor	93.7	71.4	52.3	34.0
<b>5</b> (N(CH <sub>3</sub> ) <sub>2</sub> )	major	93.3	70.1	57.3	43.0
	minor	95.1	73.9	62.0	46.5

a). In 0.1M CD<sub>2</sub>Cl<sub>2</sub>/CFCl<sub>3</sub> (15/85) at 153 K.

**Table 3.2**

$^{13}\text{C}$  NMR chemical shift data ( $\delta_a$  and  $\delta_e$ ) of C-5 for compounds 6-11 at 298 K<sup>a</sup>.



Compd (Subst)	Solvent				
	CDCl <sub>3</sub>	CD <sub>2</sub> Cl <sub>2</sub>	(CD <sub>3</sub> ) <sub>2</sub> CO	CD <sub>3</sub> CN	(CD <sub>3</sub> ) <sub>2</sub> SO
<b>6</b> NH <sub>2</sub>	45.98	46.49	54.75	46.84	45.15
<b>7</b> NHCH <sub>3</sub>	53.11	53.60	53.99	54.00	52.30
<b>8</b> N(CH <sub>3</sub> ) <sub>2</sub>	57.09	57.63	57.44	57.88	55.81
<b>9</b> NH <sub>2</sub>	44.20	44.85	54.56	45.49	44.19
<b>10</b> NHCH <sub>3</sub>	52.03	52.58	53.21	53.17	51.82
<b>11</b> N(CH <sub>3</sub> ) <sub>2</sub>	57.06	57.55	58.04	58.11	56.57

a). All NMR samples were in 0.1M solutions. Compounds **6-8** have axial substituents and compounds **9-11** have equatorial substituents.

**Table 3.3**

$^{13}\text{C}$  NMR chemical shift data ( $\delta_a$  and  $\delta_e$ ) of C-4 and C-6 for compounds 6-11 at 298 K<sup>a</sup>.

Compd (Subst)	Solvent				
	$\text{CDCl}_3$	$\text{CD}_2\text{Cl}_2$	$(\text{CD}_3)_2\text{CO}$	$\text{CD}_3\text{CN}$	$(\text{CD}_3)_2\text{SO}$
6 $\text{NH}_2$	72.93	73.39	71.57	73.73	72.01
7 $\text{NHCH}_3$	68.90	69.30	69.51	69.65	68.15
8 $\text{N}(\text{CH}_3)_2$	67.82	68.28	68.44	68.60	67.04
9 $\text{NH}_2$	73.52	73.99	71.14	74.27	69.69
10 $\text{NHCH}_3$	71.38	71.88	72.04	72.12	70.51
11 $\text{N}(\text{CH}_3)_2$	69.62	70.06	70.17	70.35	68.62

a). All NMR samples were in 0.1M solutions. Compounds 6-8 have axial substituents and compounds 9-11 have equatorial substituents.

The low temperature  $^{13}\text{C}$  NMR chemical shifts of 5-methylamino-1,3-dithiacyclohexane (13) and cis-5-methoxy-2-methyl-1,3-dithiacyclohexane (15) are collected in Table 3.4. The 2-methyl group in 15 acts as a counterpoise group to provide axial/equatorial equilibria that are not highly biased. This was necessary because the low temperature  $^{13}\text{C}$  NMR peaks of 5-methoxy-1,3-dithiacyclohexane (14) were too biased to permit accurate estimation of the equilibria. The assignments of signals to the axial and equatorial 13 are based on the induced  $\alpha$  chemical shifts of axial and equatorial 3-X-substituted-thiacyclohexanes where X =  $\text{NH}_2$ ,  $\text{NPh}$  and  $\text{NMe}_2$  (Fig.3.3).<sup>255</sup> When X is equatorial, the induced  $\alpha$  chemical shifts on C3 are all greater than when X is axial (Table 3.5) in  $\text{CD}_2\text{Cl}_2$ . The same trend is observed in the 5-amino and 5-methylamino-1,3-dioxacyclohexanes. Therefore, the major

conformer in the low temperature spectrum of **13** is assigned to that with the methylamino substituent in the axial orientation.

Figure 3.3

Conformational equilibria of 3-X-substituted-thiacyclohexanes.

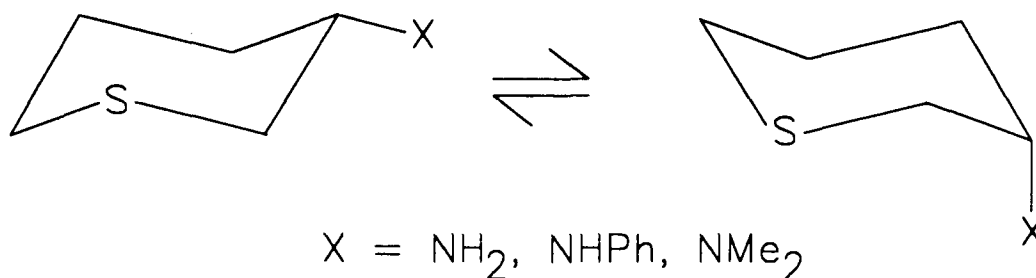


Table 3.4

Low-temperature <sup>13</sup>C NMR chemical shift data of cis-2-methyl-5-methoxy-1,3-dithiacyclohexane and 5-methylamino-1,3-dithiacyclohexanes<sup>a</sup>.

Compd (Subst)	Isomer	C2	C4, C6	C5	CH <sub>3</sub>	2-methyl
<b>15</b> (OCH <sub>3</sub> )	major	43.4	34.4	65.6	57.1	22.0 (eq Me)
	minor	36.9	28.2	78.1	b	24.2 (ax Me)
<b>13</b> (NHCH <sub>3</sub> )	major	32.4	34.4	47.3	33.6	
	minor	32.3	35.6	58.0	34.6	
<b>14</b> (OCH <sub>3</sub> )	major <sup>c</sup>	31.9	34.2	77.4	57.2	

a). All samples in 0.1M CD<sub>2</sub>Cl<sub>2</sub>/CFCl<sub>3</sub> (15/85) at 153 K.

b). Buried under solvent peaks.

c). The equilibrium was too biased. The chemical shifts of the minor conformer could not be distinguished from the noise.

Table 3.5

$^{13}\text{C}$  NMR chemical shift data of axial- and equatorial-3-X-substituted-thiacyclohexanes<sup>a</sup>.

X	$\text{NH}_2$		NHPH		$\text{NMe}_2$	
	A	E	A	E	A	E
$\delta$ C3	42.6	49.9	42.9	50.4	57.6	62.3

a). Low temperature spectra in  $\text{CD}_2\text{Cl}_2$  with temperatures ranging from 170 to 203 K: A (axial) and E (equatorial) refer to the orientation of the nitrogen functions.<sup>255</sup>

For compound **15**, the assignment of the two conformers is based on the  $\alpha$  shift of C2 due to the axial and equatorial methyl substituents. From the  $^{13}\text{C}$  NMR spectra of 56 alkyl-substituted-1,3-dithiacyclohexanes, it has been established that the  $\alpha$  chemical shift of C2 from an equatorial 2-methyl group ( $10.09 \pm 0.24$ ) is greater than from the axial one ( $5.24 \pm 0.44$ ).<sup>256</sup> As a result, the major conformer in the low-temperature spectrum of **15** is assigned to that with the 2-methyl group equatorial and the 5-methoxy group axial. The assignment is corroborated by the fact that C4,6 is shielded in the minor conformer owing to the  $\gamma$ -gauche effect of the 2-methyl group.

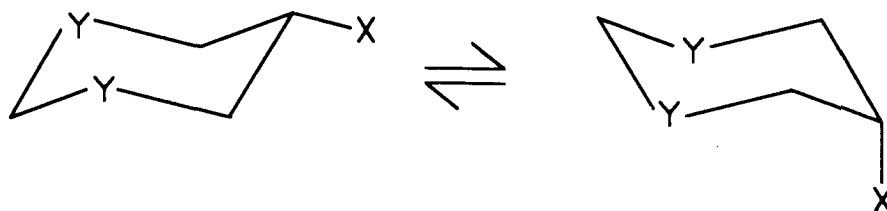
#### ii. Conformational Analysis

The equilibrium constants (K) of the 5-Z-substituted-1,3-dioxacyclohexanes and 1,3-dithiacyclohexanes are reported in Table 3.6. The values listed represent mean values obtained

from at least five integrations of each spectrum. The free energy differences  $\Delta G^\circ$  were calculated from  $\Delta G^\circ = -RT \ln K$ , and represent the equatorial = axial equilibrium. The error in the equilibrium constants (K) are the standard deviations of the integration measurements. The errors in  $\Delta G^\circ$  values were derived from the errors in K and the error in the temperature T ( $\pm 2$ K).

Table 3.6

Equilibrium data<sup>a</sup> for 5-substituted-1,3-diheterocyclohexanes.



Compd	(Subst, X)	Y	$K_{eq}$ (error)	$\Delta G^\circ$ (error) kcalmol <sup>-1</sup>
3	NH <sub>2</sub>	O	0.83 (0.03)	0.06 (0.01)
4	NHCH <sub>3</sub>	O	3.21 (0.04)	-0.36 (0.01)
5	N(CH <sub>3</sub> ) <sub>2</sub>	O	0.02 (0.00)	1.17 (0.10)
12	OCH <sub>3</sub>	O	0.53 (0.02)	0.19 (0.01)
13	NHCH <sub>3</sub>	S	4.90 (0.19)	-0.48 (0.03)
15	OCH <sub>3</sub>	S	4.81 <sup>b</sup> (0.21)	1.44 <sup>c</sup> (0.05)

a). In CD<sub>2</sub>Cl<sub>2</sub>/CFCl<sub>3</sub> (15/85) at 153 K.

b). The equilibrium constant is for 5-methoxy-2-methyl-1,3-dithiacyclohexane.

c). The  $\Delta G^\circ$  reported here is for 5-methoxy-1,3-dithiacyclohexane after the  $\Delta G^\circ$  of the 2-methyl group ( $\Delta G^\circ = -1.92 \pm 0.02$ )<sup>134</sup> has been subtracted from the  $\Delta G^\circ$  of 5-methoxy-2-methyl-1,3-dithiacyclohexane ( $\Delta G^\circ = -0.48 \pm 0.03$ ).

<sup>1</sup>H NMR and <sup>13</sup>C NMR spectra of the free systems (3-5) and anomeric 5-substituted-1,3-dioxacyclohexane systems (6-11)

were measured at ambient temperature. These data were also used to evaluate the conformational equilibria in several solvents of different dielectric constant in order to study the importance of electrostatic or dipole/dipole interactions in these systems. In solvents of low dielectric constant such as  $\text{CD}_2\text{Cl}_2$ , it is expected that the equilibria will be dominated by the dipole/dipole repulsion to a greater extent (Fig.3.4). Accordingly, the effect of dipolar interactions should be minimized in solvents of high dielectric constant. This prediction was indeed observed to be true in the above system when the substituents at the 5-position were Cl, Br,  $\text{SCH}_3$ ,  $\text{OCH}_3$  and CN.<sup>211</sup> 5-Substituted-2-isopropyl-1,3-dioxacyclohexanes were chosen to provide the "standard" vicinal coupling constants required for the evaluation of the corresponding conformational equilibria in the conformationally mobile 5-substituted-1,3-dioxacyclohexanes. It has been shown<sup>257</sup> by  $^1\text{H}$  NMR spectroscopy that isopropyl substituents at C-2 in 1,3-dioxacyclohexanes do not alter the coupling constants of H-4, H-5 and H-6. However,  $^{13}\text{C}$  NMR spectroscopy showed that substituents at C-2 did influence chemical shifts of the signals of C-4, C-5 and C-6 to a slight extent.<sup>258</sup> As a result, a correction factor (Table 3.7) was generated with each solvent for C-4, C-5 and C-6 by comparing the  $^{13}\text{C}$  chemical shifts of 1,3-dioxacyclohexane and 2-isopropyl-1,3-dioxacyclohexane.



Figure 3.4

Dipolar interactions in axial and equatorial 5-substituted-1,3-dioxacyclohexanes.

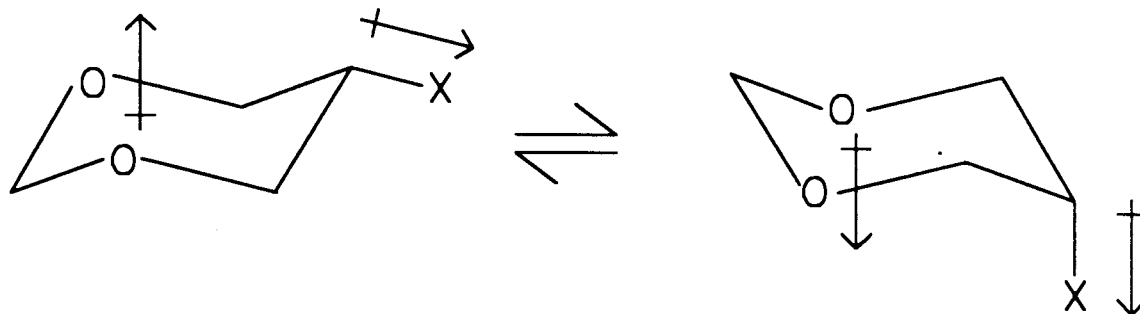


Table 3.7

2-isopropyl-induced  $^{13}\text{C}$  NMR chemical shift corrections of 1,3-dioxacyclohexane.

Carbon Signal	Solvent				
	$\text{CDCl}_3$	$\text{CD}_2\text{Cl}_2$	$(\text{CH}_3)_2\text{CO}$	$\text{CD}_3\text{CN}$	$(\text{CH}_3)_2\text{SO}$
C5	-0.48	-0.44	-0.55	-0.50	-0.63
C4, C6	0.07	0.08	0.06	0.07	-0.02

The  $^1\text{H}$  NMR spectra of compounds 3-11 at ambient temperature were recorded in different solvents and the coupling constants of H-5 with H-4's and H-6's, given by the width at half-height,  $W_{\frac{1}{2}} = |J_{\text{AX}} + J_{\text{BX}}|$ , are collected in Tables 3.8 and 3.9. The coupling constants  $W_{\frac{1}{2}} = |J_{\text{AX}} + J_{\text{BX}}|$  of the free 1,3-dioxacyclohexanes (3-5) and the coupling constants ( $J_{\text{eq}}$  and  $J_{\text{ax}}$ ) of the anancomeric systems (6-11) were used to evaluate the mole fraction of the axial conformers (Table 3.10).

Table 3.8

$^1\text{H}$  coupling constants of H-5 ( $W_3$ ) in Hz for 5-X-substituted-2-isopropyl-1,3-dioxacyclohexanes (6-11) at 298 K.

a) Axial substituted (6-8)

Compd (Subst)	Solvent				
	$\text{CDCl}_3$	$\text{CD}_2\text{Cl}_2$	$(\text{CD}_3)_2\text{CO}$	$\text{CD}_3\text{CN}$	$(\text{CD}_3)_2\text{SO}$
6 $\text{NH}_2$	15.5	15.7	16.5	15.9	15.8
7 $\text{NHCH}_3$	15.4	15.1	15.5	15.5	15.6
8 $\text{N}(\text{CH}_3)_2$	15.5	15.3	15.4	15.6	15.0

b) Equatorial substituted (9-11)

Compd (Subst)	Solvent				
	$\text{CDCl}_3$	$\text{CD}_2\text{Cl}_2$	$(\text{CD}_3)_2\text{CO}$	$\text{CD}_3\text{CN}$	$(\text{CD}_3)_2\text{SO}$
9 $\text{NH}_2$	3.6	3.6	3.6	3.7	3.6
10 $\text{NHCH}_3$	3.6	3.5	3.7	3.7	3.6
11 $\text{N}(\text{CH}_3)_2$	4.3	4.8	4.4	4.4	4.4

Table 3.9

$^1\text{H}$  Coupling constants of H-5 ( $W_3$ ) for 5-X-substituted-1,3-dioxacyclohexanes (3-5) at 298 K.

Compd (Subst)	Solvent				
	$\text{CDCl}_3$	$\text{CD}_2\text{Cl}_2$	$(\text{CD}_3)_2\text{CO}$	$\text{CD}_3\text{CN}$	$(\text{CD}_3)_2\text{SO}$
3 $\text{NH}_2$	9.8	10.6	14.7	12.3	13.2
4 $\text{NHCH}_3$	9.4	9.5	11.3	10.8	12.0
5 $\text{N}(\text{CH}_3)_2$	12.9	13.5	13.7	13.5	13.8

As an alternative method to determine the conformational equilibria of 1,3-dioxacyclohexanes (3-5), the  $^{13}\text{C}$  chemical shifts of C4 and C-6 of compounds (3-11) (Table 3.2, 3.3, and

3.11) were used to evaluate the mole fractions,  $N$ , of 1,3-dioxacyclohexanes (3-5) (Tables 3.12).

Table 3.10

Calculated mole fraction<sup>a</sup> of the axial conformers (I) at 298K.

		Solvent				
compd (subst)		CDCl <sub>3</sub>	CD <sub>2</sub> Cl <sub>2</sub>	(CD <sub>3</sub> ) <sub>2</sub> CO	CD <sub>3</sub> CN	(CD <sub>3</sub> ) <sub>2</sub> SO
3	NH <sub>2</sub>	0.48	0.42	0.16	0.34	0.25
4	NHCH <sub>3</sub>	0.51	0.48	0.34	0.40	0.30
5	N(CH <sub>3</sub> ) <sub>2</sub>	0.23	0.17	0.15	0.19	0.11

a). For an equilibrium mixture of (I) and (II) at 298 K:  $|J_{AX} + J_{BX}| = N(J_{ae} + J_{ee}) + (1-N)(J_{aa} + J_{ae})$  where  $N$  is the mole fraction of conformer (I).

Table 3.11

<sup>13</sup>C NMR chemical shift data ( $\delta_{obs}$ ) of C-4 and C-6 for compounds 3-5 at 298 K.

		Solvent				
Compd (Subst)		CDCl <sub>3</sub>	CD <sub>2</sub> Cl <sub>2</sub>	(CD <sub>3</sub> ) <sub>2</sub> CO	CD <sub>3</sub> CN	(CD <sub>3</sub> ) <sub>2</sub> SO
3	NH <sub>2</sub>	73.26	73.86	71.20	74.18	72.67
4	NHCH <sub>3</sub>	70.07	70.73	70.98	71.16	69.96
5	N(CH <sub>3</sub> ) <sub>2</sub>	69.34	69.83	69.92	70.07	68.37

Attempts at a similar analysis using C-5 as a probe for the evaluation of the conformational equilibria indicated that the chemical shifts of the averaged systems did not always occur between the extremes of the conformationally biased systems. This may be due to the close proximity of C-5 to the

electronegative substituents which affect the  $^{13}\text{C}$  chemical shifts of C-5 to different extents.

Table 3.12

Calculated mole fraction<sup>a</sup> of the axial conformer at 298 K using C-4 and C-6 as the probe.

Compd (Subst)	Solvent				
	$\text{CDCl}_3$	$\text{CD}_2\text{Cl}_2$	$(\text{CD}_3)_2\text{CO}$	$\text{CD}_3\text{CN}$	$(\text{CD}_3)_2\text{SO}$
3 $\text{NH}_2$	0.44	0.22	0.14	0.17	1.28 <sup>b</sup>
4 $\text{NHCH}_3$	0.53	0.45	0.42	0.39	0.23
5 $\text{N}(\text{CH}_3)_2$	0.16	0.13	0.14	0.16	0.16

- a). For an equilibrium mixture of axial and equatorial conformers at 298 K:  $N = (\delta_{\text{obs}} - \delta_{\text{e}})/(\delta_{\text{a}} - \delta_{\text{e}})$  where N is the mole fraction of axial conformer.
- b). Anomalous mole fraction calculated due to the anomalous chemical shifts measured in the anancomeric and conformationally free systems (see Discussion).

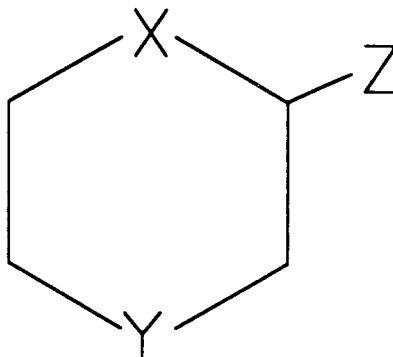
## II. 2-Methoxy and 2-methylamino-1,4-diheterocyclohexanes.

### i. NMR Analysis

The low-temperature  $^{13}\text{C}$  NMR spectra of 2-methoxy- and 2-methylamino-1,4-diheterocyclohexanes (16-22) showed two sets of signals which correspond to the axial and equatorial conformers. The chemical shifts of the major and minor conformers are collected in Table 3.13. The spectra were obtained at 153 K which was well below the coalescence temperature (190-200 K). The assignments of the 2-axial substituted conformers were based on the strong  $\gamma$  gauche substituent-induced chemical shifts. The equilibrium

constants, calculated at 153 K, as described above for the 1,3-diheterosubstituted systems, are reported in Table 3.14.

**Structure Index (compounds 16-28).**



Compd	X	Y	Z
16	S	S	NHMe
17	S	CH <sub>2</sub>	"
18	O	O	"
19	S	O	"
20	O	S	"
21	O	CH <sub>2</sub>	"
22	S	S	OMe
23	S	CH <sub>2</sub>	"
25	O	S	"
26	S	O	"
27	O	O	"
28	O	CH <sub>2</sub>	"

Table 3.13

Low-temperature  $^{13}\text{C}$  NMR chemical shifts of 2-methoxy and 2-methyl- amino-1,4-diheterocyclohexanes<sup>a</sup>.

Compd (Subst)	Isomer	C2	C3	C4	C5	C6	CH <sub>3</sub>	
16	NHCH <sub>3</sub>	major	59.5	37.6		29.9	24.5	34.4
		minor	64.6	40.7		33.5	29.1	35.9
17	NHCH <sub>3</sub>	major	64.7	29.2	27.0	27.5	36.9	33.9
		minor	61.6	28.7	24.6	27.3	35.8	34.3
18	NHCH <sub>3</sub>	major	87.2	70.5		66.3 <sup>d</sup>	65.8 <sup>d</sup>	33.1
		minor	82.9	67.6		65.7	57.7	31.3
19	NHCH <sub>3</sub>	s <sup>b</sup>	60.0	74.5		69.3	22.3	34.0
20	NHCH <sub>3</sub>	major	89.4	31.0		26.0	69.0	32.5
		minor	80.9	31.5		27.1	57.8	30.5
21 <sup>e</sup>	NHCH <sub>3</sub>	major	84.3	38.1	22.9	24.9	57.5	31.0
		minor	84.8	38.3	c	26.2	61.6	31.5
22	OCH <sub>3</sub>	major	75.3	34.0		23.2	27.6	56.0
		minor	85.1	32.7		25.3	30.7	56.9
23	OCH <sub>3</sub>	s <sup>b</sup>	81.9	28.3	21.8	25.1	35.2	56.9
25	OCH <sub>3</sub>	major	102.2	30.3		25.9	69.1	56.4
		minor	94.1	26.1		29.9	58.7	55.3
26	OCH <sub>3</sub>	s <sup>b</sup>	72.2	76.9		68.2	22.3	56.5
27	OCH <sub>3</sub>	major	95.3	68.3		66.4	58.8	55.0
		minor	98.6	65.6		c	65.0	56.4
28 <sup>f</sup>	OCH <sub>3</sub>	major	98.1	38.2	22.7	33.9	59.3	54.6
		minor	103.1	39.8	22.2	33.6	65.5	56.5

a). In ppm downfield from Me<sub>4</sub>Si in CD<sub>2</sub>Cl<sub>2</sub>/CFCl<sub>3</sub> (15/85) at 153 K.

b). S: the only conformer observed.

c). Signal not seen.

d). The chemical shift assignments for C5 and C6 may be interchanged.

e). The chemical shifts of the 4-CH<sub>3</sub> are 18.0 and 15.7 ppm for the major and minor conformers, respectively.

f). The chemical shifts of the 4-CH<sub>3</sub> are 22.7 and 22.2 ppm for the major and minor conformers, respectively.

Table 3.14

Equilibrium data obtained<sup>a</sup> for 2-substituted-1,4-dihetero-  
cyclohexanes.

Compd (Subst Z)	X	Y	$K_{e\rightleftharpoons a}$ (error)	$\Delta G^\circ$ (error) kcalmol <sup>-1</sup>
16 NHCH <sub>3</sub>	S	S	31.90 (1.60)	-1.06 (0.05)
17 "	S	CH <sub>2</sub>	0.37 (0.01)	0.31 (0.01)
18 "	O	O	0.06 (0.00)	0.89 (0.04)
19 "	S	O	b	<-1.1 <sup>c</sup>
20 "	O	S	0.19 (0.01)	0.51 (0.02)
21 "	O	CH <sub>2</sub>	2.60 <sup>d</sup> (0.15)	1.66 <sup>e</sup> (0.07)
22 OCH <sub>3</sub>	S	S	28.60 (2.07)	-1.02 (0.09)
23 "	S	CH <sub>2</sub>	b	-1.53 <sup>f</sup>
25 "	O	S	0.63 (0.02)	0.14 (0.01)
26 "	S	O	b	<-1.1 <sup>c</sup>
27 "	O	O	6.56 (0.20)	-0.57 (0.03)
28 "	O	CH <sub>2</sub>	4.53 (0.11)	-0.46 (0.02)

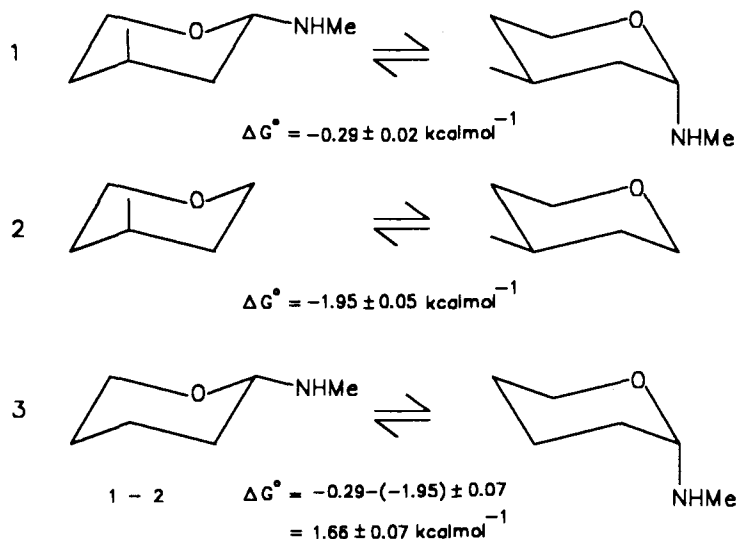
a). In CD<sub>2</sub>Cl<sub>2</sub>/CFCl<sub>3</sub> (15/85) at 153 K.

b). Only the axial conformer was seen.

c). See Experimental.

d). The equilibrium constant (K) is for 4-methyl-2-methylaminooxacyclohexane.

e). This was calculated by subtracting the  $\Delta G^\circ_{4-\text{Me}}$  of the 4-methyl substituent in oxacyclohexane ( $\Delta G^\circ_{4-\text{Me}} = -1.95 \pm 0.05$  kcalmol<sup>-1</sup>) from the  $\Delta G^\circ$  of 21 ( $\Delta G^\circ_{21} = -0.29 \pm 0.02$  kcalmol<sup>-1</sup>).<sup>210</sup>



f). From the equilibration of 2-methoxy-4-methylthiacyclohexane in CCl<sub>4</sub>.<sup>248</sup>

ii. Conformational analysis

Assuming additivity, the experimental conformational free energy differences can be represented by the following equation:-

$$\Delta G^{\circ}_{\text{expt}} = \Delta G^{\circ}_{\text{steric}} + \Delta G^{\circ}_{\text{electrostat}} + \Delta G^{\circ}_{\text{electronic}} \quad (\text{eq.3.1})$$

where

$\Delta G^{\circ}_{\text{steric}}$  is the conformational free energy difference when only the steric component is considered.

$\Delta G^{\circ}_{\text{electrostat}}$  is the conformational free energy difference when only electrostatic interactions are considered.

$\Delta G^{\circ}_{\text{electronic}}$  is the additional free energy difference when the summation of  $\Delta G^{\circ}_{\text{steric}}$  and  $\Delta G^{\circ}_{\text{electrostat}}$  cannot account for the experimentally determined free energy difference.

$\Delta G^{\circ}_{\text{steric}}$  was estimated by comparing the polar substituents (OCH<sub>3</sub> and NHCH<sub>3</sub>) with a non-polar substituent (ie; CH<sub>3</sub>) in cyclohexane and in the 2-substituted-1,4-diheterocyclohexanes (16-28). This kind of correlation was attempted by Franck<sup>259</sup> to predict the steric interaction component in 2-substituted-oxacyclohexanes. A linear correlation of  $\Delta G^{\circ}_{1-2}$  values with  $\Delta G^{\circ}_{3-4}$  values was established using substituents which were not expected to have anomeric interactions with the ring oxygen atom (Fig.3.5).

A similar approach was used here to establish the linear coefficients in the 1,4-diheterocyclohexanes. The "A" value of the methyl substituent was used to determine the



Figure 3.5

Comparison of steric requirements of substituted cyclohexane and 2-substituted-oxacyclohexane.

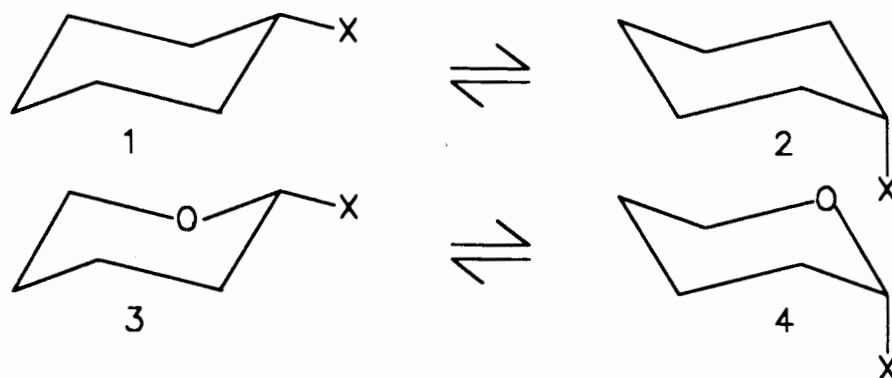
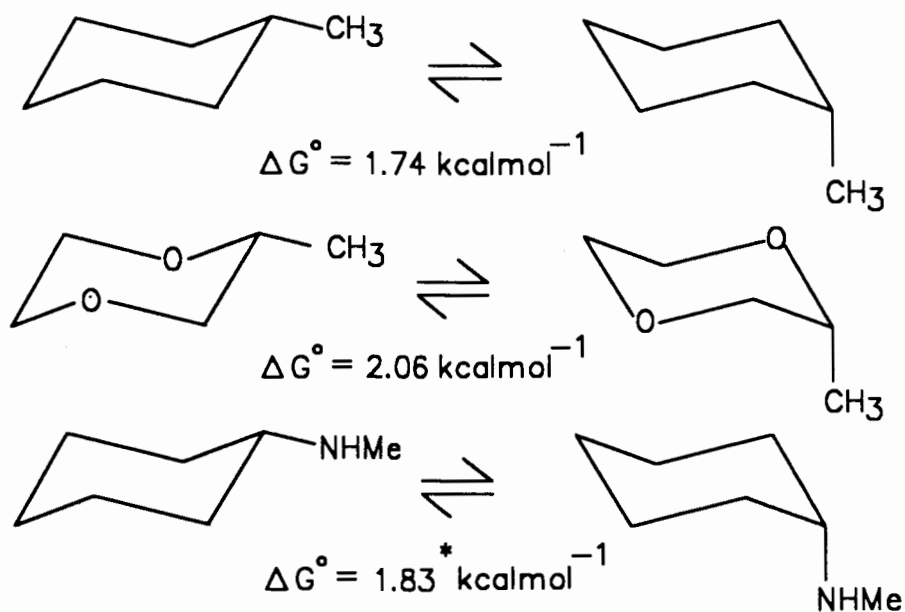


Figure 3.6

Calculated energy differences of the methyl substituent in cyclohexane and 1,4-dioxacyclohexane.



\* The substituent NHMe has the proton pointed into the cyclohexane ring. This is the expected rotamer in 2-methylaminooxacyclohexane.<sup>260</sup>

coefficients. The procedure, using the 1,4-dioxacyclohexane ring as an example, is presented in Figure 3.6. We chose to calculate the energy difference of axial and equatorial substituted heterocyclohexanes by molecular mechanics using Allinger's MM2 force field.<sup>222</sup>

The steric interaction of a methyl group in 1,4-dioxacyclohexane is 1.18 (2.06/1.74) times more severe than in cyclohexane. Therefore, the estimated steric interaction of the methylamino-substituent in the 1,4-dioxacyclohexane ring will be  $1.83 \times 1.18 = 2.17 \text{ kcal mol}^{-1}$ .

$\Delta G^{\circ}_{\text{electrostat}}$  was calculated using the molecular modelling program "PCMODEL".<sup>231</sup> In this program, the electrostatic interactions of a molecule were calculated in terms of the charge/charge model. Abraham's formula<sup>254</sup> was incorporated into a subroutine of the program to calculate the charge/charge interaction using a dielectric constant of 1.5. The results of these calculations are shown in Table 3.15.

Table 3.15

Conformational free energy data<sup>a</sup> for 2-methoxy and 2-methylamino-heterocyclohexanes and 1,4-diheterocyclohexanes.

Compd	$\Delta G^\circ_{\text{steric}}^b$	$\Delta G^\circ_{\text{electrostat}}^c$	$\Delta G^\circ_{\text{expt}}(\text{error})$	$\Delta G^\circ_{\text{electronic}}^d$
16	0.95	0.08	-1.06 (0.05)	-2.09
17	1.23	0.24	0.31 (0.01)	-1.16
18	2.20	0.13	0.89 (0.04)	-1.44
19	0.60	-0.05	<-1.1 <sup>e</sup>	<-1.65
20	2.47	0.24	0.51 (0.02)	-2.20
21	2.71	0.35	1.66 (0.07)	-1.40
22	0.27	0.13	-1.03 (0.09)	-1.43
23	0.35	-0.63	-1.53 <sup>f</sup>	-1.23
25	0.70	-0.12	0.14 (0.01)	-0.44
26	0.17	0.38	<-1.1 <sup>e</sup>	<-1.65
27	0.62	0.10	-0.58 (0.03)	-1.30
28	0.77	-0.81	-0.46 (0.02)	-0.42

a). In kcal/mol.

b). Calculated according to the corresponding "A" values of the substituents (see Discussion).

c). Calculated according to Abraham's formula<sup>254</sup> using the program "PCMODEL".<sup>231</sup>

d).  $\Delta G^\circ_{\text{electronic}} = \Delta G^\circ_{\text{expt}} - (\Delta G^\circ_{\text{steric}} + \Delta G^\circ_{\text{electrostat}})$ .

e). See Experimental.

f). From equilibration of 2-methoxy-4-methylthiacyclohexane in  $\text{CCl}_4$ .<sup>248</sup>

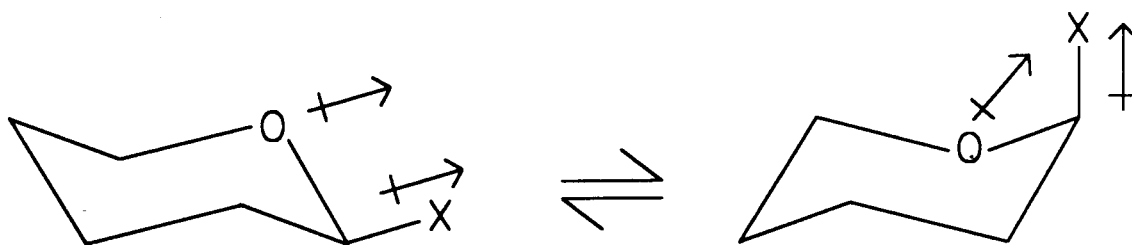
### 3.3 Discussion

#### I. Solvent Effects on the Conformational Equilibria of 5-Substituted-1,3-dioxacyclohexanes.

One of the early interpretations of the anomeric effect was based on the electrostatic interaction of the ring dipole of the carbohydrate ring and the dipole of the substituent.<sup>13</sup> In the studies of carbohydrates<sup>16,19,258</sup> and other simpler systems,<sup>264</sup> polar solvents were found to stabilize the equatorial conformers. This can be explained by the repulsive electrostatic interactions between the carbon-substituent dipole and the resultant dipole of the lone pairs on the ring oxygen since polar media are predicted to minimize dipolar interactions<sup>265</sup> (Fig.3.7).

Figure 3.7

Dipole-dipole interpretation of the anomeric interactions in 2-substituted-oxacyclohexanes.



If dipole/dipole interactions exert the dominant effect in the conformational equilibria of anomeric systems, the proportion of the equatorial conformer should increase with

increasing dielectric constant of the solvents. The anomeric effects in simple carbohydrate analogues, 2-alkoxyoxacyclohexanes, were indeed found to be higher in less polar media and lower in hydroxylic solvents.<sup>162,266</sup> However, the preference for the diaxial conformers of trans-2,3- and trans-2,5-dimethoxy-1,4-dioxacyclohexanes (Fig.3.8) and their analogues<sup>164</sup> at various temperatures and in different solvents was attributed to the dominance of hyperconjugative interaction ( $n_p \rightarrow \sigma^*_{C-X}$ ), resulting in a polar double bond-no bond structure; the authors<sup>164</sup> suggested that polar solvents should enhance this interaction (Fig.3.9). In the charge transfer model, this can be represented by the resonance structures A=B (Fig.3.10).

Figure 3.8

Trans-2,3-dimethoxy- and trans-2,5-dimethoxy-1,4-dioxacyclohexanes.



Figure 3.9

Model of  $n_p \rightarrow \sigma^*_{C-X}$  orbital interaction in truncated fragment.

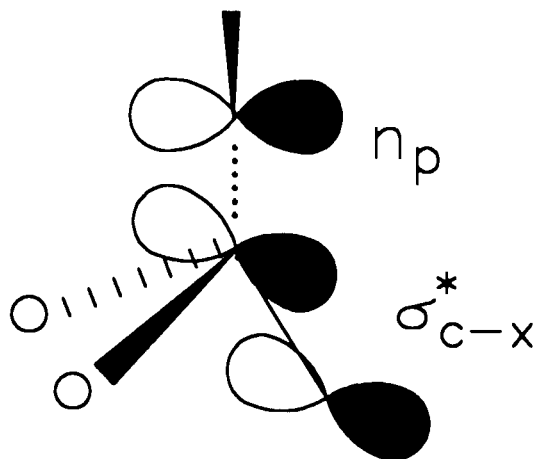
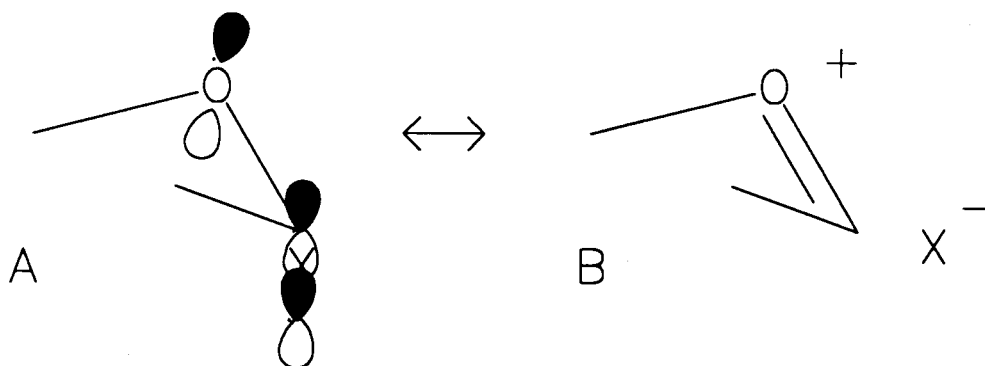


Figure 3.10

Charge transfer model of  $n_p \rightarrow \sigma^*_{C-X}$  orbital interaction.

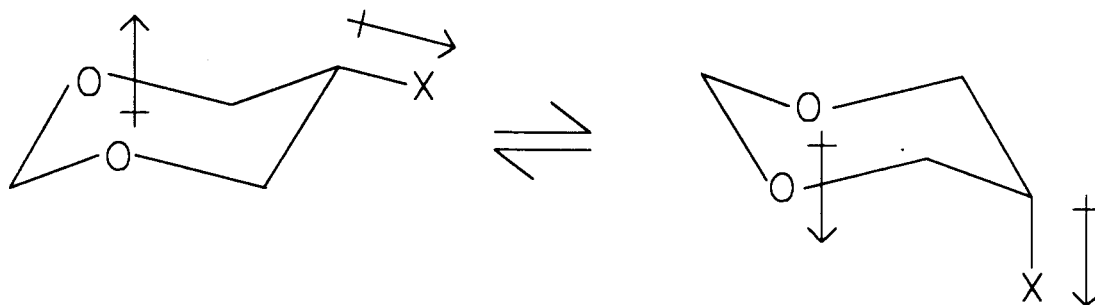


According to the original explanation, in 5-substituted-1,3-dioxacyclohexanes, the proportion of the more polar axial conformer should increase in a more polar solvent (Fig.3.11). According to the second explanation,<sup>164</sup> the opposite trend should be observed, if O-C-C-X gauche effects result in double-bond no-bond-type resonance structures. This

prediction is confirmed in the above system when X is Cl, Br, SCH<sub>3</sub>, OCH<sub>3</sub> and CN.<sup>211</sup>

Figure 3.11

Dipole-dipole interactions in 5-axial, and 5-equatorial-substituted-1,3-dioxacyclohexanes.

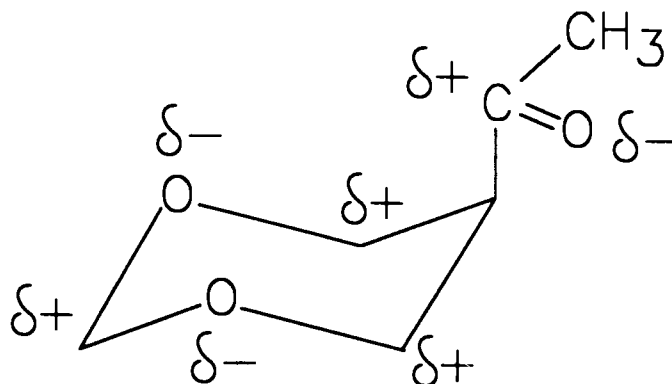


If dipole/dipole interactions make a significant contribution to the conformational equilibria of compounds 3-5 (Fig.3.11 where X=NH<sub>2</sub>, NHCH<sub>3</sub> and N(CH<sub>3</sub>)<sub>2</sub>), the mole fractions of the axial conformer should increase with more polar solvents. In fact, the opposite trend was observed for compounds 3 and 4, and compound 5 showed a very small solvent effect (see Tables 3.10 and 3.12). In the conformational equilibria of these compounds, either dipolar interactions are not important or it is overwhelmed by other effects. The latter type of behaviour was indeed reported in the study of solvent effects on the equilibria of 5-substituted-1,3-dioxacyclohexanes where the substituents were COCH<sub>3</sub> and COOCH<sub>3</sub>.<sup>211</sup> The preference for the axial conformers in polar solvents due to the alleviation of the dipolar repulsion may

be offset by the electrostatic attraction favouring the axial conformation (Fig.3.12).

Figure 3.12

Intramolecular electrostatic attraction in 5-axial-acetyl-1,3-dioxacyclohexane.



Another explanation for the greater axial preference of 3 and 4 in less polar solvents is also an electrostatic one. The NH protons of the 5-amino and 5-methylamino groups are capable of intramolecular hydrogen bonding with the ring oxygens in compounds 3 and 4. The axial preference of the 5-amino group in 5-amino-5-methyl-1,3-dioxacyclohexane has been suggested to be due to hydrogen bonding (Fig.3.13).<sup>267</sup>

This type of hydrogen bonding has been observed in 5-hydroxy-substituted-1,3-dioxacyclohexanes<sup>268,269</sup> and 3-substituted-oxacyclohexane.<sup>270</sup> It has also been suggested that the axial hydroxy group in cis-2-phenyl-5-hydroxy-1,3-dioxacyclohexane has a bifurcated hydrogen bond<sup>271</sup> (Fig.3.14).



Figure 3.13

Conformational equilibrium of 5-amino-5-methyl-1,3-dioxacyclohexane.

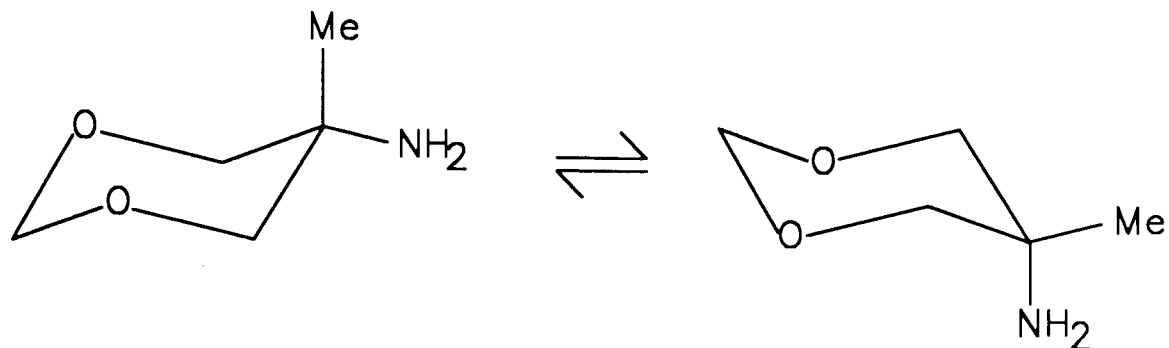
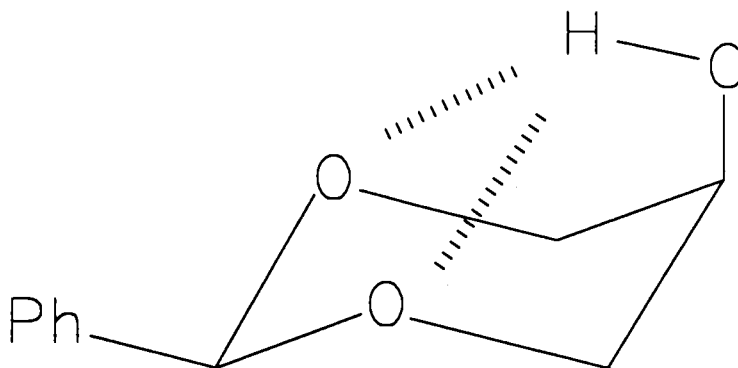


Figure 3.14

Bifurcated intramolecular hydrogen bonding in cis-2-phenyl-5-hydroxy-1,3-dioxacyclohexane.



A similar interaction was proposed for the stabilization of the axial isomer of 2-tert-butyl-5-methoxy-1,3-dithiacyclohexane and the dioxacyclohexane analogue through the protonation of the methoxy substituent in acidic solvents<sup>188</sup> (Fig.3.15). We note also that the <sup>1</sup>H NMR analysis of 5-hydroxy-1,3-dithiacyclohexane showed that H-5 was coupled to the hydroxy proton with a large trans coupling constant

( $^3J=6.2$  Hz) This suggested that H-5 was fixed in the trans orientation with respect to the hydroxy proton, probably due to hydrogen bonding with the ring sulfur atoms (Fig.3.16).

Figure 3.15

Intramolecular hydrogen bonding in protonated cis-2-tert-butyl-5-methoxy-1,3-dithiacyclohexane.

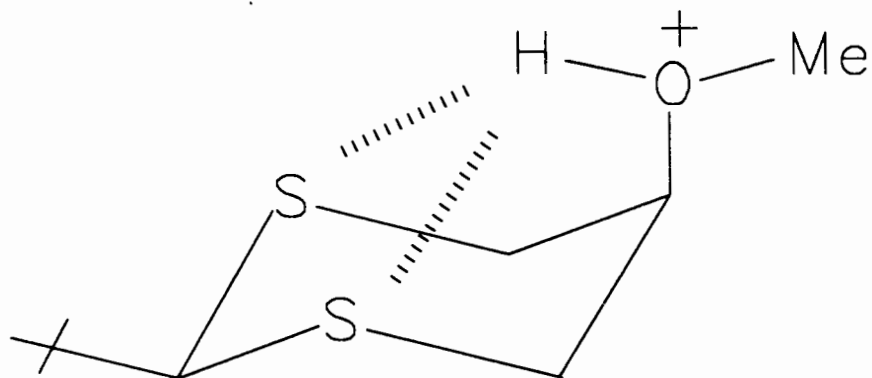
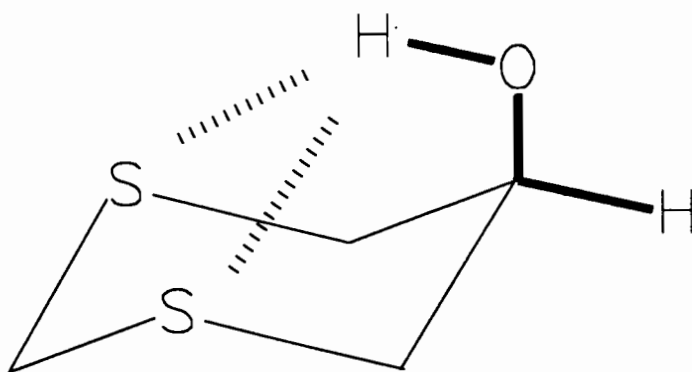


Figure 3.16

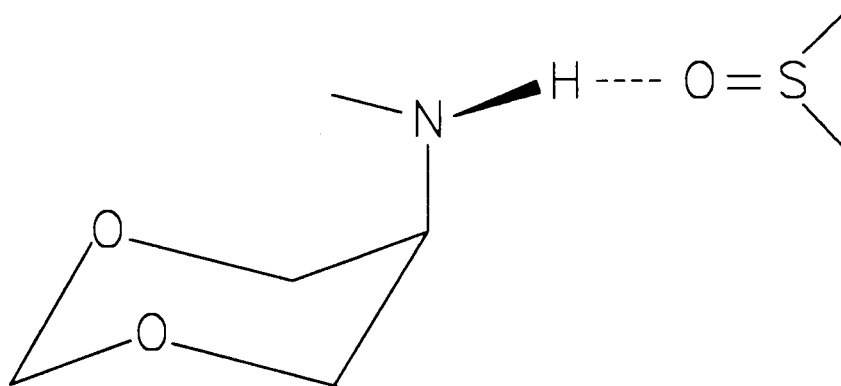
Intramolecular hydrogen bonding in 5-axial-hydroxy-1,3-dithiacyclohexane.



From the results in Tables 3.10 and 3.12, the participation of hydrogen bonding in the axial conformations of compound 3 and 4 provides a consistent explanation for their increased axial preferences in less polar media. In DMSO solvent, the mole fraction of the axial conformer of 3 and 4 was the lowest. The increases in the equatorial conformer may not only be due to the high dielectric constant of the DMSO solvent, but may also be due to its hydrogen bond forming property which destroys the intramolecular hydrogen bonding of the axial conformer of 3 or 4 (Fig.3.17). A similar explanation can be applied to account for the exceptionally low proportion of the axial conformer of 3 and 4 in acetone solvent (Tables 3.10 and 3.12).

Figure 3.17

Intermolecular hydrogen bonding of axial-amino substituted-1,3-dioxacyclohexane with solvent, dimethylsulfoxide.



The anomalous mole fraction of 3 calculated in the DMSO solvent, with the Eliel equation using the  $^{13}\text{C}$  chemical shifts of C-5 as a probe, (Table 3.12) may be a result of the competition of the intramolecular and intermolecular hydrogen bonding. The  $^{13}\text{C}$  chemical shifts of C-5 in the anomeric systems and the conformationally free system were not readily interpreted perhaps because of this solvent-solute interaction. For this reason, the equilibrium values obtained using the coupling constant information are probably more reliable than those obtained using the chemical shift information. If hydrogen bonding is the dominant conformational effect in the equilibria of compounds 3-5, the absence of a marked solvent effect in compound 5 may be due to the lack of an available proton in the dimethylamino substituent.

## II. Anomeric effect

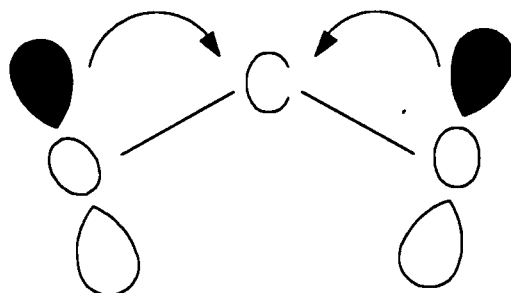
### i. 2-Methoxyoxacyclohexane

Table 3.15 summarizes the experimental conformational free energies together with the component analysis, as described in the preceding sections, for 2-methoxy and 2-methylaminoxacyclohexanes and thiacyclohexanes. From the measured conformational free energy, the axial conformer is favoured by  $0.46 \text{ kcal mol}^{-1}$ . Similar values were reported by

different research groups.<sup>23,109</sup> After the steric and electrostatic energy differences have been subtracted from the experimental value, the orbital interaction energy component has a value of  $0.42 \text{ kcalmol}^{-1}$  in favour of the axial conformer. Therefore, a combination of one exo  $n_{\text{O}} \rightarrow \sigma^*_{\text{C-O}}$  and one endo  $n_{\text{O}} \rightarrow \sigma^*_{\text{C-O}}$  orbital interaction is more stabilizing than one exo  $n_{\text{O}} \rightarrow \sigma^*_{\text{C-O}}$  orbital interaction by  $0.42 \text{ kcalmol}^{-1}$ . Although the hyperconjugative back donation is present in the O-C-O fragment of the axial conformer (Fig.3.18), summation of both the endo and the exo interactions are more stabilizing than the exo interaction. Moreover, the magnitude of the endo  $n_{\text{O}} \rightarrow \sigma^*_{\text{C-O}}$  orbital interaction should be smaller than the exo counterpart in the axial conformer since the p-type lone pair orbital of the endocyclic oxygen is not oriented at the optimal antiperiplanar plane of the exocyclic C-O bond due to geometric constraints.

Figure 3.18

Hyperconjugative interactions in the O-C-O fragments.



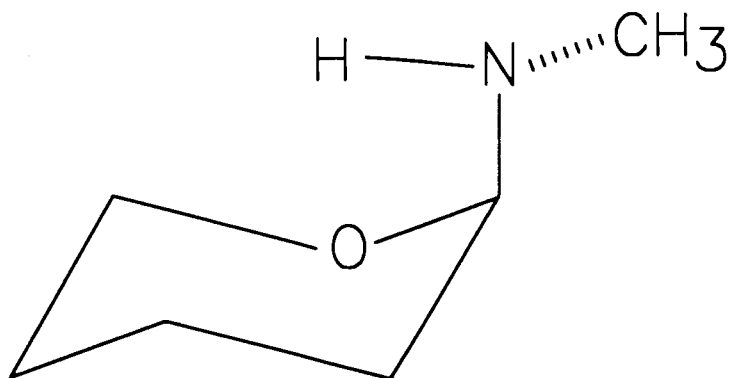
## ii. 2-Methylaminoxacyclohexane

The equatorial conformer of 2-methylaminoxacyclohexane is highly biased in the conformational equilibrium with a free energy difference of  $1.66 \text{ kcalmol}^{-1}$ . This observation was interpreted by Booth *et al.*<sup>23,106</sup> in terms of the competition between the endo and exo anomeric effects. Thus, in addition to the large steric requirement of the 2-methylamino substituent in the axial conformer, the exo stabilizing  $n_{\text{N}} \rightarrow \sigma^*_{\text{C-O}}$  orbital interaction suffers the competition from an endo anomeric effect. This results in the very strong preference for the equatorial conformer.<sup>113</sup> In our study, however, with a small electrostatic energy difference ( $0.35 \text{ kcalmol}^{-1}$ ) and a large steric energy difference ( $2.71 \text{ kcalmol}^{-1}$ ), the orbital interaction energy was calculated to be  $-1.40 \text{ kcalmol}^{-1}$  in favour of the axial conformer. From the NMR study of Booth *et al.*,<sup>260</sup> it appeared that the NH proton of the axial-2-methylamino-substituent in oxacyclohexane points inside the ring, thus enabling the optimal orientation for the p-type lone pair of the nitrogen to interact with the  $\sigma^*_{\text{C-O}}$  orbital (Fig.3.19). In the axial conformer, both the  $n_{\text{O}} \rightarrow \sigma^*_{\text{C-N}}$  and  $n_{\text{N}} \rightarrow \sigma^*_{\text{C-O}}$  orbital interactions are present. In the equatorial conformer, only the exo  $n_{\text{N}} \rightarrow \sigma^*_{\text{C-O}}$  orbital interaction is turned on. Therefore, the combination of both endo and exo anomeric effects in 2-methylaminoxacyclohexane is more stabilizing than the exo anomeric effect by  $1.4 \text{ kcalmol}^{-1}$ . It

is the accentuated steric effect that has the dominant influence on the conformational equilibrium.

Figure 3.19

Predicted orientation of the NH proton of 2-axial-methylamino-oxacyclohexane.

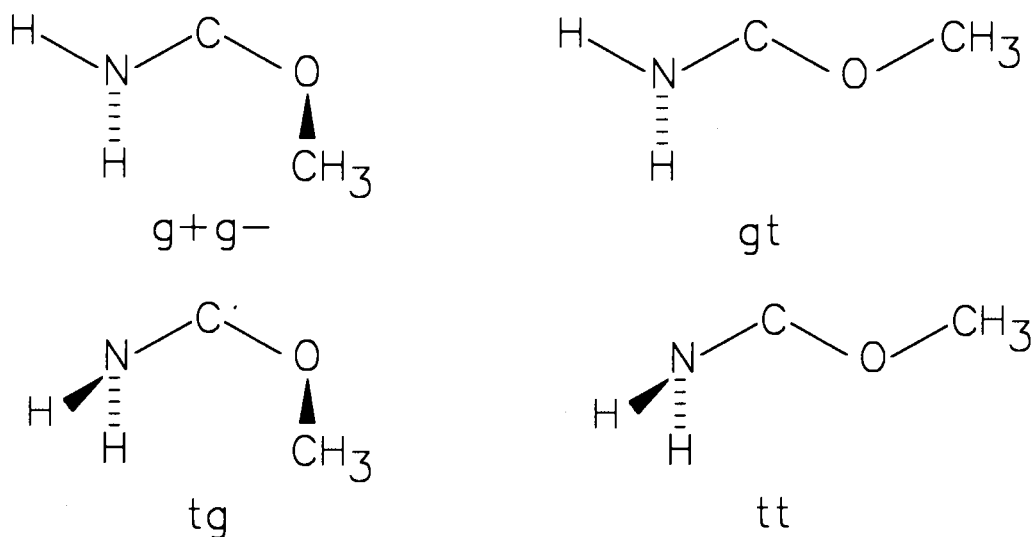


In the *ab initio* MO calculation of  $X\text{-CH}_2\text{-OCH}_3$  at the 6-31G\*//4-21G level, where  $X=\text{OCH}_3$ , a normal anomeric effect (ca 3 kcalmol<sup>-1</sup>) was indicated by the energy difference.<sup>272</sup> The normal anomeric effect was also observed for  $X=\text{NH}_2$  between the g+g- and the gt conformers (Fig.3.20). However, between the tg and the tt conformers, a "reverse" anomeric effect was observed. The authors suggested that in the tg conformer, the interaction between the nitrogen lone pair and the C-O bond was counteracted by the interaction of the lone pair of the oxygen atom.<sup>162,278</sup> Since nitrogen is a stronger electron donor and the C-N bond a weaker acceptor,<sup>273</sup> this results in the prediction of a more stable tt conformer. In our opinion,

as in the case of 2-methylaminoxacyclohexane, stabilization obtained by the summation of  $n_O \rightarrow \sigma^*_{C-N}$  and  $n_N \rightarrow \sigma^*_{C-O}$  orbital interactions is greater than one  $n_N \rightarrow \sigma^*_{C-O}$  orbital interaction. The steric repulsion brought about by the methoxy group and the two NH protons in the tg conformer of  $H_2NCH_2OCH_3$  may have a greater contribution to the energy difference between the tt and tg conformers than the orbital interactions.

Fig 3.20

The four possible stable conformations of aminomethoxymethane.



### iii. 2-Methoxythiacyclohexane

The predominance of the axial conformer of 2-methoxythiacyclohexane in the conformational equilibrium is largely due to the orbital interaction energy difference in the two conformers. The summation of the exo-anomeric  $n_O \rightarrow \sigma^*_{C-S}$  and the



endo-anomeric  $n_S \rightarrow \sigma^*_{C-O}$  interactions in the axial conformer is greater than the exo-anomeric  $n_O \rightarrow \sigma^*_{C-S}$  interaction in the equatorial conformer by  $1.23 \text{ kcal mol}^{-1}$ . This is a greater orbital interaction difference than in the case of 2-methoxyoxacyclohexane ( $\Delta E_{\text{orbital}} = -0.42 \text{ kcal mol}^{-1}$ ). The stabilizing orbital interaction energy is proportional to the square of the overlap and inversely proportional to the energy difference of the orbitals involved. Therefore, although the overlap is reduced in the case of thiacyclohexane (C-S bond in thiacyclohexane is longer than the C-O bond in oxacyclohexane), the orbital interaction energy could indicate that the energy gap factor dominates. Thus, one could argue that the energy gap between the p-type lone pair of oxygen and the  $\sigma^*_{C-S}$  orbital should be smaller than with the  $\sigma^*_{C-O}$  orbital, as indicated by the PMO calculations of dithiamethane and dihydroxymethane.<sup>140</sup> The steric interaction energy difference is less important than in the oxacyclohexane analogue, because of the longer C-S bond. The electronegativity of sulfur is smaller than oxygen. Therefore, the electrostatic interaction difference in this thiacyclohexane is smaller than in the oxacyclohexane system.

#### iv. 2-Methylaminothiacyclohexane

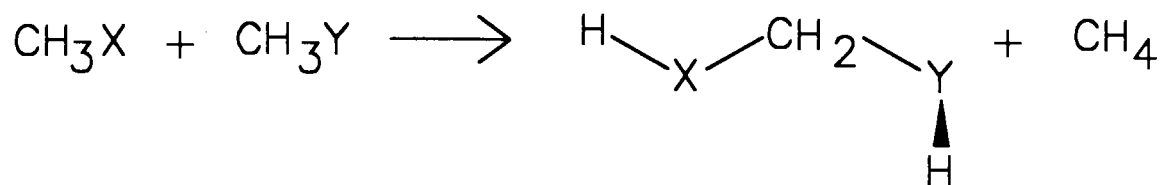
In the conformational equilibrium of 2-methylaminothia-cyclohexane, the equatorial conformer is favoured, but to a lesser extent than in the oxygen analogue. It is largely due to the large steric energy difference which favours the equatorial conformer. With a small electrostatic energy difference, the calculated energy of orbital interaction is about  $1.2 \text{ kcal mol}^{-1}$  in favour of the axial conformer. This energy difference is about the same as in the oxacyclohexane analogue. This could be explained by the dominance of the energy gap factor, as described above for 2-methoxythiacyclohexane. It is the greater  $n_{\text{N}} \rightarrow \sigma^*_{\text{C-S}}$  interaction that leads to a net orbital interaction energy of similar magnitude in the oxacyclohexane and thiacyclohexane systems.

Calculations, using the isodesmic approach, of a series of disubstituted methanes provide a comparison of the stabilization obtained by the association of different pairs of heteroatoms (Table 3.16). All of these calculations support the operation of normal anomeric interactions in these molecules, with shorter donor-carbon bonds, longer acceptor-carbon bonds and stabilizing association energies. The association energies indicate that the hyperconjugative interaction between  $\text{N} \rightarrow \text{C-O}$  is more stabilizing than  $\text{O} \rightarrow \text{C-N}$ ,  $\text{N} \rightarrow \text{C-S}$  is more stabilizing than  $\text{S} \rightarrow \text{C-N}$ , and  $\text{O} \rightarrow \text{C-S}$  is more stabilizing than  $\text{S} \rightarrow \text{C-O}$ . This is in accord with predictions

based on donor-acceptor abilities and electronegativities of these heteroatoms.<sup>273</sup>

Table 3.16

Total interaction energy (kcalmol<sup>-1</sup>) between X and Y groups in XCH<sub>2</sub>Y<sup>a</sup> calculated at the 6-31G<sup>\*</sup>//6-31G<sup>\*</sup> level.



X	O	O	N	S	N	S	O
Y	N	O	O	N	S	O	S
$\Delta E$	11.30	11.55	10.48	3.64	3.16	2.48	0.47

a). The starting and optimized geometry of XCH<sub>2</sub>Y has a trans, gauche conformation (ie. only one hyperconjugative interaction is possible).

In general, for atoms within the same group in the periodic table, the orbital energies of a lone pair orbital increase as one goes down the group, and the orbital energies of the  $\sigma^*$  orbitals decrease when one moves to the right of a row. Thus, the first ionization potential of oxacyclohexane (IP=9.5 eV)<sup>65</sup> was found to be higher than that of azacyclohexane (IP=8.70 eV)<sup>275</sup> which in turn was found to be higher than that of thiacyclohexane (IP=8.45 eV).<sup>65</sup> The PMO analysis of diheterosubstituted methanes,<sup>140</sup> also indicates that the  $\sigma^*_{\text{C-S}}$  orbital has a lower energy than the  $\sigma^*_{\text{C-O}}$

orbital, and generally, the  $\sigma^*_{C-O}$  orbital energy would be lower than that of a  $\sigma^*_{C-N}$  orbital.

### III. Ethane type gauche interactions

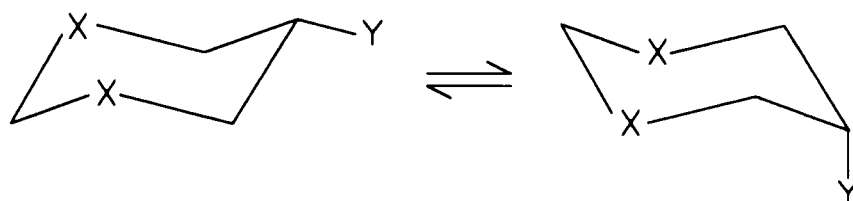
Several noteworthy trends emerged from this study. Thus, in the 5-methoxy substituted 1,3-dioxa and dithiacyclohexanes (12,14), the equatorial conformers are more stable, whereas in the 5-methylamino analogues (4,13), the axial conformers are the more stable. Since the methylamino group has a larger steric bulk than the methoxy group ( $\Delta$  values  $NHCH_3=1.70$  kcalmol<sup>-1</sup>,<sup>110</sup>  $OCH_3= 0.60$  kcalmol<sup>-1</sup>,<sup>275</sup> the above conformational preferences are not attributable to a steric effect. The equatorial preference of 5-methoxy-1,3-dithiacyclohexane (14) is stronger than in the 1,3-dioxa analogue. Based on the stronger dipole moment of C-O bonds than the C-S bonds, the opposite trend would have been predicted. The fact that the C-S bond is longer than the C-O bond would also predict a stronger equatorial preference of the 5-methoxy-1,3-dioxacyclohexane (12).

It is obvious from the foregoing discussion, that the conformational equilibria of all the 5-substituted 1,3-diheterocyclohexanes studied (4, 12-14) cannot be rationalized merely in terms of steric and electrostatic interactions. Orbital interactions may therefore make a significant

contribution to the overall equilibria. The orbital interaction energy, the steric, electrostatic and experimental energy differences, evaluated as described in the preceding sections, are collected in Table 3.17.

Table 3.17

Experimental and calculated energy differences (e = a) for 5-methoxy and 5-methylamino-1,3-dioxo and dithiacyclohexanes.



Energy difference <sup>a</sup> e = a	12		4		14		13	
	X O	Y OCH <sub>3</sub>	X O	Y NHCH <sub>3</sub>	X S	Y OCH <sub>3</sub>	X S	Y NHCH <sub>3</sub>
$\Delta E_{\text{steric}}^b$	0.26		0.74		0.38		0.76	
$\Delta E_{\text{electrostat}}^c$	1.71		-0.54		1.45		-0.37	
$\Delta E_{\text{exptl}}^d$	0.19		-0.36		1.44		-0.48	
$\Delta E_{\text{orbital}}^e$	-1.78		-0.56		-0.39		-0.87	

a). In kcalmol<sup>-1</sup>.

b). Differences between the axial and equatorial conformers were calculated by multiplying the proportionality constants, obtained from comparing the methyl substituted cyclohexane and 5-methyl-1,3-dioxo and dithiacyclohexanes, with the "A-values" of the respective substituents (See "Results" above).

c). Difference in electrostatic energies were taken from the charge/charge interaction terms in the optimized structures, using the interactive molecular modelling program PCMODEL<sup>231</sup>. This program uses a variant of the MM2 force field.

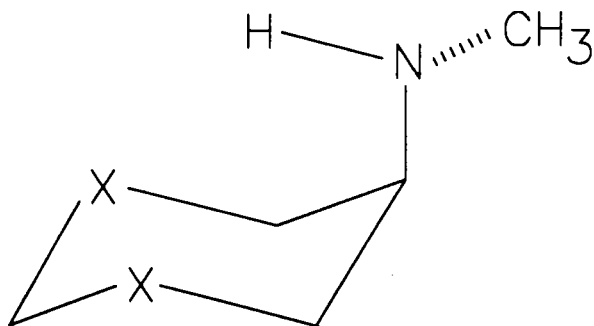
d). Experimental  $\Delta E$  values were taken from Table 3.6.

e). Difference in orbital interaction energies were calculated by subtracting the  $\Delta E_{\text{steric}}$  and  $\Delta E_{\text{electrostat}}$  from  $\Delta E_{\text{exptl}}$ .

With respect to these calculations, the following points require clarification. Since the  $^1\text{H}$  NMR coupling constant data and the solvent studies of 5-methylamino-1,3-dithiacyclohexane (13) indicated that the NH proton was pointed inside the ring with possible weak hydrogen bonding interaction (see above), the calculations of the steric and electrostatic energies, were started with a conformation in which the NH proton pointed inside the ring and the  $\text{NCH}_3$  group was gauche to the endocyclic C-C bonds (Fig.3.21). For the equatorial

Figure 3.21

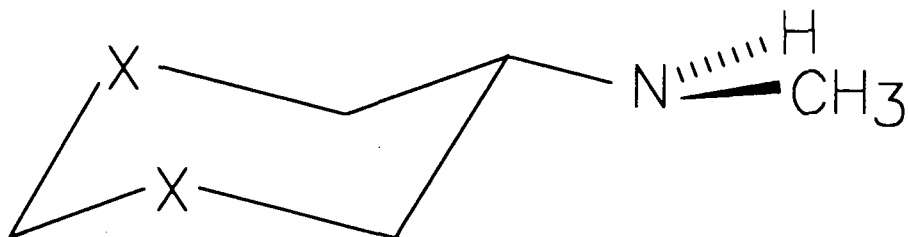
Predicted orientation of the  $\text{NHCH}_3$  group in 5-axial-methylamino-1,3-diheterocyclohexanes.



conformer, in order to minimize the steric interactions between the NH and  $\text{NCH}_3$  groups with the ring hydrogens, the optimizations started with both bonds rotated away from the ring (Fig.3.22). The same structures were assigned for the energy calculations of the analogous 5-methylamino-1,3-dioxacyclohexanes (4).

Figure 3.22

Possible orientation of the 5-methylamino substituent in 1,3-diheterocyclohexanes.



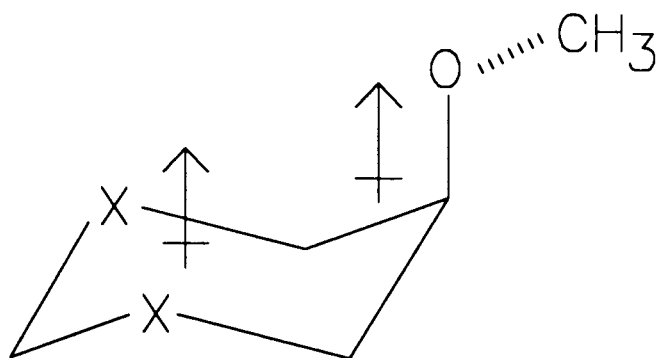
For 5-methoxy-1,3-dioxa and dithiacyclohexanes (12,14), the steric energies between the axial and equatorial conformer pairs are similar, suggesting that steric interactions only make a minor contribution to the different conformational behaviour of the two compounds. With a greater A-value than the methoxy group, the 5-methylamino group has a larger steric interaction, favouring the equatorial conformers. However, the experimental free energy differences indicated that the axial conformers were favoured.

Two different approaches are commonly used in molecular mechanics calculations of electrostatic interactions, namely, the dipole/dipole and the point charge models. The latter approach was adopted in this study. The electrostatic interaction between polar X-Y bonds are calculated using Coulomb's law, in the form of Abraham's equation.<sup>254</sup> The assigned charges on the atoms X and Y were the default values from "PCMODEL". The values obtained for (12) and (14)

reflect a strong destabilization of the axial conformers. In these two axial conformers, the resultant dipole of the two ring oxygen atoms and the dipole of the exocyclic C-O bond are strongly repulsive (Fig.3.23).

Figure 3.23

Resultant dipoles of the diheterocyclohexane ring and the methoxy substituent.



In the case of the 5-methylamino-substituted compounds, the axial conformers have overall attractive electrostatic interactions while the equatorial conformers have overall repulsive interactions. Although the charges on the ring oxygen or sulfur atoms and the nitrogen atom are repulsive in nature, the amino proton and the oxygen or sulfur lone pairs are strongly attractive in the axial conformer (Fig.3.24).

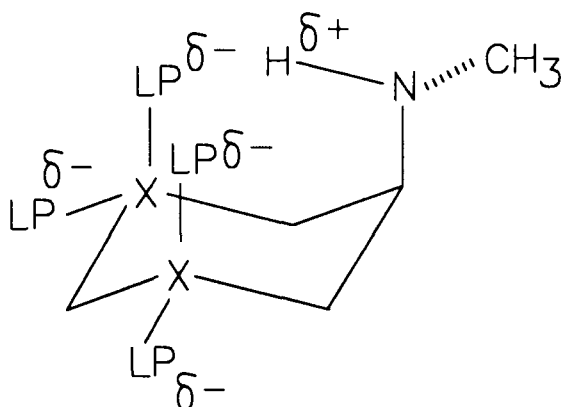
The differences in orbital interactions obtained for the series of compounds showed that the gauche interactions between O/O, O/N, S/O and S/N are all attractive. In



contrast, the experimental and "theoretical" studies on 1,2-disubstituted cyclohexanes<sup>186,187</sup> and 5-methoxy-1,3-diheterocyclohexanes,<sup>193</sup> have shown that although O/O has an attractive gauche interaction, S/O has a repulsive gauche interaction.<sup>188</sup>

Figure 3.24

Resultant charge distribution in 5-methylamino-1,3-diheterocyclohexanes.



However, 5-methylthio-1,3-dioxacyclohexane showed an attractive O/S gauche interaction.<sup>188</sup> The discrepancy in the S/O gauche interaction may be due to the limitation in assessing the charges in different atoms. Although the same methodology is adopted in the present study and the literature, lone pairs are included in the "PCMODEL" calculations.<sup>231</sup> Therefore, the destabilization in the axial conformer of 5-methoxy-1,3-dithiacyclohexane is partly accounted for by the electrostatic repulsion of the sulfur and

oxygen lone pairs. In addition, previous workers have estimated the "theoretical" values for electrostatic and steric interactions by "hand-calculations" of non-optimized geometries (Dreiding models).<sup>169,188</sup> The standard Dreiding structures for these types of molecules are very different from the minimized structures. As was pointed out by Eliel et al.,<sup>188</sup> the calculated energy difference of the axial and equatorial methylthiocyclohexane was over-estimated more than two fold from the experimental conformational free energy difference. However, good agreement between the calculated and experimental conformational energies for this molecule was obtained using the MM2 force field.<sup>276</sup> The effect of non-optimized structures was also exemplified in the calculation of the energies in 5-methoxy-2-tert-butyl-1,3-dithiacyclohexanes. The axial conformers were calculated to be more stable than the equatorial ones by 0.3 kcalmol<sup>-1</sup>. In our calculation using "PCMODEL",<sup>232</sup> the equatorial conformer of 5-methoxy-1,3-dithiacyclohexane (14) was calculated to be more stable by 0.4 kcalmol<sup>-1</sup>. Although the same charge-charge model was used in the estimation of the electrostatic interactions, the magnitudes of the charges on various atoms used in the Abraham's equation ( $E_{\text{electrostat}} = 332q_i \cdot q_j / r_{ij} \cdot \epsilon$ ) were different.<sup>254</sup> One may find different values of excessive charges  $q_i$  and  $q_j$  in the literature.<sup>254,277-280</sup>

In the interpretation of the attractive gauche interactions of the above compounds, both through bond and through space orbital interactions have to be considered [see Chapter 1]. The stabilization may be provided by the  $n \rightarrow \sigma^*$  through bond interaction and the destabilization may be due to the  $n \rightarrow n$  through space and  $n \rightarrow \sigma$  through bond interactions. The resulting bonding and antibonding combinations of the four electron destabilizing  $n \rightarrow n$  through space orbital interaction<sup>#</sup> (of the ring heteroatoms and the substituent) interact with the  $\sigma$  and  $\sigma^*$  orbitals of the intervening C-C bond. Although the lone pair orbitals involved are separated by three bonds, their interaction is found to be significant in this type of substituted heterocycle. The lone pairs of the ring oxygen and the exocyclic sulfur atom in the axial conformer of 2-isopropyl-5-t-butylthio-1,3-dioxacyclohexane were suggested to interact through space to give a lower oxidation potential than the equatorial conformer.<sup>169,186, 188,282</sup> It was also suggested that the electrochemical oxidation of thioethers is significantly facilitated by lone pair-lone pair repulsion of electron rich neighbouring groups.<sup>283</sup> As an illustration, the through space and through bond orbital interactions for 5-methylamino-1,3-dioxacyclohexane (4) are presented in Figure 3.25. It is the two orbital-two electron  $(n_1-n_2) \rightarrow \sigma^*_{C-C}$

---

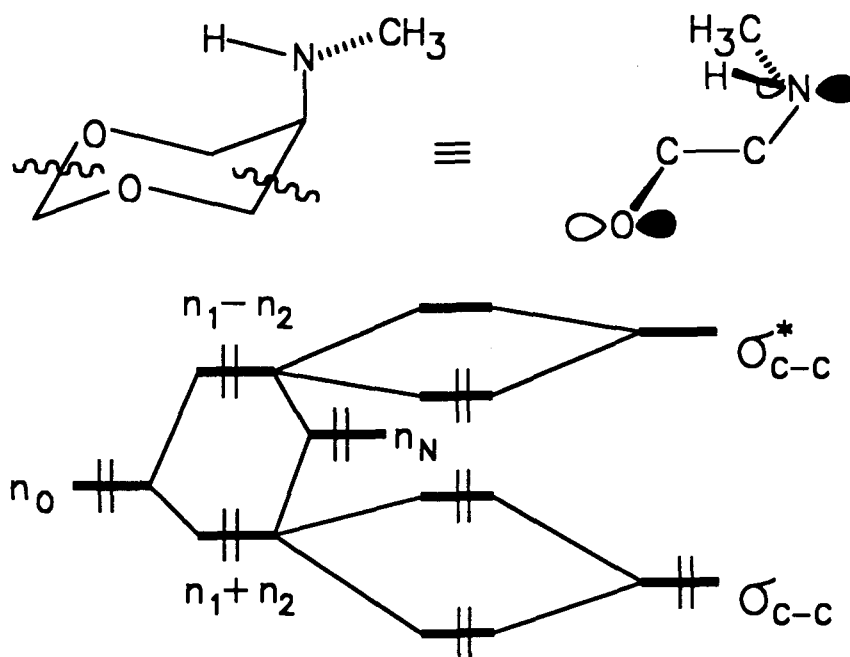
<sup>#</sup> Note that for the sake of simplicity, only one of the ring heteroatoms is considered. In fact, the two ring heteroatom orbitals also interact through space to give an  $n+$  and  $n-$  combination.<sup>65,281</sup>

interaction that is net stabilizing. The two orbital-four electron  $(n_1+n_2) \rightarrow \sigma_{C-C}$  interaction is net destabilizing.

From the  $\Delta E_{\text{orbital}}$  obtained (Table 3.17), the orbital interaction in **12** (-1.78) is greater than in **4** (-0.56) (ie;  $\Delta E_{\text{orbital}} O/O > O/N$ ). However, the magnitude of  $\Delta E_{\text{orbital}}$  for **14** (-0.39) is smaller than for **13** (-0.87) (ie;  $\Delta E_{\text{orbital}} S/O < S/N$ ).

Figure 3.25

Combinations of through space and through bond orbital interactions for 5-methylamino-1,3-dioxacyclohexane (**4**).



Assuming that the energy levels of the  $\sigma_{C-C}$  and the  $\sigma_{C-C}^*$  orbitals are constant, the amount of stabilization and

destabilization depends on the resulting energy levels of the through space bonding and antibonding orbital combinations ( $n_1+n_2$ ) and ( $n_1-n_2$ ). As the order of the energy levels of lone pair orbitals is  $n_o < n_N < n_S$ ,<sup>205</sup> the relative magnitudes of the through bond stabilizing interactions ( $\sigma^*_{C-C}$ , with ( $n_1-n_2$ )) should be  $O/O < O/N$ ;  $S/O < S/N$  since  $\Delta E_{\text{stabilizing}} \propto S^2/\Delta E$ . The relative magnitudes of the destabilizing interactions ( $\sigma_{C-C}$ , with ( $n_1+n_2$ )) may be predicted from the following analysis. The original  $n_N \rightarrow n_{O(S)}$  interaction results in a higher lying ( $n_1+n_2$ ) combination than that resulting from an  $n_o \rightarrow n_{O(S)}$  interaction. The relative magnitudes of the subsequent ( $n_1+n_2$ )  $\rightarrow \sigma_{C-C}$  interaction will be  $O/O > O/N$ ;  $S/O > S/N$  since  $\Delta E_{\text{destabilizing}} \propto S^2(E_1+E_2)$ . The results ( $O/O > O/N$ ;  $S/O < S/N$ ) suggest that in the oxygen series (4, 12),  $\Delta E_{\text{orbital}}$  is dominated by the destabilizing interaction whereas in the sulfur series (13, 14), the stabilizing ( $n_1-n_2$ )  $\rightarrow \sigma^*_{C-C}$  interactions must dominate.

It is more difficult to analyze the differences in the  $\Delta E_{\text{orbital}}$  between different pairs of heterocycles with the same substituent and different ring heteroatoms (ie; 12 vs. 14, 4 vs. 13) since in addition to the changes in the energy levels of the lone pair orbitals, changes in the orbital overlaps ( $S$ ) are also involved. The results appear to suggest that for the oxygen substituent (12, 14), the overlap factor dominates over the energy gap factor and that the order of the stabilizing

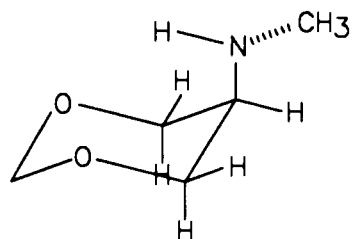
orbital interaction is  $O/O > S/O$ . The opposite appears to hold for the nitrogen substituent (4, 13), the energy gap factor being dominant and the order of the stabilizing orbital interaction being  $O/N < S/N$ . However, a conclusion in the absence of a quantitative PMO treatment is tenuous. The through space and through bond orbital interactions described above might also be complicated by the through space interaction of the two ring heteroatoms.

An alternative description may be advanced in terms of the  $\sigma_{C-H} \rightarrow \sigma^*_{C-X}$ ,  $\sigma_{C-X} \rightarrow \sigma^*_{C-Y}$  interactions. St. Jacques et al.<sup>200,284,285</sup> have suggested that the gauche effects in 3-X-substituted-1-benzoxepins<sup>290,291</sup> and 3-X-substituted-1,5-benzodioxepins<sup>200</sup> may be interpreted in terms of the latter type of orbital interactions. An analysis of such interactions in the 5-substituted-1,3-diheterocyclohexanes follows. The appropriate orbital interactions in the above compounds are shown in Figure 3.26.

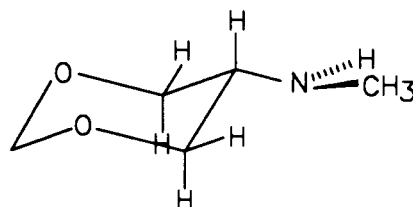
The  $\Delta E_{\text{orbital}}$  obtained in the above calculations (Table 3.17), indicates that the four  $\sigma_{C-H} \rightarrow \sigma^*_{C-X}$  orbital interactions in the axial conformers are more stabilizing than the two sets of  $\sigma_{C-X} \rightarrow \sigma^*_{C-Y}$  orbital interactions in the equatorial conformers. Indeed, *ab initio* calculations of  $CH_3X$  molecules have shown that the  $\sigma_{C-H}$  orbital is a good donor and has a higher orbital energy than the  $\sigma_{C-O}$  orbital.<sup>205-207</sup> An

Figure 3.26

Possible through bond interactions in 5-substituted-1,3-diheterocyclohexanes.

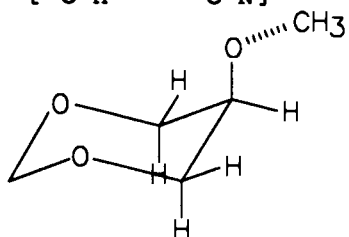


2  $[\sigma_{\text{C-H}} \rightarrow \sigma^*_{\text{C-O}}]$   
 2  $[\sigma_{\text{C-H}} \rightarrow \sigma^*_{\text{C-N}}]$

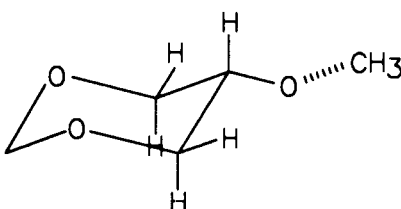


2 exo  $[\sigma_{\text{C-N}} \rightarrow \sigma^*_{\text{C-O}}]$   
 2 endo  $[\sigma_{\text{C-O}} \rightarrow \sigma^*_{\text{C-N}}]$

4

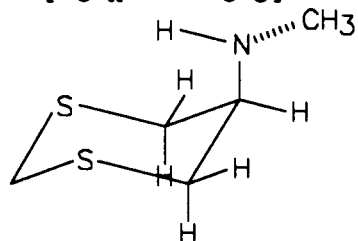


2  $[\sigma_{\text{C-H}} \rightarrow \sigma^*_{\text{C-O}}]$   
 2  $[\sigma_{\text{C-H}} \rightarrow \sigma^*_{\text{C-O}}]$

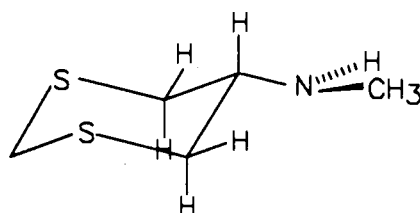


2 exo  $[\sigma_{\text{C-O}} \rightarrow \sigma^*_{\text{C-O}}]$   
 2 endo  $[\sigma_{\text{C-O}} \rightarrow \sigma^*_{\text{C-O}}]$

12

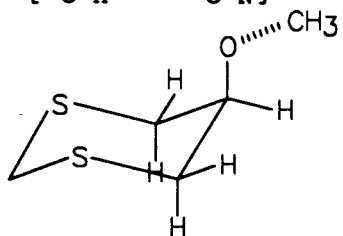


2  $[\sigma_{\text{C-H}} \rightarrow \sigma^*_{\text{C-S}}]$   
 2  $[\sigma_{\text{C-H}} \rightarrow \sigma^*_{\text{C-N}}]$

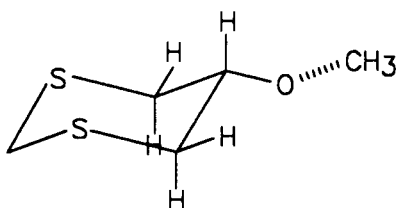


2 exo  $[\sigma_{\text{C-N}} \rightarrow \sigma^*_{\text{C-S}}]$   
 2 endo  $[\sigma_{\text{C-S}} \rightarrow \sigma^*_{\text{C-N}}]$

13



2  $[\sigma_{\text{C-H}} \rightarrow \sigma^*_{\text{C-S}}]$   
 2  $[\sigma_{\text{C-H}} \rightarrow \sigma^*_{\text{C-O}}]$



2 exo  $[\sigma_{\text{C-O}} \rightarrow \sigma^*_{\text{C-S}}]$   
 2 endo  $[\sigma_{\text{C-S}} \rightarrow \sigma^*_{\text{C-O}}]$

14

analysis of the individual systems follows. The absolute value of  $\Delta E_{\text{orbital}}$  for 5-methoxy-1,3-dioxacyclohexane (12), is greater than that for the 5-methylamino analogue (4), i.e. a greater axial preference; this can be attributed to the stronger  $\sigma_{\text{C-H}} \rightarrow \sigma^*_{\text{C-O}}$  than the  $\sigma_{\text{C-H}} \rightarrow \sigma^*_{\text{C-N}}$  orbital interaction. In their equatorial conformers, the 5-methoxy substituted compound has a stronger exo  $\sigma_{\text{C-O}} \rightarrow \sigma^*_{\text{C-O}}$  interaction but a weaker endo  $\sigma_{\text{C-O}} \rightarrow \sigma^*_{\text{C-O}}$  interaction than the corresponding  $\sigma_{\text{C-O}} \rightarrow \sigma^*_{\text{C-N}}$  and  $\sigma_{\text{C-N}} \rightarrow \sigma^*_{\text{C-O}}$  interaction, respectively in the 5-methylamino substituted compound. This is corroborated by the *ab initio* calculations of methanol and aminomethane at the 6-31G\* level which indicate that the  $\sigma_{\text{C-N}}$  and  $\sigma^*_{\text{C-N}}$  orbitals have a higher energy than the  $\sigma_{\text{C-O}}$  and  $\sigma^*_{\text{C-O}}$  orbitals, respectively. In the cases of 5-methylamino-1,3-dioxacyclohexane (4) and the corresponding 1,3-dithiacyclohexane (13), a greater axial preference is observed in the latter compound. As in the analysis of the pair of 5-substituted-1,3-dioxacyclohexanes, this trend can be explained by the dominant  $\sigma_{\text{C-H}} \rightarrow \sigma^*_{\text{C-X}}$  interaction (the  $\sigma_{\text{C-H}} \rightarrow \sigma^*_{\text{C-S}}$  interaction is stronger than the  $\sigma_{\text{C-H}} \rightarrow \sigma^*_{\text{C-O}}$  interaction). Quantitative PMO analysis of related systems has shown that  $\sigma^*_{\text{C-S}}$  has a lower orbital energy than  $\sigma^*_{\text{C-O}}$  and  $\sigma_{\text{C-S}}$  has a higher orbital energy than  $\sigma_{\text{C-O}}$ .<sup>140</sup> The observed trend might also indicate a stronger exo  $\sigma_{\text{C-N}} \rightarrow \sigma^*_{\text{C-S}}$  interaction and a stronger endo  $\sigma_{\text{C-S}} \rightarrow \sigma^*_{\text{C-N}}$  interaction in the equatorial conformer of (13) than the corresponding  $\sigma_{\text{C-N}} \rightarrow \sigma^*_{\text{C-O}}$



and  $\sigma_{C-O} \rightarrow \sigma^*_{C-N}$  interactions, respectively in the 1,3-dioxacyclohexane analogue (4), although these interactions are suggested to make only a minor contribution.

A comparison of the  $\Delta E_{\text{orbital}}$  values for 5-methoxy-1,3-dithiacyclohexane (14) and the dioxacyclohexane analogue (12) indicates a stronger net stabilizing orbital interaction component in the axial conformer of the latter derivative (12) in spite of the stronger  $\sigma_{C-H} \rightarrow \sigma^*_{C-S}$  interaction in the axial conformer of the former compound (14). The trend is consistent with a greater  $\sigma_{C-X} \rightarrow \sigma^*_{C-S}$  interaction in equatorial 5-X-1,3-dithiacyclohexane (13,14) than  $\sigma_{C-X} \rightarrow \sigma^*_{C-O}$  interaction in equatorial 5-X-1,3-dioxacyclohexane (4,12), although once again the  $\sigma_{C-X} \rightarrow \sigma^*_{C-Y}$  interactions are suggested to be less important than the  $\sigma_{C-H} \rightarrow \sigma^*_{C-X}$  interactions. Hence, the lower stabilization of axial (14) may be due to the greater diffuseness of the sulfur 3p orbital which leads to a strong n-n destabilizing orbital interaction with the methoxy oxygen  $n_p$  orbitals in this conformation. This interpretation might also explain the difference in  $\Delta E_{\text{orbital}}$  of 5-methoxy-1,3-dithiacyclohexane (14) and the 5-methylamino substituted analogue (13).

The above observations indicate that, in the absence of additional orbital repulsion, the  $\sigma_{C-H} \rightarrow \sigma^*_{C-X}$  interaction is

more important than the  $\sigma_{C-X} \rightarrow \sigma^*_{C-Y}$  interaction in ethane type gauche interactions.

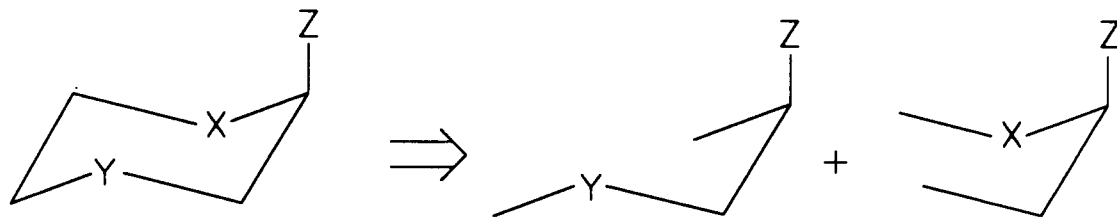
The analysis of the combination of through bond and through space interactions, and the subsequent analysis of through bond interactions in the 5-substituted-1,3-diheterocyclohexanes, suggest that the latter type of interactions might provide a more consistent interpretation of the attractive and repulsive gauche interactions. An exact evaluation will have await a detailed quantitative PMO analysis of these and other orbital interactions.

#### IV. 2- or 3-Substituted-1,4-diheterocyclohexanes

Assuming additivity, the orbital interactions in these systems might be considered as the combination of an ethane type gauche interaction and an anomeric type gauche interaction (Fig.3.27).

Figure 3.27

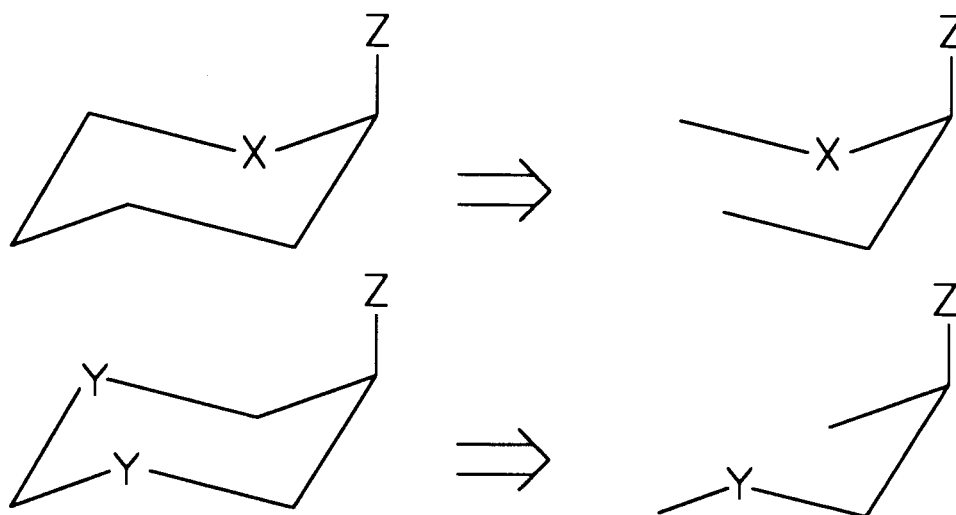
The two orbital interaction components in 2- or 3-substituted-1,4-diheterocyclohexanes.



The anomeric type gauche interaction is obtained from the orbital interactions in 2-substituted heterocyclohexanes and the ethane type gauche interaction is obtained by taking half of the orbital interactions in the 5-substituted-1,3-diheterocyclohexanes (Fig.3.28).

Figure 3.28

Gauche interactions in hetero-substituted fragments.

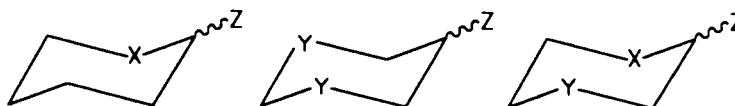


The magnitudes of the orbital interactions operating in O-C-N, S-C-N, O-C-O, S-C-O, O-C-C-N, S-C-C-N, O-C-C-O and S-C-C-O fragments have been discussed above in sections II and III. The composite orbital interactions in the 2-substituted-1,4-diheterocyclohexanes can then be compared with the two types of gauche interactions (see Table 3.18).

Table 3.18

Comparison of the orbital interactions in the 2-substituted-1,4-diheterocyclohexanes and the two corresponding types of gauche interaction in 2-substituted heterocyclohexanes and 5-substituted-1,3-diheterocyclohexanes.

$$-\Delta E_{\text{orbital e}\rightleftharpoons\text{a}} \text{ (kcalmol}^{-1}\text{)}$$



Z=OCH <sub>3</sub>	(1)	(2)	(3)	(4) <sup>a</sup>
X=S, Y=S	1.23	0.39	1.43	1.43
X=O, Y=S	0.42	0.39	0.44	0.62
X=S, Y=O	1.23	1.78	>1.65	2.12
X=O, Y=O	0.42	1.78	1.30	1.31
Z=NHCH <sub>3</sub>				
X=S, Y=S	1.16	0.23	2.09	1.28
X=O, Y=O	1.40	-0.12	1.44	1.34
X=S, Y=O	1.16	-0.12	>1.65	1.10
X=O, Y=S	1.40	0.23	2.20	1.52

a). (4) = (1) + (2)/2.

The same procedure, as described in the preceding sections, has been used for the estimation of the orbital interactions in the composite systems. However, the orientation of the methylamino substituents in the equatorial conformers is different from that of the 5-substituted-1,3-diheterocyclohexanes. In the 5-substituted-1,3-diheterocyclohexanes, in order to minimize the steric interactions of the axial protons at C-4 and C-6 of the ring and the

substituent, the methyl group and the NH proton are pointed above the ring (Fig.3.29). In the 2-substituted heterocyclohexanes, the NH proton has to be pointed down in order to maximize the exo-anomeric interaction ( $n_N \rightarrow \sigma^*_{C-O}$ ) (Fig.3.30).

Figure 3.29

Orientation of the equatorial methylamino substituent in 5-substituted-1,3-diheterocyclohexanes.

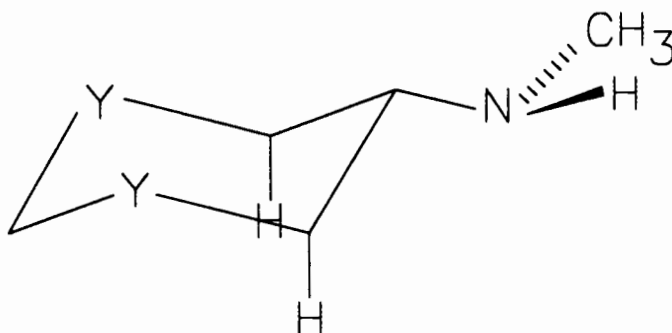
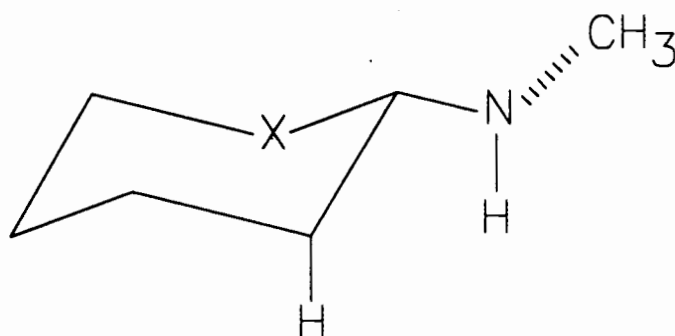


Figure 3.30

Orientation of the equatorial methylamino substituent in 2-substituted-heterocyclohexanes.

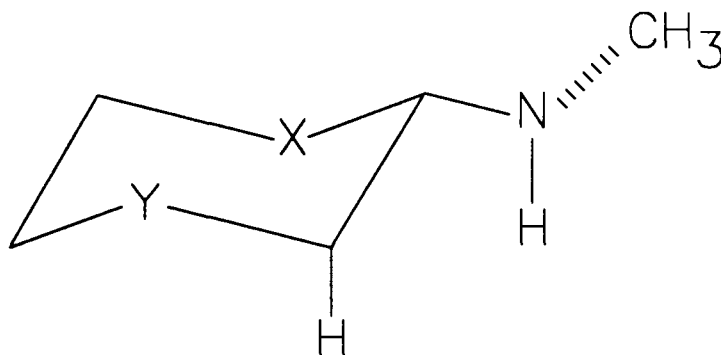


A basic tenet of conformational analysis dictates that a molecule will tend to minimize the destabilizing interactions and maximize the stabilizing interactions. Therefore, the NH

proton of the methylamino substituent in the 2-substituted-1,4-diheterocyclohexanes (16, 18-20) was pointed down in the above calculations (Fig.3.31). The data in column (3) of Table 3.18 indicate that in all cases studied, the combinations of the anomeric type and ethane type gauche orbital interactions are all attractive (ie; axial conformers are preferred). For  $Z=OCH_3$ , good agreement is obtained between the summation of the two individual interactions (column (4)), and the composite interactions, except in the case when  $X=O$  and  $Y=S$  (25). The trend indicates that the concept of additivity might be valid in these molecules. The situation is different when  $Z=NHCH_3$ ; the magnitudes of the  $\Delta E_{\text{orbital}}$  in the composite system are greater than the summation of the individual interactions for all combinations of substituents O and S.

Figure 3.31

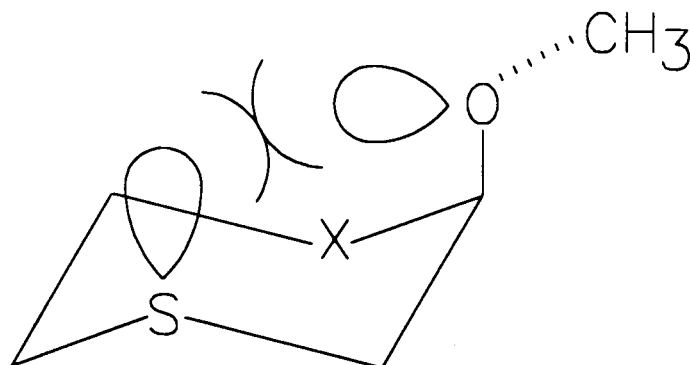
Orientation of the equatorial methylamino substituent in 2-substituted-1,4-diheterocyclohexanes.



In the axial substituted composite systems, the exocyclic C-Z bonds are shortened when compared with a similarly substituted cyclohexane. This is a general property of the anomeric type gauche interaction (see Chapter 1). For  $Z=OCH_3$  and  $Y=S$ , the shortening of the exocyclic C-O bond will increase the n-n through space orbital repulsion between the oxygen lone pairs and the sulfur lone pairs (Fig.3.32).

Figure 3.32

Through space lone pair repulsion in axial-2-methoxy-1,4-diheterocyclohexane (Y=S).

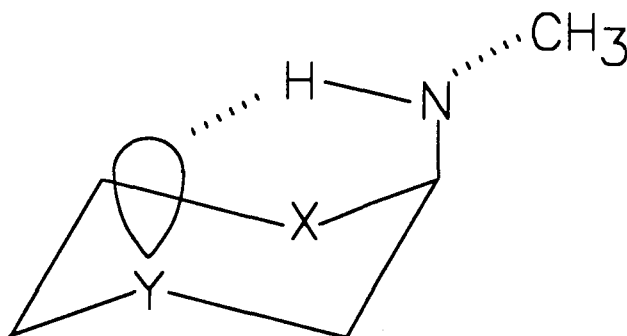


However, when  $Z=NHCH_3$ , the shortening of the C-N bond will enhance the hydrogen bond between the NH proton and the ring heteroatoms (Fig.3.33). In addition, since nitrogen is a better  $\pi$  donor and a weaker  $\sigma$  acceptor than oxygen, the endo-anomeric back donation of the  $n_O \rightarrow \sigma^*_{C-N}$  interaction will be smaller than the exo-anomeric  $n_N \rightarrow \sigma^*_{C-O}$  interaction. The same should apply to the  $n_S \rightarrow \sigma^*_{C-O}$ , and  $n_N \rightarrow \sigma^*_{C-S}$  interactions, as

indicated by the MO calculations using the isodesmic approach (Table 3.16). These bond length trends are also observed in the MO calculations of the gauche, gauche conformers of dihetero-substituted methanes  $XCH_2Y$  and the corresponding mono-substituted methanes (Table 3.19). The shortening of the exocyclic C-N bond will therefore, enhance the hydrogen bonding interaction between the NH proton and the ring heteroatom in the ethane type gauche fragment.

Figure 3.33

Hydrogen bond between NH proton and the ring heteroatom in axial-2-methylamino-1,4-diheterocyclohexanes.



One would also predict, as a result of the strong nitrogen  $\pi$  orbital donation, that the N-H bond will be strongly polarized. This prediction is supported by the Mulliken population analysis in the above calculations ( Fig.3.34). The magnitude of the hydrogen bond interactions between the positively charged NH proton and the ring heteroatom will thus be increased in the composite systems (16, 18-20, 22, 25-27).



Figure 3.34

Atomic charges on  $XCH_2Y$  ( $X=O, S; Y=NH_2$ ), given by Mulliken population analysis.

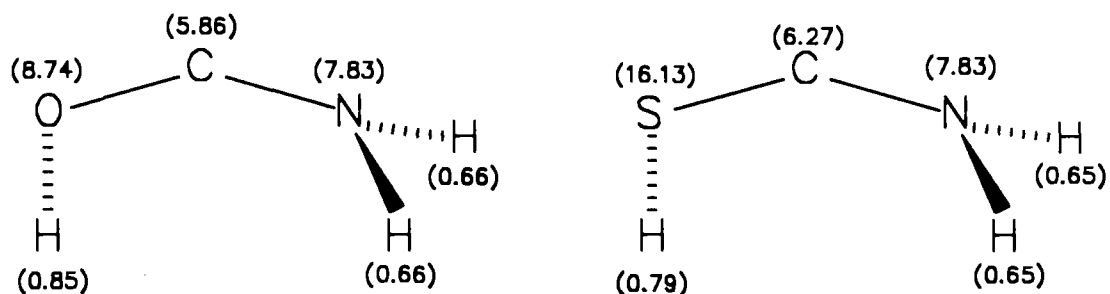


Table 3.19

Optimized bond lengths ( $\text{\AA}$ ) and bond angles ( $^\circ$ ) in the gauche, gauche conformation of  $XCH_2Y$  and the corresponding staggered mono-substituted methanes, evaluated at the 6-31G\* level.

Compound	Bond length $r_{C-X}, r_{C-Y}$	Bond length variation (%) <sup>a</sup>
$CH_3X$		
X=OH	1.400	
X=SH	1.818	
X= $NH_2$	1.453	
$XCH_2Y$		
X=OH, Y=OH	1.389, 1.389	-0.8, -0.8
X=SH, Y=OH	1.822, 1.385	+0.2, -1.1
X=OH, Y= $NH_2$	1.409, 1.434	+0.6, -1.3
X=SH, Y= $NH_2$	1.850, 1.433	+1.8, -1.4

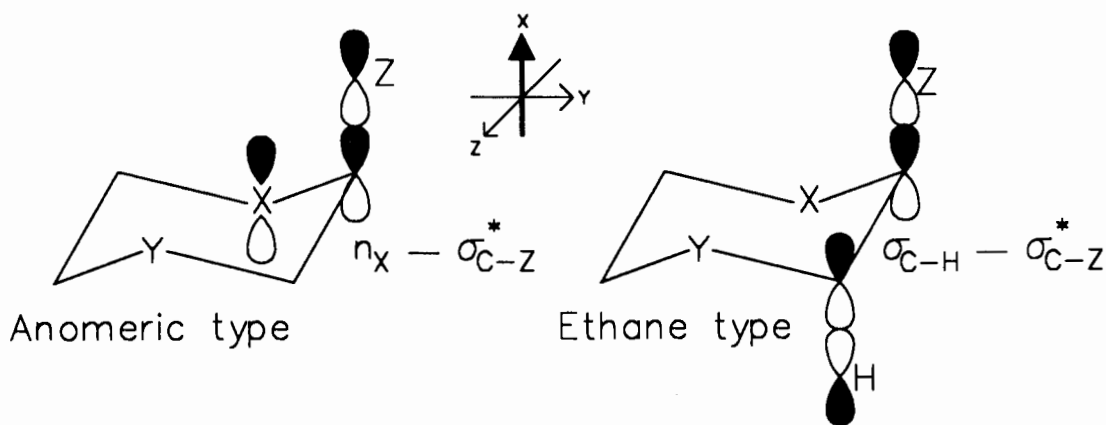
a). Bond length variation = Percentage changes in bond lengths in  $XCH_2Y$  when compared with the monosubstituted methanes.

## V. Additivity of Effects?

One of the orbital interactions in the anomeric type gauche interaction is the endo-anomeric  $n_X \rightarrow \sigma_{C-Z}^*$  interaction and one of the orbital interactions in the ethane type gauche interaction is the  $\sigma_{C-H} \rightarrow \sigma_{C-Z}^*$  interaction (Fig.3.35). In the

Figure 3.35

The  $n_X \rightarrow \sigma_{C-Z}^*$  orbital interaction in the anomeric type gauche fragment and the  $\sigma_{C-H} \rightarrow \sigma_{C-Z}^*$  orbital interaction in the ethane type gauche fragment.

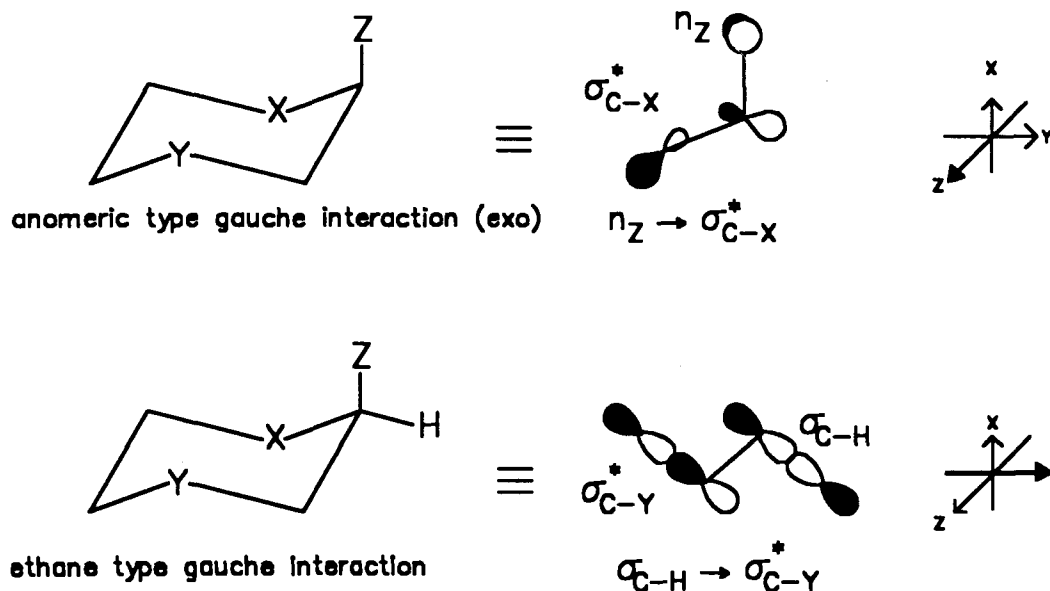


composite systems, both of these orbital interactions are operating in the same plane. The result of these three center orbital interactions might be more stabilizing than the summation of the two individual components. The other orbital interactions in the anomeric type and ethane type gauche interactions are orthogonal to each other and should, therefore, only have a minimal influence on each other in the

composite systems (Fig.3.36). Dominance of the interactions shown in Fig.3.35 will therefore, result in non-additivity whereas dominance of the interactions in Fig.3.36 will result in additivity of the individual effects. It is also clear from the above discussion that additional electrostatic stabilization, for example, NH hydrogen bonding, will also lead to non-additivity.

Figure 3.36

Orientations of the anomeric type and ethane type gauche orbital interactions.



Although good agreement is obtained for the  $\Delta E_{\text{orbital}}$  for the composite systems and the summation of the two individual components for the substituent  $Z=\text{OCH}_3$ , and arguments have been presented to account for the additivity, the discussion has

focused on the stabilizing orbital interactions. The agreement might only be fortuitous since the additional stabilizing and destabilizing interactions, brought about in the composite system might just compensate each other. The scheme of additivity might only be applicable if all the orbital interactions involved, are orthogonal to each other. The above discussion is more qualitative than quantitative. A more detailed understanding of the orbital interactions in the composite systems will have to await a quantitative perturbation molecular orbital analysis.

## CHAPTER 4

### PARAMETERIZATION OF THE MM2 FORCE FIELD FOR THE O-C-N SYSTEM

#### 4.1 Introduction

Molecular mechanics calculations, or force field calculations, treat a molecule as a collection of particles held together by simple harmonic forces. These forces are described in terms of potential energy functions. The combination of these potential energy functions is the force field.

The overall potential energy or "steric energy";  $E$ , of the molecule in the force field is derived from its energy difference from an "ideal" strain-free, zero energy structure. In its simplest form, the force field is approximated by the Westheimer equation [eq.4.1].<sup>286</sup>

$$E = E_s + E_b + E_w + E_{nb} \quad (\text{eq.4.1})$$

where

$E_s$  is the energy of bond deformation (stretching or compression)

$E_b$  is the energy of bending

$E_w$  is the torsional energy and

$E_{nb}$  is the energy of non-bonded interactions.

The force field reproduces the potential energy surface for the displacement of atoms within a molecule. The absolute energy, by itself has no physical meaning. However, it is the energy difference between different conformations of a molecule that are significant. The parameterization of the force fields relies heavily on experimental data collected. Allinger's MM2 force field has been parameterized to give excellent geometrical and relative energy results for several classes of compounds.<sup>287,288</sup> Other force fields such as those of Lifson and Warshe<sup>l</sup><sup>289-291</sup> and Boyd<sup>292,293</sup> are referred to as "consistent" force fields as they have been parameterized to reproduce vibrational frequencies as well as geometrical and thermodynamic data.

In its present form, the MM2 force field can treat hydrocarbons and most of the common type of monofunctional molecules with high accuracy.<sup>199</sup> For polyfunctional molecules, if the functional groups are separated by three or more carbons, the results are generally quite good.<sup>295</sup> The lack of reliable experimental force constants for molecules with neighbouring heteroatoms or with heteroatoms only one carbon apart, render the MM2 force field deficient in dealing with these types of molecules.<sup>294,295</sup>

This deficiency can be overcome by the proper use of quantum mechanically-derived parameters.<sup>262,296-301</sup> This idea

has been adopted by Fuchs and coworkers<sup>296</sup> in the parameterization of the N-C-N MM2 force field and by Wolfe et al. in the parameterization of peptide and penicillin force fields.<sup>297-299</sup>

This chapter describes the general procedures and strategy for the parameterization of the MM2 force field for X-C-Y systems. *Ab initio* MO calculations have been used to obtain the geometries and energies required for the parameterization. By way of example, the parameterization of the N-C-O force field is described. This parameterization would be essential for the proper evaluation of the conformational effects operating in some of the heterocyclic systems described in Chapter 3.

#### **4.2 Development of the Force Field**

The basic equation of the MM2 force field, which is an extension of the Westheimer equation, takes into account six types of interactions. The first one  $E_1$  represents the interaction between two directly bonded atoms (a stretching interaction) and the second  $E_2$  represents the interaction between two atoms bonded to a third (a bending interaction). These interactions can be represented by a simple function based on Hooke's Law. Hooke's Law, which assumes constant

force constants, overestimates the bending energy. Since a large bending deformation usually leads to a decrease in overlap between adjacent bonds, the effective force constant is reduced. To correct this, cubic terms are usually added to the stretching and bending potential functions of the MM2 force field equations [eq 4.2 and 4.3].<sup>288</sup>

$$E_1 = 143.88 (k_s/2) (\Delta l)^2 (1 + CS \cdot \Delta l) \quad (\text{eq.4.2})$$

where

143.88 = conversion factor for md/Å molecule to kcal/mol/Å<sup>2</sup>.

$k_s$  = stretching constant (md/Å).

$\Delta l = l_{ik} - l^{\circ}_{ik}$  where  $l_{ik}$  is the actual bond length and  $l^{\circ}_{ik}$  is the minimum energy bond length (Å).

CS = cubic stretch term.

$$E_2 = 0.043828 (k_b/2) (\Delta \theta)^2 (1 + SF \cdot \Delta \theta^4) \quad (\text{eq.4.3})$$

where

0.043828 = conversion factor for mdÅ/rad<sup>2</sup>/molecule to kcal/deg<sup>2</sup>/mol.

$k_b$  = bending constant (mdÅ/rad<sup>2</sup>) for angle type a-b-c.

$\Delta \theta = \theta_{abc} - \theta^{\circ}_{abc}$ , in degrees.  $\theta_{abc}$  is the actual angle and  $\theta^{\circ}_{abc}$  is the minimum energy angle for angle type a-b-c.

SF = sextic bending term.

As a bond angle is compressed, the two associated bond lengths usually become longer. To account for this compression related bond lengthening, a stretch-bend "cross term"  $E_3$  is included in the MM2 force field [eq 4.4].<sup>288</sup>

$$E_3 = 2.51118 k_{sb} (\Delta \theta_{abc}) (\Delta l_{ab} + \Delta l_{bc}) \quad (\text{eq.4.4})$$



where

2.51118 = conversion factor for md/rad/molecule to kcal/deg/mol.

$k_{sb}$  = stretch-bend constant (md/rad) for angle type a-b-c.

$\Delta l_{ab}, \Delta l_{bc} = l - l^\circ$  as defined in compression energy section.  
If atom a or c is a hydrogen or lone pair, the respective  $\Delta l = 0$ .

A fourth interaction is the non-bonded interaction  $E_4$ , represented by the Hill equation<sup>301</sup> using the Buckingham potential [eq 4.5 and 4.6].<sup>303,304</sup>

$E_4 = K_V(2.9 \times 10^5 e^{(-12.5R/r)} - 2.25(r/R)^6$  for  $r/R < 3.311$  (eq.4.5)  
and

$E_4 = 336.176(K_V(r/R)^2)$  for  $r/R > 3.311$  (eq.4.6)

where

$R$  = interatomic distance.

$r$  = sum of VDW radii.

$K_V = \sqrt{E_i \cdot E_j}$  where  $E_i$  and  $E_j$  are the hardness parameters for atoms  $i$  and  $j$ .

The Van der Waals (non-bonded) interaction energy is calculated between all pairs of atoms not bound to each other or to a common atom. The fifth interaction is the electrostatic interaction which takes into account differences in nuclear charge. This dipole/dipole type interaction  $E_5$  is calculated using Jeans' formula [eq 4.7].<sup>305</sup>

$E_5 = 14.39418(m_A \cdot m_B (\cos c - 3 \cos a_A \cdot a_B)) / r^3 \cdot \Delta E$  (eq.4.7)

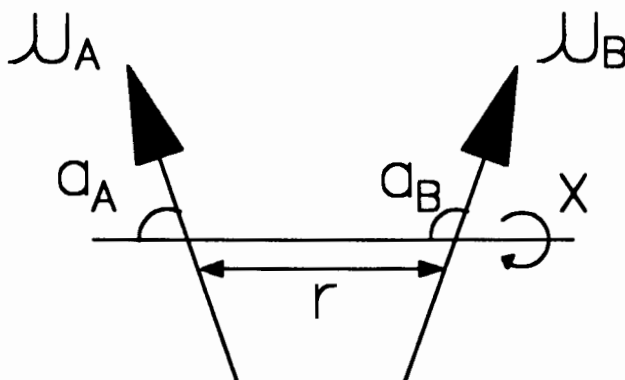
where

14.39418 = conversion factor for (ergs/molecule) to (kcal/mol)

$m_A$  and  $m_B$  = dipole moments of the two bonds.  
 $c$  = angle between the two bonds.  
 $r$  = distance between their mid points (Fig.4.1).  
 $a_A$  and  $a_B$  = angles between the bonds and the line joining their mid-points.  
 $\Delta E$  = dielectric constant parameter which is set to 1.5.

Figure 4.1

Schematic representation of a dipole/dipole interaction.



The final interaction is concerned with the torsional energy  $E_6$  which permits the accurate reproduction of conformational preferences [eq 1.7]. To a reasonable approximation, the torsional potential function is represented as a Fourier series expansion truncated at the third term.<sup>195</sup>

$$E_6 = V_1/2(1+\cos\omega) + V_2/2(1-\cos2\omega) + V_3/2(1+\cos3\omega) \quad (\text{eq.4.8})$$

where

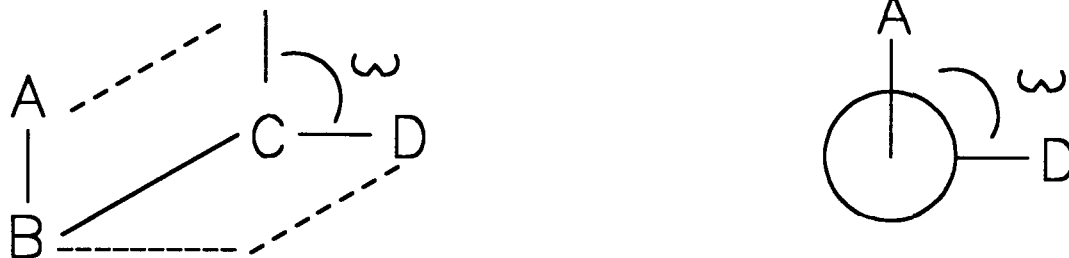
$V_1$ ,  $V_2$  and  $V_3$  = first, second and third order torsional constants.

$\omega$  = dihedral angle.

Torsional terms are incorporated explicitly into the force field for atom pairs which are separated by a chain of three bonds. For any set of four covalently bonded atoms A-B-C-D, the torsional (or dihedral) angle is defined as the angle measured about the B-C axis from the A-B-C plane to the B-C-D plane (Fig.4.2). The torsional angle is defined to be

Figure 4.2

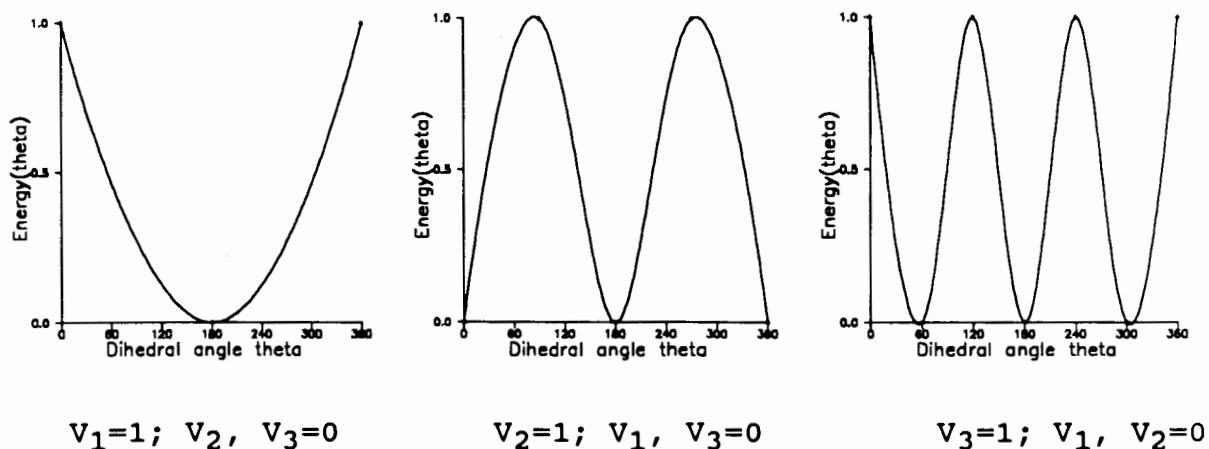
Schematic representation of a torsional angle  $\omega$  described by the connected atoms A-B-C-D.



positive when a clockwise rotation is needed to turn the A-B-C plane into the B-C-D plane when looking down the axis from B to C. This torsional function is used to reproduce multiple periodic extrema over a complete ( $360^\circ$ ) rotation. The periodicity and behaviour of these three terms are illustrated in Fig.4.3. The low periodicity ( $V_1$  and  $V_2$ ) terms tend to dominate in systems carrying heteroatoms.<sup>195</sup> Therefore, in systems that demonstrate the anomeric effect, such as the O-C-O-C fragments, the torsional behaviour is well described by the  $V_1$  and  $V_2$  terms.<sup>301</sup>

Figure 4.3

The periodicity and behaviour of the MM2 torsional terms.



### I. Ab initio calculations

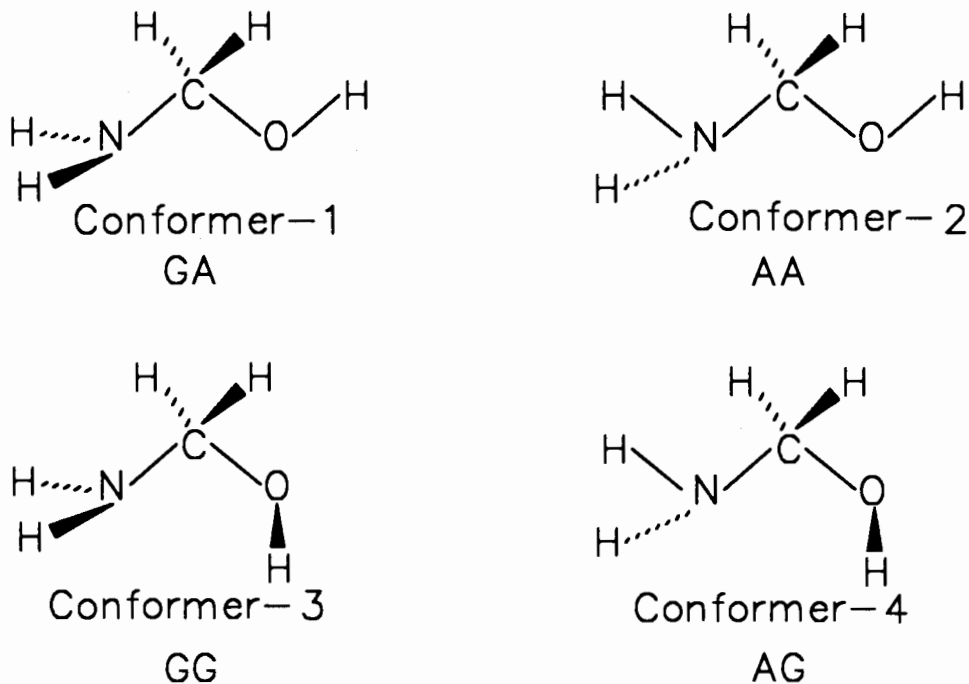
The simplest system containing the N-C-O fragment, aminomethanol (AMOL) has been calculated at the 4-21G level by Schafer and co-workers.<sup>107,306</sup> Full geometry optimization was applied to four conformers of AMOL (Fig.4.5); however, conformer-2 was transformed to conformer-1 at the end of the optimization.

In order to parameterize the MM2 force field, more than three conformers are required to evaluate the different potential energy functions. We calculated aminomethanol (AMOL, 4-1), methylaminomethanol (MAMOL, 4-2) and aminomethoxymethane (AMM, 4-3) at different minima and

transition states, using the GAUSSIAN 86 program<sup>307</sup> with full geometry optimization.

Figure 4.4

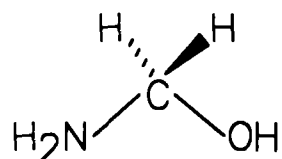
The four possible conformers of aminomethanol.



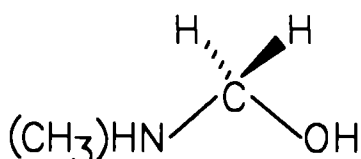
Given the size of the target molecules, and conscious of the need for computational economy at the time, the *ab initio* calculations were all performed at the 3-21G level.<sup>71</sup> It was found that the structural trends and relative energies of the three most stable conformers of AMOL were similar for computations at both the 3-21G and the 4-21G level.<sup>107</sup> The results of the calculations of the three true minima of aminomethanol are given in Table 4.1.

Figure 4.5

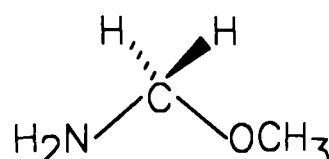
Aminomethanol (AMOL, 4-1), methylaminomethanol (MAMOL, 4-2)  
and aminomethoxymethane (AMM, 4-3).



Aminomethanol  
AMOL 4-1



Methylaminomethanol  
MAMOL 4-2



Aminomethoxymethane  
AMM 4-3

Analysis of the structural and energy parameters in Table 4.1 shows that the anomeric effect is operative in this molecule. The following are some interesting features that characterize the operation of the anomeric effect:-

1. The conformer (GG) with the most gauche arrangements of heteroatom pairs is the most stable .
2. The C-O bond length in the GA conformer is the longest and the C-N bond length is the shortest amongst the three stable conformers. This is in agreement with the  $n_N \rightarrow \sigma^*_{C-O}$  stabilizing orbital interaction.
3. Similarly, the C-N bond length in the AG conformer is the longest and the C-O bond length is the shortest due to the  $n_O \rightarrow \sigma^*_{C-N}$  orbital interaction.
4. The C-H bond lengths are also affected by a similar type of orbital interaction, but to a smaller extent.

5. The N-C-O bond angle in the GG conformer is the largest due to the highest degree of double bond character ( $n_N \rightarrow \sigma^*_{C-O}$  and  $n_O \rightarrow \sigma^*_{C-N}$  orbital interactions both turned on).

Table 4.1

Relative energies and selected structural parameters of fully optimized conformers (true minima) of aminomethanol (AMOL) at the 3-21G level: bond lengths in Å; angles in degrees.

	Conformer-1 (GA)	Conformer-3 (GG)	Conformer-4 (AG)
C1-H2	1.0823	1.0822	1.0833
C1-H3	1.0823	1.0760	1.0812
C1-O4	1.4469	1.4442	1.4352
C1-N5	1.4348	1.4383	1.4418
O4-H6	0.9666	0.9671	0.9673
N5-H7	1.0039	1.0017	0.9987
N5-H8	1.0039	1.0015	0.9972
O4-C1-N5	110.39	115.93	111.93
C1-O4-H6	111.19	110.59	108.04
C1-N5-H7	113.23	116.63	117.56
C1-N5-H8	113.23	115.34	118.09
H7-N5-H8	110.96	113.01	115.13
N5-C1-O4-H6	180.01	-62.44	-39.90
O4-C1-N5-H7	63.74	75.41	-79.33
O4-C1-N5-H8	-63.71	-60.83	135.42
-HF (Hartrees)	169.123109	169.125356	169.123360
$\Delta E$ (kcalmol <sup>-1</sup> )	1.41 (1.12)*	0.00 (0.00)*	1.25 (1.26)*

\* Calculated at the 4-21G level.<sup>107</sup>

## II. Development of anomeric bond length parameters

The C-N and C-O bonds lengths of this type of compound show a wide variation not accounted for by the anharmonic corrected Hooke's law function [eq.4.2]. The standard bond lengths ( $l_0$ ) of the C-N and C-O bonds are therefore redetermined according to the procedures of Norskov-Lauritsen and Allinger.<sup>301</sup> From eq.4.9 and 4.10, it can be seen that

For an anomeric fragment such as  $H_1-N_2-C_3-O_4-H_5$ :-

$$l_0' = l_0 - \Sigma \delta l \quad (\text{eq.4.9})$$

where

$l_0'$  = new natural bond length due to the anomeric effect  
and for the  $N_2-C_3$  bond,

$$\Sigma \delta l_{2,3} = \Sigma \{k/2[1+\cos(2\omega_{i_2,3})] - ck/2[1+\cos(2\omega_{j_3,4})]\} + d \quad (\text{eq.4.10})$$

where

- $\omega$  = dihedral angle lone pair-N-C-O.
- $i$  = summation over the lone pair on N.
- $j$  = summation over the lone pair on O.
- $k, c$  and  $d$  = constants.

the first term in eq.4.10 causes the shortening of  $l_{0,2,3}$ , and the second term causes its lengthening. There is also an overall shortening (an electrostatic effect) due to the constant  $d$ . In the MM2 calculations, the various  $l_0'$  are determined at the initial stage, and then are updated during the minimization process according to the change in the dihedral angle  $\omega$ .



The constants  $k$ ,  $c$  and  $d$  were developed using the bond length parameters obtained by the *ab initio* calculations of the four conformers of AMOL (Table 4.2). In the MM2 force field, the standard bond length  $l_0$  C-N = 1.438 and  $l_0$  C-O = 1.402. The optimized constants obtained from eq.4.9 and 4.10 were found to be

for C-N bond:  $c = 1.00$ ,  $k = 0.0047$ ,  $d = 0.0009$  and

for C-O bond:  $c = 3.33$ ,  $k = 0.0036$ ,  $d = -0.035$ .

Table 4.2

Bond lengths (in Å) obtained by the full geometry optimization of AMOL.

$l_0$ \Conformer	AG	AA*	GG	GA
C-N	1.4348	1.4491	1.4383	1.4418
C-O	1.4469	1.4428	1.4442	1.4352

\* The HNCO dihedral angles are fixed at 180° and 60°.

### III. Development of bond angle parameters

According to the bond bending function in the MM2 force field,<sup>298</sup> the bending energy for the bonded atoms N-C-O,

$$E_b = 0.043828(k_b/2)\Delta q^2_{NCO}[1+(0.007E-5)SF\Delta\theta^4_{NCO}] \quad (\text{cf. eq.4.3})$$

*Ab initio* energy values of the conformer-1 (GA) of AMOL were evaluated with different N-C-O bond angles from 100°-120° (Table 4.3). A least squares method was then used to

calculate the required parameters. The optimized parameters were found to be:

$$k_b = 1.59 \text{ md}\text{\AA}/\text{rad}^2, \theta_o = 111.35^\circ$$

Table 4.3

Relative energies E (kcalmol<sup>-1</sup>) of AMOL with different N-C-O bond angles ( $\theta$  in degrees):-

$\theta_{\text{NCO}}$	E	$\theta_{\text{NCO}}$	E
100.0	3.86	110.4	0.00
105.0	1.01	111.0	0.01
108.0	0.20	111.5	0.04
109.0	0.07	115.0	0.68
110.0	0.01	120.0	2.91

#### IV. Development of torsional parameters

This term is incorporated explicitly into the MM2 force field for the calculation of conformational energy differences with the change of torsional angle. It is the most important interaction in the force field when neighbouring heteroatom pairs are involved. The energy of torsion  $E_T$  is estimated by eq 4.11:<sup>308</sup>

$$E_T = E_{\text{QM}}(\omega) - E_{\text{MM}}(\omega) \quad (\text{eq.4.11})$$

where

- $E_{\text{QM}}(\omega)$  = quantum mechanical energy with dihedral angle  $\omega$ .
- $E_{\text{MM}}(\omega)$  = molecular mechanics energy with dihedral angle  $\omega$  (with all the torsional terms set to zero).

Since the MM2 force field calculates different types of interactions separately, it is essential to subtract  $E_{MM}$  from  $E_{QM}$  in order to obtain the energies associated with torsion. For the fragment A-B-C-D of interest, the A/D dihedral angle was varied from 0 to 180° in 30° intervals, and at each value, *ab initio* full geometry optimized MO calculations and MM2 calculations (with all the torsional terms set to zero) were performed. Each pair of energies was then subjected to analysis by eq.4.11 to give  $E_T$  values. A function of  $E_T$  against  $\omega$  was then obtained for each set of dihedral angles. The  $V_1$ ,  $V_2$  and  $V_3$  torsional terms were evaluated by means of a matrix least-squares method built into the spread sheet program SHEET.<sup>309</sup> The barriers to rotation, as well as the minima and maxima of AMOL, MAMOL and AMM are collected in Tables 4.4 to 4.6. The parameters obtained by this procedure provided good estimates for the torsional constants. This procedure is more accurate than that carried out by Fuchs et al for the parameterization of the N-C-N fragment.<sup>111,296,310</sup> In their studies, the energy potential curves calculated by molecular mechanics were adjusted through the torsional terms ( $V_1$ ,  $V_2$ , and  $V_3$ ) by trial and error, until a reasonable fit between the *ab initio* results and the MM2 curves was achieved. The magnitudes of the individual torsional terms might not reflect their actual contribution to the total energies. In this study, after the initial set of torsional

terms is obtained, only small adjustments are required to obtain the best fit between the experiment and quantum mechanical results. A list of the torsional constants are collected in Table 4.7.

Table 4.4

Relative energies E (kcalmol<sup>-1</sup>) of aminomethanol (AMOL) with different dihedral angles  $\omega$  (degrees).

a) H-N-C-O							
$\omega$	0.0	30.0	60.0	90.0	120.0	150.0	180.0
$E_{QM}$	3.90	0.77	0.00	0.73	2.00	3.29	4.60
$E_{MM}$	3.05	1.81	1.14	1.67	1.93	0.75	0.00
$E_T$	0.85	-1.14	-1.14	-0.94	0.07	2.54	4.60
b) H-O-C-N							
$\omega$	0.0	30.0	60.0	90.0	120.0	150.0	180.0
$E_{QM}$	2.20	0.73	0.00	1.60	2.10	1.86	1.40
$E_{MM}$	2.26	1.68	0.85	0.81	0.94	0.42	0.00
$E_T$	-0.06	-0.95	-0.85	0.79	1.16	1.44	1.40
c) LP-O-C-N							
$\omega$	0.0	30.0	60.0	90.0	120.0	150.0	180.0
$E_{QM}$	2.10	1.58	1.40	1.74	2.20	1.95	0.00
$E_{MM}$	0.21	0.00	0.37	1.28	1.40	0.53	0.00
$E_T$	1.89	1.58	1.03	0.46	0.80	1.42	0.00
d) LP-N-C-O							
$\omega$	0.0	30.0	60.0	90.0	120.0	150.0	180.0
$E_{QM}$	4.30	2.86	2.30	3.73	6.20	4.98	0.00
$E_{MM}$	1.92	0.77	0.00	0.80	1.96	1.62	1.14
$E_T$	2.38	2.09	2.30	2.93	4.24	3.36	-1.14

Table 4.5

Relative energies E (kcalmol<sup>-1</sup>) of methylaminomethanol (MAMOL) with different C-N-C-O dihedral angles  $\omega$  (degrees).

$\omega$	0.0	30.0	60.0	90.0	120.0	150.0	180.0
E <sub>QM</sub>	9.93	2.52	0.00	4.39	6.61	7.08	6.97
E <sub>MM</sub>	3.21	2.09	0.88	1.83	3.05	1.63	0.00
E <sub>T</sub>	6.72	0.43	-0.88	2.56	3.56	5.45	6.97

Table 4.6

Relative energies E (kcalmol<sup>-1</sup>) of aminomethoxymethane (AMM) with different C-O-C-N dihedral angles  $\omega$  (degrees).

$\omega$	0.0	30.0	60.0	90.0	120.0	150.0	180.0
E <sub>QM</sub>	5.61	1.22	0.00	2.45	3.58	2.26	2.38
E <sub>MM</sub>	4.56	2.95	1.03	1.11	2.04	0.99	0.00
E <sub>T</sub>	1.05	-1.73	-1.03	1.34	1.54	2.21	2.38

Table 4.7

Torsional constants obtained for the parameterization of the MM2 force field for the N-C-O fragment<sup>a</sup>.

Torsion Angle Type	Fourier Expansion Parameters (kcalmol <sup>-1</sup> )		
	V <sub>1</sub>	V <sub>2</sub>	V <sub>3</sub>
O-C-N-C	-2.98	-2.46	1.67
O-C-N-LP	0.62	2.20	1.38
O-C-N-H	-2.23	-1.94	-0.54
N-C-O-C	-1.55	-0.84	1.29
N-C-O-LP	1.29	-0.22	0.86
N-C-O-H	-1.80	0.65	1.59

a). The inclusion of lone-pairs is important since systems with anomeric effects have strong adjacent orbital interactions and the magnitudes of the interactions with the non-bonding n orbitals are usually significant.<sup>107</sup>

The parameterized N-C-O force field, MM2\*, has been used to examine a number of acyclic and heterocyclic molecules containing this unit. The relative energies of different conformers of aminomethanol (AMOL), methylaminomethanol (MAMOL), aminomethoxymethane (AMM) and 1-methoxy-N,N-dimethylmethanamine (MDMMA) are collected in Table 4.8 together with the corresponding literature values. The relative energies of the various axial and equatorial structures of 2-methylaminoxacyclohexane (MAOC), 1-oxa-3-azacyclohexane (OAC), 1-oxa-3,5-diazacyclohexane (ODAC) and 1,3-dioxa-5-azacyclohexane (DOAC), as calculated by MM2\* vs literature values are collected in Table 4.9. The results indicate that although the agreement is generally good, MM2\* overestimates the stabilities of the gauche conformers. This may be attributed to the choice of torsional parameters. During the parameterization of the X-N-C-O-Y torsional constants, the lone pair orbital interactions were always maximized. In order to obtain the X-N-C-O torsional constants, the Y-O-C-N unit was fixed at the conformation with the maximum lone pair orbital interaction ( $n_O \rightarrow \sigma^*_{C-N}$ ). Similarly, when parameterizing the Y-O-C-N unit, the X-N-C-O unit was fixed such that maximum  $n_N \rightarrow \sigma^*_{C-O}$  orbital interactions were present. This is a limitation of the current MM2 program since torsion about only one of the pair of bonds can be

Table 4.8

Predicted relative energies (kcalmol<sup>-1</sup>) of the conformers of aminomethanol (AMOL), methylaminomethanol (MAMOL), aminomethoxymethane (AMM) and 1-methoxy-N,N-dimethylmethanamine (MDMMA) with the newly parameterized MM2 force field, MM2\*, and *ab initio* MO calculations.

AMOL		
Conformer	MM2*	Literature <sup>a107</sup>
GG	0.0	0.0
GA	1.5	1.12
AG	3.5	1.26
AA	5.9	Failed to converge

MAMOL		
Conformer	MM2*	Literature <sup>a309</sup>
GG-	1.2	0.4
GG	0.0	0.0
GA	2.2	1.3
AG	5.1	1.6
AA	8.5	7.0
G-G-	4.8	0.7
G-A	8.1	6.6

AMM		
Conformer	MM2*	Literature <sup>a309</sup>
GA	7.4	7.3
G-A	1.2	0.7
GG	0.0	0.0

MDMMA		
Conformer	MM2*	Literature <sup>a309</sup>
GA	4.3	4.9
G-A	0.0	0.0
AG-	4.2	0.5

a). *Ab initio* MO calculation at the 4-21G level.

handled. A torsional cross term is required to appropriately treat this torsion/torsion interaction.

Table 4.9

Relative energies (kcalmol<sup>-1</sup>) of the axial and equatorial conformers of heterocycles having N-C-O units as calculated by MM2\* vs literature values.

MAOC		
Substituent	MM2*	Literature <sup>a24</sup>
A	0.5	1.5
E	0.0	0.0

OAC		
Substituent	MM2*	Literature <sup>b312</sup>
A	0.0	0.0
E	5.4	4.8

ODAC		
Substituent	MM2*	Literature <sup>b312</sup>
AA	0.0	0.0
AE	5.4	4.8
EE	12.5	15.1

DOAC		
Substituent	MM2*	Literature <sup>b312</sup>
A	0.0	0.0
E	12.3	Failed to converge

- a). Estimated by dynamic NMR spectroscopy.  
 b). *Ab initio* MO calculations at the 4-21G level.

As a result of this parameterization, the exo-anomeric effect is maximized. This is observed in both the axial and



equatorial conformers of 2-methylaminoxacyclohexane. The axial and equatorial conformers have the lowest energies when the lone pair on nitrogen is antiperiplanar to the endocyclic C-O bond. This prediction is also supported by the coupling constants and nOe enhancement analysis in axial and equatorial methylaminoxacyclohexane.<sup>24</sup>

The bond length and bond angle parameters of different conformations of aminomethanol are collected in Table 4.10.

Table 4.10

Predicted bond length (Å) and bond angle (degrees) parameters of aminomethanol, as calculated by MM2\*.

Conformer	Bond Length		Bond angle
	C-N	C-O	N-C-O
GG	1.4403	1.4232	110.80
AG	1.4391	1.4241	110.74
GA	1.4403	1.4245	111.18
AA	1.4414	1.4272	111.97

The trends in the change in bond lengths and bond angles with different conformations are also consistent with the operation of  $n \rightarrow \sigma^*$  orbital interactions. However, the absolute values of the bond lengths and bond angles differ from those obtained by *ab initio* calculations. A better fit would require further work on the optimization of the anomeric bond length parameters as a function of C-O and C-N torsion, and the

proper choice of equilibrium bond lengths and bond angles. Given the approximations of the molecular mechanics method, this level of refinement is probably unnecessary. MM2\* in its present form is adequate for sampling the conformations of molecules containing N-C-O units.#

---

# After the completion of this work, an independent report describing a parameterization of the MM2 force field for the N-C-O fragment appeared [B.Fernandez, M.A.Rios and L.Carballera, *J.Comp.Chem.*, 12, 78, 1991]. However, this parameterization involves modification of the source code of the MM2 program. The parameterization described in this chapter utilizes the MM2 program in its original form and only incorporates additional parameters.

## CHAPTER 5

### THE STUDY OF ANOMERIC SYSTEMS CONTAINING SECOND AND LOWER ROW HETEROATOMS

#### Results and Discussion

The initial theoretical studies of Schleyer *et al.*<sup>39</sup> suggested that anomeric interactions are not significant in systems containing second and third row elements. On the contrary, the experimental studies of Pinto *et al.* showed that anomeric effects involving second and third row hetero-substituents were important in determining conformations (see Chapter 1).<sup>28,29,38,157,313,314</sup> The purpose of this study is to get a direct estimate of the magnitude of anomeric interactions involving second and third row heteroatoms. The energies and geometries of various conformations (Fig.5.1) of diselenomethane  $\text{CH}_2(\text{SeH})_2$ , selenothiomethane  $\text{CH}_2(\text{SeH})(\text{SH})$  and dithiomethane  $\text{CH}_2(\text{SH})_2$  were calculated using *ab initio* MO methods (Table 5.1, 5.2, 5.3). The gauche, gauche and gauche, anti conformations correspond to the truncated fragments of the axial and equatorial 2-substituted heterocyclohexanes, respectively (Fig.5.2). The energy difference between these two conformers is therefore, a measure of the anomeric effect. The use of such truncated units can avoid the additional effects such as ring constraints and solvent interactions present in the experimental investigations.

Figure 5.1

The five relevant conformations of disubstituted methanes (for  $X=Y$ , G, A $\equiv$ A, G).

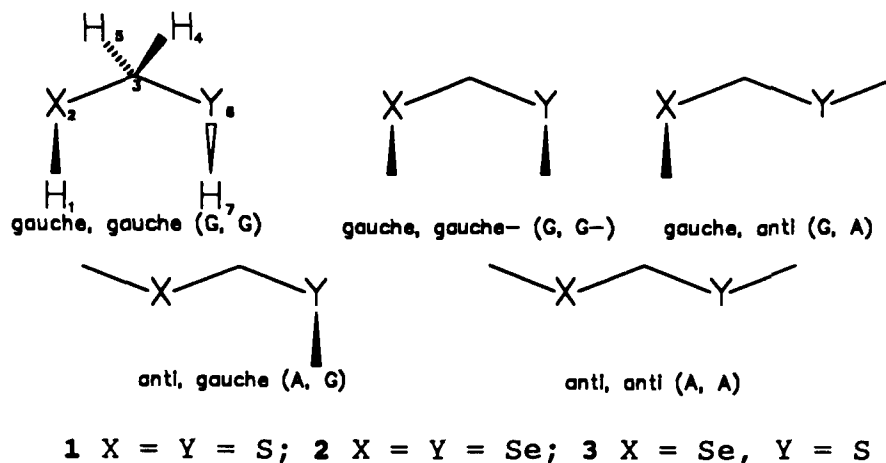
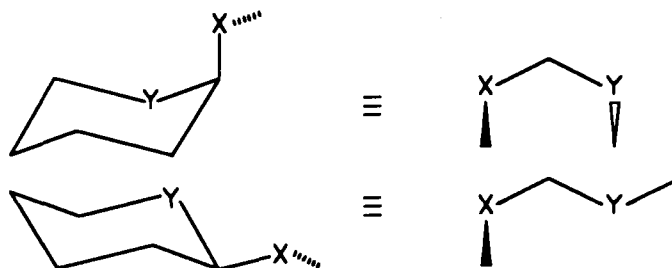


Figure 5.2

The relationship between the axial and equatorial conformations of 2-substituted-heterocyclohexanes and their truncated models.



The Gaussian86 program<sup>225</sup> was used in the calculations. The basis sets chosen for the S and Se atoms were those of Huzinaga and his group<sup>314,315</sup> and the hydrogen and carbon

basis sets were standard STO-3G three gaussian expansions.<sup>316</sup> In addition, d-polarization functions were included for S and Se, and the basis sets were denoted as MINI-1\*. Orbital exponents of 0.46 and 0.37 were employed for the 3d polarization functions of S<sup>317</sup> and Se,<sup>318</sup> respectively. Minimal basis level treatment was found to be suitable for the quantitative comparison of similar molecules. The geometry parameters of chalcogen hydrides were reasonably reproduced.<sup>319</sup> The use of polarization functions is important for describing the geometry parameters of molecules containing second and lower row substituents which are capable of expanding their valence shells.<sup>320</sup> For simple molecules, the molecular properties are described adequately with standard basis sets which comprise functions centered at the nuclear positions. Functions of higher angular quantum number such as the d-type functions on heavy atoms are required to displace the center of electron charge away from the nuclear positions. In most cases, geometric parameters especially equilibrium bond lengths calculated with polarized basis sets are in better agreement with their respective experimental values.<sup>71,321</sup> The inclusion of diffuse functions were also found to lower the total energies of different conformers of a molecule.<sup>322</sup>

In order to investigate the accuracy of Huzinaga's MINI-1\* basis set, the gauche, gauche and gauche, anti conformers

of dithiomethane were calculated at various computational levels (Table 5.4, 5.5). With the exception of the 4-31G basis set, all basis set calculations gave relative energies between the two gauche, gauche and gauche, anti conformers that were within  $0.3 \text{ kcal mol}^{-1}$  of one another. However, the bond lengths calculated using the MINI-1\* basis set, were all longer than those calculated with the 3-21G\* and 6-31G\* basis sets. In a study on compounds containing carbonyl groups, it was found that the relative energies calculated using the 6-31G\* basis set were essentially the same regardless of whether the 3-21G or 6-31G\* geometries were used.<sup>323</sup> Therefore, bond length variations with different basis sets appear to have little effect on the relative energies of different conformations. The MINI-1 basis set has been optimized for good orbital energies.<sup>314,315,317,318</sup> It predicts ionization energies of chalcogen hydrides close to experimental values.<sup>324-327</sup> In general, the ionization energies calculated are approximately 4% higher than experimental. It is known that calculations with the MINI-1 basis set give poor bond lengths but reproduce very well the bond angles. The largest discrepancies are in the C-X bond lengths; for instance, the C-S bond lengths are too long, typically of the order of 0.1 Å.<sup>319</sup> Except for the STO-3G basis set which underestimated the C-S and H-S bond lengths, all the standard basis set calculations overestimated them in the present study (Table

5.4, 5.5). The inclusion of d-functions improves these parameters and is consistent with the concept of d-orbital participation, as first proposed by Pauling.<sup>328</sup>

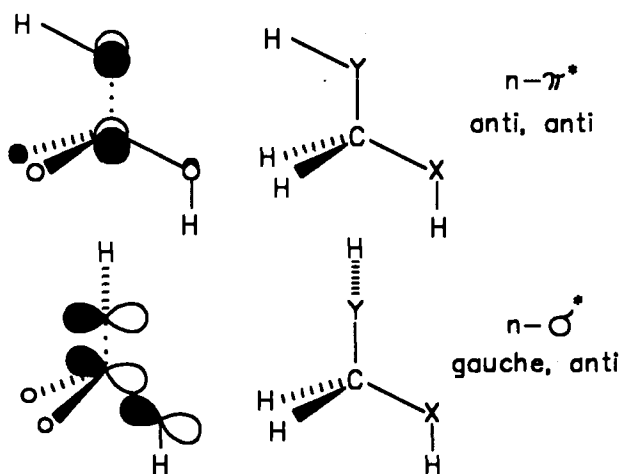
For all three compounds examined at the MINI-1\* level, the total energies of the different conformers vary in the sequence  $g,g < g,a < g,g^- < a,a$ . In the  $g,g$  arrangement, the anomeric interaction is at a maximum, and both heteroatoms can participate in the two electron-two orbital stabilizing interactions as described in Chapter 1. The  $g,g^-$  conformer, however, has an unfavourable dipole-dipole interaction as well as a destabilizing steric repulsion. In the  $g,a$  forms, only one anomeric type interaction is present. For the  $a,a$  conformers, the anomeric interaction is between the  $n_p$  orbital of the heteroatoms and the  $\sigma^*$  orbital of the trans C-H bonds. This is a weaker stabilization than the corresponding  $n \rightarrow \sigma^*_{C-X}$  interaction. In addition, the  $a,a$  conformers are destabilized by a parallel dipole-dipole repulsion. Of particular note are the relative energies between the  $g,g$  and  $g,a$  conformations; they are defined as the anomeric effects between the interacting orbitals.

As with other anomeric systems, the bond distances between atoms involved in anomeric interactions are altered according to the orientation of the heteroatom lone pairs.<sup>37</sup> For instance, the C-X and C-Y bonds in the gauche, anti

conformers of all three molecules studied are the longest and shortest, respectively amongst all the conformers. The effect of two or more electronegative atoms bonded to the same carbon, on the bond lengths appears to be general.<sup>329</sup> It has been observed experimentally<sup>20-22</sup> and theoretically.<sup>20,25,71,90,330,331</sup> These bond length variations can be understood within the framework of a perturbation molecular orbital (PMO) model<sup>22-24</sup> which can account not only for the geometric but also the energetic variations from one conformer to another, as described in Chapter 1. Within this context, the greater charge transfer to the antibonding C-X region resulting from the  $n \rightarrow \sigma^*$  interaction (Fig.5.3) gives

Figure 5.3

The orbitals involved in the  $\pi$  and  $\sigma$  type interactions in disubstituted methanes.





a longer C-X bond and a shorter C-Y bond in the gauche, anti than in the anti, anti conformer. In the gauche, gauche conformer, the two  $n \rightarrow \sigma^*$  interactions are operating against each other. While the C-Y bond is shortened due to the  $n_Y \rightarrow \sigma^*_{CH_2X}$  charge transfer, it is also lengthened by the  $n_X \rightarrow \sigma^*_{CH_2Y}$  back donation. As a result, the C-X and C-Y bond lengths are in between the two extremes. For instance, the C-Se bond lengths in the gauche, anti conformer of diselenomethane are 2.010 and 2.002 Å. The anti C-Se bond is 0.01 Å longer than the gauche C-Se bond. In the gauche, gauche conformer, the two Se atoms can participate approximately equally in the charge transfer, therefore, both C-Se bonds are almost identical (2.006 Å)<sup>a</sup>. However, for the gauche, gauche- conformer which has the proper geometry for anomeric charge transfer, the C-Se bonds are slightly longer than in the gauche, gauche conformer, probably due to the destabilizing steric repulsion between the two protons pointing in the same direction.

In the gauche, gauche conformer of selenothiomethane, the C-S bond shortening (0.006 Å) is 3 times greater than the C-Se bond shortening (0.002 Å) when compared with the anti, anti conformer. Although selenium and sulfur have nearly the same electronegativity according to most scales,<sup>332</sup> the above bond

---

<sup>a</sup> It is worthy of note that the C-Se bond lengths observed experimentally in g,g C-Se-C-Se acetal units are 1.932 (6) -1.967 (6) Å.<sup>27</sup>

length differences suggest that the  $n_S \rightarrow \sigma^*_{C-Se}$  is stronger than the  $n_{Se} \rightarrow \sigma^*_{C-S}$  orbital interaction. Moreover, the anti, gauche conformer is more stable than the gauche, anti conformer (Table 5.2).

The study of Pinto et al. on 2-[(4-methoxyphenyl)seleno]-1,3-dithiacyclohexane showed the presence of a sulfur endo-anomeric effect and a selenium exo-anomeric effect.<sup>333</sup> They also proposed a double-bond no-bond structure with a negatively charged selenium for the axial conformation. From the measured dipole moments in the equatorial and axial conformers, and the analysis of the equilibrium data by means of a dual substituent parameter approach,<sup>158,159</sup> Pinto et al.<sup>333</sup> suggested that increased electron density was present on selenium in the axial conformer. The same situation is observed in the gauche, gauche conformer of selenothiomethane; examination of the results of a Mulliken population analysis indicates that the selenium is more negatively charged and the sulfur less negatively charged when compared with the corresponding diselenomethane and dithiomethane.

Table 5.1

Optimized parameters (bond lengths in Å; bond angles in degrees) of diselenomethane<sup>a,b</sup>.

	G, G	G, G-	G, A	A, A
H <sub>1</sub> -Se <sub>2</sub>	1.4897	1.4882	1.4911	1.4903
H <sub>7</sub> -Se <sub>6</sub>	1.4891	1.4884	1.4899	1.4905
H <sub>4</sub> -C <sub>3</sub>	1.1185	1.1194	1.1179	1.1178
H <sub>5</sub> -C <sub>3</sub>	1.1185	1.1176	1.1183	1.1179
C <sub>3</sub> -Se <sub>2</sub>	2.0056	2.0067	2.0096	2.0100
C <sub>3</sub> -Se <sub>6</sub>	2.0061	2.0059	2.0016	2.0099
C <sub>3</sub> -Se <sub>2</sub> -H <sub>1</sub>	94.64	94.96	94.90	93.90
C <sub>3</sub> -Se <sub>6</sub> -H <sub>7</sub>	94.68	94.88	94.59	93.90
H <sub>4</sub> -C <sub>3</sub> -Se <sub>2</sub>	106.46	105.79	110.28	109.47
H <sub>5</sub> -C <sub>3</sub> -Se <sub>2</sub>	109.66	109.86	109.90	109.47
Se <sub>2</sub> -C <sub>3</sub> -Se <sub>6</sub>	115.26	116.39	110.40	107.35
H <sub>4</sub> -C <sub>3</sub> -Se <sub>2</sub> -H <sub>1</sub>	180.52	177.65	51.47	61.40
H <sub>5</sub> -C <sub>3</sub> -Se <sub>2</sub> -H <sub>1</sub>	62.55	60.27	-70.31	-61.08
H <sub>1</sub> -Se <sub>2</sub> -C <sub>3</sub> -Se <sub>6</sub>	-57.51	-65.12	172.73	180.17
H <sub>7</sub> -Se <sub>6</sub> -C <sub>3</sub> -H <sub>5</sub>	182.67	-54.82	173.83	61.28
-E(Hartree)	4820.61510	4820.61339	4820.61430	4820.61157
ΔE kcalmol <sup>-1</sup>	0.00	1.07	0.50	2.21

<sup>a</sup> Atom numbering is that of figure 5.1.

<sup>b</sup> This study, Huzinaga's MINI-1 basis with d polarization functions.<sup>337</sup>

Table 5.2

Optimized parameters (bond lengths in Å; bond angles in degrees) of selenothiomethane a,b.

	G, G	G, G-	A, G	G, A	A, A
H <sub>1</sub> -Se <sub>2</sub>	1.4893	1.4882	1.4905	1.4905	1.4895
H <sub>7</sub> -S <sub>6</sub>	1.3687	1.3676	1.3691	1.3698	1.3695
H <sub>4</sub> -C <sub>3</sub>	1.1199	1.1206	1.1191	1.1188	1.1193
H <sub>5</sub> -C <sub>3</sub>	1.1198	1.1189	1.1200	1.1203	1.1193
C <sub>3</sub> -Se <sub>2</sub>	2.0120	2.0123	2.0157	2.0047	2.0139
C <sub>3</sub> -S <sub>6</sub>	1.8724	1.8729	1.8692	1.8783	1.8788
C <sub>3</sub> -Se <sub>2</sub> -H <sub>1</sub>	94.47	94.77	95.03	94.47	93.83
C <sub>3</sub> -S <sub>6</sub> -H <sub>7</sub>	95.74	96.05	95.66	95.60	94.90
H <sub>4</sub> -C <sub>3</sub> -Se <sub>2</sub>	105.16	105.48	109.67	105.77	108.92
H <sub>5</sub> -C <sub>3</sub> -Se <sub>2</sub>	109.16	109.05	109.36	109.10	108.92
Se <sub>2</sub> -C <sub>3</sub> -S <sub>6</sub>	115.16	116.28	110.51	110.12	106.96
H <sub>4</sub> -C <sub>3</sub> -Se <sub>2</sub> -H <sub>1</sub>	181.14	169.73	49.99	173.86	-60.70
H <sub>5</sub> -C <sub>3</sub> -Se <sub>2</sub> -H <sub>1</sub>	63.97	53.25	-70.72	55.61	60.70
H <sub>5</sub> -C <sub>3</sub> -S <sub>6</sub> -H <sub>7</sub>	180.62	-59.74	175.32	53.17	-61.64
H <sub>1</sub> -Se <sub>2</sub> -C <sub>3</sub> -S <sub>6</sub>	-56.06	-72.92	172.21	-66.44	180.00
-E(Hartree)	2825.8482	2825.8453	2825.8473	2825.8467	2825.8442
ΔE kcalmol <sup>-1</sup>	0.00	1.80	0.57	0.92	2.51

<sup>a</sup> Atom numbering is that of Figure 5.1.

<sup>b</sup> This study, Huzinaga's MINI-1 basis with d polarization functions.<sup>337</sup>

Table 5.3

Optimized parameters (bond lengths in Å; bond angles in degrees) of dithiomethane<sup>a,b</sup>.

	G, G	G, G-	G, A	A, A
H <sub>1</sub> -S <sub>2</sub>	1.3686	1.3674	1.3695	1.3689
H <sub>7</sub> -S <sub>6</sub>	1.3685	1.3674	1.3699	1.3689
H <sub>4</sub> -C <sub>3</sub>	1.1211	1.1218	1.1204	1.1206
H <sub>5</sub> -C <sub>3</sub>	1.1211	1.1202	1.1215	1.1206
C <sub>3</sub> -S <sub>2</sub>	1.8783	1.8788	1.8835	1.8828
C <sub>3</sub> -S <sub>6</sub>	1.8778	1.8783	1.8731	1.8828
C <sub>3</sub> -S <sub>2</sub> -H <sub>1</sub>	95.57	95.92	95.68	94.90
C <sub>3</sub> -S <sub>6</sub> -H <sub>7</sub>	95.54	95.88	95.55	94.90
H <sub>4</sub> -C <sub>3</sub> -S <sub>2</sub>	106.41	105.82	110.42	109.85
H <sub>5</sub> -C <sub>3</sub> -S <sub>2</sub>	110.18	110.23	110.25	109.85
S <sub>2</sub> -C <sub>3</sub> -S <sub>6</sub>	115.01	116.05	110.18	106.68
H <sub>4</sub> -C <sub>3</sub> -S <sub>2</sub> -H <sub>1</sub>	180.37	182.82	69.99	61.02
H <sub>5</sub> -C <sub>3</sub> -S <sub>2</sub> -H <sub>1</sub>	62.15	60.28	-51.24	-61.02
H <sub>1</sub> -S <sub>2</sub> -C <sub>3</sub> -S <sub>6</sub>	-58.07	-65.70	186.92	180.00
H <sub>7</sub> -S <sub>6</sub> -C <sub>3</sub> -H <sub>5</sub>	-56.72	70.94	-65.53	180.00
-E(Hartree)	831.081177	831.079352	831.079708	831.076769
ΔE kcalmol <sup>-1</sup>	0.00	1.15	0.92	2.77

<sup>a</sup> Atom numbering is that of Figure 5.1.

<sup>b</sup> This study, Huzinaga's MINI-1 basis with d polarization functions.<sup>337</sup>

Table 5.4

Optimized geometric parameters (bond lengths in Å; bond angle in degrees) of dithiomethane at various levels of computation<sup>a, b</sup>.

	STO-3G	3-21G	3-21G*	4-31G	6-31G*	MINI-1	MINI-1*
C <sub>3</sub> -S <sub>2</sub>	1.80	1.87	1.81	1.872	1.81	1.93	1.878
C <sub>3</sub> -S <sub>6</sub>	1.80	1.87	1.81	1.872	1.81	1.93	1.877
H <sub>1</sub> -S <sub>2</sub>	1.33	1.35	1.32	1.354	1.32	1.39	1.368
H <sub>7</sub> -S <sub>6</sub>	1.33	1.35	1.32	1.354	1.32	1.39	1.368
H <sub>4</sub> -C <sub>3</sub>	1.08	1.07	1.07	1.074	1.07	1.12	1.121
H <sub>5</sub> -C <sub>3</sub>	1.08	1.07	1.07	1.074	1.07	1.12	1.121
S <sub>2</sub> -C <sub>3</sub> -S <sub>6</sub>	116.86	114.97	115.86	115.23	116.61	115.06	115.01
H <sub>7</sub> -S <sub>6</sub> -C <sub>3</sub>	95.68	97.65	97.25	97.40	97.62	96.93	95.54
H <sub>1</sub> -S <sub>2</sub> -C <sub>3</sub>	95.67	97.65	97.26	97.41	97.55	96.93	95.57
H <sub>4</sub> -C <sub>3</sub> -S <sub>6</sub>	106.39	105.87	106.19	105.79	105.85	105.99	106.41
H <sub>5</sub> -C <sub>3</sub> -S <sub>6</sub>	110.21	110.13	110.40	110.20	110.35	110.11	110.18
H <sub>7</sub> -S <sub>6</sub> -C <sub>3</sub> -S <sub>2</sub>	59.77	58.49	57.88	57.80	57.40	57.87	58.07
H <sub>1</sub> -S <sub>2</sub> -C <sub>3</sub> -S <sub>6</sub>	62.20	59.06	56.74	56.64	57.78	60.17	56.72
H <sub>4</sub> -C <sub>3</sub> -S <sub>6</sub> -H <sub>7</sub>	183.26	180.31	180.80	179.83	180.67	179.79	180.37
H <sub>5</sub> -C <sub>3</sub> -S <sub>6</sub> -H <sub>7</sub>	-61.82	-60.98	-62.66	-61.68	-63.12	-61.86	-62.15

<sup>a</sup> Atom numbering is that of Figure 5.1.

<sup>b</sup> gauche, gauche conformer

Table 5.5

Optimized geometric parameters (bond lengths in Å; bond angles in degrees) of dithiomethane at various levels of computation<sup>a,b</sup>.

	STO-3G	3-21G	3-21G*	4-31G	6-31G*	MINI-1	MINI-1*
C <sub>3</sub> -S <sub>2</sub>	1.80	1.87	1.81	1.86	1.81	1.93	1.873
C <sub>3</sub> -S <sub>6</sub>	1.81	1.88	1.82	1.88	1.82	1.94	1.884
H <sub>1</sub> -S <sub>2</sub>	1.33	1.35	1.32	1.35	1.32	1.39	1.369
H <sub>7</sub> -S <sub>6</sub>	1.33	1.35	1.32	1.35	1.32	1.39	1.370
H <sub>4</sub> -C <sub>3</sub>	1.08	1.07	1.07	1.07	1.07	1.12	1.122
H <sub>5</sub> -C <sub>3</sub>	1.09	1.07	1.07	1.07	1.08	1.12	1.120
S <sub>2</sub> -C <sub>3</sub> -S <sub>6</sub>	113.23	110.47	111.05	110.53	111.72	110.42	110.18
H <sub>7</sub> -S <sub>6</sub> -C <sub>3</sub>	95.02	97.38	97.05	97.42	97.02	96.78	95.55
H <sub>1</sub> -S <sub>2</sub> -C <sub>3</sub>	95.54	97.58	97.15	97.40	97.54	96.84	95.68
H <sub>4</sub> -C <sub>3</sub> -S <sub>6</sub>	110.25	109.71	110.24	109.94	110.14	110.02	110.42
H <sub>5</sub> -C <sub>3</sub> -S <sub>6</sub>	109.88	109.86	110.36	109.93	110.29	109.99	110.25
H <sub>7</sub> -S <sub>6</sub> -C <sub>3</sub> -S <sub>2</sub>	184.44	190.80	188.53	191.10	189.77	186.98	173.08
H <sub>1</sub> -S <sub>2</sub> -C <sub>3</sub> -S <sub>6</sub>	63.30	63.35	65.73	62.25	63.84	58.08	65.53
H <sub>4</sub> -C <sub>3</sub> -S <sub>6</sub> -H <sub>7</sub>	65.29	74.59	71.39	74.77	72.65	70.53	69.99
H <sub>5</sub> -C <sub>3</sub> -S <sub>6</sub> -H <sub>7</sub>	-51.93	-47.15	-48.89	-47.15	-47.36	-51.44	-51.24
ΔE <sup>c</sup> kcal mol <sup>-1</sup>	1.35	1.29	1.02	1.80	1.14	1.39	0.92

<sup>a</sup> Atom numbering is that of Figure 5.1.

<sup>b</sup> gauche, anti conformer

<sup>c</sup> Relative energy difference with gauche, gauche conformer

The anomeric interaction between C-X and C-Y bonds can be related to the larger X-C-Y bond angle in the gauche, gauche than in the gauche, anti conformers.<sup>37,38</sup> For diselenomethane, the Se-C-Se bond angle in the gauche, gauche conformer is 115.3° and it is 110.4° in the gauche, anti conformer. The larger than tetrahedral angle in the gauche, gauche conformer is a consequence of the anomeric charge transfer which increases the electron density around C-Se bonds. An explanation in terms of the different secondary orbital overlap effects in the two conformations has been proposed.<sup>37</sup> In the gg, gg-, ga and aa conformations of dithiomethane, the S-C-S bond angles are 115.0°, 116.1°, 110.2° and 106.7°, respectively. This trend is similar to that found in the oxygen analogs (Table 5.7), at a high level of computation with the 6-31G\* basis set. The same bond angle widening is observed in the gg conformer of selenothiomethane. When neither C-X orbital is in the orientation to interact with the  $n_x$  orbital, the Se-C-S angle is the smallest. The Se-C-S bond angles in the ga and ag conformers have intermediate values when only one anomeric interaction is operating.

The variation in geometrical parameters can also be rationalized from the Mulliken population analysis. For instance, in the gauche, anti conformer of diselenomethane, the anti C-Se bond has a lower population (0.5488)



than the gauche C-Se bond (0.5881). This gives a longer anti C-Se, and a shorter gauche C-Se bond, respectively. However, the overlap between the two selenium atoms is negative in all four conformations. This repulsive overlap is the largest in the gauche, gauche conformer and this can explain the larger Se-C-Se bond angle.

Table 5.6

Selected geometrical parameters and relative energies of HX-CH<sub>2</sub>-YH<sup>a</sup>.

	r C-X <sup>b</sup>	r C-Y <sup>b</sup>	θ X-C-Y <sup>c</sup>	ΔE <sup>d</sup>
X=S, Y=S				
g, g	1.8783	1.8778	115.01	0.00
g, g-	1.8783	1.8788	116.05	1.15
g, a	1.8731	1.8835	110.18	0.92
a, a	1.8828	1.8828	106.68	2.77
X=Se, Y=S				
g, g	2.0118	1.8726	115.17	0.00
g, g-	2.0123	1.8729	116.28	1.80
g, a	2.0047	1.8783	110.12	0.92
a, g	2.0157	1.8692	110.51	0.57
a, a	2.0139	1.8788	106.96	2.51
X=Se, Y=Se				
g, g	2.0056	2.0061	115.26	0.00
g, g-	2.0067	2.0059	116.39	1.07
g, a	2.0016	2.0096	110.40	0.50
a, a	2.0100	2.0099	107.35	2.21

<sup>a</sup> Fully optimized with MINI-1\* basis set.

<sup>b</sup> Bond lengths in Å.

<sup>c</sup> Bond angles in degrees.

<sup>d</sup> Relative energy in kcalmol<sup>-1</sup>.

Table 5.7

Optimized parameters (bond lengths in Å, bond angles in degrees) of dihydroxymethane. a, b

	r C-O	r C-O	θ O-C-O	ΔE kcalmol <sup>-1</sup>
g, g	1.3858	1.3858	112.33	0.00
g, g-	1.3865	1.3860	113.73	3.68
g, a	1.3741	1.3946	108.67	3.91
a, a	1.3824	1.3823	105.42	8.67

a). Atom numbering is that of Figure 5.1

b). Fully optimized with 6-31G\* basis set.

The energies calculated in the different conformers have been subjected to analysis using an isodesmic approach:<sup>71</sup>



The isodesmic equation represents a theoretical reaction in which the number of electron pairs and number of chemical bond types are held constant and only the relationships among the bonds are altered. In the Hartree-Fock (HF) models, the effect of electron correlation is small; therefore, the absolute errors in the theoretical total energies are cancelled. As a result, even simple levels of theory will provide an adequate description of the overall energetics. The energy difference calculated in the isodesmic process is termed the bond separation energy or the methyl stabilization energy. These energy differences characterize the interactions between neighbouring bonds. A positive bond separation energy reflects stabilization as a result of

neighbouring interaction. Conversely, a negative bond separation energy reflects destabilization.

The calculated bond separation energies for the gauche, gauche (g,g) and the gauche, anti (g,a) conformers of  $\text{HXCH}_2\text{YH}$  are reported in Table 5.8.

Table 5.8  
Calculated bond separation energies ( $\text{kcal mol}^{-1}$ ) for  $\text{XCH}_2\text{Y}$ .



Gauche, Gauche			Gauche, Anti		
X\Y	SH	SeH	X\Y	SH	SeH
SH	1.46	1.07	SH	0.54	1.07
SeH		0.63	SeH	0.15	0.13

From the results in Table 5.8 in which the bond separation energies decrease in the order  $\text{S/S} > \text{S/Se} > \text{Se/Se}$ , it is evident that the neighbouring group stabilization energy decreases as one goes down a column of the periodic table. This corroborates the results of an earlier study of second row anomeric effects by Schleyer and coworkers.<sup>39</sup> In comparison, the gauche, gauche conformer of dihydroxymethane, calculated with the 6-31G\* basis set, has a strong methyl stabilization energy which reproduces the quantitative experimental data by Benson<sup>334</sup> (Table 5.9). Even the anti, anti conformer has a large methyl stabilization energy. It is

important to note that even though small methyl stabilization energies were obtained for 1-3 with the MINI-1\* calculation, the 6-31G\* calculation of dithiomethane gave *negative* energies (Table 5.9) in all four conformations. Therefore, the isodesmic approach seems to be basis set dependent. However, the total energy difference between the gauche, gauche and gauche, anti conformers of dithiomethane is only approximately 3.4 times smaller than that in the oxygen analogs. The same trend is observed at other levels of computation.<sup>38,39</sup>

Table 5.9

Calculated relative energies ( $\Delta E$ ) and methyl stabilization energies ( $\Delta MS$ ) of dithiomethane and dihydroxymethane<sup>a</sup>.



a) X=S

Conformer	-E(hartrees)	$\Delta E(\text{kcalmol}^{-1})$	$\Delta MS(\text{kcalmol}^{-1})$
gauche, gauche	835.2049971	0.00	-0.29
gauche, -gauche	835.2028034	1.36	-1.65
gauche, anti	835.2031733	1.14	-1.44
anti, anti	835.1993123	3.55	-3.84

b) X=O

Conformer	-E(hartrees)	$\Delta E(\text{kcalmol}^{-1})$	$\Delta MS(\text{kcalmol}^{-1})$
gauche, gauche	189.9006192	0.00	15.6
gauche, -gauche	189.8947344	3.68	11.9
gauche, anti	189.8943745	3.91	11.7
anti, anti	189.8867695	8.67	6.90

a). HF/6-31G\* basis, fully optimized.

b). CH<sub>4</sub> -E (hartrees)=40.1951719; CH<sub>3</sub>SH -E(hartrees)=437.7003198; CH<sub>3</sub>OH -E(hartrees)=115.0354183.

Experimentally, Pinto et al.<sup>157</sup> estimated the Se/S and Se/Se anomeric effect to be about 1 kcalmol<sup>-1</sup>. The lower limit on the O/O anomeric interaction in six-membered analogs was estimated to be 2.1 kcalmol<sup>-1</sup>.<sup>166</sup> Therefore, in six-membered ring systems, the O/O anomeric effect is only twice as large as the Se/Se anomeric effect. This energy difference is smaller than that obtained from the computed energies of the truncated units. The crowded nature of the central methine carbon rather than a methylene group in the disubstituted methanes may contribute to this difference. In a recent study of CH<sub>3</sub>CHXY, which is a better truncated model for the corresponding six-membered ring systems, at the 6-31G\* level of computation, the energy difference between the gauche, gauche and gauche, anti conformers is 3.34 kcalmol<sup>-1</sup> when X=OH and Y=OH. When X=OH and Y=SH, the energy difference is 3.12 kcalmol<sup>-1</sup>.<sup>140</sup> The addition of a methyl group at the central carbon, indeed, decreases the energy difference between the gauche, gauche and gauche, anti conformers. It is also noteworthy that a recent experimental study of dimethoxymethane has given an energy difference of 2.5 kcalmol<sup>-1</sup> between the g,g and g,a conformers.<sup>335</sup>

The foregoing discussion has presented results obtained with the MINI-1\* basis set since this basis set was the only one available to us at the time. Recently, however a 3-21G\* basis set for selenium and tellurium developed by W.Hehre and

S.Kahn<sup>228</sup> was made available to us. Since the MINI-1\* optimized bond lengths, especially the C-X bonds were all too long and were of some concern to us, we decided to reexamine the systems described above with the 3-21G\* basis set. We have also extended the calculations to include systems containing tellurium. The relative energies and selected geometrical parameters of a series of dichalcogenides are reported in Tables 5.10-5.15.

Table 5.10

Optimized parameters (bond lengths in Å; bond angles in degrees) of diselenomethane<sup>a,b</sup>.

	G, G	G, G-	A, G	A, A
H <sub>1</sub> -Se <sub>2</sub>	1.4630	1.4642	1.4689	1.4655
H <sub>7</sub> -Se <sub>6</sub>	1.4630	1.4642	1.4636	1.4655
H <sub>4</sub> -C <sub>3</sub>	1.0820	1.0836	1.0802	1.0801
H <sub>5</sub> -C <sub>3</sub>	1.0820	1.0803	1.0816	1.0801
C <sub>3</sub> -Se <sub>2</sub>	1.9558	1.9562	1.9581	1.9629
C <sub>3</sub> -Se <sub>6</sub>	1.9559	1.9563	1.9547	1.9630
C <sub>3</sub> -Se <sub>2</sub> -H <sub>1</sub>	95.15	95.01	95.50	94.24
C <sub>3</sub> -Se <sub>6</sub> -H <sub>7</sub>	95.16	95.01	94.94	94.24
H <sub>4</sub> -C <sub>3</sub> -Se <sub>2</sub>	106.45	105.94	110.74	109.46
H <sub>5</sub> -C <sub>3</sub> -Se <sub>2</sub>	109.91	110.03	110.11	109.45
Se <sub>2</sub> -C <sub>3</sub> -Se <sub>6</sub>	115.38	116.08	109.92	107.68
H <sub>4</sub> -C <sub>3</sub> -Se <sub>2</sub> -H <sub>1</sub>	180.22	175.30	51.85	61.23
H <sub>5</sub> -C <sub>3</sub> -Se <sub>2</sub> -H <sub>1</sub>	62.81	58.34	-69.93	-60.95
H <sub>1</sub> -Se <sub>2</sub> -C <sub>3</sub> -Se <sub>6</sub>	-57.50	-67.46	173.35	180.15
H <sub>7</sub> -Se <sub>6</sub> -C <sub>3</sub> -H <sub>5</sub>	-57.51	67.26	-69.43	179.90
-E (Hartree)	4817.369753	4817.368423	4817.369767	4817.366003
ΔE kcalmol <sup>-1</sup>	0.01	0.84	0.00	2.36

a). At the 3-21G\* level of calculation.

b). Fully optimized with molecular symmetry disabled.

Table 5.11

Optimized parameters (bond lengths in Å; bond angles in degrees) of selenothiomethane<sup>a,b</sup>.

	G, G	G, G-	A, G	G, A	A, A
H <sub>1</sub> -Se <sub>2</sub>	1.4633	1.4646	1.4674	1.4638	1.4651
H <sub>7</sub> -S <sub>6</sub>	1.3262	1.3266	1.3268	1.3302	1.3278
H <sub>4</sub> -C <sub>3</sub>	1.0832	1.0839	1.0814	1.0832	1.0813
H <sub>5</sub> -C <sub>3</sub>	1.0824	1.0814	1.0822	1.0815	1.0813
C <sub>3</sub> -Se <sub>2</sub>	1.9609	1.9618	1.9663	1.9567	1.9679
C <sub>3</sub> -S <sub>6</sub>	1.8058	1.8062	1.8049	1.8103	1.8136
C <sub>3</sub> -Se <sub>2</sub> -H <sub>1</sub>	94.98	94.80	94.96	94.82	93.62
C <sub>3</sub> -S <sub>6</sub> -H <sub>7</sub>	97.57	97.63	97.44	97.60	96.90
H <sub>4</sub> -C <sub>3</sub> -Se <sub>2</sub>	105.80	105.53	109.63	105.71	108.78
H <sub>5</sub> -C <sub>3</sub> -Se <sub>2</sub>	109.38	109.07	109.44	109.20	108.78
Se <sub>2</sub> -C <sub>3</sub> -S <sub>6</sub>	115.85	116.69	111.30	110.14	107.71
H <sub>4</sub> -C <sub>3</sub> -Se <sub>2</sub> -H <sub>1</sub>	179.16	170.18	46.17	171.59	-60.26
H <sub>5</sub> -C <sub>3</sub> -Se <sub>2</sub> -H <sub>1</sub>	62.89	54.46	-73.69	54.10	60.30
H <sub>1</sub> -Se <sub>2</sub> -C <sub>3</sub> -S <sub>6</sub>	-57.45	-72.37	169.21	-68.45	180.02
H <sub>7</sub> -S <sub>6</sub> -C <sub>3</sub> -Se <sub>2</sub>	-56.06	63.75	-66.20	174.83	179.92
-E(Hartree)	2824.3523	2824.3506	2824.3514	2824.3516	2824.3479
ΔE kcalmol <sup>-1</sup>	0.00	1.09	0.58	0.43	2.79

a). At the 3-21G\* level of calculation.

b). Fully optimized with molecular symmetry disabled.



Table 5.12

Optimized parameters (bond lengths in Å; bond angles in degrees) of dithiomethane<sup>a, b</sup>.

	G, G	G, G <sup>-</sup>	A, G	A, A <sup>C</sup>
H <sub>1</sub> -S <sub>2</sub>	1.3266	1.3273	1.3291	1.3239
H <sub>7</sub> -S <sub>6</sub>	1.3266	1.3273	1.3270	1.3239
H <sub>4</sub> -C <sub>3</sub>	1.0837	1.0846	1.0827	1.0823
H <sub>5</sub> -C <sub>3</sub>	1.0838	1.0826	1.0837	1.0823
C <sub>3</sub> -S <sub>2</sub>	1.8105	1.8115	1.8178	1.8242
C <sub>3</sub> -S <sub>6</sub>	1.8109	1.8115	1.8070	1.8242
C <sub>3</sub> -S <sub>2</sub> -H <sub>1</sub>	97.43	97.43	97.09	99.59
C <sub>3</sub> -S <sub>6</sub> -H <sub>7</sub>	97.44	97.43	97.35	99.59
H <sub>4</sub> -C <sub>3</sub> -S <sub>2</sub>	105.89	105.61	110.37	
H <sub>5</sub> -C <sub>3</sub> -S <sub>2</sub>	110.49	110.22	110.33	
S <sub>2</sub> -C <sub>3</sub> -S <sub>6</sub>	116.27	117.12	111.29	
H <sub>4</sub> -C <sub>3</sub> -S <sub>2</sub> -H <sub>1</sub>	179.27	174.61	48.92	
H <sub>5</sub> -C <sub>3</sub> -S <sub>2</sub> -H <sub>1</sub>	62.99	58.86	-71.27	
H <sub>1</sub> -S <sub>2</sub> -C <sub>3</sub> -S <sub>6</sub>	-57.64	-68.19	171.71	180.00
H <sub>7</sub> -S <sub>6</sub> -C <sub>3</sub> -H <sub>5</sub>	-56.85	68.22	-65.80	180.00
-E(Hartree)	831.3352258	831.3330123	831.3335899	831.3239287
ΔE kcalmol <sup>-1</sup>	0.00	1.38	1.02	7.07

a). At the 3-21G\* level of calculation.

b). Fully optimized with molecular symmetry disabled.

c). With C<sub>2v</sub> symmetry.

Table 5.13

Optimized parameters (bond lengths in Å; bond angles in degrees) of ditelluromethane<sup>a, b</sup>.

	G, G	G, G-	A, G	A, A
H <sub>1</sub> -Te <sub>2</sub>	1.6753	1.6765	1.6821	1.6779
H <sub>7</sub> -Te <sub>6</sub>	1.6753	1.6765	1.6763	1.6779
H <sub>4</sub> -C <sub>3</sub>	1.0826	1.0854	1.0805	1.0802
H <sub>5</sub> -C <sub>3</sub>	1.0826	1.0801	1.0824	1.0803
C <sub>3</sub> -Te <sub>2</sub>	2.1763	2.1762	2.1746	2.1802
C <sub>3</sub> -Te <sub>6</sub>	2.1763	2.1762	2.1769	2.1799
C <sub>3</sub> -Te <sub>2</sub> -H <sub>1</sub>	94.52	94.30	94.44	93.21
C <sub>3</sub> -Te <sub>6</sub> -H <sub>7</sub>	94.51	94.31	93.99	93.22
H <sub>4</sub> -C <sub>3</sub> -Te <sub>2</sub>	106.39	105.72	110.21	108.69
H <sub>5</sub> -C <sub>3</sub> -Te <sub>2</sub>	109.00	109.40	109.51	108.68
Te <sub>2</sub> -C <sub>3</sub> -Te <sub>6</sub>	117.53	117.96	112.63	111.22
H <sub>4</sub> -C <sub>3</sub> -Te <sub>2</sub> -H <sub>1</sub>	187.56	186.70	52.00	60.50
H <sub>5</sub> -C <sub>3</sub> -Te <sub>2</sub> -H <sub>1</sub>	71.05	70.45	-68.48	-60.23
H <sub>1</sub> -Te <sub>2</sub> -C <sub>3</sub> -Te <sub>6</sub>	-50.03	-55.39	173.72	180.15
H <sub>7</sub> -Te <sub>6</sub> -C <sub>3</sub> -H <sub>5</sub>	-50.03	55.12	-66.19	179.92
-E(Hartree)	13206.50564	13206.50488	13206.50669	13206.50438
ΔE kcalmol <sup>-1</sup>	0.65	1.13	0.00	1.44

a). At the 3-21G\* level of calculation.

b). Fully optimized with molecular symmetry disabled.

Table 5.14

Optimized parameters (bond lengths in Å; bond angles in degrees) of tellurothiomethane<sup>a,b</sup>.

	G, G	G, G-	A, G	G, A	A, A
H <sub>1</sub> -Te <sub>2</sub>	1.6754	1.6779	1.6802	1.6758	1.6777
H <sub>7</sub> -S <sub>6</sub>	1.3262	1.3263	1.3269	1.3306	1.3282
H <sub>4</sub> -C <sub>3</sub>	1.0837	1.0845	1.0814	1.0837	1.0813
H <sub>5</sub> -C <sub>3</sub>	1.0824	1.0817	1.0819	1.0815	1.0813
C <sub>3</sub> -Te <sub>2</sub>	2.1838	2.1842	2.1864	2.1783	2.1885
C <sub>3</sub> -S <sub>6</sub>	1.8057	1.8062	1.8072	1.8088	1.8113
C <sub>3</sub> -Te <sub>2</sub> -H <sub>1</sub>	93.73	93.29	94.08	93.64	92.22
C <sub>3</sub> -S <sub>6</sub> -H <sub>7</sub>	98.02	97.97	97.73	97.61	97.49
H <sub>4</sub> -C <sub>3</sub> -Te <sub>2</sub>	106.27	105.61	109.47	105.77	108.08
H <sub>5</sub> -C <sub>3</sub> -Te <sub>2</sub>	108.25	108.24	108.86	108.04	108.09
Te <sub>2</sub> -C <sub>3</sub> -S <sub>6</sub>	116.84	117.68	112.28	111.41	108.82
H <sub>4</sub> -C <sub>3</sub> -Te <sub>2</sub> -H <sub>1</sub>	179.07	169.80	45.57	170.78	-59.75
H <sub>5</sub> -C <sub>3</sub> -Te <sub>2</sub> -H <sub>1</sub>	63.46	54.73	-73.49	54.02	59.80
H <sub>1</sub> -Te <sub>2</sub> -C <sub>3</sub> -S <sub>6</sub>	-56.39	-72.13	169.24	-68.48	180.02
H <sub>7</sub> -S <sub>6</sub> -C <sub>3</sub> -Te <sub>2</sub>	-56.50	59.67	-66.39	176.17	179.92
-E(Hartree)	7018.9195	7018.9182	7018.9196	7018.9191	7018.9170
ΔE kcalmol <sup>-1</sup>	0.11	0.88	0.00	0.32	1.66

a). At the 3-21G\* level of calculation.

b). Fully optimized with molecular symmetry disabled.

Table 5.15

Optimized parameters (bond lengths in Å; bond angles in degrees) of selenotelluromethane<sup>a,b</sup>.

	G, G	G, G-	A, G	G, A	A, A
H <sub>1</sub> -Te <sub>2</sub>	1.6749	1.6769	1.6820	1.6760	1.6779
H <sub>7</sub> -Se <sub>6</sub>	1.4631	1.4638	1.4636	1.4691	1.4657
H <sub>4</sub> -C <sub>3</sub>	1.0825	1.0844	1.0803	1.0824	1.0801
H <sub>5</sub> -C <sub>3</sub>	1.0820	1.0803	1.0815	1.0804	1.0801
C <sub>3</sub> -Te <sub>2</sub>	2.1781	2.1783	2.1762	2.1756	2.1828
C <sub>3</sub> -Se <sub>6</sub>	1.9556	1.9558	1.9578	1.9569	1.9610
C <sub>3</sub> -Te <sub>2</sub> -H <sub>1</sub>	94.00	93.71	94.85	93.76	92.88
C <sub>3</sub> -Se <sub>6</sub> -H <sub>7</sub>	95.60	95.37	95.20	95.36	94.69
H <sub>4</sub> -C <sub>3</sub> -Te <sub>2</sub>	106.96	106.02	110.84	106.35	108.80
H <sub>5</sub> -C <sub>3</sub> -Te <sub>2</sub>	109.01	109.65	109.75	108.76	108.80
Te <sub>2</sub> -C <sub>3</sub> -Se <sub>6</sub>	116.26	116.77	110.45	111.24	108.94
H <sub>4</sub> -C <sub>3</sub> -Te <sub>2</sub> -H <sub>1</sub>	184.12	183.49	50.97	171.71	-60.55
H <sub>5</sub> -C <sub>3</sub> -Te <sub>2</sub> -H <sub>1</sub>	67.15	66.85	-70.82	53.63	60.59
H <sub>1</sub> -Te <sub>2</sub> -C <sub>3</sub> -Se <sub>6</sub>	-52.67	-58.95	173.00	-68.36	180.02
H <sub>7</sub> -Se <sub>6</sub> -C <sub>3</sub> -Te <sub>2</sub>	-58.48	65.11	-70.17	174.68	179.92
-E(Hartree)	9011.9374	9011.9364	9011.9387	9011.9375	9011.9352
ΔE kcalmol <sup>-1</sup>	0.79	1.41	0.00	0.73	2.16

a). At the 3-21G\* level of calculation.

b). Fully optimized with molecular symmetry disabled.

The validity of the 3-21G\* basis set was checked against the 6-31G\* basis set for dithiomethane. It would appear from the relative energies of the dithiol series that 3-21G\* tracks 6-31G\* quite well (Table 5.16). The geometrical parameters obtained by use of the 3-21G\* basis set also follow very closely those obtained by the 6-31G\* calculation (cf Tables 5.5 and 5.12).

Table 5.16

Calculated conformational energies of different conformers of dithiomethane.

Conformer	HF/3-21G*		HF/6-31G*		Isodesmic Reaction	
	-E	E <sub>rel</sub>	-E	E <sub>rel</sub>	3-21G*	6-31G*
g,g	831.33523	0.0	835.20500	0.0	0.22	-0.29
g,g-	831.33301	1.39	835.20280	1.38	-1.17	-1.67
g,a	831.33359	1.03	835.20318	1.14	-0.81	-1.43
a,a	a	----	835.19929	3.58 <sup>b</sup>	----	-3.87
a,a <sup>c</sup>	831.32393	7.09	835.19429	6.72	-6.51	-7.00

- a). Relaxes without barrier to the g,a conformer.  
 b). Normal mode with one imaginary frequency.  
 c). Input geometry with C<sub>2v</sub> symmetry constraint.

With the 3-21G\* basis set, the C-Se bond lengths of the gauche, gauche conformer of diselenomethane are much closer to the experimental values<sup>28</sup> than with the MINI-1\* basis set. The trends in geometrical changes within the conformers are the same as those obtained with the MINI-1\* basis set.

However, the energy differences between the various conformers are unexpected. The gauche,gauche and gauche,anti forms are stabilized to the same extent vis-a-vis the isodesmic reaction, even though they differ in the number of anomeric interactions. In the case of diselenomethane, the methyl stabilization energy is the same for these two conformers, and for ditelluromethane, the anti,gauche form is less destabilized than the gauche,gauche form (Table 5.17).

Table 5.17

Calculated relative<sup>a</sup> energies ( $\Delta E$ ) and methyl stabilization energies ( $\Delta MS$ )<sup>b</sup> of diheterosubstituted methanes<sup>c</sup>.

X,Y	Conformer	$\Delta E(\text{kcalmol}^{-1})$	$\Delta MS(\text{kcalmol}^{-1})$
S,S	g,g	0.0	0.22
	a,g	1.03	-0.81
S,Se	g,g	0.0	0.15
	a,g	0.54	-0.42
S,Te	g,g	0.11	-1.04
	a,g	0.0	-0.93
Se,Se	g,g	0.01	0.32
	a,g	0.0	0.33
Te,Te	g,g	0.66	-1.07
	a,g	0.00	-0.42

a). HF/3-21G\* basis, fully optimized.

b).  $\text{CH}_4$  -E(hartrees)=40.007494;  $\text{CH}_3\text{SH}$  -E(hartrees)=435.671188;  $\text{CH}_3\text{SeH}$  -E(hartrees)=2428.688369;  $\text{CH}_3\text{TeH}$  -E(hartrees)=6623.257421.

c). The calculation of selenotelluromethane is in progress.

Perhaps in the heavier chalcogenides there is a sizeable difference between the first and second anomeric interactions.

Perhaps the second interaction attenuates the first. Therefore, the energy difference between the gauche, gauche and gauche, anti conformers may not provide a true measure of the anomeric effect. There is no "anomeric" stabilization of heteroatom lone pairs in the anti,anti conformers and one such interaction is present in the gauche,anti conformer. Perhaps the energy difference between these conformers is a better measure of the anomeric stabilization in diheterosubstituted methanes.<sup>#</sup> Our calculations indicated that, in general, the anti,anti forms either relaxed without barrier to another conformer or were not true minima. This result indicated that, in a relative sense, the anti,anti forms were unstable because they lacked anomeric stabilization.

After this study was completed, Schleyer *et al.*<sup>336</sup> published their results on a similar study of  $\text{CH}_2(\text{SeH})_2$  1. The MO calculations were performed using a mixed basis set with electron correlation. The 6-31G\* basis set was used for carbon and hydrogen, and since there was no 6-31G\* basis set for Se in the Gaussian programs, Huzinaga's 43321/4321/4 split valence basis set<sup>337</sup> was used. With these higher levels of computation including electron correlation, the methyl stabilization energy (Table 5.18) is higher for all conformers

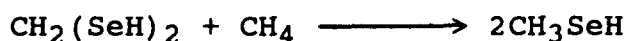
---

<sup>#</sup> In the estimation of the O/O anomeric effect ( $3.91 \text{ kcal mol}^{-1}$ ) by Wiberg and Murcko,<sup>322</sup> the energy differences between the gauche,anti and anti,anti conformers of dimethoxymethane and methyl propyl ether were used.

and the trend in the relative energies (Table 5.19) is slightly different; however, the trend in geometric parameters (Table 5.20) of different conformers remain the same as calculated at the levels of computation used in our study.

From Table 5.18, it is clear that the addition of zero point energy (ZPE) correlation raises the relative energies of diselenomethane conformers for the isodesmic reaction. Theoretical MO energies refer to isolated molecules at 0 K with stationary nuclei. In order to obtain energies more comparable with experimental data, ZPE correction may be needed.

Table 5.18  
The methyl stabilization energies<sup>a</sup> of diselenomethane calculated by the isodesmic reaction:



	G,G	G,G-	G,A	A,A
MIX <sup>b,c</sup> (MP4SDTQ)	1.23	0.33	0.49	-1.39
MIX <sup>b,c</sup> (MP4SDTQ+ZPE)	1.94	1.19	1.27	-0.41
MINI-1* (HF)	0.63	-0.44	0.13	-1.58
3-21G* (HF)	0.32	-0.52	0.33	-2.03

a). in kcalmol<sup>-1</sup>.

b). Mixed basis set C6-31G//Se43321/4321/4//H31.

c). Reference 336.



Table 5.19

Relative energies<sup>a</sup> of diselenomethane at different levels of computation.

	MIX <sup>b,c</sup>			
	HF	MP4SDTQ	MINI-1*	3-21G*
G,G	0.00	0.00	0.00	0.01
G,G-	1.04	0.91	1.07	0.84
G,A	0.71	0.74	0.50	0.00
A,A	2.23	2.66	2.21	2.36

a). in kcalmol<sup>-1</sup>.

b). Mixed basis set C6-31G//Se43321/4321/4//H31.

c). Reference 336.

The effect of electron correlation is seen to generally increase the energy differences between different conformers of a molecule. This can be noticed from the relative energies of dimethoxymethane conformers, calculated with electron correlation (Table 5.21).<sup>322</sup> At the 6-31G\* level, the O/O anomeric effect in dimethoxymethane was calculated to be 5.4 kcalmol<sup>-1</sup> after the destabilizing gauche COCC interaction was subtracted.<sup>322</sup> This COCC gauche interaction was estimated from the energy difference between the g,a and the a,a conformers of methyl propyl ether. The calculated energy difference was multiplied by a scaling factor of 1.5 to account for the intrinsic differences between methyl propyl ether and dimethoxymethane.<sup>259</sup> In a personal communication from Schleyer and Salzner, we have learned that the S/S anomeric effect in dithiomethane at the 6-31G\* level with

electron correlation was calculated (using relative energies) to be 1.28 kcalmol<sup>-1</sup>. At this highest level of computation, the anomeric stabilization of S/S is only 4 times smaller than in the O/O counterpart.

Table 5.20

Optimized parameters of diselenomethane at different levels of computation.

	G,G	G,G-	G,A	A,A
<u>r (C-Se)</u>				
Mix <sup>a,b</sup>	1.977	1.977	1.972, 1.985	1.984
MINI-1*	2.006	2.007, 2.006	2.002, 2.010	2.010
3-21G*	1.956	1.956	1.955, 1.958	1.963
<u>r (C-H)</u>				
Mix <sup>a,b</sup>	1.077	1.076, 1.078	1.077, 1.076	1.075
MINI-1*	1.119	1.118, 1.119	1.118	1.118
3-21G*	1.082	1.080, 1.083	1.080, 1.082	1.080
<u>θ (HCSe)</u>				
Mix <sup>a,b</sup>	96.4	96.2	96.2, 95.8	94.9
MINI-1*	106.5, 109.7	105.8, 109.9	110.3, 109.9	109.5
3-21G*	106.4, 109.9	105.9, 110.0	110.7, 110.1	109.5
<u>θ (SeCSe)</u>				
Mix <sup>a,b</sup>	117.4	118.0	112.2	108.1
MINI-1*	115.3	116.4	110.4	107.4
3-21G*	115.4	116.1	109.9	107.7

a). Mixed basis set C6-31G//Se43321/4321/4//H31.

b). Reference 336.

Table 5.21

Effect of Electron Correlation on Relative Energies<sup>a</sup> of Dimethoxymethane.<sup>322</sup>

Conformer	6-31G* Basis Set			
	RHF	MP2	MP3	MP4 (SDTQ)
gauche, gauche	0.00	0.00	0.00	0.00
gauche, -gauche	3.55	4.20	4.00	4.13
gauche, anti	2.71	3.46	3.23	3.43
anti, anti	6.03	7.38	6.94	7.33

a). in kcalmol<sup>-1</sup>.

The anomeric effect was first noted by Edward<sup>13</sup> and is today generally defined as the sum of the free energy difference for the axial/equatorial equilibrium in a 2-substituted heterocyclohexane and the "scaled A-value" for the same substituent in the heterocycle (see Chapter 1).

Throughout this thesis, the anomeric effect in disubstituted methanes has been defined as the energy difference between the gauche, gauche and gauche, anti conformations. The alternative description in terms of the isodesmic reaction predicted "anomeric effects" that were substantially less in the 2<sup>nd</sup> and 3<sup>rd</sup> row than in the 1<sup>st</sup> row analogs. However, it is now clear from both the relative energy criterion and the isodesmic criterion (using results at higher levels of computation) that second and third row anomeric interactions do exist. Indeed, Schleyer and Salzner<sup>336</sup> also now conclude that the trends in bond angles, bond lengths and total energies of various conformations of CH<sub>2</sub>(SeH)<sub>2</sub> provide

evidence for anomeric stabilization. Finally, if the 3-21G\* basis set is a reasonable replacement for the 6-31G\* basis set, it would appear that anomeric stabilization is possible with tellurium. The latter prediction remains to be tested by experiment.

## CHAPTER 6

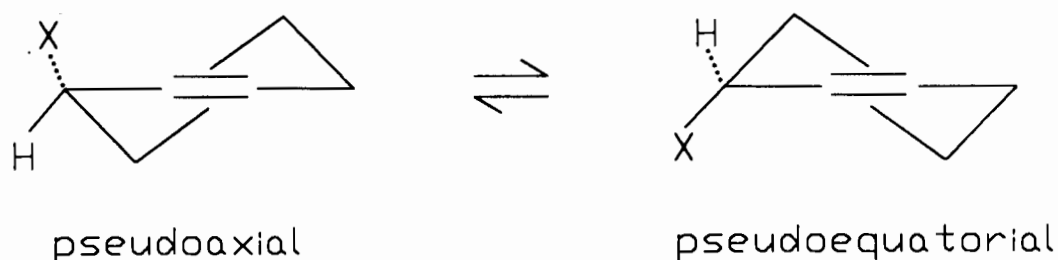
### THEORETICAL INVESTIGATION OF THE ALLYLIC ANOMERIC EFFECT

#### 6.1 Introduction

The anomeric effect is an important factor in the determination of conformations in heteroatom-containing systems. The fact that electronegative substituents in 2-substituted oxacyclohexanes prefer the axial orientation is well studied (see Chapter 1). Similar axial preferences have also been observed in cyclohexanones and methylenecyclohexanes bearing polar adjacent (C(2)) substituents.<sup>12,338-348</sup> 3-Substituted cyclohexenes in the half-chair conformation with electronegative groups such as hydroxy and acetoxy,<sup>349</sup> chloro and bromo,<sup>350,351</sup> also tend to favour a pseudo-axial form (Fig.6.1). With a 3-methyl substituent, the equatorial conformer is dominant.<sup>351</sup>

Figure 6.1

Conformational equilibrium of 3-substituted cyclohexenes in the half-chair conformation.

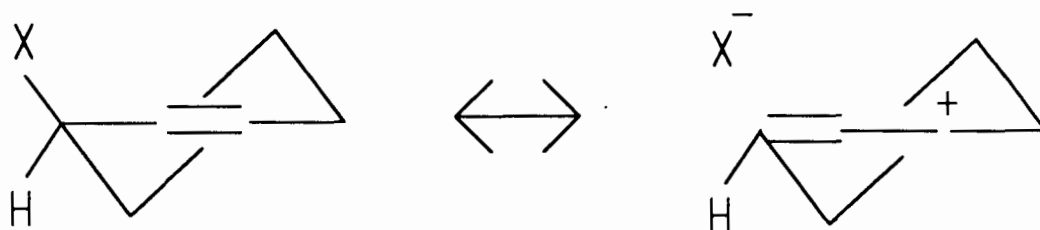


These conformational preferences involving  $\pi$ -systems have been referred to as examples of an "allylic anomeric effect".<sup>347,348, 352,353</sup> More recently, similar behaviour has been called the "vinylogous" anomeric effect by Denmark et al.<sup>311</sup> Although it is clear that conformational "abnormality" is observed in these allylic systems, the interpretations of the origin of the effect differ.

The pseudo-axial preference of some 3-substituted cyclohexenes has been interpreted by Lessard et al.<sup>351</sup> simply in terms of a double bond-no bond resonance interaction (Fig.6.2).

Figure 6.2

Double bond-no bond resonance interaction in 3-substituted cyclohexenes.



Two factors have been invoked to rationalize the axial preference of 2-halo- and 2-methoxycyclohexanones. Firstly, the axial orientation of the substituents insures the minimum dipole-dipole interactions of the polar bonds

(Fig.6.3).<sup>354,355</sup> Secondly, the  $\sigma_{C-X}$  orbital is stabilized by the two electron-two orbital  $\sigma_{C-X} \rightarrow \pi^*_{C=O}$  interaction. Maximum stabilization is achieved when these two orbitals are in the same plane (Fig.6.4).<sup>356,357</sup>

Figure 6.3

Dipole-dipole interactions in the axial and equatorial 2-substituted cyclohexanones.

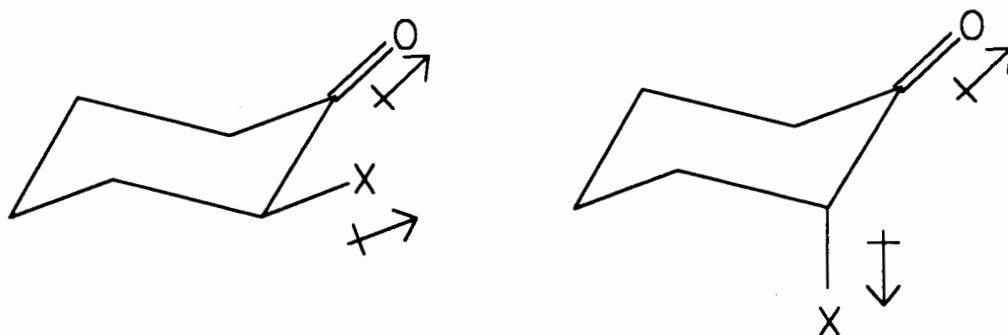
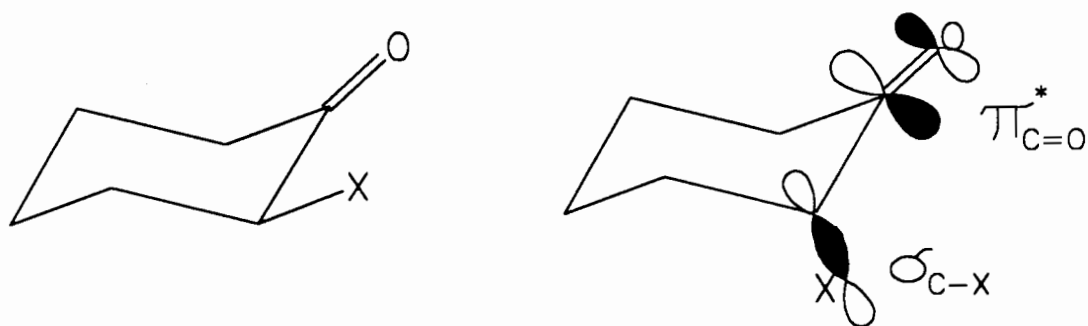


Figure 6.4

The two electron-two orbital  $\sigma_{C-X} \rightarrow \pi^*_{C=O}$  interaction in the axial conformation of 2-substituted cyclohexanones.

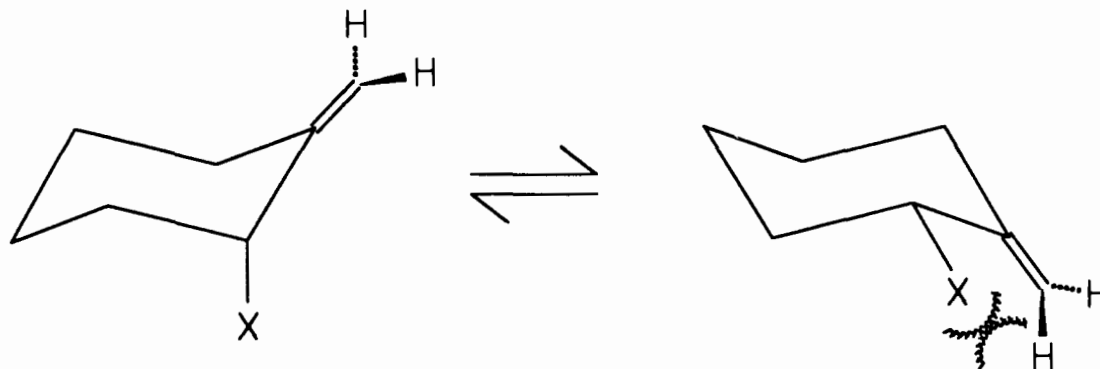


For methylenecyclohexanes, several explanations have been offered to interpret the general axial preference of polar 2-

substituents. Since one of the methylene carbons of the cyclohexane ring is replaced by an ethylene group, an additional steric interaction is introduced between the 2-substituent and one of the allylic hydrogens. This is the allylic A<sup>1,3</sup> strain<sup>358</sup> and is clearly more important for the substituents in the equatorial position (Fig.6.5). Zefirov

Figure 6.5

Allylic A<sup>1,3</sup> strain steric interaction in the equatorial conformation of 2-substituted methylenecyclohexanes.



and coworkers suggested that the  $n_o \rightarrow \pi^*_{c=c}$  orbital interaction was the major factor governing the conformational characteristics in 2-methoxy- and 2-acetoxymethylenecyclohexanes (Fig.6.6).<sup>353</sup>

However, Lessard et al. had clear evidence against the dominance of the  $n_o \rightarrow \pi^*_{c=c}$  orbital interaction in 2-methoxymethylenecyclohexanes (Fig.6.7).<sup>345</sup> With different X



Figure 6.6

The  $n_{OR} \rightarrow \pi_{C=C}^*$  orbital interaction in axial-2-methoxy- and 2-acetoxymethylenecyclohexanes.

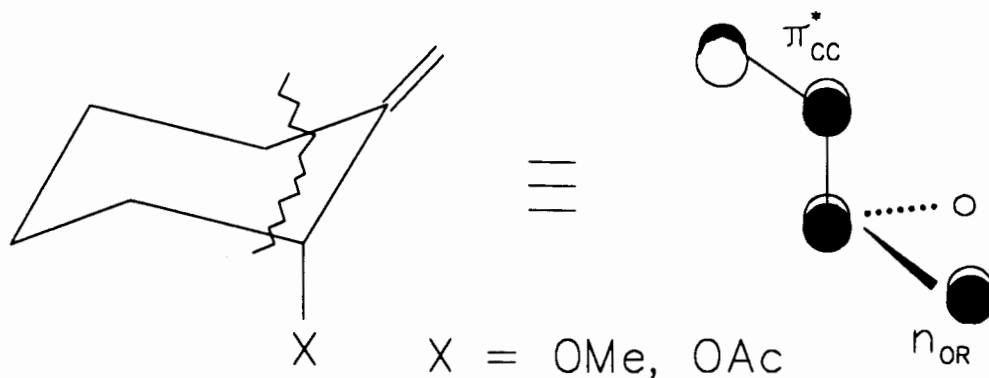
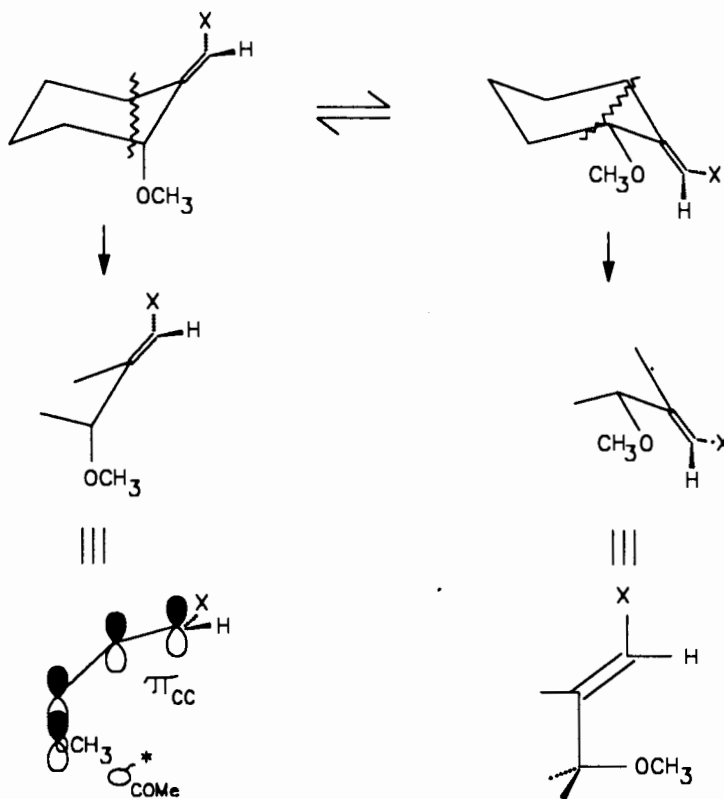


Figure 6.7

Orbital interactions in 7-X-substituted-2-methoxymethylenecyclohexanes.



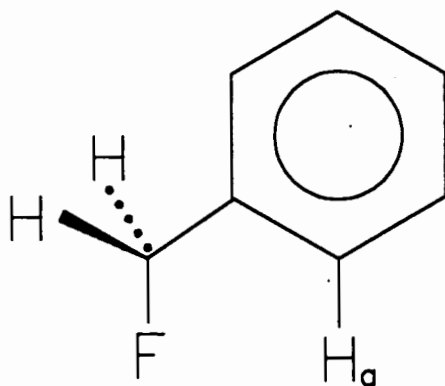
X = H, OMe, Ph, CN

in 7-X-substituted-2-methoxymethylenecyclohexanes , they found that the proportion of the axial conformer decreased as X became less electron donating. The results can be explained in terms of a dominance of a  $\pi_{C=C} \rightarrow \sigma^*_{C-O}$  stabilizing orbital interaction, analogous to that found in the generalized anomeric effect. The pseudo-axial orientation of 3-oxocyclohexenes can also be rationalized in term of  $\pi_{C=C} \rightarrow \sigma^*_{C-O}$  stabilization,<sup>344</sup> ie.the double bond-no bond interaction proposed by Lessard et al..<sup>346,351</sup> Similarly, the origin of the increase in axial preference upon oximation of 2-chlorocyclohexanones has been interpreted in terms of an enhanced  $\pi_{C=N} \rightarrow \sigma^*_{C-X}$  hyperconjugation of the azomethine linkage.<sup>311</sup> Furthermore, the photoelectron spectroscopic studies of Brown et al.<sup>359,360</sup> on conformationally rigid and flexible allylic ethers and alcohols have shown that the  $\pi_{C=C}$  ionization potentials are higher for those with the gauche arrangement of the allylic fragment (dihedral angle RO-C-C=C close to 90°). On the other hand, the axial preference may simply be a result of the destabilization effect of the equatorial conformers. When a substituent such as 2-methoxy is equatorial, the olefinic  $\sigma_{C-C}$  orbital is coplanar with the  $\sigma_{C-OMe}$  orbital. The result is destabilization of the equatorial conformer due to the four electron-two orbital  $\sigma_{C-OMe} \rightarrow \sigma_{C-C}$  interaction.<sup>68</sup>

From the above experimental and theoretical studies, it appears that the gauche arrangements of allylic systems with electronegative substituents cannot be rationalized in terms of one single conformational factor. Dipole-dipole, steric, and orbital interactions could all contribute to the observed effect. Electrostatic interactions between the electronegative substituents and the double bond may also play a role.<sup>345,346,351,361</sup> Thus, the planar conformational preference of benzyl fluoride has been attributed to the electrostatic attraction between the strong electronegative fluorine atom and the syn-periplanar ortho-hydrogen (Fig.6.8).<sup>361</sup>

Figure 6.8

The planar conformation of benzyl fluoride.



The same rationale may apply to the preference of the cis form of allyl fluoride in the gas-phase;<sup>362</sup> the gauche form is preferred for allyl chloride and bromide.<sup>363</sup> For allyl

alcohol (propen-1-ol), although both theoretical and experimental results agree that only two rotamers (the cis and gauche) around the C<sub>1</sub>-C<sub>2</sub> bond are the predominant species, the most stable species and the existence of an allylic anomeric effect is less certain.<sup>364-368</sup>

In view of the discrepancies present in the literature on the origin and significance of the gauche preferences of electronegative groups in allylic systems, we chose to probe these systems further through theoretical studies.

## 6.2 Result and Discussion

A series of 1-X-substituted-2-propenes (X=H, CH<sub>3</sub>, OCH<sub>3</sub>, OCOCH<sub>3</sub>, F and Cl) were subjected to semi-empirical molecular orbital and molecular mechanics calculations. The MNDO program<sup>236</sup> introduced by Dewar and Thiel in 1977<sup>229</sup> was used for the semi-empirical MO calculations and Allinger's MM2 program<sup>222</sup> was used for the molecular mechanics calculations. The energies were calculated with full geometry optimization at each C=C-C-X dihedral angle ( $\phi$ ) from 0° to 180° at 30° intervals. The relative energies of the cis ( $\phi=0^\circ$ ) and gauche ( $\phi=120^\circ$ ) (Fig.6.9) rotamers are reported in Table 6.1. The energies calculated by these two methods were analyzed in terms of a Fourier-type expansion of the potential energy function into one-fold ( $V_1$ ), two-fold ( $V_2$ ), and three-fold

Figure 6.9

Cis and gauche rotamers of 1-X-substituted-2-propene.

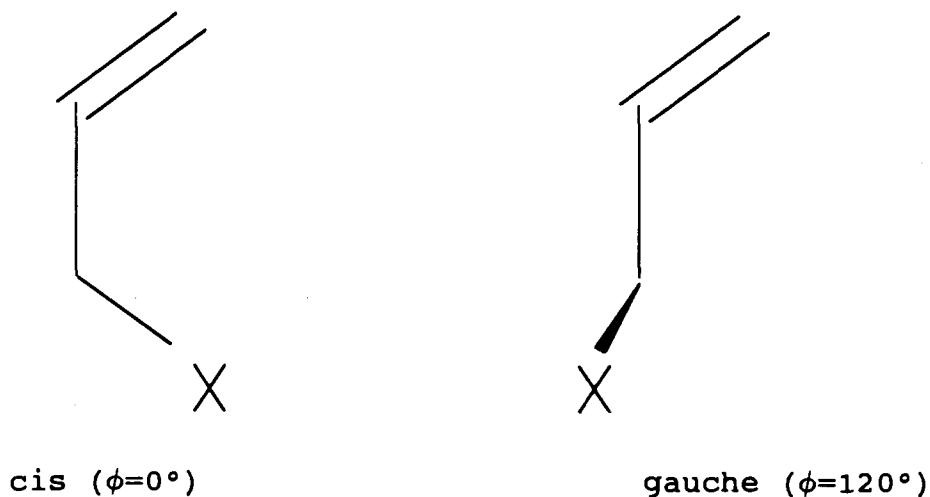


Table 6.1

Relative energies of cis and gauche rotamers of 1-X-substituted-2-propene.

Substituent X	Dihedral angle C=C-C-X ( $\phi$ )	Relative Energies (kcalmol <sup>-1</sup> )	
		MM2	MNDO
H	0.0	0.00	0.13
	120.0	0.00	0.00
CH <sub>3</sub>	0.0	0.43	0.43
	120.0	0.00	0.00
OCH <sub>3</sub>	0.0	0.35	1.30
	120.0	0.00	0.00
OCOCH <sub>3</sub>	0.0	0.73	0.58
	120.0	0.00	0.00
F	0.0	0.00	0.00
	120.0	0.51	0.01
Cl	0.0	0.26	1.41
	120.0	0.00	0.00

(V<sub>3</sub>) components (eq.1.7).<sup>195</sup> This analysis gives the relative

$$V(\phi) = 1/2 V_1(1 - \cos\phi) + 1/2 V_2(1 - \cos 2\phi) + 1/2 V_3(1 - \cos 3\phi) \quad (\text{eq.1.7})$$

importance of the dipole-dipole (V<sub>1</sub>), stereoelectronic (V<sub>2</sub>) and steric (V<sub>3</sub>) interactions. Since the torsional terms are not parameterized for this particular kind of fragment in the MM2 force field, the relative energies obtained from the MM2 calculations do not contain the stereoelectronic components. The torsional terms obtained from the MM2 and MNDO calculations are reported in Table 6.2. The stereoelectronic term (V<sub>2</sub>) has significant values when compared with the steric term (V<sub>3</sub>) in the MNDO calculations. The dipole-dipole term (V<sub>1</sub>) is also important in the cases of electronegative substituents. In the Fourier expansion analysis of the MM2 calculations, the steric component (V<sub>3</sub>) dominates the rotameric preferences.

This study shows that orbital interactions are important in allylic compounds having electronegative substituents, as manifested in the large V<sub>2</sub> terms obtained in the MNDO calculations. However, the types of orbital interactions involved cannot be evaluated by means of these analyses. In order to evaluate the types of orbital interactions involved, allyl alcohol was chosen as the candidate for a more detailed analysis by *ab initio* MO calculations.

Table 6.2

Torsional terms obtained from the Fourier expansion analysis of the total potential functions of 1-X-substituted-2-propenes.

MM2			
Substituents X	V <sub>1</sub>	V <sub>2</sub>	V <sub>3</sub>
H	0.09	-0.15	2.09
CH <sub>3</sub>	-0.06	-0.15	1.43
OCH <sub>3</sub>	-0.04	-0.05	1.35
OCOCH <sub>3</sub>	-0.02	-0.05	1.33
F	-0.59	1.26	2.43
Cl	0.76	-0.80	1.18

MNDO			
Substituents X	V <sub>1</sub>	V <sub>2</sub>	V <sub>3</sub>
H	0.08	-0.01	0.21
CH <sub>3</sub>	0.08	-0.12	0.65
OCH <sub>3</sub>	0.20	-0.16	0.14
OCOCH <sub>3</sub>	0.24	-0.19	0.18
F	-0.09	0.23	0.09
Cl	0.80	-0.58	0.37

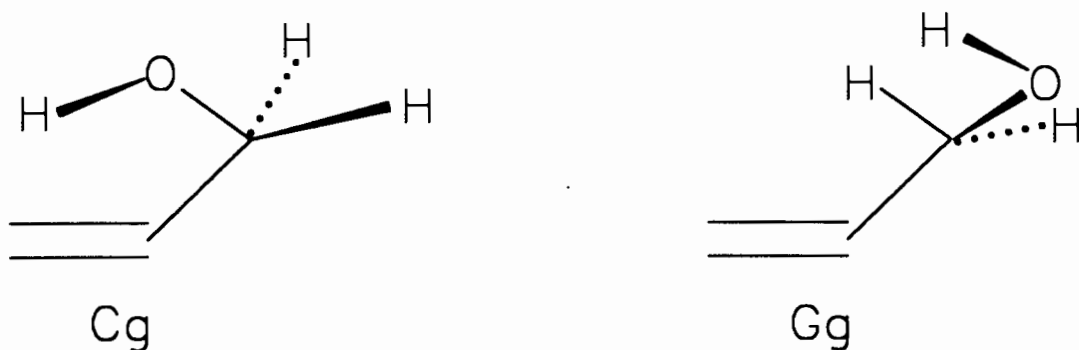
Allyl alcohol has been studied experimentally by various spectroscopic methods<sup>362-366</sup>. The results indicate that the Cg and Gg forms (Fig.6.9) are the lowest energy conformers with the hydroxylic hydrogen gauche to the  $\pi$  system.<sup>#</sup>

<sup>#</sup> The notation used for the conformers of allyl alcohol follows the usage of Murty and Curl.<sup>365</sup> With respect to the O-C-C=C dihedral angle ( $\phi_1$ ), there exists the cis conformer ( $\phi_1=0^\circ$ ) and gauche conformer ( $\phi_1=120^\circ$  and  $-120^\circ$ ); these arrangements are designated as C, G and G' respectively. For the H-O-C-C dihedral angle ( $\phi_2$ ), it is either gauche ( $\phi_2=60^\circ$  and  $-60^\circ$ ) or trans ( $\phi_2=180^\circ$ ); these are designated as g, g' and t, respectively.

Since the IR and NMR studies of cis- and trans-5-t-butyl-2-cyclohexenol and 2-cyclopentenol showed no indications of intramolecular hydrogen bonds, Bakke et al.<sup>369</sup> suggested that the preference of the Cg and Gg rotamers of allyl alcohol is not influenced by an intramolecular hydrogen bond. The conformational preference was suggested to be determined by weak repulsion between the lone pair electrons of the oxygen and the  $\pi$  electrons of the double bond<sup>370</sup> and an overlap between the  $n_o$  and the  $\pi^*_{c=c}$  orbital.<sup>369</sup> *Ab initio* MO calculations at the 4-31G and 4-21G levels showed that the Cg and Gg rotamers have almost equal energy content.<sup>364</sup>

Figure 6.10

The Cg and Gg forms of allyl alcohol.



Although it is known that  $\pi$  electrons are weak proton acceptors, intramolecular  $\text{OH}\cdots\pi$  electron bonding is possible for the Cg and Gg rotamers of allyl alcohol. The 4-31G basis set calculated bond populations between the hydroxylic



hydrogen and the p atomic orbitals of the CC double bond indicate the existence of such interactions.<sup>366</sup> Such hydrogen bonding was also suggested to be present in the two possible conformations of 3-buten-2-ol (Fig.6.11).<sup>371</sup> As the Gg and Cg rotamers of allyl alcohol are of almost equal energy, the Gt and Ct rotamers might also have similar energies (Fig.6.12).

Figure 6.11

The gauche and cis conformations of 3-buten-2-ol.

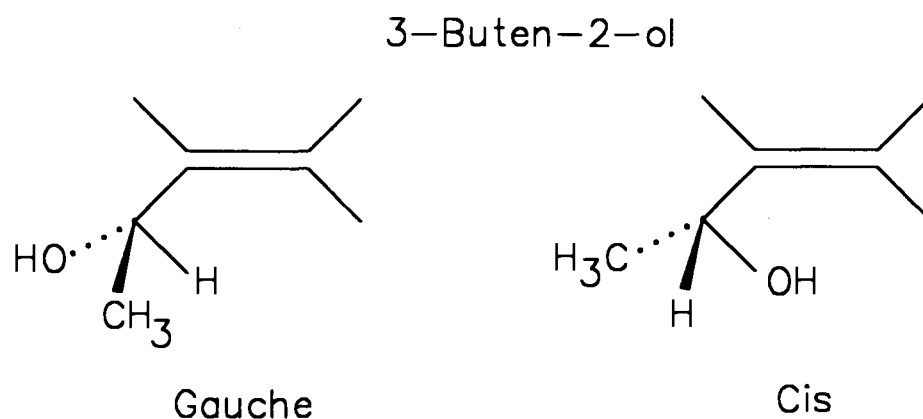
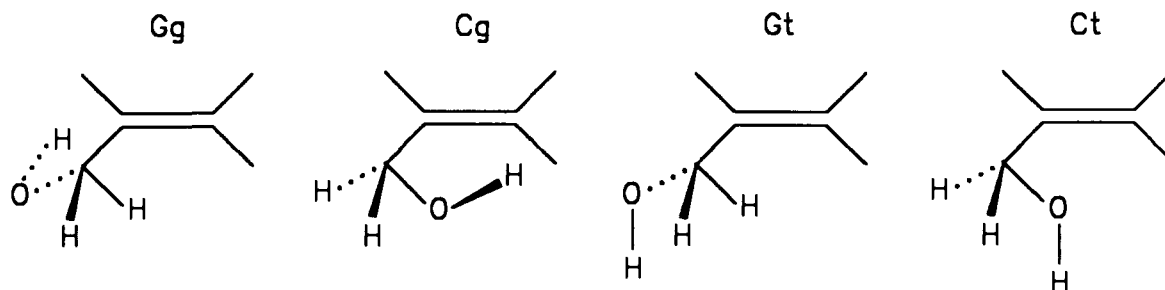


Figure 6.12

The two different sets of rotamers of allyl alcohol in the gauche and cis conformations.



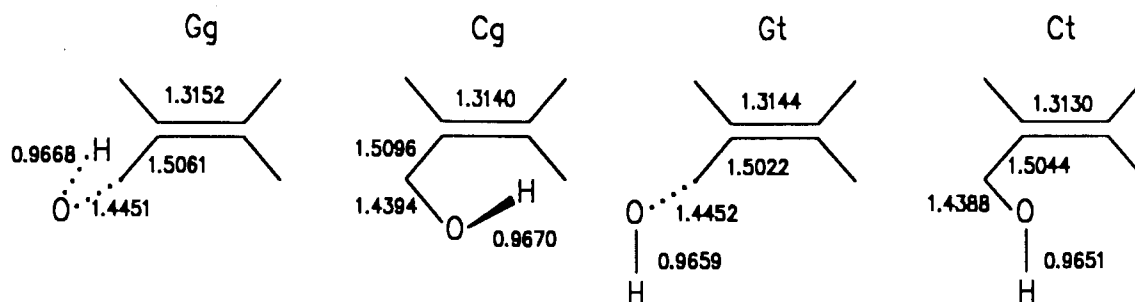
The other conformations have high energy contents and are not included in the analysis. The precise order of energies is sensitive to the level of computation. Results from the 6-31G and 3-21G level calculations are given in Tables 6.3 and 6.4, respectively.

The 6-31G calculation shows that the rotamer pairs, Gg, Cg and Gt, Ct have similar energy contents. However, in the 3-21G calculation, the Cg is the most stable rotamer with the Gg rotamer  $1.11 \text{ kcal mol}^{-1}$  higher in relative energy. The Ct rotamer is more stable than the Gt rotamer by  $1.56 \text{ kcal mol}^{-1}$ . Although the relative energies of the four rotamers are different at the two levels of computation, the change in the geometrical parameters follows the same trend. At both levels, the C=C bond length of the Gg rotamer is longer than that in the Cg rotamer and that of Gt is longer than that of Ct. The C-C bond length of rotamer Cg is longer than that in Gg and that of Ct is longer than that of Gt. The C-O bond length of rotamer Gg is longer than that in Cg and that of Gt is longer than that of Ct. The bond lengthening of C-O and C=C for the Gg and Gt rotamers compared with the Cg and Ct, respectively are explained by the  $\pi_{\text{C=C}} \rightarrow \sigma_{\text{C-O}}^*$  orbital interaction (Fig.6.13). This can also explain the shortening of C-C bonds of the Gg and Gt rotamers relative to the Cg and Ct, respectively. This  $\pi_{\text{C=C}} \rightarrow \sigma_{\text{C-O}}^*$  interaction is analogous to

the  $n \rightarrow \sigma^*_{C-X}$  interaction postulated as the origin of the anomeric effect in acetal systems.

Figure 6.13

The bond lengths (Å) of allyl alcohol calculated at the 6-31G level.



However, in spite of this stabilizing interaction, the Gg and Gt rotamers are less stable than the Cg and Ct rotamers, respectively<sup>#</sup>. In the cis rotamers, the p type lone pairs on the oxygen atoms can interact with the  $\pi^*$  orbitals of the double bond. This is the  $n \rightarrow \pi^*$  interaction as suggested by Zefirov *et al.* in the rationalization of the conformational equilibrium of 2-methoxy and 2-acetoxymethylenecyclohexane.<sup>353</sup> The latter interaction might well be the dominant one.

<sup>#</sup> This applies to the 6-31G results. In the 3-21G calculation, the Gg and Cg rotamers have about the same energy contents, and the Ct is more stable than the Gt.

Table 6.3

Ab initio MO calculation for allyl alcohol at the 6-31G basis level. The bond lengths are in Å, angles in degrees, relative energy ( $\Delta E$ ) in kcalmol<sup>-1</sup>.

	Gg	Cg	Gt	Ct
C1-C2	1.3233	1.3222	1.3221	1.3210
C2-C3	1.4992	1.5026	1.4942	1.4964
C3-O4	1.4372	1.4299	1.4369	1.4306
O4-H5	0.9514	0.9514	0.9507	0.9499
H6-C1	1.0731	1.0729	1.0729	1.0733
H7-C1	1.0754	1.0729	1.0751	1.0710
H8-C2	1.0761	1.0771	1.0749	1.0772
H9-C3	1.0793	1.0806	1.0866	1.0870
H10-C3	1.0844	1.0863	1.0841	1.0870
C3-C2-C1	124.52	125.23	124.62	125.19
O4-C3-C2	111.70	113.74	107.52	109.71
H5-O4-C3	112.80	112.93	113.48	113.50
H6-C1-C2	121.60	121.47	121.71	121.20
H7-C1-C2	121.91	121.70	122.09	121.33
H8-C2-C3	11.13	114.79	114.67	114.35
H9-C3-C2	110.94	110.44	110.12	109.69
H10-C3-C2	110.82	109.82	110.85	109.69
O4-C3-C2-C1	-127.26	10.73	-133.71	0.00
H5-O4-C3-C2	60.93	65.30	184.18	180.00
H6-C1-C2-C3	180.77	179.73	181.64	180.00
H7-C1-C2-C3	0.37	0.57	1.86	0.00
H8-C2-C3-C4	52.79	190.08	47.04	180.00
H9-C3-C2-C1	116.67	-107.10	106.98	-121.13
H10-C3-C2-C1	-3.43	134.81	-12.58	121.13
-E(Hartree)	191.8426652	191.8421830	191.8405954	191.840982
$\Delta E$	0.00	0.30	1.30	1.05

Table 6.4

Ab initio MO calculation for allyl alcohol at the 3-21G basis level. The bond lengths are in Å, angles in degrees, relative energy ( $\Delta E$ ) in kcalmol<sup>-1</sup>.

	Gg	Cg	Gt	Ct
C1-C2	1.3152	1.3140	1.3144	1.3130
C2-C3	1.5061	1.5096	1.5022	1.5044
C3-O4	1.4451	1.4394	1.4452	1.4388
O4-H5	0.9668	0.9670	0.9659	0.9651
H6-C1	1.0730	1.0724	1.0728	1.0730
H7-C1	1.0751	1.0721	1.0748	1.0702
H8-C2	1.0748	1.0755	1.0736	1.0755
H9-C3	1.0804	1.0813	1.0870	1.0874
H10-C3	1.0850	1.0865	1.0845	1.0874
C3-C2-C1	124.34	123.14	124.50	123.53
O4-C3-C2	111.44	112.76	106.76	108.74
H5-O4-C3	109.71	109.81	110.65	110.93
H6-C1-C2	121.95	122.00	121.72	121.57
H7-C1-C2	121.85	120.78	122.08	120.72
H8-C2-C3	114.83	115.66	114.13	115.14
H9-C3-C2	110.21	109.95	109.36	109.23
H10-C3-C2	110.42	109.73	110.54	109.23
O4-C3-C2-C1	-132.22	11.13	-140.20	0.00
H5-O4-C3-C2	60.92	68.01	185.45	180.00
H6-C1-C2-C3	181.06	179.63	181.76	180.00
H7-C1-C2-C3	0.80	0.54	2.14	0.00
H8-C2-C3-C4	48.25	190.43	40.93	180.00
H9-C3-C2-C1	111.89	-106.34	100.43	-121.36
H10-C3-C2-C1	-7.63	135.68	-18.53	121.36
-E(Hartree)	190.8524870	190.8542666	190.8495109	190.8519966
$\Delta E$	1.11	0.00	2.98	1.42

The Gg and Cg rotamers are capable of intramolecular hydrogen bonding. The presence of this  $\text{OH}\cdots\pi$  interaction is supported by the following observations:-

- (1) The Gg and Cg rotamers are more stable than the Gt and Ct rotamers, respectively<sup>§</sup> by about  $1.5 \text{ kcalmol}^{-1}$ .
- (2) The OH bond lengths of Gg and Cg are longer than those of Gt and Ct.
- (3) The bond populations of Gg and Cg are larger than in the other two conformers.
- (4) The distances between the hydroxylic hydrogen and C1 and C2, respectively are 3.55 and 2.66 Å for Gg, and 2.93 and 2.73 Å for Cg. The sum of the van der Waals radii of H and of the aromatic carbon is 2.90 Å.<sup>46</sup> Therefore, the distances to C2 have contracted in both rotamers.

The above analysis suggests that the conformational preferences of allyl alcohol are controlled by more than one type of orbital interaction. This could also be the case for other members of the series. To probe this suggestion further, the *ab initio* wave functions of allyl fluoride and allyl chloride at the 3-21G\* level were subjected to a quantitative PMO analysis.<sup>78,374</sup>

The orbital interactions that contribute to the HOMO's of the gauche and cis rotamers of the allyl halides are presented in Figs. 6.14 and 6.15, respectively. In each case,

---

<sup>§</sup> This applies to the 6-31G calculation. In the 3-21G calculation, the energy difference is about  $1.0 \text{ kcalmol}^{-1}$ .

interactions 1 and 2 are destabilizing, and interactions 3-5 are stabilizing. In Fig.6.14,  $\pi^+$  is the in-phase combination of  $\pi_{CH_2}$  with  $\pi_X$ ,  $\pi^-$  is the out-of phase combination of  $\pi_{CH_2}$  with  $\pi_X$ , and  $\pi^*$  is the out-of phase combination of  $\pi^*_{CH_2}$  with  $\pi_X$ . In Fig.6.15,  $\sigma_1$  is the in-phase combination of the  $2a_1$   $CH_2$  orbital with  $\pi_X$ ,  $\sigma_2$  is the in-phase combination of the  $1b_1$   $CH_2$  orbital with  $\pi_X$ , and  $\sigma^*$  is the out-of-phase combination of  $1b_1$  with  $\pi_X$ . The results of the quantitative PMO analysis are summarized in Tables 6.5 and 6.6.

Figure 6.14

The orbital interactions of allyl halides in the cis rotameric form.

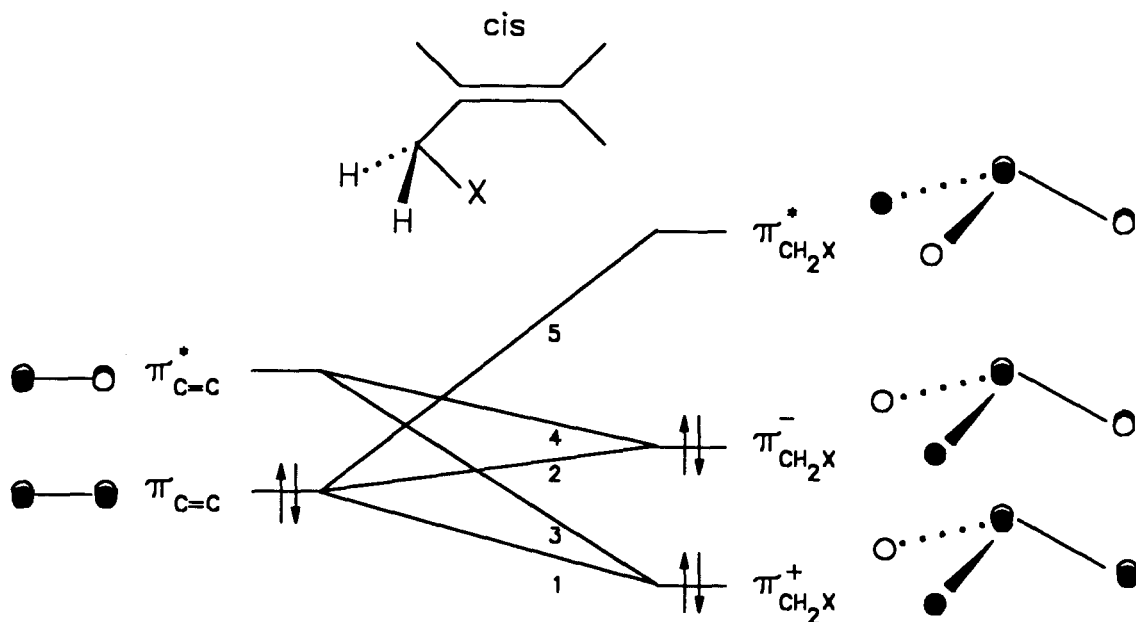
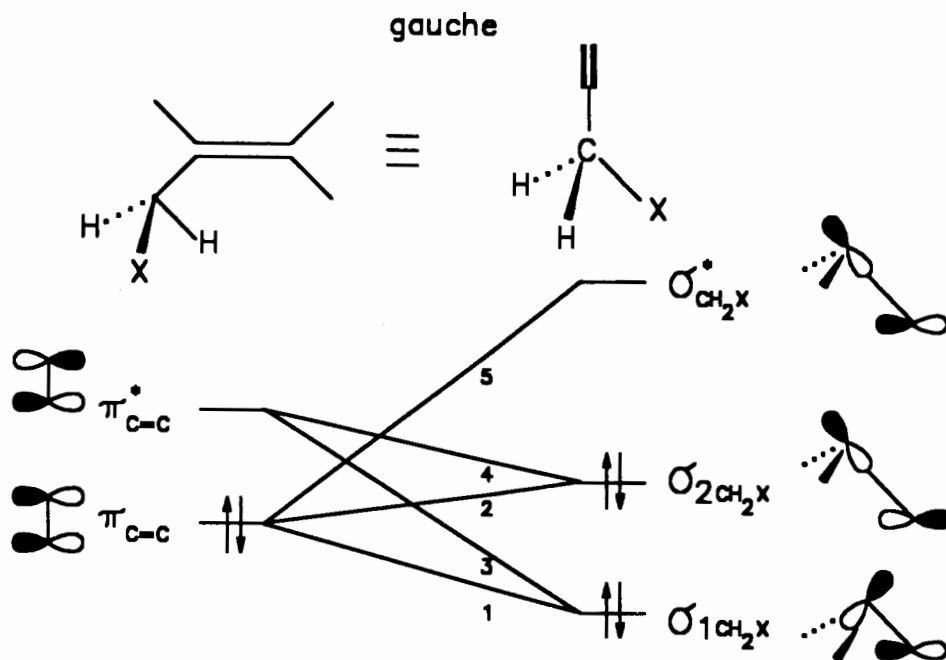


Figure 6.15

The orbital interaction of allyl halides in the gauche rotameric form.



For allyl fluoride, the PMO analysis predicts the relative destabilization of the cis structure by 3.17 (5.83-2.66) kcalmol<sup>-1</sup>, in agreement with the trend in the orbital interactions that contribute to the HOMO's of these two structures but in disagreement with the relative total energies. In addition, the relative destabilization of the cis rotamer is caused almost entirely by the destabilizing interactions; there is no significant contribution from the  $\pi \rightarrow \sigma^*$  interaction which is analogous to the  $n \rightarrow \sigma^*$  anomeric-type interaction, in the gauche rotamer. However, the total relative energies predict a more stable cis structure. The strong electronegative fluorine atom plays a major role. In



the cis structure, there is a strong electrostatic interaction between the fluorine atom and  $H_a$ , the syn-periplanar hydrogen atom on C1. From the atomic charges on the fluorine and on  $H_a$ , and the internuclear distance, the coulombic interaction is calculated to be  $3.37 \text{ kcalmol}^{-1}$ . When this interaction is taken into account in the analysis, the cis structure is more stable than the gauche form by  $0.2 \text{ kcalmol}^{-1}$ . The coulombic interaction, and not an anomeric-type effect is, therefore, the origin of the cis preference of allyl fluoride. A similar result was obtained in the PMO analysis of the benzylic anomeric effect in benzyl fluoride.<sup>361</sup>

Table 6.5

Orbital interactions in allyl fluoride.

Conformation	Orbital	Orbital energy (au)	Orbital interaction	Orbital interaction energy ( $\text{kcalmol}^{-1}$ )
Cis	$\pi_{C=C}$	-0.403	$\pi^+_{CH_2F} \rightarrow \pi_{C=C}$	4.70
	$\pi^*_{C=C}$	0.144	$\pi^-_{CH_2F} \rightarrow \pi^*_{C=C}$	1.79
	$\pi^+_{CH_2F}$	-0.682	$\pi^*_{CH_2F} \rightarrow \pi_{C=C}$	-0.22
	$\pi^-_{CH_2F}$	-0.522	$\pi^+_{CH_2F} \rightarrow \pi^*_{C=C}$	0.00
	$\pi^*_{CH_2F}$	0.307	$\pi^-_{CH_2F} \rightarrow \pi^*_{C=C}$	-0.44
			Total	$5.83 - 3.37^a$ $= 2.46$
Gauche	$\pi_{C=C}$	-0.408	$\sigma_1 \rightarrow \pi_{C=C}$	1.38
	$\pi^*_{C=C}$	0.140	$\sigma_2 \rightarrow \pi^*_{C=C}$	1.55
	$\sigma_1$	-0.697	$\sigma^* \rightarrow \pi_{C=C}$	-0.14
	$\sigma_2$	-0.642	$\sigma_1 \rightarrow \pi^*_{C=C}$	-0.02
	$\sigma^*$	0.254	$\sigma_2 \rightarrow \pi^*_{C=C}$	-0.11
			Total	2.66

a). Refers to the coulombic interaction between F and  $H_a$ .

Table 6.6

Orbital interactions in allyl chloride.

Conformation	Orbital	Orbital energy (au)	Orbital interaction	Orbital interaction energy (kcalmol <sup>-1</sup> )
Cis	$\pi_{C=C}$	-0.407	$\pi^+_{CH_2Cl} \rightarrow \pi_{C=C}$	5.86
	$\pi^*_{C=C}$	0.138	$\pi^-_{CH_2Cl} \rightarrow \pi^*_{C=C}$	0.22
	$\pi^+_{CH_2Cl}$	-0.692	$\pi^*_{CH_2Cl} \rightarrow \pi_{C=C}$	-0.18
	$\pi^-_{CH_2Cl}$	-0.434	$\pi^+_{CH_2Cl} \rightarrow \pi^*_{C=C}$	-0.16
	$\pi^*_{CH_2Cl}$	0.284	$\pi^-_{CH_2Cl} \rightarrow \pi^*_{C=C}$	-0.14
			Total	5.60-0.63 <sup>a</sup> =4.97
Gauche	$\pi_{C=C}$	-0.412	$\sigma_1 \rightarrow \pi_{C=C}$	1.11
	$\pi^*_{C=C}$	0.132	$\sigma_2 \rightarrow \pi^*_{C=C}$	3.35
	$\sigma_1$	-0.634	$\sigma^* \rightarrow \pi_{C=C}$	-0.37
	$\sigma_2$	-0.540	$\sigma_1 \rightarrow \pi^*_{C=C}$	-0.04
	$\sigma^*$	0.163	$\sigma_2 \rightarrow \pi^*_{C=C}$	-0.11
			Total	3.94

a). Refers to the coulombic interaction between Cl and H<sub>g</sub>.

For allyl chloride, the PMO analysis predicts net stabilization of the gauche structure by 1.66 (5.60-3.94) kcalmol<sup>-1</sup>, in agreement with the trend in the relative energies of the HOMO's of these two structures and also in agreement with the trend in the total energies. The coulombic interaction in the cis rotamer is calculated to be 0.63 kcalmol<sup>-1</sup>; taking this into account, the gauche rotamer is predicted to be more stable than the cis rotamer by 1.03 kcalmol<sup>-1</sup>. As in the case of allyl fluoride, the two-orbital four-electron destabilizing interactions are the dominant interactions in determining the stability of the cis and

gauche rotamers. Moreover, the gauche preference of allyl chloride appears to be the result of the  $\pi^+_{\text{CH}_2\text{Cl}} \rightarrow \pi_{\text{C}=\text{C}}$  destabilizing interaction in the cis rotamer.

In conclusion, the gauche preference of electronegative substituents at C<sub>1</sub> of propenes is attributed to the dominance of destabilizing orbital interactions in the cis conformers. The hyperconjugative interactions of the anomeric type do not dominate. Thus, whereas the allylic or vinylogous anomeric effect may exist as a phenomenological effect, its origin in terms of charge transfer (anomeric) interactions must be questioned.

## Chapter 7

### ROTATIONAL BARRIERS IN STERICALLY HINDERED DICHALCOGENIDES

#### 7.1 INTRODUCTION

The rotation about the chalcogen-chalcogen bond in dichalcogenides has been the subject of investigations both experimentally<sup>373-377</sup> and theoretically.<sup>378-383</sup> The key features of interest are (1) the nature of rotational transition state and (2) the relative magnitudes of the rotational barriers as a function of the chalcogen atom. Thus, Fraser *et al.*<sup>374</sup> reported the effects of substitution on the barriers to rotation about the sulfur-sulfur bond in acyclic disulfides, and argued that conformational interconversion between enantiomeric ground states proceeds by way of a *syn* transition state (see Figure 7.1). In contrast, Jorgensen and Snyder<sup>378</sup> concluded, on the basis of molecular mechanics calculations on dialkyl disulfides, that rotation proceeds by way of the *anti* transition state. They argued further that Fraser *et al.*<sup>374</sup> had no definitive experimental evidence for the operation of steric retardation to disulfide rotation, a premise on which the original hypothesis was based. That steric retardation does play some role is indicated by the greater magnitude of the barrier in bis(2,4,6-tri-*tert*-butylphenyl) disulfide (7.1)<sup>373</sup> compared with those in non-hindered disulfides.<sup>374</sup>

Figure 7.1

Chalcogen-chalcogen bond rotation in acyclic dichalcogenides.

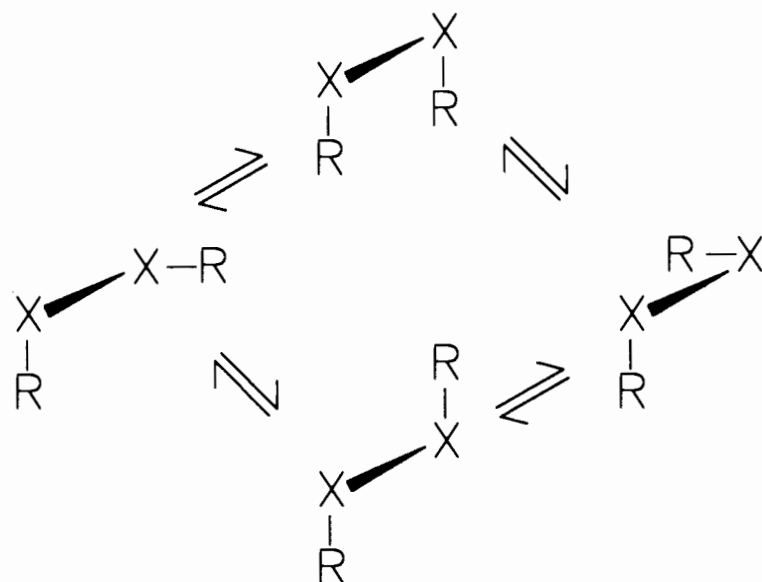
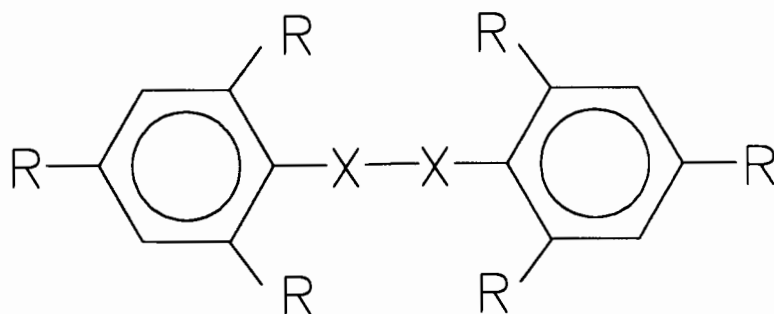


Figure 7.2

Structure of bis(2,4,6-tri-substituted-phenyl)dichalcogenides.



7.1 X=S, R=t-Bu

7.2 X=Se, R=t-Bu

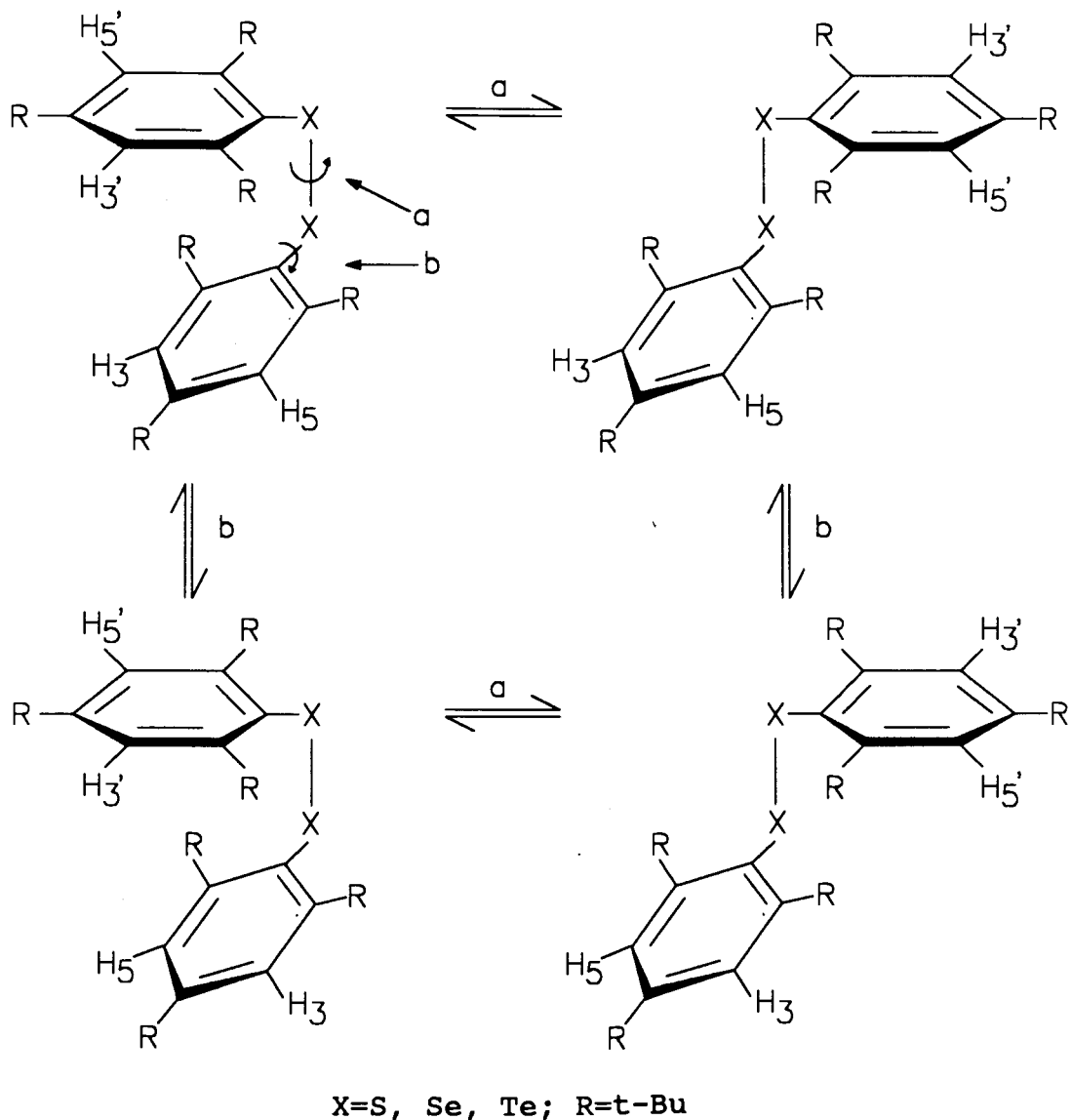
7.3 X=Te, R=t-Bu

7.4 X=Te, R=CH<sub>3</sub>

Restricted rotation about the selenium-selenium bond in diselenides has also been reported.<sup>373,376</sup> Thus, Anderson and Henriksen<sup>376</sup> have measured a barrier of 6.3 kcalmol<sup>-1</sup> in phenyl benzyl diselenide; this is approximately 1.4 kcalmol<sup>-1</sup> lower than that in the corresponding disulfide.<sup>374</sup> Similarly, a reduction in barrier was observed by Kessler and Rundel<sup>373</sup> on substitution of sulfur for selenium in the sterically hindered derivative 7.1, and rotational barriers of 16.2 and 12.5 kcalmol<sup>-1</sup> for the sulfur and selenium analogues, 7.1 and 7.2, respectively, were derived using the coalescence method. Regarding the latter results, it should be noted, as Fraser et al.<sup>374</sup> have pointed out, that the values represent minimal values for the rotational barriers about the chalcogen-chalcogen (X-X) bond, since rotation about the carbon-chalcogen (C-X) bonds must also have been restricted to permit observation of separate <sup>1</sup>H NMR signals for the *meta* protons<sup>375</sup> (see Figure 7.3). Thus, rapid rotation about the C-X bond (bond *b*) would render all *ortho*-R groups isochronous, either by interchanging the groups within one aryl moiety or by operation of the C<sub>2</sub> symmetry axis; the same is true for the *meta*-protons. If rotation about *b* is the low-energy process and rotation about the X-X bond (bond *a*) is the high-energy process, then a true measure of the barrier to rotation about *a* cannot be obtained and the barrier might be higher than the measured value. On the other hand, if rotation about *a* is the

Figure 7.3

Rotation about the chalcogen-chalcogen (X-X) bond and about the carbon-chalcogen (C-X) bond in sterically hindered dichalcogenides.



low-energy process and the true barrier is below the measured value, then the *ortho* (and *meta*) signals would become isochronous by rotation about a regardless of the rate of

rotation about *b*. In this case, the barrier to rotation about *b* would be higher than measured. The problem presents an unusual situation in that only the lower barrier can be measured, in contrast to the normal situation in kinetics in which only the higher barrier can be measured. Despite these complications, it would appear that the effect of the chalcogen atom on X-X rotational barriers in dichalcogenides can be assessed even in these sterically hindered candidates, since similar differences in barriers (ca 20%) are observed<sup>376</sup> for phenyl benzyl disulfide and diselenide or dibenzyl disulfide and diselenide. It is noteworthy that *ab initio* molecular orbital calculations of HSSH and HSeSeH have yielded<sup>381</sup> similar barriers to rotation about the chalcogen-chalcogen bond, a result that is in agreement with the findings of an earlier theoretical study on MeSSMe and MeSeSeMe.

The extension of experimental studies of this nature to the fourth-row analogues, namely the ditellurides, is unknown, although *ab initio* MO calculations of HXXH give barriers of similar magnitudes where the cognate atom X is sulfur, selenium or tellurium.<sup>381,383</sup> An independent report describing the crystal structure and rotational barrier in bis(2,4,6-tri-*tert*-butylphenyl) ditelluride (7.3) appeared<sup>384</sup> after this work has been completed.



As part of a program of research designed to examine the properties, conformations and reactions of organochalcogens, we report here the first example of restricted rotation in a ditelluride, bis(2,4,6-tri-tert-butylphenyl) ditelluride (7.3). The rotational barriers in 7.3 and in the corresponding diselenide 7.2 (for purposes of comparison) have been measured by total line-shape analysis of variable-temperature  $^1\text{H}$  NMR spectra. Compound 7.3 serves as an initial candidate with which to probe further the factors affecting conformational interconversion in dichalcogenides.

## 7.2 COMPOUNDS

The compounds required for the experimental work were synthesized by Dr. R.D.Sharma.

Bis(2,4,6-tri-tert-butylphenyl) diselenide (7.2) and bis(2,4,6-tri-tert-butylphenyl) ditelluride (7.3) were prepared from 2,4,6-tri-tert-butylphenyllithium and elemental selenium and tellurium, respectively, in THF, followed by air oxidation, as also reported by du Mont and coworkers.<sup>385,386</sup>

*Diselenide 7.2*: orange needles (hexane), m.p. 251-252°C;  $^1\text{H}$  NMR (286 K),  $\delta$ 1.38 (s, 18H, 4,4'CMe<sub>3</sub>),  $\approx$ 1.38 (br.pk., 2,6,2'6'CMe<sub>3</sub>), 7.34 (s, 4H, H-3,5,3',5');  $^1\text{H}$  NMR (209 K),  $\delta$ 1.12 (s, 18H, 2,2'CMe<sub>3</sub>), 1.37 (s, 18H, 4,4'CMe<sub>3</sub>), 1.69 (s, 18H, 6,6'CMe<sub>3</sub>), 7.02 (s, 2H, H-3,3'), 7.42 (s, 2H, H-5,5')

Anal. Calcd. for  $C_{36}H_{58}Se_2$ : C 66.85, H 9.01. Found, C 66.64, H 9.38%.

*Ditelluride 7.3*: red needles (hexane), m.p.  $190^\circ C$ , lit.<sup>385</sup>  $192-193^\circ C$ ;  $^1H$  NMR (293 K),  $\delta$ 1.37 (s, 18H, 4,4' $Me_3$ ), 1.45 (s, 36H, 2,6,2',6' $Me_3$ ), 7.30 (s, 4H, H-3,5,,3',5');  $^1H$  NMR (178 K),  $\delta$ 1.12 (s, 18H, 2,2' $Me_3$ ), 1.31 (s, 18H, 4,4' $Me_3$ ), 1.60 (s, 18H, 6,6' $Me_3$ ), 7.11 (s, 2H, H-3,3'), 7.31 (s, 2H, H-5,5').

Anal. Calcd. for  $C_{36}H_{58}Te_2$ : C 57.96, H 7.84. Found, C 57.80, H 8.00%.

Bis(2,4,6-trimethylphenyl) ditelluride (7.4) was prepared as described by Akiba *et al.*<sup>387</sup> and was obtained as orange-red prisms from diethyl ether, m.p.  $131-132^\circ C$ , lit.<sup>387</sup>  $125-127^\circ C$ ;  $^1H$  NMR (238 K),  $\delta$ 2.36 (s, 6H, 4,4' $Me$ ), 2.39 (s, 12H, 2,6,2',6' $Me$ ), 6.88 (s, 4H, H-3,5,3',5');  $^1H$  NMR (146 K),  $\delta$ 2.31 (s, 12H, 2,6,2',6' $Me$ ), 2.35 (s, 6H, 4,4' $Me$ ), 6.87 (s, 4H, H-3,5,3',5').

### 7.3 RESULTS

The conformational processes of interest in compounds of type 7.1-7.4 are the restricted rotation about the C-X and X-X bonds, as illustrated in Figure 7.3. Previous work<sup>373,374</sup> on relatively non-hindered diaryl disulfides has shown that the

magnitude of the S-S rotational barrier is significantly lower than that for C-S rotation, permitting the study of the latter process without interference from the former. However, in the case of hindered disulfide 7.1 and diselenide 7.2, restricted rotation about both C-X and X-X bonds was observed at low temperature, and the changes in line shape with temperature were assigned<sup>373</sup> to the X-X dynamic process.

Dynamic <sup>1</sup>H NMR spectroscopy is a convenient method for determining the rotational barriers in 7.2 and 7.3. The signals for the *tert*-butyl groups at the 2 and 6 positions in 7.2 and 7.3 exhibit coalescence behaviour at about 277 and 209 K, respectively, whereas those for the *meta* protons, H-3 and H-5, exhibit coalescence behaviour at about 266 and 204 K in the spectra of 7.2 and 7.3, respectively. Below these respective temperatures separate signals are observed for each of the 2,2'-*tert*-butyl or 6,6'-*tert*-butyl groups and the H-3,3' or H-5,5' protons. The *meta*-proton signals appear as broadened singlets and do not exhibit *J* coupling. The signals for the 4,4'-*tert*-butyl groups in the spectra of both 7.2 and 7.3 do not exhibit changes due to an exchange process. Thus, the conformational behaviour of ditelluride 7.3 does indeed resemble that of its lighter congeners 7.1 and 7.2 in exhibiting restricted rotation about both C-X and X-X bonds at low temperature. The changes in line shape observed with changes in temperature in the spectra of 7.2 and 7.3 were

simulated by total line-shape analysis using a program for classical two-site exchange.<sup>218</sup> For the diselenide 7.2 both the *tert*-butyl and phenyl signals were used for line-shape matching. In the case of the ditelluride 7.3, however, only the data for the phenyl resonances are presented, since line-shape matching of the *tert*-butyl signals was judged to be less reliable owing to the presence of an impurity. The rate constants derived from the line-shape analysis are listed in Table 7.1. Activation parameters were calculated as described in Chapter 2 and the results are presented in Table 7.2. The <sup>1</sup>H NMR spectra are not of sufficient complexity that their line shapes show significant changes over considerable temperature ranges and, as expected,<sup>388</sup> the uncertainties in  $\Delta H^\ddagger$  and  $\Delta S^\ddagger$  are relatively large. Furthermore, it is likely that the errors have been underestimated, since no attempt has been made to evaluate systematic errors in the line-shape analysis. The free energies of activation derived from careful line-shape analysis are not affected severely by these problems, however, and only these values will be used for purposes of comparison.

Table 7.1

Rate constants (k) derived from line-shape analysis.

Compound	Temperatures (K)	No. of points	Phenyl signals		<i>tert</i> - Butyl signals		
			$k$ ( $s^{-1}$ )	Error	No. of points	$k$ ( $s^{-1}$ )	Error
7.2	209	12	-	-	12	2.0	0.8
	220		6.0	0.2		7.0	1.0
	230		13	2		13.0	0.8
	241		31	3		-	-
	250		80	3		-	-
	257		122	3		137	6
	262		167	3		182	10
	264		244	12		256	3
	270		385	15		370	7
	272		-	-		455	10
	273		417	17		500	13
	277		500	13		556	15
	280		625	20		625	20
	286		1000	50		1000	50
7.3	178	8	4.0	0.3	Not calculated; see Results		
	194		64	2			
	198		145	4			
	199		156	5			
	202		244	12			
	206		457	21			
	217		2904	48			
	221		5538	154			

The free energy of activation for conformational interconversion in the ditelluride 7.3 is  $9.4 \pm 0.1$  kcalmol<sup>-1</sup> at 204 K, the coalescence temperature. The corresponding value for the diselenide 7.2 is  $11.8 \pm 0.1$  kcalmol<sup>-1</sup> at 204 K. The  $\Delta G^\ddagger$  value calculated at 254 K, the coalescence temperature reported previously<sup>373</sup> for the *tert*-butyl signals, is  $12.4 \pm 0.1$  kcalmol<sup>-1</sup>, and compares favorably with the earlier value ( $\Delta G_c^\ddagger = 12.6$  kcalmol<sup>-1</sup>) derived by the coalescence method.<sup>373</sup>

Table 7.2

Activation parameters for restricted rotation in 7.2 and 7.3.<sup>a</sup>

Compound	No. of points	Signals	T <sub>c</sub> (K)	$\Delta H^\ddagger$ (kcalmol <sup>-1</sup> )	$\Delta S^\ddagger$ (calmol <sup>-1</sup> K <sup>-1</sup> )	$\Delta G^\ddagger_{204\text{ K}}$ (kcalmol <sup>-1</sup> )	$\Delta G^\ddagger_{254\text{ K}}$ (kcalmol <sup>-1</sup> )
2	24	<i>tert</i> -Butyl and phenyl	277	9.3±0.5	-12.4±2.2	11.8±0.1	12.4±0.1
			266				
3	8	phenyl	204	13.3±0.7	17.9±3.8	9.4±0.1	8.5±0.2

a). Uncertainties in the parameters are at the 95% confidence level.

#### 7.4 DISCUSSION

The difference in the free energy of activation in the ditelluride 7.3 compared with the diselenide 7.2 can be accounted for in terms of (1) ground-state destabilization, (2) transition-state stabilization, (3) transition-state stabilization which overrides a ground-state stabilizing

effect, (4) ground-state destabilization which overrides a transition-state destabilizing effect in the former compound. In order to facilitate further discussion, it is useful first to consider the nature of the stabilizing and destabilizing interactions in the ground state and transition state of simple dichalcogenides.

### I. Interactions in the ground state

In the general case, the ground state is represented by one of two enantiomeric perpendicular conformers which can interconvert by way of a *syn* or *anti* transition state (Figure.7.1). That the ground states of disulfides, diselenides and ditellurides resemble one another in the above context is indicated by x-ray crystallographic data for the diaryl dichalcogenides (see Table 7.3).<sup>389-395</sup> Furthermore, theoretical calculations of the dichalcogen dihydrides and simple dialkyl derivatives support this contention.<sup>378,380,381,383</sup> The stabilization of *gauche* forms has been rationalized in terms of the minimal repulsion of lone pairs in this conformation.<sup>389-395</sup> In addition, stabilizing hyperconjugative interactions might also play some role.<sup>381-383</sup>

Table 7.3

Critical structural data for diaryl dichalcogenides in the solid state.

Compound	Structural feature			Ref.
	Bond length (Å) C - X	Bond length (Å) X - X	C - X - X - C dihedral angle (°)	
S <sub>2</sub> (C <sub>6</sub> H <sub>5</sub> ) <sub>2</sub>	1.789 (3)	2.023 (1)	96.2	389,390
Se <sub>2</sub> (C <sub>6</sub> H <sub>5</sub> ) <sub>2</sub>	1.93 (5)	2.29 (1)	82.0 (±3.0)	391
Se <sub>2</sub> (C <sub>6</sub> H <sub>4</sub> NO <sub>2</sub> <sup>-p</sup> ) <sub>2</sub>	1.920 (3)	2.3018 (8)	87.8 (1)	392
Te <sub>2</sub> (C <sub>6</sub> H <sub>5</sub> ) <sub>2</sub>	2.115 (16)	2.712 (2)	88.5	395

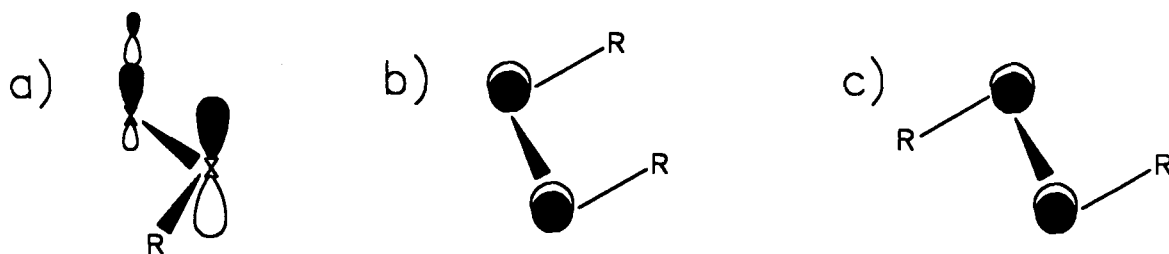
The dominant stabilizing interactions in the ground state of these compounds may be treated, within the framework of perturbational molecular orbital (PMO) theory,<sup>69,70</sup> in terms of two-orbital two-electron interactions that contribute to the HOMO of the molecules. The relevant interaction involves a doubly occupied non-bonding orbital on the chalcogen atom, the highest occupied p-type orbital ( $n_x$ ), and an unoccupied acceptor orbital, the antibonding  $\sigma^*_{x-c}$  orbital, associated with the remaining fragment (see Figure 7.4). The magnitude of this interaction is proportional to the square of the overlap between the interacting orbitals and inversely proportional to their energy difference. Application of the PMO analysis to the dichalcogenides requires prior knowledge of the relative energies of the  $n_x$  and  $\sigma^*_{x-c}$  orbitals and also the differences in overlap. The first ionization potentials



measured for  $H_2X$  ( $X = S, Se, Te$ ) indicate that the  $n_x$  orbital energy decreases in the sequence  $Te > Se > S$ ,<sup>397</sup> a result that is also substantiated by theoretical calculations.<sup>381</sup>

Figure 7.4

Dominant orbital interactions that contribute to the HOMO of R-X-X-R molecules in the (a) perpendicular, (b) syn and (c) anti conformations.



*Ab initio* MO calculations by Lehn et al.<sup>398</sup> have shown also that the  $\sigma^*_{se-c}$  orbital is lower lying than the  $\sigma^*_{s-c}$  orbital, and it is likely that the  $\sigma^*_{te-c}$  orbital lies even lower. Thus, on the basis of an energy-gap argument, one would predict a more favourable  $n_x \rightarrow \sigma^*_{x-c}$  interaction for  $X = Te$  than  $X = Se$ , and a greater stabilization of the ditelluride relative to the diselenide. The effect of differences in overlap is not readily evaluated in the absence of a quantitative PMO analysis.<sup>399</sup> Thus, although the longer Te-Te bond (see Table 7.3) might be predicted to lead to lesser overlap between interacting orbitals and lesser stabilization, because the 5p lone-pair orbitals on Te extend outward more

than the 4p lone-pair orbitals on Se it is conceivable that greater stabilization will be present in the case of the ditellurides. *Ab initio* MO calculations of H-X-X-H (X = S, Se, Te)<sup>381</sup> show that, in the ground state, the total energies of these molecules decrease in the sequence S > Se > Te, thereby suggesting that overlap effects are greater in the case of the ditelluride and/or that the energy-gap effects are dominant.

## II. Interactions in the transition state

Regarding the transition state for rotation, either the *syn* (dihedral angle 0°) or *anti* (dihedral angle 180°) conformations (see Fig.7.1) are destabilized owing to repulsion between the lone pairs on the chalcogen atoms. Within the PMO framework, such interaction is treated in terms of two-orbital, four-electron destabilizing orbital interactions.<sup>69,70</sup> The magnitude of this interaction is proportional to the square of the overlap between interacting orbitals and to the sum of their orbital energies. An argument based on consideration of orbital energies therefore predicts that the transition state of the ditellurides is more destabilized than that of the diselenides. Calculated X-X overlap populations in H-X-X-H (X = S, Se, Te) molecules are nearly equal,<sup>383</sup> and a net destabilization of the transition state in the case of ditellurides is, therefore, predicted.

(These results also have a bearing on the previous discussion regarding ground states, and suggest that energy-gap effects are dominant in that case.)

### III. Effects on the rotational barriers

Overall, on the basis of electronic arguments presented in the foregoing discussion, one predicts a greater destabilization of the transition state and stabilization of the ground state in ditellurides relative to diselenides (a negatively reinforced situation; for a summary of this terminology, see Ref.400), and a greater rotational barrier in the former compounds. However, one predicts also that non-bonded repulsion between substituents will decrease in the sequence  $S > Se > Te$  owing to the longer C-X and X-X bonds as one descends the group, and it is logical that both the ground state and transition state will decrease in stability in the order  $Te > Se > S$ . Therefore, on steric grounds, a clear prediction regarding the relative magnitudes of the rotational barriers as a function of the chalcogen atom is difficult, since the ground state and transition state effects are balanced.<sup>400</sup> What is clear, however, is that the influence of steric and electronic effects on the transition state is opposite in nature, the former stabilizing and the latter destabilizing in the ditellurides compared with the diselenides. On the other hand, both steric and electronic

effects act to stabilize the ground state of the ditellurides relative to the diselenides. One might expect that as the substituents on the chalcogen atoms increase in size, steric interactions would play a more important role and eventually dominate over the countervailing electronic effects in the transition state; lower barriers in the ditellurides would be predicted. This might well account for the discrepancy in the behaviour of simple vs complex dichalcogenides, namely the experimentally observed differences in rotational barriers in complex disulfides vs diselenides<sup>373,376</sup> and the calculated barriers of similar magnitudes in simple dichalcogen dihydrides.<sup>381,383</sup>

Returning to the case of the sterically hindered diselenide 7.2 and ditelluride 7.3, the lower barrier to rotation in 7.3 may be attributed, in light of the foregoing arguments, to the relative stabilization of the transition state (owing to a dominance of steric interactions) which counteracts the effect of concomitant ground-state stabilization in the ditelluride 7.3. That steric retardation to rotation about the chalcogen-chalcogen bond in the transition state is important is evident from the lower rotational barriers reported for simple diaryl disulfides and dialkyl disulfides,<sup>373-375</sup> and further by the observation that the variable-temperature <sup>1</sup>H NMR spectra of dimesityl ditelluride (7.4) show no changes attributable to a dynamic

process, even at 146 K. The results also support the hypothesis<sup>374</sup> that conformational interconversion proceeds by way of the *syn* transition state.

Finally, we comment on the assignment of the measured rotational barriers to the X-X or the C-X rotational process. As explained in section 7.1, the measured barriers can only represent minimal values for X-X or C-X rotation since both processes must be slow in order that line broadening be observed. Consequently, it is difficult to prove, on the basis of the present work, that the observed effects are due to the X-X process rather than the C-X process.

#### **7.5 Theoretical investigation of the rotational barriers in dichalcogenides**

The steric bulk of the methyl substituents in the dimesityl ditelluride (7.4) is much smaller than that of the *t*-butyl groups in the bis(2,4,6-tri-*tert*-butylphenyl) diselenide (7.2) and ditelluride (7.3) (Fig.7.2). According to the steric retardation suggestion of Fraser et al.,<sup>374</sup> the rotational barrier about the Te-Te bond (7.4) should be lower than in the *t*-butyl analog (7.2 & 7.3). This is indeed what we found experimentally. However, as has been pointed out by Kessler and Rundel<sup>373</sup>, both C-X and X-X bond rotations have to be restricted for separation of the meta proton signals to be

observed by NMR spectroscopy in these compounds. Although no changes attributable to a dynamic process can be observed for (7.4), even at 146 K, the rotation between the Te-Te bond may already be restricted, the  $C_2$  symmetry of the molecule rendering the ortho-Me and meta-protons isochronous. As mentioned in section 7.1, only the lower barrier can be measured in these compounds. The use of an asymmetric molecule in which one of the phenyl substituents is replaced by another group such as the benzyl group may be used to solve this problem. The proposal of steric retardation also faces some challenges. Jorgensen and Snyder<sup>378,379</sup> argued that the the experimental energy difference obtained by Fraser et al.<sup>373</sup> ( $\Delta\Delta G^\ddagger=1.8$  kcalmol<sup>-1</sup>) was small and that the analysis of the free energy of activation data was complicated by the possible operation of other effects. They also concluded, on the basis of molecular mechanics calculations on a series of dialkyl disulfides using Allinger's MM force field, that rotation proceeds by way of the anti transition state. The same result was also obtained from the *ab initio* MO calculations of dichalcogen hydrides.<sup>380,382</sup> Experimental investigations using photoelectron spectroscopy and x-ray crystallographic analysis also support the fact that rotation occurs via the anti transition state. In substituted disulfides, as the steric bulk of the R group increases, the

dihedral angle R-S-S-R increases towards the anti conformation (see Table 7.4).

Table 7.4

(CSSC) Dihedral angles ( $\omega(^{\circ})$ ) of disulfides with bulky substituents.<sup>378</sup>

Compound	CSSC $\omega(^{\circ})$	Method of determination
Diadamantyl disulfide	103	PES
t-Butyl disulfide	110	PES/MO calculation
D-penicillamine disulfide	115	X-ray analysis

Although the trend in the change in the dihedral angles of dichalcogenides were reproduced by the molecular mechanics calculations,<sup>222</sup> other geometrical parameters were not. A survey of the MM2 force field revealed that it is not fully parameterized for the dichalcogenide systems. However, the changes in dihedral angles and other geometrical parameters were observed in the MNDO calculation of dialkyl disulfides (Table 7.5). Thus, in the present study, MNDO MO calculations of a series of dialkyl disulfides were performed on an IBM PC using the program "PCMODEL".<sup>231</sup> The subroutines in the semiempirical calculations are the PC version of the MOPAC program released by QCPE.<sup>230</sup> All the geometrical parameters were optimized except for the R-S-S-R dihedral angles that were fixed at  $0^{\circ}$  and  $180^{\circ}$  for the syn and anti conformers, respectively. When R=t-butyl, the C-S-S-C dihedral angle is

Table 7.5

Optimized parameters<sup>a</sup> (bond lengths in Å; bond angles in degrees) of dialkyl disulfides.

Conformation	$\omega$	r(R-S)	r(S-S)	Heat of Formation (kcalmol <sup>-1</sup> )	$\Delta E$ (kcalmol <sup>-1</sup> )
(1) R=H					
syn	0.2	1.3049	1.9323	5.99	5.20
gauche	-91.6	1.3089	1.9112	0.80	0.00
anti	180.0	1.3060	1.9292	2.63	1.80
(2) R=CH <sub>3</sub>					
syn	0.0	1.7288	1.9394	-12.21	6.71
gauche	-102.4	1.7349	1.9237	-18.92	0.00
anti	180.5	1.7321	1.9402	-17.31	1.61
(3) R=CH <sub>2</sub> CH <sub>3</sub>					
syn	0.0	1.7414	1.9369	-23.71	6.11
gauche	107.4	1.7489	1.9214	-29.80	0.00
anti	-178.0	1.7442	1.9400	-28.91	0.89
(4) R=CH(CH <sub>3</sub> ) <sub>2</sub>					
syn	0.0	1.7576 1.7564	1.9360	-27.00	8.65
gauche	-108.6	1.7643 1.7642	1.9201	-35.65	0.00
anti	180.0	1.7603 1.7597	1.9393	-33.83	1.82

a). From MNDO calculation.

131.4 for the gauche conformer. Unfortunately, the calculations failed to achieve self-consistency in the case of the syn and anti conformers. The results of the calculations also showed that the H-S and C-S bond lengths of the disulfide hydrides and dialkyl disulfides, respectively were the longest in the gauche conformations. In this conformation, the p-type



lone pairs on sulfurs can have maximum overlap with the antiperiplanar  $\sigma^*_{\text{S-C(H)}}$  orbitals. The shortening of the central S-S bonds also supports the operation of the stabilizing  $n_{\text{S}} \rightarrow \sigma^*_{\text{C-S}}$  orbital interaction.

The syn and anti rotational barriers obtained by the MNDO calculations agree with the results obtained by *ab initio* calculation of methyl disulfide<sup>141</sup> and hydrogen disulfide<sup>383</sup> in that the syn barriers are always higher than the anti barriers (Table 7.6).

Table 7.6

*Ab initio* MO calculated rotational barrier (in kcalmol<sup>-1</sup>) of disulfide hydride and methyl disulfide.

Molecule	Syn barrier	Anti barrier	Level of calculation	Ref.
H-S-S-H	8.8	6.2	3-21G*	132
	8.5	6.1	6-31G*	132
CH <sub>3</sub> -S-S-CH <sub>3</sub>	16.49	8.0	DH+d <sup>a</sup>	141
	11.69	5.8	3-21G*	this study

a). DH + d = Dunning-Hay basis set with inclusion of d orbitals: same as the DH basis set<sup>401</sup> except that the contracted set for S was augmented with a 3d function.

The results obtained from the calculation of alkyl disulfides may also be extended to the analysis of diselenides. It was found that the magnitudes of the rotational barriers in dimethyl disulfide and dimethyl diselenide were very similar<sup>141</sup> and that the rotational

barriers about different chalcogen-chalcogen bonds in dichalcogen hydrides appeared to be almost identical.<sup>381</sup>

The rotational barrier obtained for the hydrogen disulfide is very different from that in its oxygen analog. While the gauche conformer of hydrogen peroxide is the global minimum, the anti conformer is only slightly less stable than the gauche conformer. However, the syn conformer is destabilized by 9.05 kcalmol<sup>-1</sup> relative to the gauche conformer (Table 7.7).

Table 7.7

Potential energy profile for internal rotation of hydrogen peroxide at the 6-31G\* level of calculation.

Dihedral angle $\omega$ H-O-O-H	0.0	30.0	60.0	90.0	125.3	150.0	180.0
Relative Energy kcalmol <sup>-1</sup>	0.0	-1.8	-5.6	-8.2	-9.1	-8.5	-8.2

The change in the energies for hydrogen peroxide was subjected to a Fourier decomposition analysis of the potential function (eq.1.7).<sup>195</sup> The separation of the potential function into one-fold ( $V_1$ ), two-fold ( $V_2$ ), and the three-fold ( $V_3$ ) components facilitates the analysis of the results. For the three potential constants (Fig.7.5),  $V_3$  (-0.39) is very small and negative, indicating a slight preference for staggered conformations. The large and negative  $V_1$  (-7.80)

term reflects the importance of dipole interactions (Fig.7.6). The gauche conformation provides the optimum orientation for the  $n_{\text{O}} \rightarrow \sigma^*_{\text{OH}}$  orbital interaction. This can be seen from the negative  $V_2$  term (-4.23). The magnitudes of these potential constants are very close to those obtained by Radom *et al.*<sup>195</sup> ( $V_1 = -7.08$ ,  $V_2 = -3.51$ , and  $V_3 = -0.22$ ) with a rigid rotor assumption, calculated at the 4-31G level.

Figure 7.5

Fourier decomposition analysis of the potential function for hydrogen peroxide.

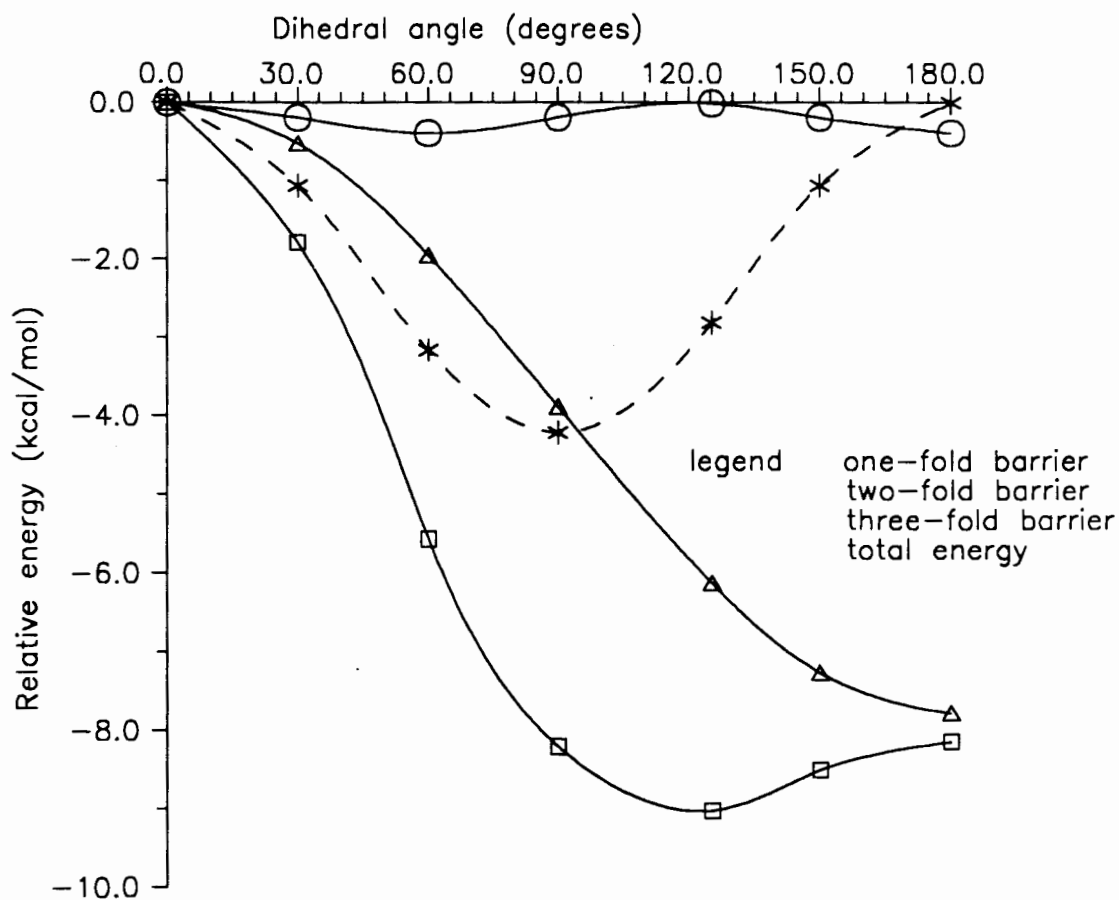
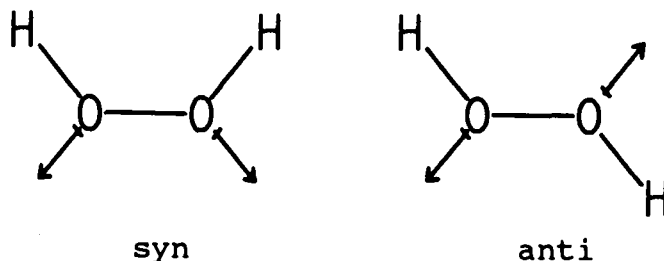


Figure 7.6

Dipolar interactions in the syn and anti rotameric forms of hydrogen peroxide.



In the case of hydrogen disulfide (Table 7.8), Fourier decomposition analysis of the potential function indicates that the stability of the gauche conformer is dominated by the  $V_2$  term (-7.24); the greater magnitude of this term than in hydrogen peroxide implies that the  $n_S \rightarrow \sigma^*_{S-H}$  orbital interaction is more important in controlling the stability of the gauche conformation of hydrogen disulfide. The  $V_1$  term (-1.74) is much smaller than in hydrogen peroxide, indicating that the dipole interaction is of less significance. As expected, a slight preference for the staggered conformations is reflected by the small and negative  $V_3$  term (-0.64) (Fig.7.7).

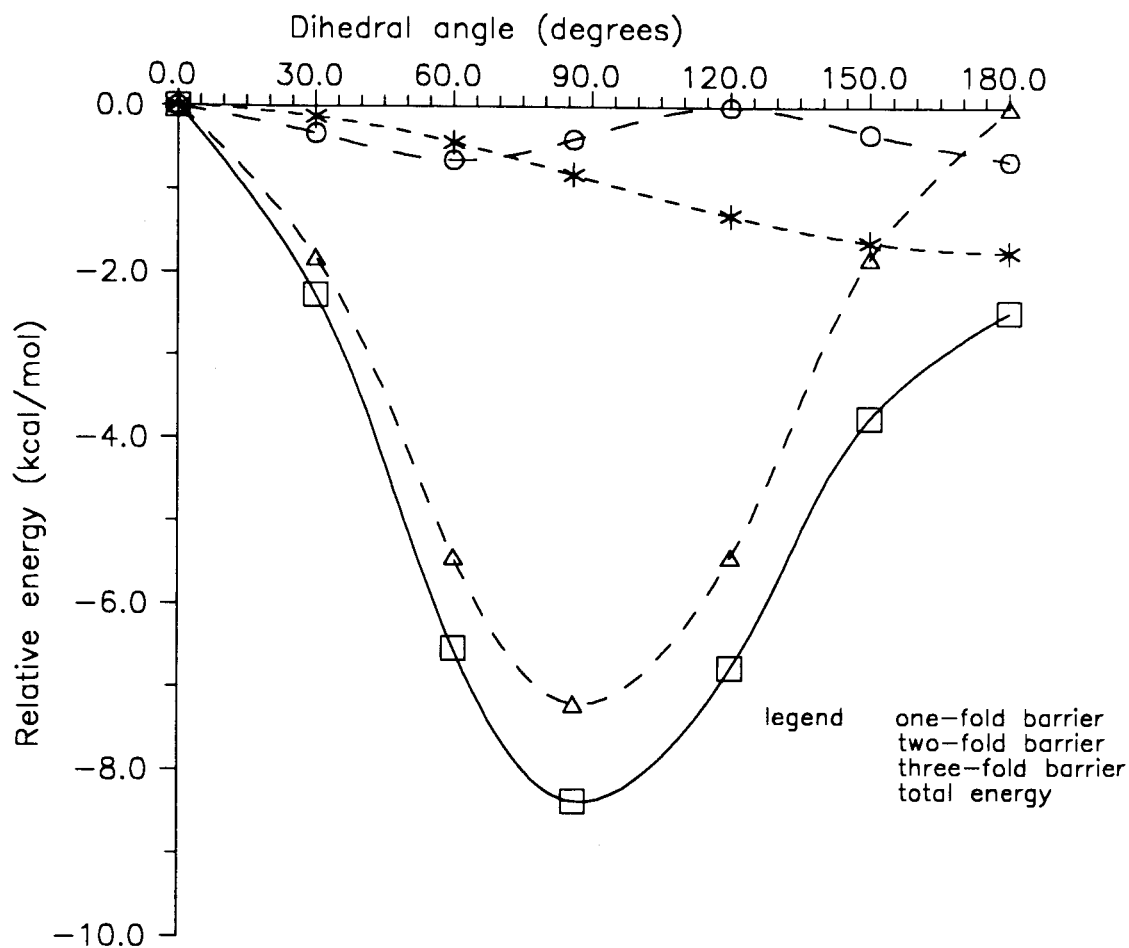
Table 7.8

Potential energy profile for internal rotation of hydrogen disulfide at the 6-31G\* level of calculation.

Dihedral angle $\omega$ H-S-S-H	0.0	30.0	60.0	86.0	120.0	150.0	180.0
Relative energy kcalmol <sup>-1</sup>	0.0	-2.3	-6.5	-8.4	-6.8	-3.8	-2.5

Figure 7.7

Fourier decomposition analysis of the potential function for hydrogen disulfide .



In conclusion, all of the above calculations indicate that the anti transition state for chalcogen-chalcogen rotation is favoured over the syn transition state. The experimental evidence on the sterically hindered compounds suggests otherwise.<sup>402</sup> It would appear that further studies

are necessary in order to resolve the discrepancy and to further probe the proposed steric retardation process.

## REFERENCES

1. J.H.van't Hoff, Bull.Soc.Chim.France, 23, 295, 1875.
2. J.A.Le Bel, Bull.Soc.Chim.France, Series 2 22, 337, 1874.
3. H.Sachse, Chem.Ber., 23, 1363, 1890.
4. W.N.Haworth, "The constitution of sugars", Edward Arnold & Co., London, 1929, p.90.
5. K.W.F.Kohlrausch, A.W.Reitz and W.Stockmair, Z.Phys.Chem., B32, 229, 1936.
6. O.Hassel, Quart.Rev., 7, 221, 1953.
7. D.H.R.Barton, Experientia, 6, 316, 1950.
8. E.L.Eliel, "Stereochemistry of carbon compounds", McGraw-Hill, N.Y., 1962.
9. M.Hanack, "Conformation theory", Academic Press, N.Y., 1965.
10. E.L.Eliel, N.L.Allinger, S.J.Angyal and G.A.Morrison, "Conformational analysis", Interscience, N.Y., 1965.
11. F.A.L.Anet, J.Krane, W.Kitching, D.Dodderel and D.Praeger, Tetrahedron Lett., 3255, 1974.
12. N.S.Zefirov, Tetrahedron, 33, 3193, 1977.
13. J.T.Edward, Chem.Ind.(London), 1102, 1955.
14. R.U.Lemieux, Abstr.Pap.Am.Chem.Soc., 5E, 135, 1959.
15. R.U.Lemieux and P.Chu., Abstr.Pap.Am.Chem.Soc., 31N, 133, 1958.
16. R.U.Lemieux, "Molecular Rearrangements", Vol.2, Edited by P.de Mayo, Interscience, N.Y., 1964.
17. E.L.Eliel, Acc.Chem.Res., 3, 1, 1970.

18. N.S.Zefirov and N.M.Shekhtman, *Russ.Chem.Rev.*, **40**, 315, **1971**.
19. S.Wolfe, *Acc.Chem.Res.*, **5**, 102, **1972**.
20. W.A.Szarek and D.Horton, *ACS Symp.Ser.*, **87**, **1979**.
21. S.Wolfe, M-H.Whangbo, and D.J.Mitchell, *Carbohydr.Res.*, **69**, 1, **1979**.
22. A.J.Kirby, "The anomeric effect and related stereoelectronic effects of oxygen", Springer Verlag, Berlin, **1983**.
23. P.Deslongchamps, "Stereoelectronic effects in organic chemistry", Pergamon, Oxford, **1983**.
24. H.Booth and K.A.Khedhair, *J.Chem.Soc., Chem.Commun.*, 467, **1985**.
25. B.Fuchs, A.Ellenweig, E.Tartakovsky and P.Aped, *Angew.Chem., Int.Ed.Engl.*, **25**, 287, **1986**.
26. B.M.Pinto, H.B.Schlegel and S.Wolfe, *Can.J.Chem.*, **65**, 1658, **1987**.
27. A.E.Reed and P.v.R.Schleyer, *J.Am.Chem.Soc.*, **109**, 7362, **1987**.
28. B.M.Pinto, R.J.Batchelor, B.D.Johnston, F.W.B.Einstein and I.D.Gay, *J.Am.Chem.Soc.*, **110**, 2990, **1988**.
29. B.M.Pinto, B.D.Johnston and R.Nagelkerke, *Heterocycles*, **28**, 389, **1989**.
30. E.Juaristi, E.A.Gonzalez, B.M.Pinto, B.D.Johnston and R.Nagelkerke, *J.Am.Chem.Soc.*, **111**, 6745, **1989**.
31. P.L.Durette and D.Horton, *Adv.Carbohydr.Chem.*, **26**, 49, **1971**.
32. R.U.Lemieux, *Pure Appl.Chem.*, **25**, 527, **1971**.



33. C.Romers, C.Altona, H.R.Buys and E.Havinga, *Top.Stereochem*, **4**, 1969, p.39-97.
34. D.G.Gorenstein and D.Kar, *J.Am.Chem.Soc.*, **99**, 672, 1977.
35. I.Tvaroska, T.Bleha, *J.Mol.Struct.*, **24**, 249, 1975.
36. G.A.Jeffrey, J.A.Pople and L.Radom, *Carbohydr.Res.*, **38**, 81, 1974.
37. G.A.Jeffrey and J.H.Yates, *Carbohydr.Res.*, **79**, 155, 1980.
38. B.M.Pinto, H.B.Schlegel and S.Wolfe, *Can.J.Chem.*, **65**, 1658, 1987.
39. P.v.R.Schleyer, E.D.Jemmis and G.W.Spitznagel, *J.Am.Chem.Soc.*, **107**, 6393, 1985.
40. R.O.Hutchins, L.D.Kopp and E.L.Eliel, *J.Am.Chem.Soc.*, **90**, 174, 1968.
41. E.L.Eliel, *Angew.Chem.Int.Ed.Engl.*, **11**, 739, 1972.
42. Y.A.Zhdanov, R.M.Minyaev and V.I.Minkin, *J.Mol.Struct.*, **16**, 357, 1973.
43. N.J.Chü, Ph.D. Thesis, University of Ottawa, Ottawa, Ontario, Canada, 1959, p.97.
44. L.O.Brockway, *J.Phys.Chem.*, **41**, 185, 1937.
45. J.Hine, *J.Am.Chem.Soc.*, **85**, 3239, 1963.
46. L.Pauling, "The nature of the chemical bond", Cornell University Press, Ithaca, N.Y., 3<sup>rd</sup> ed., 1960, p.314.
47. C.Altona, Ph.D. Thesis, University of Leiden, 1964.
48. C.Altona, C.Knobler and C.Romers, *Acta.Cryst.*, **16**, 1217, 1963.
49. C.Altona, C.Knobler and C.Romers, *Recl.Trav.Chim.Pays-Bas*, **82**, 1089, 1963.

50. C.Altona and C.Romers, Recl.Trav.Chim.Pays-Bas, 82, 1080, 1963.
51. C.Altona and C.Romers, Acta.Cryst., 16, 1225, 1963.
52. H.T.Kalff and C.Romers, Recl.Trav.Chim.Pays-Bas, 85, 198, 1966.
53. N.de.Wolf, C.Romers and C.Altona, Acta.Cryst., 22, 715, 1967.
54. E.A.C.Lucken, J.Chem.Soc.III, 2954, 1959.
55. S.David, O.Eisenstein, W.J.Hehre, L.Salem and R.Hoffmann, J.Am.Chem.Soc., 95, 3806, 1973.
56. Z.De Weck-Ardalan, E.A.C.Lucken and J.Weber, J.Mol.Struct., 32, 101, 1976.
57. L.Guibè, J.Augé, S.David and O.Eisenstein, J.Chem.Phys., 58, 5579, 1973.
58. C.H.Townes and B.P.Dailey, J.Chem.Phys., 17, 782, 1949.
59. S.David in "Anomeric effect, origin and consequences", ACS Symp.Ser. 87, Chap.1, W.A.Szarek and D.Horton, Eds., ACS, Washington, D.C., 1979.
60. J.Augé and S.David, Nouv.J.Chim., 1, 57, 1977.
61. A.S.Perlin, Can.J.Chem., 49, 1972, 1971.
62. P.Deslongchamps, P.Atlani, D.Frehel, A.Malaval and C.Moreau, Can.J.Chem., 52, 3651, 1974.
63. S.J.Angyal and K.James, Aust.J.Chem., 23, 1209, 1970.
64. J.M.Lehn, G.Wipff and H.Bürgi, Helv.Chim.Acta, 57, 493, 1974.

65. D.W.Sweigart and D.W.Turner, *J.Am.Chem.Soc.*, **94**, 5599, **1972**.
66. C.R.Brundle and D.W.Turner, *Proc.Roy.Soc.*, **A307**, 27, **1968**.
67. C.Baird and R.M.West, *J.Am.Chem.Soc.*, **93**, 4427, **1971**.
68. R.Hoffmann, *Acc.Chem.Res.*, **4**, 1, **1971**.
69. N.D.Epiotis, W.R.Cherry, S.Shaik, R.L.Yates and F.Bernadi, *Topics in Current Chemistry: Structural Theory of Organic Chemistry*, Vol. 70/ Springer-Verlag, Berlin, **1977**.
70. T.A.Albright, J.K.Burdett and M.-H.Whangbo, "Orbital Interactions in Chemistry", Wiley, N.Y., **1985**.
71. W.J.Hehre, L.Radom, P.v.R.Schleyer and J.A.Pople, "Ab initio Molecular Orbital Theory", John Wiley and Sons, **1986**.
72. F.S.Jorgensen and L.Norskov-Lauritsen, *Tetrahedron Lett.*, **23**, 5221, **1982**.
73. F.S.Jorgensen, *J.Chem.Res.(S)*, 212, **1981**.
74. O.Eisenstein, N.T.Anh, Y.Jean, A.Devaquet, J.Cantacuzene and L.Salem, *Tetrahedron*, **30**, 1717, **1974**.
75. G.Baddeley, *Tetrahedron Lett.*, 1645, **1973**.
76. G.L.Bendazzoli, F.Bernardi and P.Palmieri, *J.Chem.Soc., Faraday Trans.,II*, **69**, 579, **1973**.
77. P.Palmieri and A.M.Mirri, *J.Mol.Struct.*, **37**, 164, **1977**.
78. M-H.Whangbo, H.B.Schlegel and S.Wolfe, *J.Am.Chem.Soc.*, **99**, 1296, **1977**.
79. W.L.Jorgensen and L.Salem, "The organic chemist's book of orbitals", Academic Press, N.Y., **1973**.

80. J.E.Eilers and D.R.Whitman, *J.Am.Chem.Soc.*, 95, 2067, 1973.
81. B.J.Duke and B.O'Leary, *Chem.Phys.Lett.*, 20, 459, 1973.
82. J.E.Eilers, B.O'Leary, A.Liberles and D.R.Whitman, *J.Am.Chem.Soc.*, 97, 5979, 1975.
83. B.O'Leary, B.J.Duke and J.E.Eilers, *Adv.Quantum Chem.*, 9, 1, 1975.
84. D.L.Lichtenberger and R.F.Fenske, *J.Chem.Phys.*, 64, 4247, 1976.
85. P.Luger, P.L.Durette and D.Horton, *Chem.Ber.*, 107, 2616, 1974.
86. H.Paulsen, P.Luger and F.R.Heiker, "Anomeric effect, origin and consequences", *ACS Symp.Ser. No.87, Chapt.2*, p.63-79, W.A.Szarek and D.Horton, Eds., ACS, Washington, D.C., 1979.
87. R.U.Lemieux, A.A.Pavia, J.C.Martin and K.A.Watanabe, *Can.J.Chem.*, 47, 4427, 1969.
88. R.U.Lemieux, S.Koto and D.Voisin, "Anomeric effect, origin and consequences", *ACS Symp.Ser. No.87, Chapt.2*, p.17, W.A.Szarek and D.Horton, Eds., ACS, Washington, D.C., 1979.
89. B.Fuchs, L.Schleifer and E.Tartakovsky, *Nouv.J.Chim.*, 8, 275, 1984.
90. G.A.Jeffery, J.A.Pople, J.S.Binkley and S.Vishveshwara, *J.Am.Chem.Soc.*, 100, 373, 1978.
91. P.Deslongchamps, D.D.Rowan, N.Pothier, T.Sauvé and J.K.Saunders, *Can.J.Chem.*, 59, 1105, 1981.
92. R.U.Lemieux, *Ann.N.Y. Acad.Sci.*, 222, 915, 1973.

93. R.U.Lemieux, T.L.Nagabhushan and B.Paul, *Can.J.Chem.*, 50, 773, 1972.
94. L.T.J.Delbaere, M.N.G.James and R.U.Lemieux, *J.Am.Chem.Soc.*, 95, 7866, 1973.
95. I.Tvaroska and T.Bleha, *Adv.Carbohydr.Chem.Biochem.*, 47, 45, 1989.
96. H.Paulsen, P.Luger and F.R.Heiker, "Anomeric effect, origin and consequences", ACS Symposium Ser. No.87, Chapt.2, p.17, W.A.Szarek and D.Horton, Eds., ACS, Washington, D.C., 1979.
97. H.Thögensen, R.U.Lemieux, K.Bock and B.Meyer, *Can.J.Chem.*, 60, 44, 1982.
98. R.U.Lemieux, A.P.Venot, U.Spoehr, P..Bird, G.Mandal, N.Morishima, O.Hindsgaul and D.R.Bundle, *Can.J.Chem.*, 63, 2664, 1985.
99. T.C.Wu, P.G.Goekjian and Y.Kishi, *J.Org.Chem.*, 52, 4819, 1987.
100. E.Khadem, H.S.Horton, *J.Org.Chem.*, 33, 734, 1968.
101. R.U.Lemieux and A.R.Morgan, *Can.J.Chem.*, 43, 2205, 1965.
102. P.Finch and A.G.Nagpurkar, *Carbohydr.Res.*, 49, 275, 1976.
103. G.Ricart, C.Glacet and D.Couturier, *C.R.Acad.Sci.Ser.C*, 284, 319, 1977.
104. J.Tesse, C.Glacet and D.Couturier, *C.R.Acad.Sci.Ser.C*, 280, 1525, 1975.
105. G.Ricart, D.Barby, C.Glacet and D.Couturier, *C.R.Acad.Sc.Paris*, 292, 1981.
106. H.Booth, K.A.Khedhair and S.A.Readshaw, *Tetrahedron*, 43, 4699, 1987.

107. L.Schafer, C.van Alsenoy, J.O.Williams and J.N.Scarsdale, *J.Mol.Struct.*, 76, 349, 1981.
108. B.M.Pinto, Ph.D. Thesis, Queen's University, 1980.
109. H.Booth, T.B.Grindley and K.A.Khedhair, *J.Chem.Soc., Chem.Comm.*, 1047, 1982.
110. R.U.Lemieux, Proceedings VIIth International Symposium on Medicinal Chemistry, Vol.1, Swedish Pharmaceutical Press, Stockholm, 1985, p329.
111. P.Aped, Y.Apeloig, A.Elleneweig, B.Fuchs, I.Goldberg, M.Karni and E.Tartakovsky, *J.Am.Chem.Soc.*, 109, 1486, 1987.
112. B.Fuchs, A.Elleneweig, *Nouv.J.Chim.*, 3, 145, 1977.
113. B.Fuchs, A.Elleneweig, J.Burkert, *Tetrahedron*, 40, 2011, 1984.
114. C.B.Anderson and D.T.Sepp, *J.Org.Chem.*, 32, 607, 1967.
115. W.F.Bailey and E.L.Eliel, *J.Am.Chem.Soc.*, 96, 1798, 1974.
116. Z.Ardalan and E.A.C.Lucken, *Helv.Chim.Acta*, 56, 1715, 1973.
117. B.M.Pinto and S.Wolfe, *Tetrahedron Lett.*, 3687, 1982.
118. F.S.Jorgensen and L.Norskov-Lauritsen, *Tetrahedron Lett.*, 5221, 1982.
119. S.Desilets and M.St.-Jacques, *J.Am.Chem.Soc.*, 109, 1641, 1987.
120. J.E.Dubois, A.Cosse-Barbi and D.G.Watson, *Tetrahedron Lett.*, 30, 163, 1989.
121. A.Cosse-Barbi, D.G.Watson and J.E.Dubois, *Tetrahedron Lett.*, 30, 167, 1989.

122. T.Sugawara, H.Iwamura and M.Oki, *Bull.Chem.Soc.Jpn.*, **47**, 1496, **1974**.
123. N.S.Zefirov, V.S.Blagoreshchenskii, I.V.Kazimirchik and O.P.Yakovleva, *J.Org.Chem. USSR (Engl.Transl.)*, **7**, 599, **1971**.
124. J.B.Lambert and R.L.Whistler, *J.Org.Chem.*, **46**, 3193, **1981**.
125. E.Juaristi, L.Valle, C.Mora-Uzeta, B.A.Valenzuela, P.Joseph-Nathan and M.F.Frederich, *J.Org.Chem.*, **47**, 5038, **1982**.
126. P.Deslongchamps and D.Guay, *Can.J.Chem.*, **63**, 2757, **1985**.
127. E.Juaristi, L.Valle, C.Mora-Uzeta, B.A.Valenzuela and M.A.Aguilar, *J.Am.Chem.Soc.*, **108**, 2000, **1986**.
128. M.Mikolajczyk, P.Graczyk and P.Balczewski, *Tetrahedron Lett.*, **28**, 573, **1987**.
129. H.Matsuura, H.Murata and M.Sakakibara, *J.Mol.Struct.*, **96**, 267, **1983**.
130. E.L.Eliel, A.A.Hartmann and A.G.Abatjoglou, *J.Am.Chem.Soc.*, **96**, 1807, **1974**.
131. K.Arai, H.Iwamura and M.Oki, *Bull.Chem.Soc.Jpn.*, **48**, 3319, **1975**.
132. W.J.Hehre, R.Ditchfield, L.Radom and J.A.Pople, *J.Am.Chem.Soc.*, **92**, 4796, **1970**.
133. H.T.Kalff and C.Romers, *Acta.Cryst.*, **20**, 490, **1966**.
134. E.L.Eliel and R.O.Hutchins, *J.Am.Chem.Soc.*, **91**, 2703, **1969**.
135. K.Pihlaja and H.Nikander, *Acta.Chem.Scand.*, **B31**, 265, **1977**.
136. A.J.de Hoog, Ph.D.Thesis, University of Leiden, **1971**.

137. P.Luger, P.L.Durette and H.Paulsen, *Chem.Ber.*, 107, 2615, 1974.
138. P.Luger, G.Kothe and H.Paulsen, *Chem.Ber.*, 109, 1850, 1976.
139. P.Luger and H.Paulsen, *Acta.Cryst.*, B35, 2079, 1979.
140. S.Wolfe, B.M.Pinto, V.Varma and R.Y.N.Leung, *Can.J.Chem.*, 68, 1051, 1990.
141. S.Vishveshwara and V.S.R.Rao, *Carbohydr.Res.*, 104, 21, 1982.
142. R.O.Hutchins and B.E.Maryanoff, *J.Am.Chem.Soc.*, 94, 3266, 1972.
143. L.D.Hall and R.B.Malcolm, *Can.J.Chem.*, 50, 2092, 1972.
144. H.J.Geise, *Recl.Trav.Chim.Pays-Bas.*, 86, 362, 1967.
145. J.A.Mosbo and J.G.Verkaide, *J.Org.Chem.*, 52, 1549, 1977.
146. H.F.van Woerden and E.Havinga, *Recl.Trav.Chim.Pays-Bas.*, 86, 341, 1967.
147. G.W.Wood, J.M.McIntosh and M.A.Miskow, *Can.J.Chem.*, 49, 1202, 1971.
148. G.W.Wood, J.M.McIntosh and M.A.Miskow, *Can.J.Chem.*, 50, 521, 1972.
149. G.W.Buchanan, J.B.Stothers and G.W.Wood, *Can.J.Chem.*, 51, 3746, 1973.
150. A.E.Reed and P.v.R.Schleyer, *Inorg.Chem.*, 27, 3969, 1988.
151. A.E.Reed, C.Schade, P.v.R.Schleyer, P.V.Kamath and J.Chandrasekhar, *J.Chem.Soc., Chem.Commun.*, 67, 1988.
152. Y.Apeloig and A.Stanger, *J.Organometal.Chem.*, 346, 305, 1988.



153. E.Juarisri, B.A.Valenzuela, L.Valle and A.T.McPhail, *J.Org.Chem.*, **49**, 3026, **1984**.
154. E.Juaristi, J.Tapia and R.Mendez, *Tetrahedron*, **42**, 1253, **1968**.
155. M.Mikolajczyk, P.Balczewski, K.Wroblewski, J.Karolak -Wojciechowska, A.Miller, M.Wieczorek, M.Y.Antipin and Y.T.Struchkov, *Tetrahedron*, **40**, 4885, **1984**.
156. R.J.Batchelor, F.W.B.Einstein, I.D.Gay, J.H.Gu, B.D.Johnston and B.M.Pinto, *J.Am.Chem.Soc.*, **111**, 6582, **1989**.
157. B.M.Pinto, B.D.Johnston and R.Nagelkerke, *J.Org.Chem.*, **53**, 5668, **1988**.
158. S.Ehrensens, R.T.C.Brownlee and R.W.Taft, *Progr.Phys.Org.Chem.*, **10**, 1, **1973**.
159. R.D.Topson, *Progr.Phys.Org.Chem.*, **12**, 1, **1976**.
160. F.A.L.Anet and M.J.Kopelevich, *J.Chem.Soc., Chem.Comm.*, 595, **1987**.
161. R.U.Lemieux and A.A.Pavia, *Can.J.Chem.*, **47**, 4441, **1969**.
162. J.-P.Praly and R.U.Lemieux, *Can.J.Chem.*, **65**, 213, **1987**.
163. R.J.Ouellette and S.H.William, *J.Am.Chem.Soc.*, **93**, 466, **1971**.
164. B.Fuchs, A.Ellencweig, E.Tartakovsky and P.Aped, *Agew.Chem., Int.Ed.Engl.*, **25**, 287, **1986**.
165. C.B.Anderson and D.T.Sepp, *Tetrahedron*, **24**, 1707, **1968**.
166. E.L.Eliel and C.A.Giza, *J.Org.Chem.*, **33**, 3754, **1968**.
167. S.Wolfe, A.Rauk, L.M.Tel and I.G.Csizmadia, *J.Chem.Soc., B*, 136, **1971**.

168. S.Wolfe, L.M.Tel, W.J.Haines, M.A.Robb and I.G.Csizmadia, *J.Am.Chem.Soc.*, 95, 4863, 1973.
169. E.Juaristi, *J.Chem.Educ.*, 56, 438, 1979.
170. R.Bucourt, *Top.Stereochem.*, 8, 159, 1974.
171. G.J.Szasz, N.Sheppard and D.H.Rank, *J.Chem.Phys.*, 16, 704, 1948.
172. P.B.Woiler and E.W.Garbisch, Jr., *J.Am.Chem.Soc.*, 94, 5310, 1972.
173. R.J.Abraham and R.H.Kemp, *J.Chem.Soc., B*, 1240, 1971.
174. P.Walchli-Huber and Hs.H.Gunthard, *Chem.Phys.Lett.*, 30, 347, 1975.
175. W.C.Harris, J.R.Holtzclaw and V.F.Kalasinaky, *J.Chem.Phys.*, 67, 3330, 1977.
176. R.J.Abraham and J.R.Monasterios, *Org.Magn.Reson.*, 5, 305, 1973.
177. E.I.Snyder, *J.Am.Chem.Soc.*, 88, 1165, 1966.
178. R.J.Abraham and G.Gatti, *J.Chem.Soc., B*, 961, 1969.
179. L.H.L.Chia, H.H.Huang and P.K.K.Lim, *J.Chem.Soc., B*, 608, 1969.
180. T.M.Connor and K.A.McLauchlan, *J.Phys.Chem.*, 69, 1888, 1965.
181. R.G.Snyder and G.Zerbi, *Spectrochim.Acta.*, 23A, 391, 1967.
182. J.E.Mark and P.J.Flory, *J.Am.Chem.Soc.*, 87, 1415, 1965.
183. J.E.Mark and P.J.Flory, *J.Am.Chem.Soc.*, 88, 3702, 1966.
184. Y.Hoppilliare and D.Solgadi, *Tetrahedron*, 36, 377, 1980.
185. R.J.Abraham, H.D.Banks, E.L.Eliel, O.Hofer and M.K.Kaloustian, *J.Am.Chem.Soc.*, 94, 1913, 1972.

186. N.S.Zefirov, L.G.Gurvich, A.S.Shashkov, M.Z.Krimer and G.A.Vorobeva, *Tetrahedron*, 32, 1211, 1976.
187. N.S.Zefirov, V.V.Samoshin, O.A.Subboin, V.I.Baranenkov and S.Wolfe, *Tetrahedron*, 34, 2953, 1978.
188. E.L.Eliel and E.Juaristi, *J.Am.Chem.Soc.*, 100, 6114, 1978.
189. L.C.Allen, *Chem.Phys.Lett.*, 2, 597, 1968.
190. L.Salem, *J.Am.Chem.Soc.*, 90, 543, 1968.
191. N.S.Zefirov, *J.Org.Chem.*, USSR, 6, 1768, 1970.
192. R.Gleiter, M.Kobayashi, N.S.Zefirov and V.A.Palyulin, *Dokl.Chem.*, 235, 396, 1977.
193. D.Gonbeau, M.Loudet and G.Pfister-Guillouzo, *Tetrahedron*, 36, 381, 1980.
194. N.D.Epiotis, S.Sarkanen, D.Bjorkquist, L.Bjorkquist and R.Yates, *J.Am.Chem.Soc.*, 96, 4075, 1974.
195. L.Radom, W.J.Hehre and J.A.Pople, *J.Am.Chem.Soc.*, 94, 2371, 1972.
196. L.Radom, W.A.Lathan, W.J.Hehre and J.A.Pople, *J.Am.Chem.Soc.*, 95, 693, 1973.
197. N.L.Allinger and Y.H.Yuh, *QCPE*, 12, 395, 1980.
198. L.Norskov-Lauritsen and N.L.Allinger, *J.Comput.Chem.*, 1, 99, 1980.
199. N.L.Allinger, *J.Am.Chem.Soc.*, 99, 8127, 1977.
200. P.Dionne and M.St.-Jacques, *J.Am.Chem.Soc.*, 109, 2616, 1987.
201. T.K.Brunck and F.Weinhold, *J.Am.Chem.Soc.*, 101, 1700, 1979.

202. V.Minkin, B.Simkine and R.Mihiaev, "Theorie de la structure moleculaire (couches electroniques)". French translation: Mir, Moscow, 1982, pp 132, 249, 250.
203. R.F.Hudson, *Angew.Chem.Int.Ed.Engl.*, 12, 36, 1973.
204. Y.Karton and A.Pross, *Tetrahedron Lett.*, 3827, 1978
205. K.Kimura, S.Kesumata, Y.Achiba, T.Y.Amazaki and S.Iwaka, "Handbook of the HeI photoelectron spectra of fundamental organic molecules", Japan Scientific Societies Press, Tokyo, Halsted Press, N.Y., 1981.
206. N.D.Epiotis, W.R.Cherry, S.Shalk, R.L.Yates and F.Bernardi, *Top.Curr.Chem.*, 70, 1977.
207. R.C.Bingham, *J.Am.Chem.Soc.*, 97, 6743, 1975.
208. P.Dionne and M.St.-Jacques, *Can.J.Chem.*, 67, 11, 1989.
209. J.L.G.Ruano, J.Rodriguez, F.Alcudia, J.M.Llera, E.M.Olefirowicz and E.L.Eliel, *J.Org.Chem.*, 52, 4099, 1987.
210. E.L.Eliel, K.D.Hargrave, K.M.Pietrusiewicz and M.Manoharan, *J.Am.Chem.Soc.*, 104, 3635, 1982.
211. M.K.Kaloustian, N.Dennis, S.Mager, S.A.Evans, F.Alcudia and E.L.Eliel, *J.Am.Chem.Soc.*, 98, 956, 1976.
212. F.Alcudia, A.L.Campos, J.M.Llera and F.Zorrilla, *Phosphorus and Sulfur*, 36, 29, 1988.
213. R.D.McKelvey, T.Sugawara and H.Iwamura, *Magn.Reson.Chem.*, 23, 330, 1985.
214. A.S.Cieplak, *J.Am.Chem.Soc.*, 103, 4540, 1981.
215. A.L.Van Geet, *Anal.Chem.*, 42, 679, 1970.
216. D.S.Raiford, C.L.Fisk, E.D.Becker, *Anal.Chem.*, 51, 2050, 1979.

217. D.R.Bundle, T.Iversen, S.Josephson, *Am.Laboratory*, 12, 93, 1980.
218. G.Binsch, *Top.Stereochem.*, 3, 97, 1968.
219. B.M.Pinto, T.B.Grindley and W.A.Szarek, *Magn.Reson.Chem.*, 24, 323, 1986.
220. J.R.Wolberg, "Prediction Analysis", Chap.3. Van Nostrand, N.Y. 1967.
221. N.L.Allinger, S.M.U.Chang, D.H.Glaser, and H.Honig, *Isr.J.Chem.*, 20, 5, 1980.
222. MM2(85), QCPE Program no. MM2 85. Indiana University, Bloomington, Indiana.
223. C.C.J.Roothaan, *Rev.Mod.Phys.*, 23, 69, 1951.
224. P.Pulay, *Mol.Phys.*, 17, 197, 1969.
225. M.J.Frisch, J.S.Binkley, H.B.Schlegel, K.Raghavachari, C.F.Melius, R.L.Martin, J.J.P.Stewart, F.W.Bobrowicz, C.M.Rohlfing, L.R.Kahn, D.J.Defrees, R.Seeger, R.A.Whiteside, D.J.Fox, E.M.Fluder, and J.A.Pople, GAUSSIAN86, Gaussian Inc. Pittsburgh, PA 15213.
226. W.J.Pietro, M.M.Francl, W.J.Hehre, D.J.Defrees, J.A.Pople, and J.S.Binkley, *J.Am.Chem.Soc.*, 104, 5039, 1982.
227. J.S.Binkley, J.A.Pople, and W.J.Hehre, *J.Am.Chem.Soc.*, 102, 939, 1980.
228. R.F.Hout Jr., M.M.Francl, S.D.Kahn, K.D.Dobbs, E.S.Blurock, W.J.Pietro, M.P.McGrath, R.Steckler and W.J.Hehre, "Gaussian85", University of Illinois (Urbana-Champaign) and University of California (Irvine), 1988.

229. "Ground states of molecules. 38. The MNDO method. Approximations and Parameters.", M.J.S.Dewar and W.Thiel, J.Am.Chem.Soc., 99, 4899, 1977.
230. W.Thiel, Program no. 464, QCPE, Indiana University, Bloomington, Indiana.
231. PCMODEL with MNDO calculations, Serena Software, Box 3076, Bloomington, Indiana. MNDO calculations revised by K.E.Gilbert and J.J.Gajewski, Indiana University. PCMODEL is a 300 atom version of C.Still's (Columbia University) Macromodel program,<sup>262</sup> modified by Kosta Steliou (University of Montreal), and ported to the IBM-PC by M.M.Midland (University of California, Riverside).
232. R.Fletcher and M.J.D.Powell, Comp.J., 6, 163, 1963.
233. W.C.Davidon, Comp.J., 10, 406, 1968.
234. A.Komornicki and J.W.McIver, Chem.Phys.Lett., 10, 303, 1971.
235. J.Egyed, Bull.Soc.Chim.Fr., 2287, 1972.
236. E.L.Eliel and Sr.M.C.Knoeiber, J.Am.Chem.Soc., 90, 3444, 1968.
237. S.M.Trister and H.Hibbert, Can.J.Res., 148, 415, 1936.
238. G.Braun, Org.Synth.Coll.Vol II, p256.
239. M.L.Moore, Org.React. 5, 301, 1949.
240. W.E.Parham and H.E.Holmquist, J.Am.Chem.Soc., 73, 913, 1951.
241. C.T.Bishop and F.P.Cooper, Can.J.Chem., 40, 224, 1962.
242. R.L.Willer and E.L.Eliel, J.Am.Chem.Soc., 99, 1925, 1977.
243. G.Sosnovsky and N.C.Yang, J.Org.Chem., 25, 899, 1960.
244. W.E.Parham and M.D.Bhavsar, J.Org.Chem., 28, 2686, 1963.

245. J.M.Cox and L.N.Owen, *J.Chem.Soc.(C)*, 1130, 1967.
246. A.A.Marei and R.A.Raphael, *J.Chem.Soc.*, 886, 1960.
247. W.E.Parham, L.Christensen, S.H.Groen and R.M.Dodson, *J.Org.Chem.*, 29, 2211, 1964.
248. D.M.Vyas and W.A.Szarek, *Carbohydr.Res.*, 30, 225, 1973.
249. W.A.Szarek, D.M.Vyas, A.M.Sepulchre, S.D.Gero and G.Lukacs, *Can.J.Chem.*, 52, 2041, 1974.
250. J.Reisse, J.C.Celotti, D.Zimmermann and G.Chiurdoglu, *Tetrahedron Lett.*, 2145, 1964.
251. W.E.Parham, I.Gordon and J.D.Swalen, *J.Am.Chem.Soc.*, 74, 1824, 1952.
252. C.Glacet and D.Veron, *Bull.Soc.Chim.Fr.*, 1789, 1965.
253. Reference 21, p.7.
254. R.J.Abraham, Z.L.Rossetti, *J.Chem.Soc.*, *Perkin Trans. 2*, 582, 1973.
255. E.Brunett and P.Azpeitia, *Tetrahedron* 44, 1751, 1988.
256. E.L.Eliel, V.S.Rao and F.G.Riddell, *J.Am.Chem.Soc.*, 98, 3583, 1976.
257. H.R.Buys and E.L.Eliel, *Tetrahedron Lett.*, 2779, 1970.
258. A.J.Jones, E.L.Eliel, D.M.Grant, M.C.Knoeber and W.F.Bailey, *J.Am.Chem.Soc.*, 93, 4772, 1971.
259. R.W.Franck, *Tetrahedron*, 39, 3251, 1983.
260. H.Booth, J.M.Dixon, K.A.Khedhair and S.A.Readshaw, *Tetrahedron*, 46, 1625, 1990.
261. L.M.J.Kroon-Batenburg and J.A.Kanters, *J.Mol.Struct.*, 105, 417, 1983.

262. Macromodel is a molecular mechanics program developed by C.Still (Chemistry Department, Columbia University) that excutes simulation and energy minimization routines. Energy minimizations were performed with the Allinger's MM2(85) force field.
263. S.J.Angyal, *Angew.Chem.Int.Ed.Engl.*, 8, 157, 1969.
264. Reference 21, p9.
265. M.K.Kaloustian, *J.Chem.Educ.*, 51, 777, 1974.
266. Reference 21, p8-10.
267. E.Coene and M.Anteunis, *Tetrahedron Lett.*, 595, 1970.
268. N.Baggett, J.S.Brimacombe, A.B.Foster, M.Stacey and D.H.Whiffen, *J.Chem.Soc.*, 2574, 1960.
269. E.L.Eliel and M.K.Kaloustian, *J.Chem.Soc., Chem.Commun.*, 290, 1970.
270. S.A.Baker, J.S.Brimacombe, A.B.Foster, D.H.Whiffen and G.Zweifel, *Tetrahedron*, 7, 10, 1959.
271. J.C.Jochims and Y.Kobayashi, *Tetrahedron Lett.*, 2065, 1976.
272. M.C.Krol, C.J.M.Huige and C.Altona, *J.Comput.Chem.*, 11, 765, 1990.
273. P.Aped, L.Scheifer and B.Fuchs, *J.Comput.Chem.*, 10, 265, 1989.
274. M.D.Rozeboom and K.N.Houk, *J.Am.Chem.Soc.*, 104, 1189, 1982.
275. E.L.Eliel and M.H.Gianni, *Tetrahedron Lett.*, 97, 1962.
276. N.L.Allinger and M.J.Hickey, *J.Am.Chem.Soc.*, 97, 5167, 1975.
277. B.E.Smart, *J.Org.Chem.*, 38, 2039, 1973.



278. J.A.Pople and M.S.Gordon, *J.Am.Chem.Soc.*, 89, 4253, 1967.
279. R.J.Abraham and K.Parry, *J.Chem.Soc.(B)*, 539, 1970.
280. R.D.Stolow, D.I.Lewis and P.A.D'Angelo, *Tetrahedron*, 26, 5831, 1970.
281. D.A.Sweigart and D.W.Turner, *J.Am.Chem.Soc.*, 94, 5592, 1972.
282. E.Juaristi, R.Martinez, R.Mendez, R.A.Toscano, M.Soriano-Garcia, E.L.Eliel, A.Petasm and R.S.Glass, *J.Org.Chem.*, 52, 3806, 1987.
283. B.R.Coleman, R.S.Glass, W.N.Setzer, U.D.B.Prabhu and G.S.Wilson, "Electrochemical and Spectrochemical Studies of Biological Redox Components", K.M.Kadish, Ed., *Advances in Chemistry* 201, American Chemical Society, Washington, DC, p417-441, 1982.
284. D.Ménard and M.St.-Jacques, *J.Am.Chem.Soc.*, 106, 2055, 1984.
285. D.Ménard and M.St.-Jacques, *Can.J.Chem.*, 59, 1160, 1981.
286. F.H.Westheimer, "Steric effects in organic chemistry", M.S.Newman, Ed., John Wiley and Sons, N.Y., 1956.
287. N.L.Allinger, M.T.Trubble, M.A.Miller and D.H.Wertz, *J.Am.Chem.Soc.*, 93, 1637, 1971.
288. U.Burkert and N.L.Allinger, "Molecular Mechanics", American Chemical Society, Washington, D.C., 1982.
289. S.Lifson and A.Warshel, *J.Chem.Phys.*, 49, 5116, 1968.
290. A.Warshel, *J.Chem.Phys.*, 55, 5613, 1972.
291. A.Warshel and M.Karplus, *J.Am.Chem.Soc.*, 96, 5677, 1974.
292. R.H.Boyd, *J.Chem.Phys.*, 49, 2574, 1968.

293. S.Chang, D.McNally, S.Shary-Tehrany, M.J.Hickey and R.Boyd, J.Am.Chem.Soc., 92, 3109, 1970.
294. T.Hirano and E.Osawa, Croatica Chemica Acta, 57, 1633, 1984.
295. J.Kao, D.Leister and M.Sito, Tetrahedron Lett., 26, 2403, 1985.
296. P.Aped, L.Schleifer, B.Fuchs and S.Wolfe, J.Comput.Chem., 10, 265, 1989.
297. S.Wolfe, S.Bruder, D.F.Weaver and K.Yang, Can.J.Chem., 66, 2703, 1988.
298. S.Wolfe, M.Khalil and D.F.Weaver, Can.J.Chem., 66, 2715, 1988.
299. S.Wolfe, K.Yang and M.Khalil, Can.J.Chem., 66, 2733, 1988.
300. S.Grigoras and T.H.Lane, J.Comput.Chem., 9, 25, 1988.
301. N.L.Allinger and L.Norskov-Lauritsen, J.Comput.Chem., 5, 326, 1984.
302. T.L.Hill, J.Chem.Phys., 16, 399, 1948.
303. R.A.Buckingham, Proc.Roy.Soc.London,Ser.A, 168, 264, 1938.
304. A.Warshel, J.Chem.Phys., 49, 5116, 1968.
305. J.H.Jeans, "The Mathematical Theory of Electricity and Magnetism", 5<sup>th</sup>ed., Cambridge University Press, London, eq.354, p379, 1925.
306. C.van Alsenoy, K.Siam, J.D.Ewbank and L.Schafer, J.Mol.Struct., 136, 77, 1986.
307. A.J.Hopfinger and R.A.Pearlstein, J.Comput.Chem., 5, 486, 1984.

308. A PC scientific spreadsheet program "SHEET", written by I.D.Gay (Simon Fraser University).
309. P.Aped, Ph.D. Thesis, Tel-Aviv University, 1988.
310. L.Carballeira, B.Fernandez, R.A.Mosquera and M.A.Rios, *J.Mol.Struct.*, 205, 235, 1990.
311. S.E.Denmark, M.S.Dappen, N.L.Sear and R.T.Jacobs, *J.Am.Chem.Soc.*, 112, 3466, 1990.
312. B.M.Pinto, J.Scandoval-Ramirez and R.D.Sharma, *Tetrahedron Lett.*, 26, 5235, 1985.
313. B.M.Pinto, B.D.Johnston, J.Sandoval-Ramirez and R.D.Sharma, *J.Org.Chem.*, 53, 3766, 1988.
314. Y.Sakai, H.Tatewaki and S.Huzinaga, *J.Comput.Chem.*, 2, 100, 1981.
315. Y.Sakai, H.Tatewaki and S.Huzinaga, *J.Comput.Chem.*, 3, 6, 1982.
316. J.L.Whitten, *J.Chem.Phys.*, 39, 349, 1963.
317. Y.Sakai, H.Tatewaki and S.Huzinaga, *J.Comput.Chem.*, 2, 108, 1981.
318. H.Tatewaki and S.Huzinaga, *J.Comput.Chem.*, 1, 205, 1980.
319. R.Laitinen and T.Pakkanen, *J.Mol.Struct.*, 91, 337, 1983, and references cited therein.
320. J.B.Collins, P.v.R.Schleyer, J.S.Binkley and J.A.Pople, *J.Chem.Phys.*, 64, 5142, 1976.
321. B.T.Luke, J.A.Pople, M.B.Krogh-Jesperen, Y.Apeloig, J.Chandrasekhar and P.v.R.Schleyer, *J.Am.Chem.Soc.*, 108, 260, 1986.
322. K.B.Wiberg and M.A.Murcko, *J.Am.Chem.Soc.*, 111, 4821, 1989.

323. K.B.Wiberg and M.A.Murcko, *J.Comput.Chem.*, 9, 488, 1988.
324. A.W.Potts and W.C.Price, *Proc.Roy.Soc. (London)*, 326A, 165, 1972.
325. A.W.Potts and W.C.Price, *Proc.Roy.Soc. (London)*, 326A, 181, 1972.
326. G.Herzberg, "Molecular Spectra and Molecular Structure III. Electronic Spectra and Electronic Structure of Polyatomic Molecules", Van Nostrand, Princeton, New Jersey, 1966.
327. L.S.Cederbaum, G.Hohlneicher and W.von Niessen, *Mol.Phys.*, 26, 1405, 1973.
328. Reference 45, p.36.
329. E.Astrup, *Acta Chem.Scand.*, 27, 327, 1973.
330. P.v.R.Schleyer and A.J.Kos, *Tetrahedron*, 39, 1141, 1983.
331. J.D.Dill, P.v.R.Schleyer and J.A.Pople, *J.Am.Chem.Soc.*, 98, 1663, 1976.
332. F.A.Cotton and G.Wilkinson, "Advanced Inorganic Chemistry", 3<sup>rd</sup> ed., Wiley, New York, 1972, p.115.
333. B.M.Pinto, J.Sandoval-Ramirez, R.D.Sharma, A.C.Willis and F.W.B.Einstein, *Can.J.Chem.*, 64, 732, 1986.
334. S.W.Benson, *Angew.Chem.,Int.Ed.Engl.*, 17, 812, 1978.
335. A.Abe, K.Inomata, E.Tanisawa and I.Ando, *J.Mol.Struct.*, 238, 315, 1990.
336. U.Salzner and P.v.R.Schleyer, *J.Chem.Soc., Chem.Commun.*, 2, 190, 1990.
337. S.Huzinaga, Ed., "Gaussian basis for molecular calculations (Physical Sciences Data 16)", Elsevier, 1984.

338. J.B.Lambert, "The Conformational Analysis of Cyclohexenes, Cyclohexadienes, and Related Hydroaromatic Compounds", P.Rabideau, Ed., VCH: Weinheim, 1989, Chapter 2.
339. E.J.Corey and J.Burke, J.Am.Chem.Soc., 77, 5418, 1955.
340. E.M.Kosower, G.S.Wu and T.S.Sorensen, J.Am.Chem.Soc., 83, 3147, 1961.
341. N.L.Allinger, J.C.Tai and M.A.Miller, J.Am.Chem.Soc., 88, 4495, 1966.
342. J.Cantacuzene, R.Jantzen and D.Ricard, Tetrahedron, 28, 717, 1972.
343. J.Cantacuzene and M.Tordeux, Can.J.Chem., 54, 2759, 1976.
344. A.Ouedraogo, M.T.P.Viet, J.K.Saunders and J.Lessard, Can.J.Chem., 65, 1761, 1987.
345. J.Lessard, J.K.Saunders and M.T.P.Viet, Tetrahedron Lett., 23, 2059, 1982.
346. M.T.P.Viet, J.Lessard and J.K.Saunders, Tetrahedron Lett., 317, 1979.
347. N.S.Zefirov and I.V.Baranenkov, Tetrahedron, 39, 1769, 1983.
348. N.S.Zefirov and I.V.Baranenkov, J.Org.Chem., USSR (Engl.Transl.), 4875, 1979.
349. Y.Senda and S.Imaizumi, Tetrahedron, 30, 3813, 1974.
350. K.Sakashita, Bull.Chem.Soc.Jpn., 81, 49, 1966.
351. J.Lessard, P.V.M.Tan, R.Martino and J.K.Saunders, Can.J.Chem., 55, 1015, 1977.
352. N.S.Zefirov and I.V.Baranenkov, Tetrahedron Lett., 50, 4875, 1979.

353. N.S.Zefirov, I.V.Baranenkov, and I.G.Mursakulov,  
J.Org.Chem., USSR, (Engl.Transl.), 15, 2005, 1979.
354. Q.Shen, J.Mol.Struct., 96, 133, 1982.
355. H.Ozbal and W.W.Zajac, Tetrahedron Lett., 4821, 1979.
356. E.J.Corey, J.Am.Chem.Soc., 75, 2301, 1953.
357. E.J.Corey, J.Am.Chem.Soc., 75, 3297, 1953.
358. F.Johnson, Chem.Rev., 68, 375, 1968.
359. R.S.Brown and R.W.Marcinko, J.Am.Chem.Soc., 100, 5721,  
1978.
360. R.S.Brown, R.W.Marcinko and A.Tse, Can.J.Chem., 57, 1890,  
1979.
361. G.H.Penner, T.Schaefer, R.Sebastian and S.Wolfe,  
Can.J.Chem., 65, 1845, 1987.
362. E.Hirota, J.Chem.Phys., 42, 2071, 1965.
363. C.Sourisseau and B.Pasquier, J.Mol.Struct., 12, 1, 1972.
364. F.Vanhouteghem, W.Pyckhout, C.van Alsenoy, L.V.D.Enden  
and H.J.Geise, J.Mol.Struct., 140, 33, 1986.
365. A.N.Murty and R.F.Curl, Jr., J.Chem.Phys., 46, 4176,  
1967.
366. A.Aspiala, T.Lotta, J.Murto and M.Rasanen, J.Chem.Phys.,  
79, 4183, 1983.
367. S.Racine, A.Schrivier, L.Schrivier and J.P.Perchard,  
J.Mol.Struct., 118, 197, 1984.
368. H.Brouwer and J.B.Stothers, Can.J.Chem., 50, 1361, 1972.
369. J.M.Bakke, A.M.Schie and T.Skjetne, Acta Chem.Scand.,  
B40, 703, 1986.
370. R.J.Abraham and J.M.Bakke, Acta Chem.Scand., B37, 865,  
1983.

371. Z.Smith, N.Carballe, E.B.Wilson, K.M.Marstokk and H.Mollendal, *J.Am.Chem.Soc.*, 107, 1951, 1985.
372. M.H.Whangbo and S.Wolfe, *Isr.J.Chem.*, 20, 36, 1980.
373. H.Kessler and W.Rundel, *Chem.Ber.*, 101, 3350, 1968.
374. R.R.Fraser, G.Boussard, J.K.Saunders, J.B.Lambert and C.E.Mixan, *J.Am.Chem.Soc.*, 93, 3822, 1971.
375. H.Kessler, A.Rieker and W.Rundel, *J.Chem.Soc., Chem.Commun.*, 475, 1968.
376. J.E.Anderson and L.Henriksen, *J.Chem.Soc., Chem.Commun.*, 1397, 1985.
377. H.G.Guttenberger, H.J.Bestmann, F.L.Dickert, F.S.Jorgensen and J.P.Snyder, *J.Am.Chem.Soc.*, 103, 159, 1981.
378. F.S.Jorgensen and J.P.Snyder, *Tetrahedron*, 35, 1399, 1979.
379. F.S.Jorgensen and J.P.Snyder, *J.Org.Chem.*, 45, 1015, 1980.
380. V.Renugopalakrishnan and R.Walter, *J.Am.Chem.Soc.*, 106, 3413, 1984.
381. R.Laitinen and T.Pakkanen, *J.Mol.Struct.*, 124, 293, 1985.
382. R.Laitinen and T.Pakkanen, *J.Mol.Struct.*, 108, 263, 1984.
383. C.S.Ewig, E.H.Mei and J.R.van Wazer, *Mol.Phys.*, 40, 241, 1980.
384. W.-W.du Mont, L.Lange, H.H.Karsch, K.Peters, E.M.Peters and H.G.von Schnering, *Chem.Ber.*, 121, 11, 1988.
385. L.Lange and W.-W.du Mont, *J.Organomet.Chem.*, 286, C1, 1985.

386. W.-W. du Mont, S. Kubiniok, K. Peters and H.-G. von Schnering, *Angew. Chem., Int. Ed. Engl.*, 26, 780, 1987.
387. A. Akiba, M. V. Lakshmikantham, K.-Y. Jen and M. P. Cava, *J. Org. Chem.*, 49, 4819, 1984.
388. D. A. Kleier, G. Binsch, A. Steigel and J. Sauer, *J. Am. Chem. Soc.*, 92, 3787, 1970.
389. J. D. Lee and M. W. R. Byan, *Acta Crystallogr., Sect. B*, 25, 2094, 1969.
390. M. Sacerdoti, G. Gilli and P. Domiano, *Acta Crystallogr., Sect. B*, 31, 327, 1975.
391. R. E. Marsch, *Acta Crystallogr.*, 5, 458, 1952.
392. G. D. Morris and F. W. B. Einstein, *Acta Crystallogr., Sect. C*, 42, 1433, 1986.
393. C. M. Woodward, D. S. Brown, J. D. Lee and A. G. Massey, *J. Organomet. Chem.*, 121, 333, 1976.
394. S. Ludlow and A. E. McCarthy, *J. Organomet. Chem.*, 219, 169, 1981.
395. P. G. Llabres, O. Dideberg and L. Dupont, *Acta Crystallogr., Sect. B*, 28, 2438, 1972.
396. L. Pauling, *Proc. Natl. Acad. Sci., U.S.A.*, 35, 495, 1949.
397. R. A. Poirier and I. G. Csizmadia, "The Chemistry of Organic Selenium and Tellurium Compounds", Ed. S. Patai and Z. Rappoport, Vol. 1, Chap. 2. Wiley, N.Y., 1986.
398. J.-M. Lehn, G. Wipff and J. Demuynck, *Helv. Chim. Acta*, 60, 1239, 1977.
399. For example, A. H. Cowley, D. J. Mitchell, M.-H. Whangbo and S. Wolfe, *J. Am. Chem. Soc.*, 101, 5224, 1979.
400. E. Buncel and H. Wilson, *J. Chem. Educ.*, 57, 629, 1980.



401. S.Vishveshwara, Chem.Phys.Lett., 59, 30, 1978.

402. B.M.Pinto, R.Y.N.Leung and R.D.Sharma, Magn.Reson.Chem.,  
26, 729, 1988.